ISSN: 2067-3809

Universitatea Politehnica Timișoara

ACTA TECHNICA CORVINIENSIS – Bulletin of Engineering

Fascicule 2
[April–June]
Tome XVI [2023]

Editura POLITEHNICA

ACTA TECHNICA CORVINIENSIS

Bulletin of Engineering

Edited by:

UNIVERSITY POLITEHNICA TIMISOARA

Universitatea Politehnica Timişoara

Editor / Technical preparation / Cover design:

Assoc. Prof. Eng. KISS Imre, PhD.
UNIVERSITY POLITEHNICA TIMISOARA,
FACULTY OF ENGINEERING HUNEDOARA

Commenced publication year:
2008

ACTA TECHNICA CORVINIENSIS
Bulletin of Engineering

ASSOCIATE EDITORS and REGIONAL COLLABORATORS

The Editor and editorial board members do not receive any remuneration. These positions are voluntary. The members of the Editorial Board may serve as scientific reviewers.

We are very pleased to inform that our journal ACTA TECHNICA CORVINIENSIS – Bulletin of Engineering is going to complete its ten years of publication successfully. In a very short period it has acquired global presence and scholars from all over the world have taken it with great enthusiasm. We are extremely grateful and heartily acknowledge the kind of support and encouragement from you.

ACTA TECHNICA CORVINIENSIS – Bulletin of Engineering seeking qualified researchers as members of the editorial team. Like our other journals, ACTA TECHNICA CORVINIENSIS – Bulletin of Engineering will serve as a great resource for researchers and students across the globe. We ask you to support this initiative by joining our editorial team. If you are interested in serving as a member of the editorial team, kindly send us your resume to redactie@fih.upt.ro.

ISSN: 2067-3809

INTERNATIONAL SCIENTIFIC COMMITTEE MEMBERS and SCIENTIFIC REVIEWERS

The SCIENTIFIC COMMITTEE MEMBERS AND REVIEWERS do not receive any remuneration. These positions are voluntary.

We are extremely grateful and heartily acknowledge the kind of support and encouragement from all contributors and all collaborators!

ACTA TECHNICA CORVINIENSIS – Bulletin of Engineering is dedicated to publishing material of the highest engineering interest, and to this end we have assembled a distinguished Editorial Board and Scientific Committee of academics, professors and researchers.

ACTA TECHNICA CORVINIENSIS – Bulletin of Engineering publishes invited review papers covering the full spectrum of engineering. The reviews, both experimental and theoretical, provide general background information as well as a critical assessment on topics in a state of flux. We are primarily interested in those contributions which bring new insights, and papers will be selected on the basis of the importance of the new knowledge they provide.

ACTA TECHNICA CORVINIENSIS – Bulletin of Engineering encourages the submission of comments on papers published particularly in our journal. The journal publishes articles focused on topics of current interest within the scope of the journal and coordinated by invited guest editors. Interested authors are invited to contact one of the Editors for further details.

ACTA TECHNICA CORVINIENSIS – Bulletin of Engineering accept for publication unpublished manuscripts on the understanding that the same manuscript is not under simultaneous consideration of other journals. Publication of a part of the data as the abstract of conference proceedings is exempted.

Manuscripts submitted (original articles, technical notes, brief communications and case studies) will be subject to peer review by the members of the Editorial Board or by qualified outside reviewers. Only papers of high scientific quality will be accepted for publication. Manuscripts are accepted for review only when they report unpublished work that is not being considered for publication elsewhere.

The evaluated paper may be recommended for:

- **Acceptance without any changes** – in that case the authors will be asked to send the paper electronically in the required .doc format according to authors' instructions;
- **Acceptance with minor changes** – if the authors follow the conditions imposed by referees the paper will be sent in the required .doc format;
- **Acceptance with major changes** – if the authors follow completely the conditions imposed by referees the paper will be sent in the required .doc format;
- **Rejection** – in that case the reasons for rejection will be transmitted to authors along with some suggestions for future improvements (if that will be considered necessary).

The manuscript accepted for publication will be published in the next issue of ACTA TECHNICA CORVINIENSIS – Bulletin of Engineering after the acceptance date.

All the authors and the corresponding author in particular take the responsibility to ensure that the text of the article does not contain portions copied from any other published material which amounts to plagiarism. We also request the authors to familiarize themselves with the good publication ethics principles before finalizing their manuscripts.

ISSN: 2067–3809

Fascicule 2
[April – June]
tome XVI [2023]

ACTA Technica CORVINIENSIS
BULLETIN OF ENGINEERING

ISSN: 2067-3809

TABLE of CONTENTS

ACTA TECHNICA CORVINIENSIS – Bulletin of Engineering
Tome XVI [2023], Fascicule 2 [April – June]

The ACTA TECHNICA CORVINIENSIS – Bulletin of Engineering, Tome XVI [2023], Fascicule 2 [April–June] includes original papers submitted to the Editorial Board, directly by authors or by the regional collaborators of the Journal.

Also, the ACTA TECHNICA CORVINIENSIS – Bulletin of Engineering, Tome XVI [2023], Fascicule 2 [April–June], includes scientific papers presented in the sections of:

- IRMES 2022 – 10th International Conference on Research and Development of Mechanical Elements and Systems: "Machine design in the context of Industry 4.0 – Intelligent products", organized under the auspices of the Association for Design, Elements and Constructions (ADEKO) and University of Belgrade, Faculty of Mechanical Engineering, Department of General Machine Design, in 26 May 2022, Belgrade (SERBIA). The current identification numbers of the selected papers are the #01–03, according to the present contents list.
- IIZS 2021 – XI International Conference on Industrial Engineering and Environmental Protection, organized by Department of Mechanical Engineering, Department of Environmental Protection and Department of Industrial Engineering in Exploitation of Oil and Gas, Technical Faculty Mihajlo Pupin Zrenjanin, University of Novi Sad (SERBIA), in cooperation with partners University Politehnica Timisoara, Faculty of Engineering, Hunedoara (ROMANIA), University St. Kliment Ohridski, Technical Faculty, Bitola (MACEDONIA), Aurel Vlaicu University of Arad, Faculty of Engineering, Arad (ROMANIA), University of East Sarajevo, Faculty of Mechanical Engineering East Sarajevo (BOSNIA & HERZEGOVINA) and University of Giresun, Faculty of Engineering, Giresun (TURKEY), in Zrenjanin, SERBIA, in 06–07 October, 2022. The current identification numbers of the selected papers are the #11–13, according to the present contents list.
- ISB–INMA TEH' 2022 – International Symposium (Agricultural and Mechanical Engineering), organized by Politehnica University of Bucharest – Faculty of Biotechnical Systems Engineering (ISB), National Institute of Research–Development for Machines and Installations Designed to Agriculture and Food Industry (INMA Bucharest), Romanian Agricultural Mechanical Engineers Society (SIMAR), National Research & Development Institute for Food Bioresources (IBA Bucharest), National Institute for Research and Development in Environmental Protection (INCDPM), Research–Development Institute for Plant Protection (ICDPP), Research and Development Institute for Processing and Marketing of the Horticultural Products (HORTING), Hydraulics and Pneumatics Research Institute (INOE 2000 IHP) and "Food for Life Technological Platform", in Bucharest, ROMANIA, between 06–07 October, 2022. The current identification numbers of the selected papers are the #14–17 and #19, according to the present contents list.

ACTA TECHNICA CORVINIENSIS – Bulletin of Engineering is a good opportunity for the researchers to exchange information and to present the results of their research activity. Scientists and engineers with an interest in the respective interfaces of engineering fields, technology and materials, information processes, research in various industrial applications are the target and audience of ACTA TECHNICA CORVINIENSIS – Bulletin of Engineering. It publishes articles of interest to researchers and engineers and to other scientists involved with materials phenomena and computational modeling.

The journal's coverage will reflect the increasingly interdisciplinary nature of engineering, recognizing wide–ranging contributions to the development of methods, tools and evaluation strategies relevant to the field. Numerical modeling or simulation, as well as theoretical and experimental approaches to engineering will form the core of ACTA TECHNICA CORVINIENSIS – Bulletin of Engineering's content, however approaches from a range of environmental science and economics are strongly encouraged.

Publishing in ACTA TECHNICA CORVINIENSIS – Bulletin of Engineering is free of charge. There are no author fees. All services including peer review, copy editing, typesetting, production of web pages and reproduction of color images are included. The journal is free of charge to access, read and download. All costs associated with publishing and hosting this journal are funded by ACTA TECHNICA CORVINIENSIS – Bulletin of Engineering as part of its investment in global research and development.

ISSN: 2067–3809

Fascicule 2
[April – June]
tome XVI [2023]

ACTA Technica CORVINIENSIS
BULLETIN OF ENGINEERING

ISSN: 2067-3809

ACTA TECHNICA CORVINIENSIS – BULLETIN OF ENGINEERING
TOME XVI [2023] | FASCICULE 2 [APRIL – JUNE]

[1.]Sanjin TROHA,[2.]Željko VRCAN, [3.]Jelena STEFANOVIĆ– MARINOVIĆ, [4.]Miloš SEDAK

COMPARISON OF THE SIZE AND EFFICIENCY OF A TWO– CARRIER PLANETARY GEAR TRAIN AND KINEMATICALLY EQUIVALENT PLANETARY GEAR TRAIN

[1,2.]University of Rijeka, Faculty of Engineering, Vukovarska 58, 51000 Rijeka, CROATIA
[3.]University of Niš, Faculty of Mechanical Engineering, Aleksandra Medvedeva 14, 18000 Niš, SERBIA
[4.]University of Belgrade, Faculty of Mechanical Engineering, Kraljice Marije 16, 11120 Belgrade, SERBIA

Abstract: A two– carrier planetary gear train (PGT) developed for a specific purpose is discussed in this paper. This PGT is suitable for applications which require negative transmission ratios in the range from – 3 up to – 143. The mechanical and dimensional characteristics of the planetary gear train for nominal negative transmission ratios of – 30 and – 40 have been considered. Many combinations of ideal torque ratios of the PGT were obtained for the mentioned transmission ratios, from which only the combinations providing the minimum radial dimensions of the planetary gear units were selected. It was found that the minimum radial dimensions of the PGT will be obtained when the ratio of the reference diameters of the planetary unit ring gears of is close to unity, i.e., when the PGT housing is cylindrical rather than stepped. An introduction to single speed two– carrier planetary gear trains is given, in addition to an overview of the application of the DVOBRZ software package used to synthesize different gearboxes for the required transmission ratio. Acceptable gearboxes were selected from all PGTs according to the criteria of minimum dimensions and acceptable efficiency, and their construction concepts were created.
Keywords: two– carrier planetary gear train; transmission ratio; efficiency

INTRODUCTION

All machines require some form of mechanical power transmission, as it enables the transfer of mechanical energy from the driving machine to the driven machine. Besides that, the transmission provides other useful functions, such as changing the direction, frequency or magnitude of forces or torques acting on the driven machine [1].

Geared transmissions are some of the most used forms of power transmission, and planetary gear trains (PGTs) are a special variant of geared transmission which offers several advantages in relation to conventional gear trains. The most notable advantage is a compact design and improved durability and reliability due to the beneficial effect of power being split over several planet gears, which may be even further enhanced by vibration analysis and customized bearing solutions [2]. This has enabled the design of PGTs having high power ratings combined with a wide range of transmission ratios. However, a large diversity of kinematic schemes and the need for relatively complex calculations in comparison to conventional gearboxes, means that systematic research must be undertaken to realize the full potential of planetary gearboxes.

Current research shows that industrial applications use transmission with ratios in the range from 18 to 90 [3]. A basic type of PGT designated as 1AI is usually used for transmission ratios in the range from 3 to 8 and may be exceptionally used up to 12. This means that compound PGTs, created by combining two PGTs of basic type must be used to achieve the required transmission ratios [4– 8]. Gearboxes using such compound PGTs have found a range of applications in cranes and transportation technology in general. Machine tool gearboxes are also an important area of application and optimization of two– carrier two– speed PGTs with brakes on coupled shafts which was covered in [9]. The possibility of optimization of two– carrier two– speed PGTs with brakes on single shafts for fishing boat main propulsion gearboxes is covered in [10].

Planetary gear trains have been widely used in the aviation industry, due to their small size and weight, quiet, smooth running, high loading capacity and long service life. A method for predicting the reliability of planetary gear train in partial load state was presented in [11].

The application of PGTs in the automobile and automation industries is also important, notably in automatic transmissions containing any number of simple, compound or complex– compound planetary gear sets [12]. New concepts for the calculation of internal power flows such as the split– power ratio and the virtual split– power ratio have been introduced and presented in [13].

PGTs are also used in electric vehicles because of their high power density and ability to be designed and operated as a multi speed transmission. A hybrid dynamic model for helical PGTs that operate in conditions of high and variable input speed was proposed in [14].

There has been relatively little research into two– carrier PGTs, mostly sporadic, however some systematic research into multi– carrier PGTs has been carried out in the last decade or so. The structures or means of connection between the component gear trains have been systematically researched in [15] and methodology has been provided to determine the transmission ratios and efficiency by means of lever analogy.

The kinematic properties of the structures have been extensively researched in [16,17] as well as the efficiencies of single and two– speed PGTs by means of the torque method from [18,19].

Furthermore, within the research carried out in [3] the DVOBRZ software was developed, enabling the synthesis, analysis, and optimal selection of two– carrier PGTs. Some of the results obtained by means of this software package have been used in this paper. The mechanical and dimensional characteristics of the planetary gear train for nominal negative transmission ratios of – 30 and – 40 have been considered. Several combinations of ideal torque ratios of the PGT were obtained, from which the combinations providing the minimum radial dimensions of the planetary gear units were selected. The best gearboxes were selected according to the criteria of minimum dimensions and acceptable efficiency, and their construction concepts were created.

THE RESEARCHED TWO– CARRIER, SINGLE SPEED PLANETARY GEAR TRAIN

The subject of this paper is a single speed two– carrier PGT. The application constraints require a kinematically negative transmission ratio of – 30 and – 40, with the component PGTs being of similar size. This will result in the casing having the simplest possible shape, which will in turn reduce manufacturing costs.

This type of casing can be achieved if the relation of maximum and minimal values of the ring gear diameters is close to one, and it is for this reason that the relation with ring gear diameters is considered.

Both component gear trains are the most commonly used simple PGT, 1AI, which is shown in Figure 1 together with the specific torques on its shafts and its Wolf– Arnaudov symbol [7]. It is of relatively simple construction, its parts being the sun gear 1, the planet gears 2, the ring gear (annulus) 3 and planet carrier S.

The Wolf– Arnaudov symbol simplifies the representation of PGTs as the train shafts are represented by lines of different thickness and a circle. The sun gear shaft 1 is represented by a thin line, the ring gear shaft 3 by a thick line and the carrier shaft S by two parallel lines. The carrier shaft is the summary element because a negative transmission ratio is obtained by locking the planet carrier.

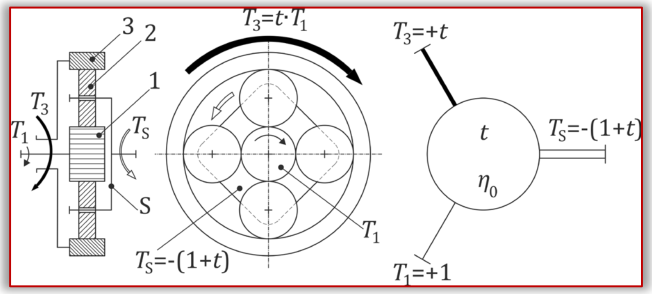

Figure 1. 1AI, the most used simple PGT with the specific torques on its shafts and its Wolf– Arnaudov symbol

It should be noted that the ideal torque ratio t of the PGT is given by Eq. (1), while the shaft torque ratio is given by Eq. (2), where z_1 is the number of teeth of the sun gear, z_3 is the number of teeth of the ring gear, T_1 is the torque acting on the sun gear shaft, T_3 is the torque acting on the ring gear shaft, T_S is the torque acting on the planet carrier shaft, and T_D is the differential torque:

$$t = \frac{T_3}{T_1} = \frac{T_{D\max}}{T_{D\min}} = \frac{|z_3|}{z_1} > +1 \qquad (1)$$

$$T_1 : T_3 : T_S = +1 : +t : -(1+t) \qquad (2)$$

Multi– carrier PGTs are created by connecting the shafts of simple PGTs (1AI) [6]. As two– carrier PGTs are the subject of this paper, we shall consider one– speed, two– carrier PGTs with three external shafts composed of two simple basic PGTs. Two of the three external shafts are single shafts and the third one is a compound shaft, as indicated in Figure 2.

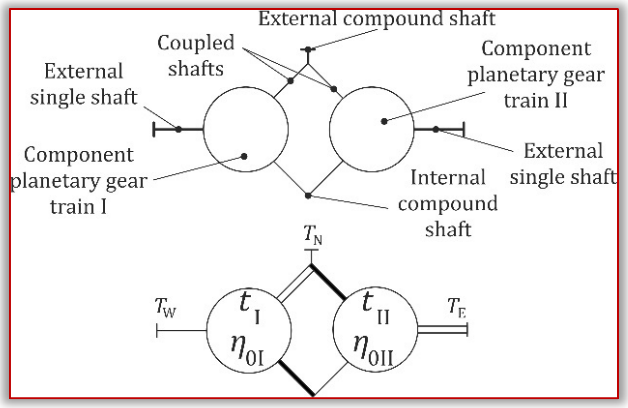

Figure 2. Two– carrier PGT symbol with shafts and respective torques marked

The torque markings of the external shaft torques (T_W, T_N and T_E) follow the cardinal directions (W, N, E), and are ordered from power input to power output. The symbol contains the markings of the ideal torque ratio (t_I and t_{II}) and efficiency (η_{0I} and η_{0II}) for every basic component PGT [10].

An overview of possible structures of two– carrier single speed PGTs has been given in Table 1 [7]. It shows that the simple component PGTs can be combined in 36 possible ways, giving 36 different PGT symbols. As some layouts are isomorphous, this is reduced to 21 practical layouts. Every PGT can provide six different operating modes, as the stationary member may be any of three external shafts, with the remaining two external shafts acting as input and output.

Table 1. Existing PGT layout

	...1 t_{II}	...2 t_{II}	...3 t_{II}	...4 t_{II}	...5 t_{II}	...6 t_{II}
1... t_I	11	12	13	14	15	16
2... t_I	21≡12	22	23	24	25	26
3... t_I	31≡13	32≡23	33	34	35	36
4... t_I	41≡14	42≡24	43≡34	44	45	46
5... t_I	51≡15	52≡25	53≡35	54≡45	55	56
6... t_I	61≡16	62≡26	63≡36	64≡46	65≡56	66

Therefore, it is possible to achieve a total of 126 different transmission variants [7]. The scheme and operating mode are noted with a matrix type designation (e. g. S15 – line 1, column 5), while the power input and output are marked by cardinal directions, the stationary element being placed in parentheses. Therefore, S15WN(E) points to layout 15 with power input being in the west, power output being in the north, and the eastern shaft being locked. However, as we explicitly state that the PGT has three external shafts, it is enough to write just S15WN to fully designate a PGT.

DVOBRZ SOFTWARE PACKAGE

Since the DVOBRZ software was used to identify variable solutions under application constraints, the principle of operation of the software is explained in detail in [20] and will be briefly presented in this paper. The DVOBRZ program was originally developed to identify the variants of two– carrier PGTs and their parameters that fulfil the kinematic requirements, and list them in order of priority according to the selection criterion, e.g., maximal efficiency, minimal weight, or size. The program can provide solutions for two– speed and single– speed gearboxes, depending on whether the actual gearbox will have a fixed transmission ratio or a user operated shifting mechanism.

The program operates by checking the ideal torque ratios of every possible combination of simple component gear trains and discards those that cannot provide the required transmission ratios. The transmission ratio for both gears is calculated for every possible combination of ideal torque ratios and is checked whether it is within the tolerance range for the desired transmission ratios. The ideal torque ratios are represented using the numbers of teeth on sun and ring gears for both component gear trains (Eq. 3 and Eq. 4):

$$t_I = \frac{|z_{3I}|}{z_{1I}} \qquad (3)$$

$$t_{II} = \frac{|z_{3II}|}{z_{1II}} \qquad (4)$$

The tooth numbers of the sun gears z_{1I} and z_{1II} must be set on program initialization. The program will then enlarge one ring gear (usually z_{3I}) by one tooth and check whether the ideal torque ratio is valid, which is achieved if the simple component gear train satisfies the assembly conditions. If it does not, the ideal torque ratio is discarded, and the ring gear enlarged by one more tooth. This procedure is repeated until a valid ideal torque ratio is found or the maximum allowable ideal torque ratio for that component gear train is reached. The same procedure will then be carried out for the second simple component gear train.

The program calculates and stores the values of different parameters for each valid member of the set of ratios (basic geometry of component gear trains, component efficiency, transmission ratios, overall efficiency for each transmission ratio etc.) as a function of the ideal torque ratios of the component gear trains t_I and t_{II}. The resulting database is then used to select the best gearbox variant for the application, whether according to a single criterion (overall efficiency, minimal ratio of ring gear reference diameters, reference diameter of the largest ring gear etc.), or by multi– criteria optimization. In the case of multi– criteria optimization, the weighting coefficients for each optimization criteria must be determined according to the application conditions, depending on how important each criterion is for the application demand.

However, a kinematic scheme must be created for any selected layout variant to check out whether the solution is kinematically valid, and that it meets the relevant design and technological criteria.

APPLICATION OF THE DVOBRZ SOFTWARE PACKAGE

— Example 1

The DVOBRZ software package was used to determine the basic parameters of transmissions fulfilling the application demands. The most important input data is summarized as follows:

- Overall transmission ratio i=– 30,
- Number of teeth of the first sun gear z_{1I} = 21(selected value),
- Number of teeth of the second sun gear z_{1II} = 21 (selected value),
- Number of planets per PGT k = 3 (application demand),
- Gear material 16MnCr4 steel (application demand),
- Average value of planet bearing losses coefficient k_b = 0,065 [3,5],

- Average value of seal frictional losses coefficient k_s = 0,05 [3,5],
- Average value of churning losses coefficient k_c = 0,125 [3,5],
- Gear width to diameter ratio b / d_1 = 0,7 (selected value),
- Efficiency $\eta \geq 0{,}93$ (application demand).

The design parameters required to manufacture the PGT were determined from constraints suggested in the literature, although it is expected that all gears will be made from the same material.

The analysis module finds 16 variants of transmissions which require demands, however due to isomorphy there are only 10 different variants. The schematic review of these variants is shown in Figure 3.

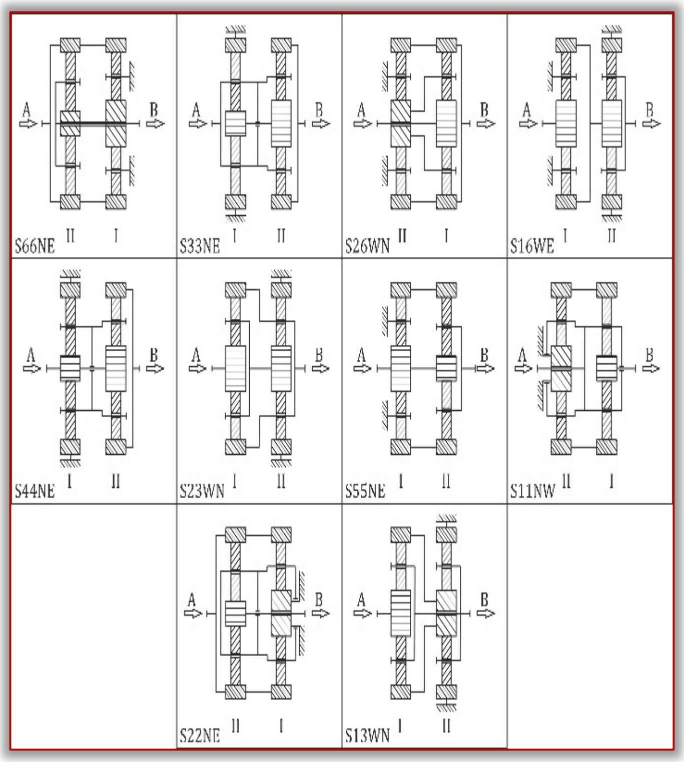

Figure 3. Single speed transmission variants

Analysis of the program results shows that the optimal solution in accordance with the criteria of maximum efficiency provides a borderline increase in efficiency in relation to the solution for minimal dimensions, however the component PGTs will have different outside diameters. Therefore, it can be concluded that the better solution is to optimise for equal outside diameters, as the decrease in overall efficiency will be negligible. The indicator of approximately equal outside diameters is the relation of maximal and minimal values of outside diameters of the two component gear trains which has to be close to unity.

The research results are condensed in Table 2 taking into consideration the following criteria: housing shape, efficiency and maximum transmission diameter.

Table 2. Research results in Example 1

Variant	t_I	t_{II}	d_{max}/d_{min}	d_{max}	η	m_I	m_{II}
S66NE	4	3,83	1,043	216	0,52	3	3
S55NE	3,17	3,67	1,081	231	0,77	3,75	3,5
S26WN	6,5	3	1,020	234	0,97	2	4,25
S16WE	6,83	3,33	1,025	246	0,97	2	4
S44NE	3,67	3,17	1,022	247,5	0,77	3,75	4,25
S23WE	7,33	3,5	1,014	267,7	0,97	2	4,25
S33NE	5,17	5	1,033	279	0,50	3	3
S13WN	7,83	3,83	1,022	282	0,97	2	4
S22NE	4	4,17	1,008	378	0,52	5,25	5
S11NW	5	4,83	1,017	435	0,50	4,75	5

The variant S13WN shown in Figure 4 is chosen as the optimal transmission, even though it has internal power circulation. However, it is insignificant [21], and the internal power flow may be seen in Figure 5. The reason for such a decision is the fact that this variant is easy for manufacturing and it has been already studied in literature [22].

This gear train layout is composed of component gear trains I and II. Input A is connected to sun gear I, while planet carriers I and II are connected to a common shaft leading to output B. Ring gear I is connected to hollow sun gear II, through which the shaft connecting planet carriers I and II is passing. A large rolling bearing supports the rotation of ring gear I, while ring gear II is locked to the gear train casing.

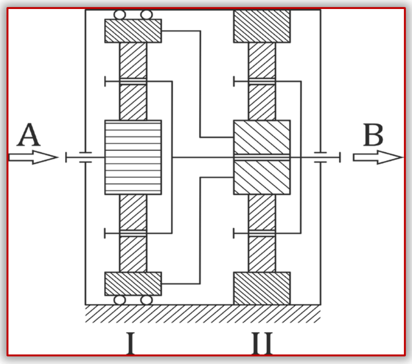

Figure 4. Schematic overview of the two– carrier, single speed planetary gear train S13WN

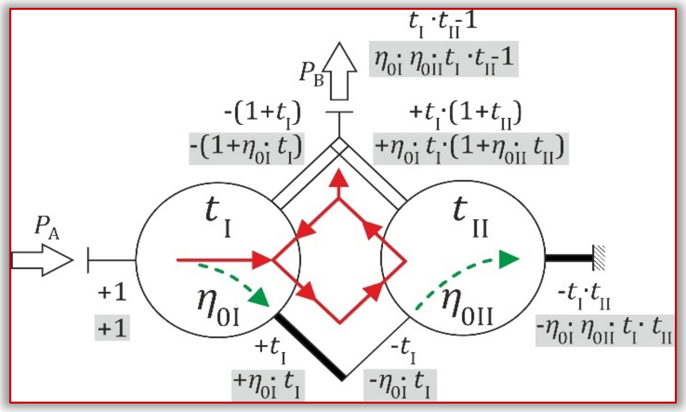

Figure 5. Torque method PGT analysis – ideal and real specific torques on all PGT shafts.

The analysis module finds possible solutions or combinations of ideal torque ratios for layout variants which provide the required transmission ratio. This data enables the creation of graphic representations of dependencies of different parameters.

The first graph is shown in Figure 6. A considerable connection of values at x– and y– axes can be seen to exist. This makes sense since it is about maximum of ring gear diameter and relation of maximum and minimum of ring diameter: an increase at the y– axis implicates an increase at the x– axis, and the points (x, y) form a cloud in the x– y plane.

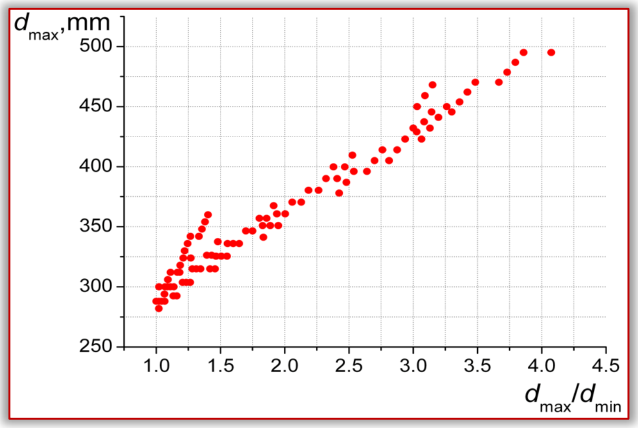

Figure 6. Correlation between maximal diameter of transmission and relation of ring gear reference diameters

The other dependencies from the analysis module are given in Figs. 7, 8 and 9.

Every point in the domain (horizontal x– y plane) presents a pair of ideal torque ratios enabling an overall torque ratio in the desired range. The vertical (z) axis on Figure 7 presents the size ratio of the larger and smaller PGT ring gear diameters. The chart shows that this ratio can variate between 1 and more than 4. Further analysis of the results has shown that PGTs with z – axis values equal or close to one will have minimal radial dimensions.

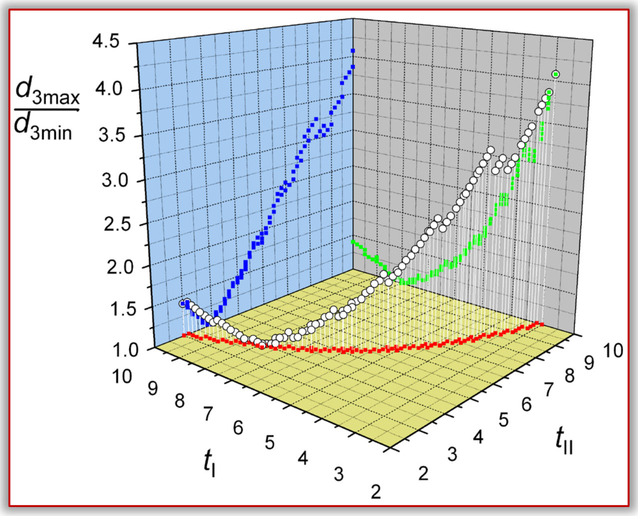

Figure 7. The influence of ideal torque ratios on the size ratio of of the larger and smaller ring gears diameters

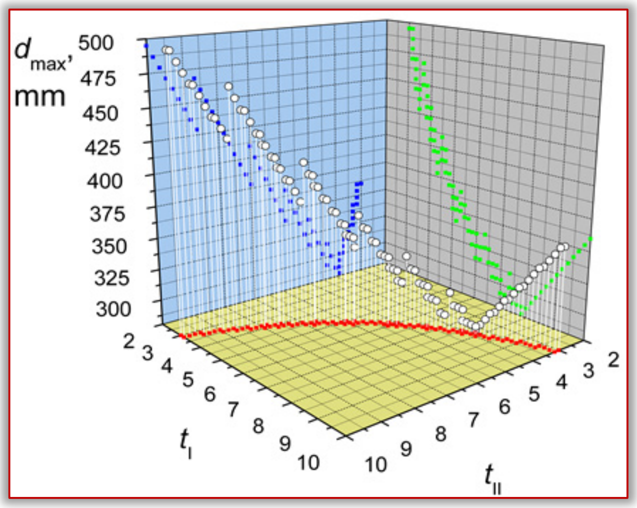

Figure 8. The influence of ideal torque ratios on maximal diameter of transmission in Example 1

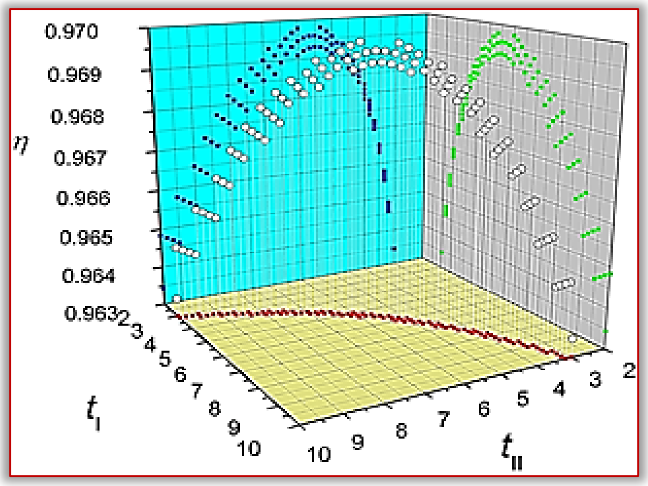

Figure 9. The influence of ideal torque ratios on overall efficiency

Every point in the x– y plane of Figure 8 also presents a pair of ideal torque ratios, while the z – axis presents the maximal diameter of the transmission.

The z – axis in Figure 9 is used to represent the overall efficiency of the PGT in relation to the combination of ideal torque ratios. The chart shows that for torque ratios in the 2 to 10 range, efficiencies ranging from 0,944 to 0,969 can be achieved.

— Example 2

In this example of application of the DVOBRZ software, only the overall transmission ratio is different, i = – 40. The other input data is the same as in Example 1. The analysis module has also found 16 variants of transmissions which are in accordance with application demands. Due to isomorphy, there are only 10 different variants which is identical to Example 1.

The research results were processed in the same way as in Example 1 and are condensed in Table 3, taking into consideration all the criteria: housing shape, efficiency and maximum transmission diameter.

Table 3. Research results in Example 2

Variant	t_I	t_{II}	d_{max}/d_{min}	d_{max}	η	m_I	m_{II}
S26WN	7,67	3,67	1,016	280,5	0,97	2	4,25
S16WE	7,83	4	1,021	288	0,97	2	4
S66NE	5,83	5,67	1,03	288,7	0,49	2,75	2,75
S55NE	3,83	4,33	1,06	292,5	0,97	4	3,75
S44NE	4,33	3,83	1,064	312	0,76	4	4,25
S23WE	8,83	4	1,039	318	0,97	2	4,25
S13WN	8,67	4,67	1,077	336	0,50	2	4
S33NE	6,83	6,67	1,025	338,2	0,97	2,75	2,75
S22NE	5,67	5,83	1,029	551,2	0,52	5,25	5,25
S33NE	6,67	6,83	1,025	615	0,47	5	5

The variant S13WN was chosen in Example 2, for the same reasons as in Example 1.

There are 71 combinations of ideal torque ratios combination which satisfy the demands for *i* =– 40, and they enable different dependencies between design parameters to be shown in Figs. 10, 11, 12, and 13.

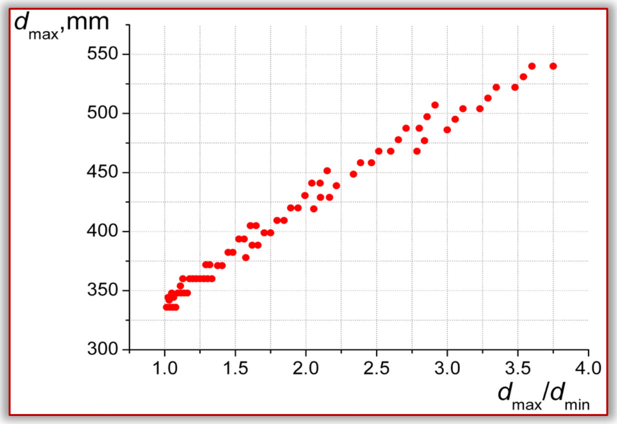

Figure 10. Correlation between maximal diameter of transmission and relation of ring gear reference diameters

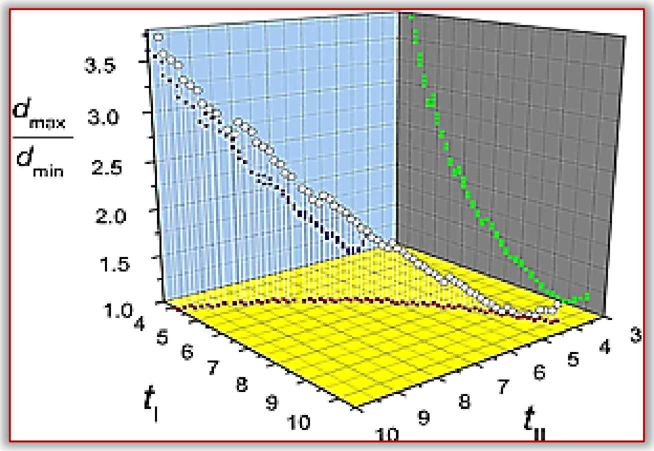

Figure 11. The influence of ideal torque ratios on the size ratio of of the larger and smaller ring gears diameters

First, the relation of the maximum transmission diameter and maximum to minimum ring gear diameter ratio is given in Figure 10. The graph resembles Figure 6, as the increase on y– axis implicates an increase on x– axis, and the points (x, y) form a cloud in the x– y plane. The difference is in the values at the x– axis and y– axis. The maximum value on the y– axis is higher than the value in Figure 6, and the value at the x– axis is smaller than the value in Figure 6.

Figure 11 presents the size ratio of the larger and smaller PGT ring gear at the z– axis, while the horizontal x– y plane presents a pair of ideal torque ratios of the component gear trains. The chart shows that this ratio can variate between 1 and 4, and that the ideal torque ratios are in the range from 3 to 10.

Further analysis of the results has shown that PGTs with z – axis values equal or close to one will have minimal radial dimensions.

In Figure 12, every point in the x– y plane presents a pair of ideal torque ratios (range from 3 to 10), while the z– axis presents the maximal diameter of transmission. The graph has a shape similar to the graph in Figure 8, with slightly larger values at the z– axis.

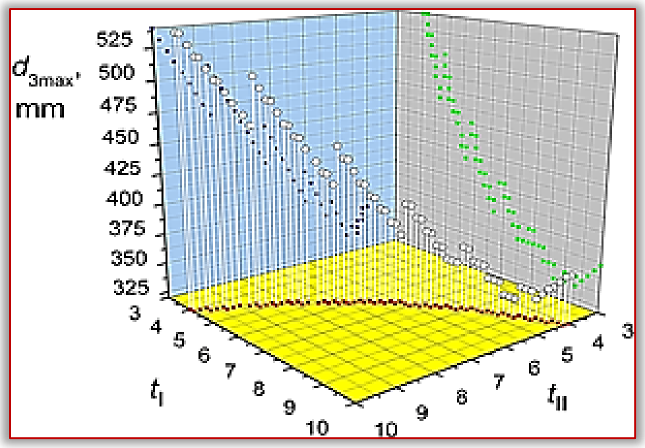

Figure 12. The influence of ideal torque ratios on maximal diameter of transmission in the example 2

Also, the ideal torque ratios are in relation with the overall efficiency of the PGT which is presented in Figure 13. The z – axis in Figure 13 is used to represent efficiency, while the x– axis and y– axis are used to represent the horizontal plane. The chart shows that for torque ratios in the 3 to 10 range, efficiencies ranging up to 0,972 can be achieved, which is a slightly larger value in comparision with the value in Example 1.

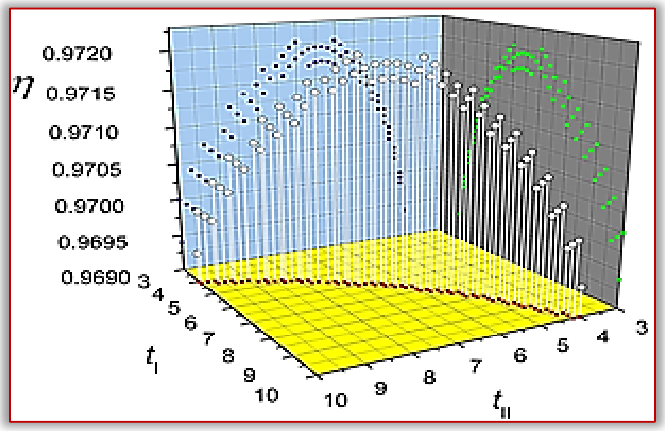

Figure 13. The influence of ideal torque ratios on overall efficiency

It is possible to determine the relation of the transmission efficiency to the overall transmission ratio, as visible in Figure 14. It has been determined that the efficiency increases with the transmission ratio for this PGT type. Furthermore, it can be concluded from the diagram in Figure 14 that PGTs with transmission ratios in the interval from – 30 to – 40 interval have very small variations in efficiency. The efficiency variations at transmission ratio of – 40 are less pronounced than at transmission ratio of – 30. This indicates that there is a very small window for PGT maximum efficiency optimization.

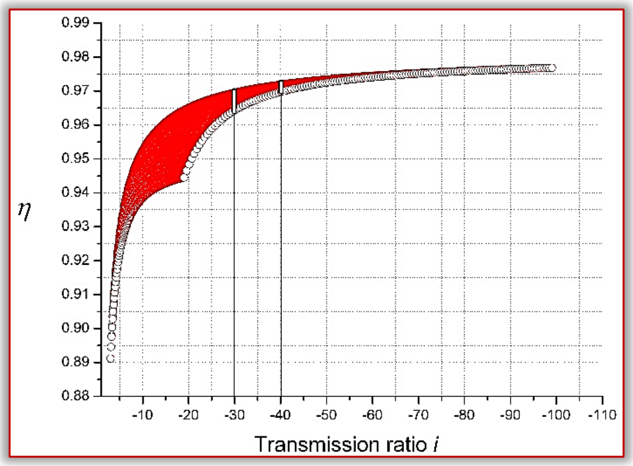

Figure 14. Influence of the overall transmission ratio on efficiency

Also, there is a slight increase in maximal diameter of the transmission at transmission ratio of – 40 in comparison to the maximal diameter of transmission at transmission ratio of – 30. The curves change in the same way in the both examples.

Based on the analysis provided in the paper it can be concluded that more two variants provide necessary conditions, but detailed analyse is required. It is about variants S26WN and S16WE, shown in Figure 15.

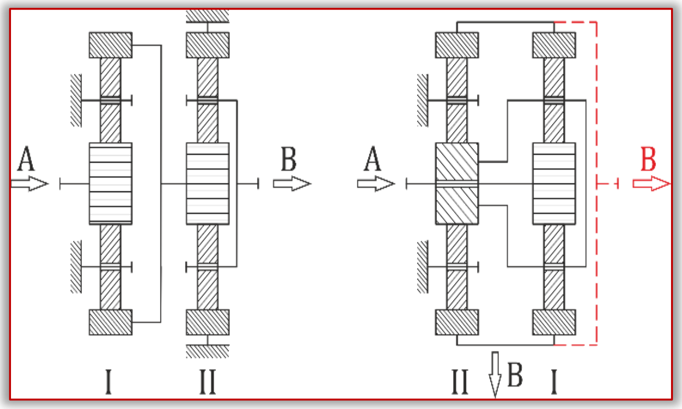

Figure 15. Schematic overview of the two– carrier, single speed planetary gear trains S16WE and S26WN (the original output located as in Figure 3 has been added in dashed red lines for clarity)

Variant S16WE having the input and output shafts on opposite sides, while variant S26WN in an alternative configuration using the connecting outer ring gear shaft as the output. Variant S16WE is commonly used for marine propulsion and industrial applications, as the calculations for both component PGTs of S16WE are relatively simple and can be performed independently of each other. On the other hand, variant S26WN, in particular the alternate configuration described above, has recently found use as a replacement for elevator worm gear drives due to its high efficiency [23].

By comparing the parameters of variant S13WN and the other possible solutions, S26WN and S16WE it can be seen that solutions S26WN and S16WE have better values of maximal transmission diameters, while the efficiency remains in the same range of values. The relations of ring gear reference diameters are equal for the transmission ratio of – 30, while solutions S26WN and S16WE have values closer to one for the transmission ratio of – 40, providing a better solution than S13WN. However, S13WN remains the better solution if the selection criteria are limited to technological demands.

CONCLUSIONS

This paper deals with the analysis of a two– carrier PGT developed for a specific application, having a transmission ratio of – 30 and – 40. The application conditions request demand the type S13WN PGT to be used. The DVOBRZ software package was used to determine the variants and basic parameters of two– carrier drives within the application constraints, while taking into consideration the design parameters such as gear geometry of the component gear trains, overall transmission ratio, average value of internal losses, gear material and overall efficiency.

The values of different parameters for all valid PGTs were calculated and stored as a function of the ideal torque ratios of the component gear trains, and the resulting database was used to select the best gearbox variant for the application according to two criteria. The first criterion was minimization of the PGT dimensions, while the second was maximization of PGTefficiency.

Analysis has shown that the efficiency of a PGT optimised for minimum size will be borderline smaller than of a PGT optimised for maximum efficiency, but the PGT optimised for minimum size will be considerably easier to manufacture, due to both ring gears being of the same size.

Further analysis and comparison to all the other kinematically equivalent PGTs has shown that S13WN does not present the best solution according to either criterion. It has been determined that both S16WE and S26WN provide valid solutions according to both the criteria of minimum size and maximum efficiency. It must be also considered that those variants have no internal power circulation, resulting in a considerably lighter build in relation to S13WN. However, variant S13WN still retains precedence due to technological demands and the fact that this variant is thoroughly examined in literature.

Acknowledgment

This research was financially supported by the Ministry of Education, Science and Technological Development of the Republic of Serbia (Contract No. 451– 03–9/2021– 14/200109)

References

[1] Jovanović, V., Janošević, D., Pavlović, J.: Analysis of the influence of the digging position on the loading of the axial bearing of slewing platform drive mechanisms in hydraulic excavators. Facta Universitatis– Series Mechanical Engineering, Vol. 19, No. 4, pp. 705– 718, 2021, 2021

[2] Liu, J., et al.: Influence of support stiffness on vibrations of a planet gear system considering ring with flexible support. Journal of Central South University, Vol. 27, No. 8, pp. 2280—2290, 2020

[3] Karaivanov, D.: Theoretical and experimental studies of the influence of the structure of coupled two– carrier planetary gear trains on its parameters, Ph.D. Thesis, University of Chemical Technology and Metallurgy, Sofia, 2000.

[4] Kudrjyavtsev, V.N., Kirdyiashev, I.N.: Planetary gear trains handbook, Mashinostroenie, Leningrad, 1977.

[5] Looman, J.: Zahnradgetriebe– Grundlagen, Konstruktion, Anwendung in Fahrzeugen, 3. Aufgabe, Springer– Verlag, Berlin, 1996

[6] Mueller, H.W.: Die Umlaufgetriebe– Auslegung und vielseitige Anwendungen, 2. Aufgabe, Springer– Verlag, Berlin, 1998

[7] Arnaudov, K., Karaivanov, D.P.: Planetary gear trains, CRC Press, Taylor & Francis Group, Boca Raton, FL, 2019

[8] Troha, S., et al.: Coupled two– carrier planetary gearboxes for two– speed drives, Machines, Technologies, Materials, Vol. 15, No. 6, pp. 212– 218, 2021

[9] Troha, S., et al.: The selection of optimal reversible two– speed planetary gear trains for machine tool gearboxes, Facta Universitatis– Series Mechanical Engineering, Vol. 18, No. 1, pp. 121– 134, 2020

[10] Stefanović– Marinović, J., Troha, S., Milovančević, M.: An application of multicriteria optimization to the two– carrier two– speed planetary gear trains, Facta Universitatis – Series Mechanical Engineering, Vol. 15, No. 1, pp. 85– 95, 2017

[11] Ming, L., Liyang, X., Lijun, D.: Load sharing analysis and reliability prediction for planetary gear train of helicopter, Mechanism and Machine Theory, Vol. 115, pp. 97– 113, 2017

[12] Kahraman, A, et al.: A Kinematics and Power Flow Analysis Methodology for Automatic Transmission Planetary Gear Trains, Journal of Mechanical Design, Vol. 126, pp. 1071– 1081, 2004

[13] Chen, C.: Power flow and efficiency analysis of epicyclic gear transmission with split power, Mechanism and Machine Theory, Vol. 59, pp. 96– 106, 2013

[14] Changhao, L., et al.: Hybrid dynamic modeling and analysis of the electric vehicle planetary gear system, Mechanism and Machine Theory, Vol. 150, Article no. 103860, 2020

[15] Arnaudov, K., Karaivanov D., Engineering analysis of the coupled two– carrier planetary gearing through the lever analogy, Proceedings of the International Conference on Mechanical Transmissions, Chongqing, China, 44– 49, 2001.

[16] Troha, S.: Analysis of a planetary change gear train's variants, Ph.D. Thesis, Faculty of Engineering, University of Rijeka, Rijeka, 2011.

[17] Karaivanov, D.P., Troha, S.: Optimal Selection of the Structural Scheme of Compound Two– Carrier Planetary Gear Trains and their Parameters, pp.339403, In: Radzevich, S.P., (Ed.), Recent Advances in Gearing: Scientific Theory and Applications, First Edition, Springer, Cham, 2022

[18] Arnaudov, K., Karaivanov, D.: Systematik, Eigenshaften und Moeglichkeiten von zusammengesetzen Mehrsteg– Planetengetriebe. Antriebstechnik, Vol. 5, pp. 58– 65, 2005

[19] Karaivanov, D. P., et al.: Analysis of Complex Planetary Change– Gears Through the Torque Method, Proceedings of XIII International Congress "Machines, Technologies, Materials" 2016, Borovets, Bulgaria, Vol. 25, No. 3, pp. 51– 55, 2016.

[20] Vrcan, Ž. et al.: Research into the Properties of Selected Single Speed Two– Carrier Planetary Gear Trains. Journal of. Applied and. Computational. Mechanics, Vol. 8, No. 2, pp. 699–709, 2022

[21] Pavlović, A., Fragassa, A., Geometry optimization by FEM simulation of the automatic changing gear, Reports in Mechanical Engineering, Vol. 1, No. 1, pp. 199– 205, 2020

[22] Handschuh, R F., Epicyclic Gear Trains, In: Wang, Q.J., Chung, Y.W. (Eds.), Encyclopedia of Tribology, Springer, Boston, MA, 2013.

[23] Janovsky, L.: Elevator Mechanical Design, Third Edition, Elevator World, Mobile, AL, 2011.

Note: This paper was presented at IRMES 2022 – 10th International Conference on Research and Development of Mechanical Elements and Systems: "Machine design in the context of Industry 4.0 – Intelligent products", organized under the auspices of the Association for Design, Elements and Constructions (ADEKO) and University of Belgrade, Faculty of Mechanical Engineering, Department of General Machine Design, in 26 May 2022, Belgrade (SERBIA).

ISSN: 2067– 3809

ACTA TECHNICA CORVINIENSIS – BULLETIN OF ENGINEERING
TOME XVI [2023] | FASCICULE 2 [APRIL – JUNE]

1.Biljana MARKOVIĆ, 2.Aleksija ĐURIĆ, 3.Marija PERENDIJA

RESEARCH OF ADHESIVE AL– SHEET JOINTS IN THE DEVELOPMENT OF LIGHTWEIGHT STRUCTURES

1-3. University of East Sarajevo, Faculty of Mechanical Engineering, Vuka Karadžića bb, 71123 East Sarajevo, BOSNIA & HERZEGOVINA

Abstract: Adhesion is a major element of the bonding technologies used today. This way of joining meets the requirements of mechanical load, with high reliability of the product, and in connection with the production and climatic conditions. Bonding is the process of making inseparable bonds in mechanical engineering with non–metallic material, through adhesion and cohesion forces, without significant impact on the structure of the parts to be joined. Gluing (adhesive joint), as a way of making joints in mechanical engineering, is gaining importance in the development of spacecraft and aircraft, as well as the automotive industry. This requires high load–bearing capacity and stiffness, with minimal weight, so alloys such as aluminum and titanium are used. Adhesive joining is increasingly displacing the dominant rivets when joining light metals, and is used to join thin sheets made of different types of materials. In this paper, the possibilities of adhesive joining and the characteristics of glued joints made of aluminum alloy AW– 5754 were researched, using static tests, and their fractography was analyzed.
Keywords: adhesive joints, light constructions, static testing, Al alloys

INTRODUCTION

In order to increase energy efficiency, the concept of sustainable lightweight (LW) design has been used for the last few years. This concept of lightweight design, which is currently used, refers to the reduction of the weight of the structure by using lighter materials, which include aluminum. The choice of materials for light constructions also means the choice of joining technology, which is of essential importance [1].

In order to think in the right direction when designing and constructing light structures, the prerequisites are the properties of the material such as: stiffness, strength, ability to absorb energy. Usage the maximum potentials of high– performance materials allows choosing the right way to connect them [2].

Adhesion is a major element of the bonding technologies used today [3–5]. This way of joining meets the requirements of mechanical load, with high reliability of the product, and in connection with the production and climatic conditions.

Adhesives used to achieve adhesion must be resistant to crash at high loads, allow uniform application of adequate force, stress distribution, weight reduction and allow better rigidity of components, durability, as well as properties shown in the crash test. In addition, these types of adhesives have advantages that are reflected in low thermal impact on materials, the ability to damping vibrations and to improve sealing [1].

Bonding is the process of making inseparable bonds in mechanical engineering with non–metallic material, through adhesion and cohesion forces, without significant impact on the structure of the parts to be joined (Figure 1). Adhesion is a state in which two different surfaces made of different (or the same) materials are held together by the interaction of attractive forces due to the interaction of molecules, atoms or ions.

Cohesion or internal strength is the action between two surfaces of a material, ie attractive forces of identical atoms or molecules. Cohesion strength depends on the material and temperature. Metals have the highest cohesive strength, and liquids and gases have the lowest. The molecular weight of the polymer is an important factor in determining the cohesion strength of the adhesive.

Double action of optimal adhesion and cohesion is required to connect the forces and to achieve the optimal strength of the bonded joint. When optimal adhesion forces are achieved in the preparation of the bonding material, then the cohesive strength of the bonded joint is the decisive criterion for its strength [6].

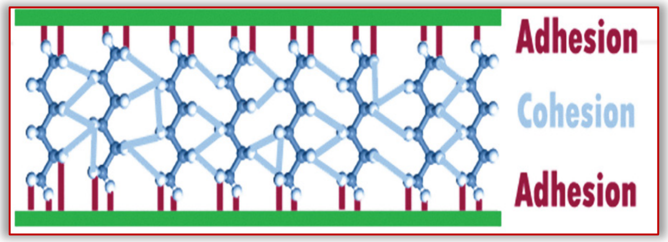

Figure 1. Adhesion and cohesion bonds in adhesive joint [7]

The mechanisms of adhesion have been intensively researched in recent years; so many theories have been put forward that explain the principles of adhesion. However, none of them fully explain adhesion. It can be concluded that the adhesion of the adhesive to the surface of the part to be bonded is the result of mechanical, physical and chemical forces that overlap and affect each other.

After Fe (iron), aluminum is the second metal used in modern mechanical engineering. It is used as a pure metal in electrical engineering, metal processing, food and chemical industries, but its application is much more important in the form of various multicomponent alloys that are widely used in the mechanical industry [8– 10]. Joining of aluminum sheets can be achieved by applying the following technologies [3– 5, 11, 12]:

- Welding;
- Connection with mechanical elements (screws, rivets);
- Gluing (adhesive bonding);
- Hybrid merger.

Adhesion, due to its low specific weight, as well as due to the thin layer of adhesive in the joints, has an advantage over welded and mechanical joints [13]. Aluminum and its alloys are characterized by extraordinary mechanical properties, which have opened many technological sectors. Although they are much lighter than other metals, they have a very high mechanical strength, which is why they are widely used in the aerospace industry (50%, 68%, depending on the manufacturer and model of the aircraft). It is considered that aluminum constructions can be competitive in applications where low specific weight, corrosion resistance, functionality of construction forms and profiles are important.

In this paper, the analysis of the mechanical properties of the adhesive joint of aluminum alloy AW 5754 with a thickness of 1 mm will be presented. Commercial adhesive, Loctite EA 3430, Henkel, (two– component epoxy adhesive) was used for adhesion.

DESIGN OF ADHESIVE JOINTS

The rules for forming adhesive joints are similar to those for solder joints. However, adhesive technology is more complicated and error– prone. The choice of adhesive largely depends on the type of material to be joined, the required joint strength, external influences (humidity, temperature, corrosion) [14].

The possibility of fast and reliable adhesion of all types of materials is the reason why today adhesives are considered a standard part of many production processes. Almost all types of materials such as steel, aluminum, synthetic and composite materials, glass and ceramics can be combined with the help of adhesives. In this way, manufacturers can choose materials without restrictions related to joining different materials [15].

The decisive role, however, is played by the position of the sheets to be joined, with the appropriate parameters of the manufacturer, which relate to the choice of adhesive. E.g [13]:

- Butt joints are undesirable, pipe butt joints are particularly unfavorable, folding joints with beveled edges are more favorable;
- Angle joints cause stress concentration, so they need to be strengthened at the ends;
- In order to avoid stress concentration, the shear load is the most favorable;

The strength of the adhesive joint depends not only on the correct choice of adhesive, but also on a number of other factors. Thus, numerous tests have shown that in addition to the type of adhesive (including correctly implemented adhesive technology), environmental conditions, temperature, duration of load, type of load, surface treatment, etc. are also influential.

Adhesive joints are subject to changes in mechanical properties, depending on the time elapsed in operation regardless of the load (the so– called aging effect of the adhesive). This effect occurs even without load, after long– term storage of the joined elements. The aging of metal adhesives depends primarily on the type of adhesive, the condition of the surfaces before bonding, but mostly on the environment in which the bond is glued (dry air or sea water). Resistance against aging is generally higher with hot–setting adhesives than with cold–setting adhesives [16, 17]. The thickness of the adhesive layer in the bonded joint also affects the strength of the joint. It is always more advantageous that the thickness of the adhesive layer is smaller. An adhesive layer thickness of 0.05 to 0.15 mm is considered optimal for most adhesives [18]. This is all true for folding and butt joints of sheets and similar shapes, where it is relatively difficult to control the thickness of the adhesive layer. Otherwise, the exact thickness of the adhesive layer can be achieved only by connecting pipes and similar elements with a closed contour.

Surface treatment significantly affects the strength of the adhesive joints of aluminum alloys. Yasmin Boutar et al [19] founded that the decrease in surface roughness was found to increase the shear strength of single lap joints. Experimental results show that rougher surfaces have less wettability which is in coherent with shear strength tests. The author's C. Borsellino et al [20] also conclude that roughness significantly affects the the strength of the adhesive joints of aluminum alloys.

The strength of the adhesive joints is highly temperature dependent [21], with cold binder adhesives being more sensitive to temperature rise than hot binders. Hot– melt adhesives are used for temperatures up to about 250 C (there are also special high– temperature adhesives up to 350 C), so that the maximum allowable permanent temperature of the loaded adhesive joint (excluding other influences) is determined by these values.

TESTING OF ADHESIVE JOINTS

The failure mode of the adhesive joint depends on a number of factors: adhesive properties (cohesion and adhesion strength), bonding material properties (free surface energy, surface roughness, surface cleanliness, mechanical properties), adhesion process and flow, pressure, temperature, time, humidity etc.), the design of the adhesive joint (adhesive layer thickness, substrate thickness, joint types and dimensions) and load conditions (load type– static or dynamic: mode, time, temperatures, loads, etc.).

Adhesive joints should be shaped so that they are primarily shear stress (folding joint) and to a lesser extent tension / pressure (butt joint), therefore, in these joints the working force should act in the plane where the joint is made. Bending and twisting stresses should be avoided [14].

Testing of adhesive joints involves static and dynamic testing. Adhesive joints are tested in the following three ways [22]:

- a tensile– shear test known as the TS test (Figure 2a);
- L tensile test (Figure 2b);
- H tensile test (Figure 2c).

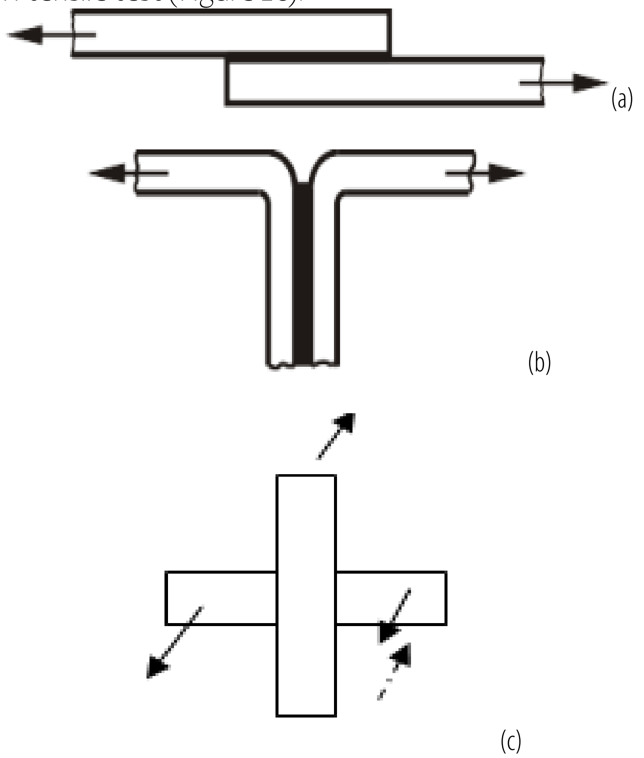

Figure 2. Methods for testing the adhesive joint: a) TS test; b) L test; c) CT test

The values of the degree of safety of the adhesive joint is in the range S = 2– 5. The most important influencing factors on the load– bearing capacity of adhesive joints are the type of material to be joined, the thickness of the adhesive in the joint, the roughness of the adhesive joints surfaces, the environment during operation and similar.

Different types of fractures can occur during tensile testing. Four types of fractures are characteristic for an adhesive joint [23]:

- Adhesive fracture (Figure 3 a);
- Adhesive– cohesive fracture (Fig 3 b);
- Cohesive fracture (Fig 3 c);
- Subtractive fracture (Fig 3 d).

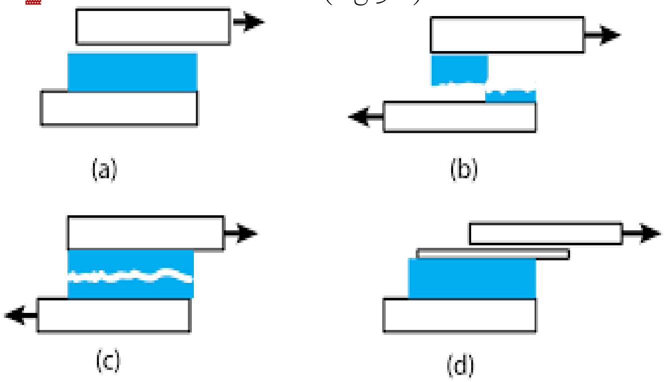

Figure 3. Types of fracture in adhesive joints [23]

EXPERIMENTAL RESEARCH

The test was adjusted to the equipment of the Faculty of Mechanical Engineering of the University of East Sarajevo (SHIMADZU AGS– X test machine). Tension– shear test was performed, i.e. TS test. The speed of the traverse during the test was 2 [mm/min]. The aim of the test is to determine the maximum force that the adhesive joint can withstand. The test was done for three samples.

Preparation of test specimens was performed in accordance with available research, experientially sheet thickness 1mm (Figure 4). Cutting and bending of the samples was done by hand with the use of auxiliary tools. The first sanding was performed with P120 sandpaper, and the final sanding with P240 granulation paper. At the end of grinding, the samples were cleaned with alcohol, Ethanol 96%. This is a common process of preparing samples for adhesion and the goal of sanding and cleaning is to remove impurities from the metal surface that can affect the quality of the joint.

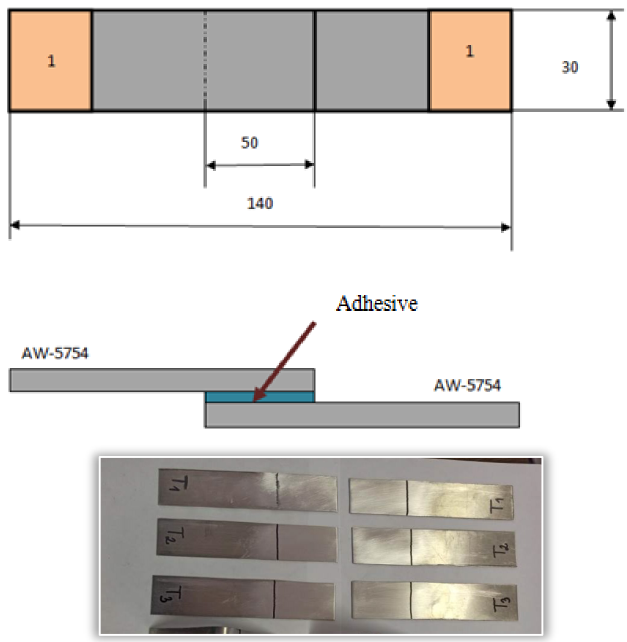

Figure 4. Prepared samples for adhesion

The samples were adhesived with Loctite EA 3430 (Henkel). It is a two– component epoxy adhesive that has great application in industry. Adhesion time 10 minutes, taking into account the viscosity of the adhesive.

After the adhesion process, the samples were clamped with plastic clamps to prevent movement during the drying process. The drying process lasted 24 hours at room temperature (approximately 20 °).

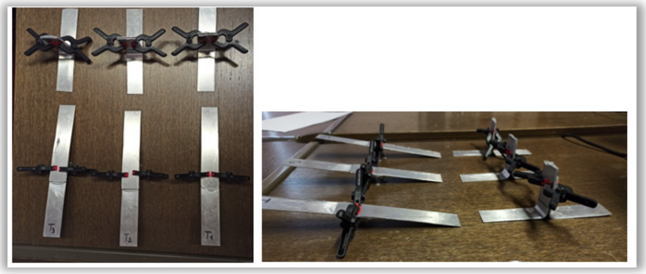

Figure 5. Samples during drying

The results of the tensile test (TS test) are shown in Figures 6, 7, 8.

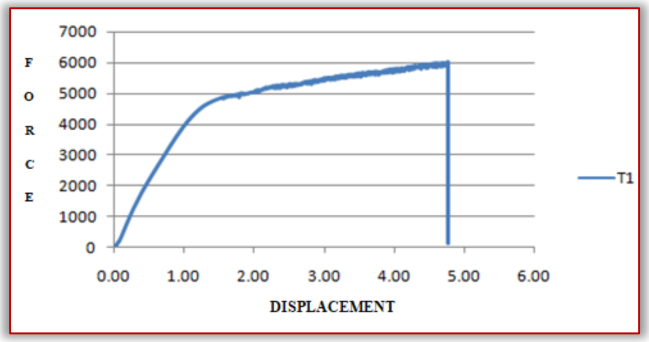

Figure 6. Force–displacement diagram for sample T1

The figures show that the adhesive joint withstood a force in the range of 6000– 6500 [N]. Taking into account the thickness of aluminum alloy sheets AW– 5754, which is 1 [mm], and width 30 [mm], and tensile strength Rm = 245 [N / mm2] it is concluded that sheet metal of these dimensions and this material can withstand a force of approximately 7350 [N]. Comparing this value with the value obtained in the tensile test, it can be concluded that the given joint gives satisfactory mechanical characteristics because the load– bearing capacity of the base material (sample) is only 11% higher than the load– bearing capacity of the adhesive joint.

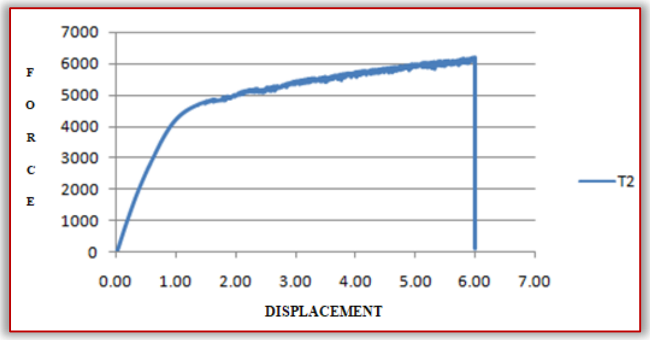

Figure 7. Force–displacement diagram for sample T2

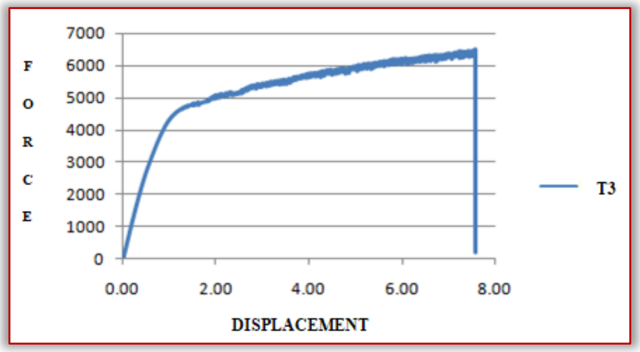

Figure 8. Force–displacement diagram for sample T3

In all three diagrams, it can be noticed that when the moment the force reaches approximately 4000 [N], a zigzag line appears, which manifests itself from the occasional tearing (cracking) of the adhesive.

Figure 9 shows the T (T1, T2, T3) samples after fracture, while Figures 10, 11, 12 show the fractography of the compound.

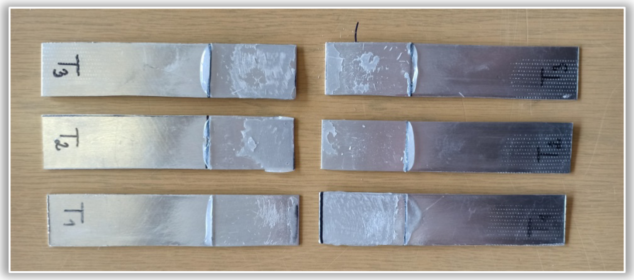

Figure 9. Display of T samples after fracture

Fractography of the compound was performed on a Leica EZ4 microscope, and from the analysis of the result it can be concluded that in these cases there is an adhesive–cohesive fracture.

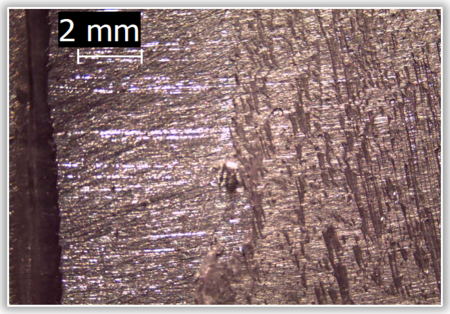

Figure 10. Fractography of the T1 sample compound

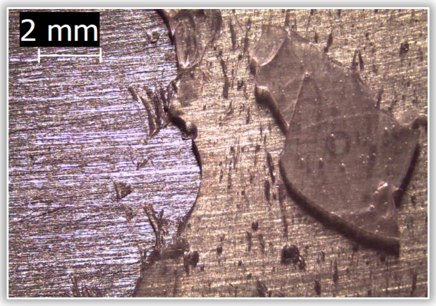

Figure 11. Fractography of the T2 sample compound

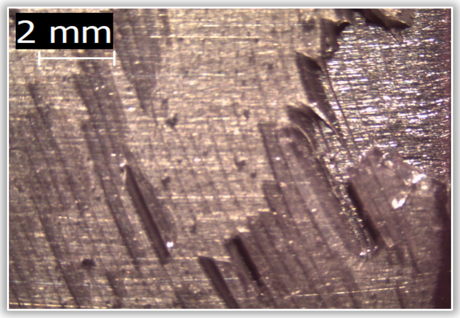

Figure 12. Fractography of the T3 sample compound

CONCLUSIONS

Considering the trend of design development for lightweight structures and the requirements for high productivity in industrial production, the increased use of structural adhesives is expected. Mentioned adhesives will be more and more represented, because the design focused on lightweight constructions means saving resources, and this is impossible to achieve, among other things, without the use of adhesives. There is a clear trend of increasing use of composite materials and aluminum alloys, primarily in the automotive and aerospace industries because weight reduction is very important in these industries. In the future, the success of metalworking companies will largely depend on their ability to exploit the innovative potential of using composite materials. In this sense, structural adhesion is an important factor and key technology (industrial production) in choosing the way of joining in the machine industry, both homogeneous and heterogeneous materials, 21st century. Adhesion is most often used for joining dissimilar materials, but in this paper, bonding of homogeneous materials is presented.

Cohesion and adhesion forces are responsible for the strength of the adhesive joint. Although many mechanisms are known to work in the adhesive material and between the adhesive and the surface of the parts to be joined by adhesion, it is still not possible to determine exactly which mechanism is most responsible for creating the adhesive joint, i.e. which mechanism achieves the highest joint strength.

The procedure for adhesion of aluminum alloy sheets AW– 5754 is presented and analyzed. Loctite EA 3430 epoxy two– component adhesive from Henkel was used for adhesion. Testing of previously prepared samples was performed using test, namely, the tensile– shear test TS. The test results show that specimens prepared and tested for tensile– shear or TS test can withstand a force in the range of 6000– 6500 [N]. Analyzing the fractography of the joint samples tested by TS test, it can be concluded that adhesive– cohesive fracture has occurred.

The results of the performed experiment are satisfactory from the aspect of durability of the adhesive joint.

Acknowledgment

The results presented in this paper were obtained through project "Research and analysis of advanced joining technology of dissimilar materials that are used in the development of lightweight structures" BI– BA/21– 23– 026 in the framework of the bilateral scientific cooperation between the Republic of Slovenia and Bosnia and Herzegovina.

References

[1] Ickert L., Adhesive technology – Key to future of lightweight design?. Adhes Adhes Sealants 9, pp. 49–53, 2012.
[2] Meschut, G., Janzen, V., Olfermann, T. Innovative and Highly Productive Joining Technologies for Multi– Material Lightweight Car Body Structures. J. of Materi Eng and Perform 23, pp. 1515–1523, 2014.
[3] Junya, N., Reiichi, S. Multi– material Automotive Bodies and Dissimilar Joining Technology to Realize Multi– material, Kobelco technology review, No. 38, pp. 32– 37, 2020.
[4] Ji, H. K., Lyang, S. W., Kaushalya. P., Payam. H., Jami. J. S., Pete, E. Knowledge based design advisory system for multi– material joining, Journal of Manufacturing Systems, Vo. 52, Part B, ISSN 0278– 6125, pp. 253– 263, 2019.
[5] Delzendehrooy, F., Akhavan– Safar, A., Barbosa, A.Q., Beygi, R., Cardoso, D., Carbas, R.J.C., Marques, E.A.S., Da Silva, L.F.M. A comprehensive review on structural joining techniques in the marine industry, Composite Structures, V. 289, ISSN 0263– 8223, 2022.
[6] Bujanis B., Magdalenis Bujanis J., Mehanizmi stvaranja ljepljenog spoja, Tehnički glasnik, Vo. 5, No. 2, ISSN 1864– 6168, pp. 89– 93, 2011.
[7] Zotti, A., Zuppolini, S., Zarrelli, M. , Anna Borriello, A. . Fracture Toughening Mechanisms in Epoxy Adhesives. In: Rudawska, A., editor. Adhesives– Applications and Properties, London: IntechOpen. 2016.
[8] Hirsch, J. Aluminium in Innovative Light– Weight Car Design, Materials Transactions, Vol. 52, No. 5 pp. 818– 824, 2011.
[9] Udoye, N. E., Inegbenebor, A. O., Fayomi, O. S. I., The Study on Improvement of Aluminium Alloy for Engineering Application: A Review, International Journal of Mechanical Engineering and Technology, Vol. 10, No. 3, pp. 380– 385, 2019.
[10] Rambabu, P., Eswara Prasad, N., Kutumbarao, V.V., Wanhill, R.J.H. Aluminium Alloys for Aerospace Applications. In: Prasad, N., Wanhill, R. (eds) Aerospace Materials and Material Technologies. Indian Institute of Metals Series. Springer, Singapore. 2019.
[11] Richard, R., Paul, K,, Belinga, M,. Jukka, M. Trends in aluminium alloy development and their joining methods, Reviews on Advanced Materials Science, Vol. 44, No. 4, pp. 383– 397, 2016.
[12] Barnes, T.A., Pashby, I. R. Joining techniques for aluminium spaceframes used in automobiles: Part II — adhesive bonding and mechanical fasteners, Journal of Materials Processing Technology, Vo. 99, No. 1–3, pp. 72– 79, 2000.
[13] EAA Aluminium Automotive Manual – Joining, 9. Adhesive bonding, European Aluminium Association, 2015.
[14] Miltenović, V., Marković, B., Tica, M. Konstrukcuini elementi u mašinogradnji 1, Mašinski fakultet Univerziteta u Istočnom Sarajevu, 2018.
[15] Sarah, K., Cindy, J., Steve, L., Guest, E. Enabling sustainable transportation through joining of dissimilar lightweight materials, MRS Bulletin, Vol. 44, No. 8, pp. 608– 612, 2019.
[16] Gerald, D., Richard, A. P. Environmental effects on the ageing of epoxy adhesive joints, International Journal of Adhesion and Adhesives, Vo. 29, No. 1, pp. 77– 90, 2009.
[17] Hirulkar, N.S., Jaiswal, P.R., Reis, P.N.B., Ferreira, J.A.M. Effect of hygrothermal aging and cyclic thermal shocks on the mechanical performance of single– lap adhesive joints, International Journal of Adhesion and Adhesives, Vol. 99, 2020.

[18] Rośkowicz, M., Godzimirski, J., Komorek, A., Jasztal, M. The Effect of Adhesive Layer Thickness on Joint Static Strength. Materials, 2021, Vol. 14, No. 6, 1499.
[19] Yasmina, B., Sami, N., Salah, M., Moez, B. S. A. Effect of surface treatment on the shear strength of aluminium adhesive single– lap joints for automotive applications. International Journal of Adhesion and Adhesives, Vol. 67, pp. 38–43, 2016.
[20] Borsellino, C., Di Bella, G., Ruisi, V.F. Adhesive joining of aluminium AA6082: The effects of resin and surface treatment, International Journal of Adhesion & Adhesives, Vol. 29 , pp. 36–44, 2009.
[21] Banea, M.D., Da Silva, L.F.M., Campilho, R.D.S.G. Effect of temperature on the shear strength of aluminium single lap bonded joints for high temperature applications, Journal of Adhesion Science and Technology, Vol. 28, No. 14–15, pp. 1367–1381, 2014.
[22] Abd– El Salam, M. H., Khaliel, J. A., Hassan, H. H. Factors affecting the adhesive force between metallic substrate and carbon black filled rubber composites, Journal of Reinforced Plastics and Composites, Vol. 32, No. 13, pp. 974–986, 2013.
[23] Natu, A. V., Ankit, R. S., Nitinkumar, R. A. Variation of Adhesive Strength in Single Lap Joint (SLJ) with Surface Irregularities. American Journal of Mechanical Engineering, Vol. 7, No. 2, pp. 61– 67, 2019.

Note: This paper was presented at IRMES 2022 – 10th International Conference on Research and Development of Mechanical Elements and Systems: "Machine design in the context of Industry 4.0 – Intelligent products", organized under the auspices of the Association for Design, Elements and Constructions (ADEKO) and University of Belgrade, Faculty of Mechanical Engineering, Department of General Machine Design, in 26 May 2022, Belgrade (SERBIA).

ACTA TECHNICA CORVINIENSIS
Bulletin of Engineering

ISSN: 2067-3809

1.Milan RACKOV

INNOVATIVE DESIGN SOLUTIONS OF GEAR TRANSMISSIONS FOR INDUSTRY 4.0

1. University of Novi Sad, Faculty of Technical sciences, Trg D. Obradovića 6, Novi Sad, SERBIA

Abstract: Gear transmissions are relatively simple mechanisms whose quality, price, delivery time and design appearance are almost equal. This is the common reason why it is very difficult for all gear manufacturers to ensure the successful placement of their products on the market. However, regardless of their simplicity, gear transmissions may have different design and technical solutions, and due to different limitations of individual components, the calculation of load capacity and other technical characteristics can be quite complicated. In accordance with the basic settings of Industry 4.0, smart transmissions are being developed that will be able to provide a certain advantage over the competition and thus, for sure, ensure the successful business of these innovative companies. This paper describes the basic principles of construction using new technologies, primarily using the Internet of Things and digital twins. The paper includes an analysis of approaches to the creation of Digital Twins. Describe why Industry 4.0 is so different and specific, define what is Cyber–physical systems and the Internet of Things, and what is predictive monitoring with using different sensors.
Keywords: Innovative design, Gear transmissions, Digital twin

INTRODUCTION

Due to the very strong competition, all gear manufacturers are trying to create some advantage over the competition in order to improve the placement of their products on the market. Many manufacturers try to attract customers by short delivery times. Other manufacturers try to achieve this with high quality, although there are also manufacturers who try to obtain customers with low prices (which is achieved with either cheaper labour, a more favourable conceptual solution, or slightly lower quality of their gearboxes). Of course, some manufacturers obtain customers with a high–quality level of gear transmissions and also with a more attractive appearance of their gearboxes. [1]

Gears, depending on their application, have different dimensions, design, technical characteristics, as well as different damages, failures and limited conditions under which they are determined. They are certainly among the most complicated mechanisms for calculation, design and construction and have a very important and general significance in modern mechanical engineering. [2] Modern solutions of universal helical gearboxes are characterized, first of all, by large torque capacity and high values of gear ratio in the frame of relatively small overall dimensions of the gear unit. [1]

The rapid development of information and communication technologies (ICT) has led to the development of the fourth industrial revolution, i.e. Industry 4.0, which is based on the use of information and communication technologies (ICT) and their communication using the Internet. This brings additional new components that are necessary for modern power transmissions, and without which it is impossible today to perform modern design, production, supervision and maintenance.

IMPLEMENTATION OF INDUSTRY 4.0 AS A MODERN DEVELOPMENT OF GEAR DRIVES

Industry 4.0 offers huge potential for improvement and success not only in the field of gear drives production but mostly for product innovation. Efficient engineering of the new generation of smart products and services is appeared, as well as new business models that are used in their marketing. In order to be able to successfully use this potential, manufacturers are facing a great process of transformation, i.e. cardinal changes where they have to overcome many challenges.

The focus of these changes is mostly related to process models, methods, IT tools and information models in the development of smart products and services. The development of products and services is the most important phase of engineering since in this phase lies the greatest innovation potential and the characteristics of future products are determined here. [3]

The essential goal of Industry 4.0 is to make manufacturing, but also related industries (e.g. logistics) faster, more efficient and more related to customer, while at the same time going beyond automation and optimization and detecting new business opportunities and models. In that way, personalization and customization of gear drive manufacturing will be established.

The fourth industrial revolution arose in the correlation between the existing traditional industry and innovations in the field of the Internet, i.e. in the field of information and communication technologies (ICT).

Innovations based on ICT can be divided into five categories (Figure1):

- Internet (Internet of Things, Internet service, ...);
- Hardware (smart devices, cloud computing, augmented reality, ...);
- Software (service–oriented architecture, semantic and Big–Data technologies, ...);
- Communication (5G, WiFi, ...);
- Built–in microsystems (microprocessors, microsensors, microactuators, ...). [3]

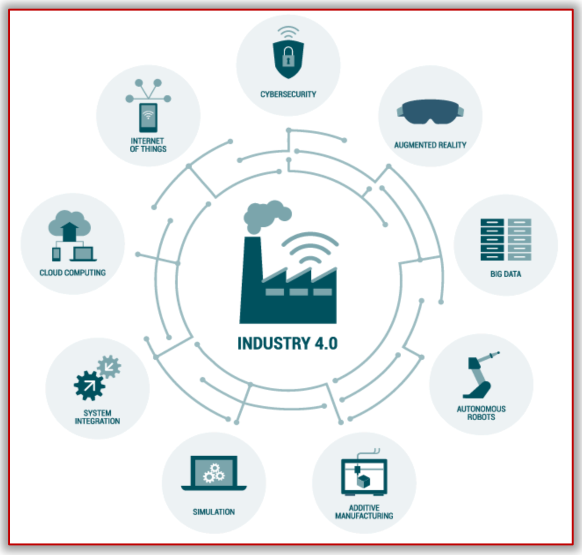

Figure 1. Industry 4.0 – the digital transformation

Trends in the development of modern technical facilities and their production largely refer to the ideology of Industry 4.0, in which a key role is played by the development of the sensor base and intellectualization of machines and materials [4], the Internet of things (IoT) and the creation of digital twins of items.

Industry 4.0 is characterized by much better automation, the bridging of the physical and digital world through cyber–physical systems, enabled by Industrial IoT. A central industrial control system is shifted to one where smart products define the production steps, there are closed–loop data models and control systems and personalization and customization of products are applied.

The basic structure of industrial products (BMS), in this case, gear transmission, consists of mechanical components (gears, shafts, bearings, etc.) (Figure2). In further evolutionary development, this structure was supplemented by electronic components and software, thus creating mechatronic products (MP). As a result of the development of miniature microcomputers and further software development, mechatronic products were equipped with artificial intelligence, so intelligent mechatronic products (IMP) appeared. In the next evolutionary step, products are enhanced by the ability to communicate with other products and the Internet. These products are called "Cyber–Physical Systems" (CPS). [3]

Cyber–physical systems define the basis of Industry 4.0 (e.g., smart machines). They use modern control systems, have embedded software systems and dispose of an Internet address to connect and be addressed via the Internet of Things (IoT). [6]

The cyber–physical systems are the basis and enable new capabilities in areas such as product design, prototyping and development, remote control, services and diagnosis, condition monitoring, proactive and predictive maintenance, track and trace, structural health and systems health monitoring, planning, innovation capability, agility, real–time applications and more. [6]

Since the Industry 4.0 is the next new stage in the organization and control of the value chain across the lifecycle of products, this ongoing improvement in which CPS fits started from mechanical systems and moved to mechatronics (where controllers, sensors and actuators are used) and adaptronics, and is now entering this stage of the rise of cyber–physical systems.

Cyber–physical systems result to new possibilities in areas such as structural health monitoring, track and trace, remote diagnosis, remote services, remote control, condition monitoring, systems health monitoring and so forth. [6]

Characteristics of cyber–physical systems:

- CPS represents an evolution in manufacturing, mechanics and engineering because they provide digital and physical bridging of system components, which is possibly thanks to Internet technology, and the bridging/convergence of Information Technology and Operational Technology;
- CPS can communicate since they have intelligent control systems, embedded software and communication capabilities as they can be connected in a network of cyber–physical systems;
- CPS can be uniquely identified because they dispose of an IP (Internet Protocol) address which means that they use Internet technology and are part of an Internet of Everything in which they can be uniquely addressed (each system has an identifier);
- CPS must have controllers, sensors and actuators (but this was already the case in previous stages before cyber–physical systems in mechatronics and adaptronics);
- CPS are the basic building blocks of Industry 4.0 and the enablers of additional capabilities in manufacturing such as track and trace and remote control;
- Smart factories, smart logistics (Logistics 4.0) and other smart areas of applications are enabled by cyber–physical systems.

Industry 4.0 offers multiple benefits for the production of gear transmissions. Central requirements from gear drive production are increased productivity, flexibility, quality and speed production (Figure 3). One of the first goals of

Industry 4.0 is productivity through optimization and automation. In other words: saving costs, increasing profitability, reducing waste, automating to prevent errors and delays, speeding up production to work more in real–time and in the function of the overall value chain, where speed is crucial for everyone, digitizing paper–based flows, being able to intervene faster in case of production issues.

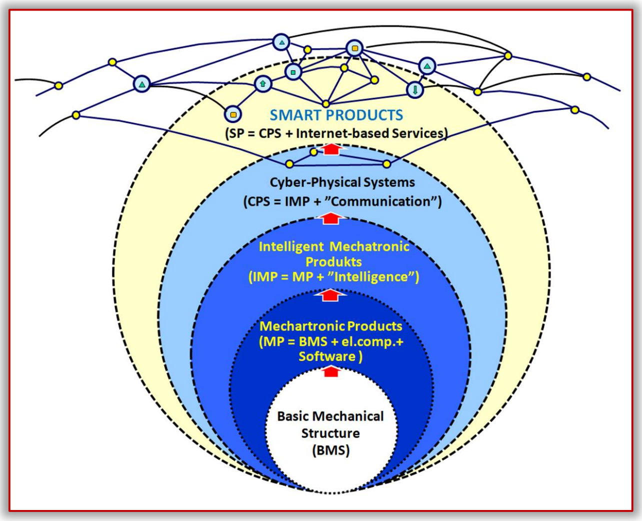

Figure 2. Evolution of stages from machine products (BMS) to smart products (SP) [5]

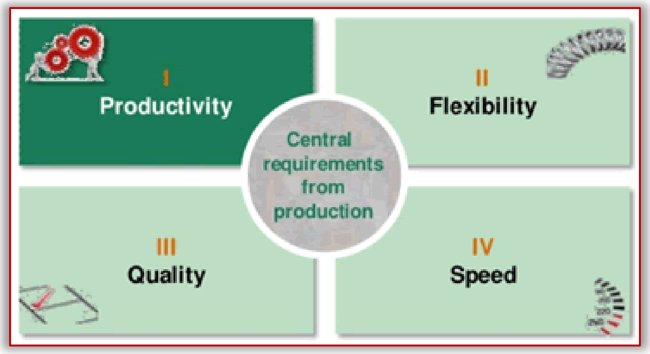

Figure3. Industry 4.0 offers multiple benefits for production

Productivity increasing of gear drives can be obtained by using a higher level of automation that reduces production time and enables better asset utilization and inventory management. The flexibility of gearbox manufacturing can be realized through machines and robots that can execute the production steps for a large number of products. Sensors and actuators that monitor the current production in real–time and quickly intervene in case of errors increase gear transmission quality. Production speed is increased by using consistent data and, e.g. new simulation opportunities.

There is also improvement of manufacturing conditions. For example, occupational safety is improved through increased automation. Ergonomically adapted workstations offer better working conditions. Increased collaboration in the product network is the result of consistent data availability. Environment is better protected by using optimized use of resources (e.g., more energy–efficient operation of machinery). Inovative capability is increased through new technological possibilities in manufacturing.

New generations of automated sensors connected to the Internet and supported by developed hardware and software tools enable the creation of fully digitalized factories. Industry 4.0 has already been introduced in many countries, thus ensuring the survival of the industry and its competitive development in modern conditions. Modern digital technologies such as the Internet of Things (IoT), robotics, cloud computing, cyber–physical systems and scalable big data analytics are key to implementing the Industry 4.0 concept. Industry 4.0 implies complete digitalization of all production processes and application of the mentioned digital technologies when creating an idea about a product, product engineering, production organization, production realization, process control and provision of industrial services. [4]

INTERNET OF THINGS AND INDUSTRY 4.0 AT GEAR DRIVES DEVELOPMENT

Trends in the development of modern technical facilities and their production largely refer to the ideology of Industry 4.0, in which a key role is played by the development of the sensor base and intellectualization of machines and materials, the Internet of things (IoT) and the creation of digital twins of items.

New generations of automated sensors connected to the Internet and supported by developed hardware and software tools enable the creation of fully digitalized factories. Industry 4.0 has already been introduced in many countries, thus ensuring the survival of the industry and its competitive development in modern conditions. Modern digital technologies such as the Internet of Things (IoT), robotics, cloud computing, cyber–physical systems and scalable big data analytics are key to implementing the Industry 4.0 concept. Industry 4.0 implies complete digitalization of all production processes and application of the mentioned digital technologies when creating an idea about a product, product engineering, production organization, production realization, process control and provision of industrial services. [4]

The Internet of Things (IoT) is a new type of communication between intelligent devices. Practically, a parallel internet is being created in which things communicate with each other, exchange information, manage each other, react and influence the environment in which they find themselves, without the influence of people. [3]

The presence of an IP address by definition means that cyber–physical systems, as objects, are connected to the Internet (of Things). An IP address also means that the cyber–physical system can be uniquely identified within the network. This is a key characteristic of the Internet of Things as well.

Cyber–physical systems are also equipped with sensors, actuators and all the other elements which are part of the Internet of Things. Cyber–physical systems, just like the Internet of Things need connectivity.

The Internet of Things consists of objects with embedded or attached technologies that enable them to sense data, collect them and send them for a specific purpose. Depending on the object and goal this could be capturing data regarding movement, location, presence of gasses, temperature, 'health' conditions of devices, the list is endless. [7]

IoT devices can also receive data and instructions, again depending on the 'use case'. All this applies to cyber–physical systems as well, which are essentially connected objects. There are more similar characteristics, but there are already many common things.

The Internet of Things focuses on looking for all the influences that surround a machine system to provide the right hardware and software to give this system a market advantage. In Industry 4.0, technology is required to be more scalable and flexible enough to respond well to changes in the supply chain as well as the entire product line. The main difference that makes both IoT and Industry 4.0 technologies key components of advanced industry transformation is connectivity. IoT seeks to connect everything to the Internet, and Industry 4.0 describes the idea of connecting sensors, actuators, control units, logistics services, other planning systems, and so on. [4] Because data–intensive industries require secure and reliable technology that is capable of storing and processing data in the cloud for better availability.

The advanced companies that introduced Industry 4.0 strive to manage their business remotely to achieve better results in an economical price structure. IoT allows remote monitoring of each device in real–time. It also keeps data secure and requires less manual work through all of these operations.

Machine systems are required to have efficient tools or systems that help manage big data and use it to infer outcomes based on different situations. IoT technology includes sensors and advanced connections of all components that are controlled and monitored. This way of connecting enables quick answers and better decision making at the right time.

The Internet of Things promotes effective machine system management strategies and improves their performance thanks to a constant control system. This helps to reduce their workload through manual handling of each task and to automate the entire industrial processing. Thus, it leads to relatively simpler maintenance of the device and simplifies the decision–making process.

MAJOR DIFFERENTIATORS OF IoT AND INDUSTRIAL IoT

The term internet of things (IoT) is often used these days. This technology is nothing but smart devices that are having good connectivity and can communicate with each other seamlessly. The number of IoT devices is growing exponentially with each passing day.

An almost identical term used is Industrial IoT (IIoT). Although both of these terms sound almost the same, because they are both based on the same technology and depend on the interconnection of devices, there are significant differences in these two concepts. [7] IoT is usually used by consumers, and as the name suggests, industrial IoT is for industry, such as manufacturing, transportation, etc. Table 1 shows the basic differences between these two terms.

Table 1. Differences between IoT and Industrial IoT [7]

Points of distinction	IoT	Industrial IoT
Security	Not critical	Is a crucial element
Scalability	Limited data processing	Support large scale network
Development focus	To improve consumer convenience	To make industrial operations efficient and effective
Interoperability	Not much integration required	Integration with legacy Operational Technologies
Precision	Can be close to accurate	Should be accurate

In the IoT interconnected system, safety is not a huge deal because consumer data does not require any security. The security of industrial IoT is becoming a key element when it comes to data entry and transmission. The disruption of production systems that involve industrial IoT costs huge financial resources and disrupts the economic activity of a large number of people and processes. Therefore, industrial IoT solutions consist of a series of advanced security measures, using security and resilient system architectures, encryption and authentication, specialized chipsets and threat detection.

Industrial IoT solutions must coexist with older operating technologies such as SCADA, M2M and other production execution systems. It is difficult to make older operating technologies disappear quickly. Industrial IoT will replace them, but to do so, it must first integrate with them, so industrial IoT solutions must support different protocols and datasets. [7]

In the contrast to IoT solutions, the Industrial IoT solutions must be very precise and accurate. From data entry to analysis, accuracy and precision should not be compromised because the automatic high–speed, high–volume manufacturing processes are synchronized to milliseconds. The quality assurance systems detect small dimensional variations in the data and take an immediate course of actions which are entirely dependent on those measurements. In the Industrial environment, "close enough" isn't good enough, and can cause downtimes, which ultimately results in lost revenues or loss of life.

DIGITAL TWINS – A CRITICAL MILESTONE TOWARD THE SMART INDUSTRY

Although the concept of a digital twin exists for quite a time, only thanks to the Internet of Things (IoT) it has become cost–effective for implementation.

Simply, the digital twin is a virtual model of a process, product, or service. This pairing of the virtual and physical worlds allows data analysis and system monitoring to solve problems before they even occur, prevent downtime, develop new features, and even plan for the future using simulations. [8]

The digital twin of an item is a computer image corresponding to a real one. It is created for each item during the design process, and then the digital twin is detailed during the production of the item and becomes its exact (in the ideal case) digital copy, which allows the reproduction of all the basic properties of the item. Then the digital twin goes through all the stages of the life cycle of a physical object.

Since the gear transmissions are among the most difficult mechanisms to calculate and design, the methods of their calculation, design and diagnostics have a general significance in machine building. Certainly, it is unrealistic to use a single and universal model that describes all the properties of a technically complicated mechanism, such as gear transmission.

Creating a digital twin based on a set of models and methods that reflect the transmission behaviour as a whole in functional and reliable aspects (lifetime mechanics) is an effective way to solve the problem of transmission design and maintenance during its life cycle. [2]

The central concept of Industry 4.0 is a cyber–physical system (CPS), which is characterized by a physical object, for example, a machine, and its digital twin, in the form of a model or a set of models that are implemented in software simulating the behaviour of the physical object.

Fundamentally, new parts in Industry 4.0 are components that are largely developed in mechanics. The most important ones are the model approach and the digital twin of the product, as well as sensor bases, wireless data transmission, diagnostics and analytics.

Digital twins are ready to transform manufacturing processes and offer new ways to reduce costs, monitor assets, optimize maintenance, reduce downtime and enable the creation of connected products.

Faults and defects of mechanical transmissions increase costs and overload employees in the production process. To alleviate these problems, manufacturers can use the digital twin, as one of the Industrial IoT functions. The digital twin replicates the mechanical transmission during its development into digital form. By upgrading the sensors, manufacturers collect data on the entire working mechanism of their equipment and the expected output of each unit. The data entered from the digital model allows manufacturers to analyze the efficiency, effectiveness and accuracy of the system. It also helps identify potential congestions in the production of a mechanical transmission, which helps the manufacturer create a better version of the product. [9]

The digital twin can allow companies to have a complete digital footprint of their products from design and development through the end of the product life cycle. This, in turn, may enable them to understand not only the product as designed but also the system that built the product and how the product is used in the field. With the creation of the digital twin, companies may realize significant value in the areas of speed to market with a new product, improved operations, reduced defects, and emerging new business models to drive revenue.

The digital twin may enable companies to solve physical issues faster by detecting them sooner, predict outcomes to a much higher degree of accuracy, design and build better products, and, ultimately, better serve their customers. With this type of smart architecture design, companies may realize value and benefits iteratively and faster than ever before. [10]

APPROACHES FOR CREATING DIGITAL TWINS

Three approaches can be distinguished when creating digital twins.

- The first approach considers general methodology for any field of application. The main tool is the use of big data and analytics. This approach is mainly used to improve items that have relatively short lifetimes. At the same time, models of workflows of items are not considered in detail. So, in one paper [11], operational data is used to improve the production process and service. Another paper [12] considers the possibility of applying operational data to the design process. Digital twin–driven product design (DTPD) is proposed and analyzed. DTPD is expected to be most useful for the iterative redesign of an existing product instead of a novel design or a completely new product.
- The second approach is based on the use of universal methods and software based on certain physical (mechanical, etc.) models. At the same time, modelling the workflow of an item is widely used. To simulate the behaviour of items, the finite element method and methods of multibody dynamics are widely used. Siemens AG gives typical examples of the second approach.

The digital twin can be considered as the virtual copy of a real–world asset. It integrates here with all data, models and other structured information related to the product, plant, infrastructure system or production process. This data can be generated during design, engineering, manufacturing, commissioning, operation or service. The fast adoption of the digital twin concept builds on advances in simulation methods, computing power, availability of IoT data and artificial intelligence. [13]

Two key elements of the digital twin are that it is holistic and dynamic. Holistic implies that all information is integrated and consistently consumed at various parts of the life cycle, connected through a digital thread. Dynamic implies that the digital thread grows over the life cycle, completing the system description and adding higher levels of detail when these become available and updating the underlying models based on the actual product use.

At its highest level, a digital thread is a continuous, seamless strand of data that connects each stage of the product life cycle from design, to build, to in–the–field usage. It provides, in effect, the channel through which data about the product travel. Such data—their storage, ready access, modelling, and analysis—are what create the ability to model production and drive efficient supply chain communications. [10]

- The third approach includes special models and methods related to specific objects. In this case, these are gears and transmissions.

Some papers give different modern representations of digital twins in the field of gears and transmissions. A paper [14] describes a simulation–based model meant to predict the fatigue endurance of tooth root. The model can be regarded as a digital twin of performance and enables the prediction of the fatigue behaviour of tooth roots even for conditions which are not covered by the standards yet.

One publication [15] describes an efficient and goal–oriented way, which presents the immense advantages of the use of digital twins, shown in the example of spur gear stage design, the definition of macro geometry and the final microgeometry optimization of the tooth flank.

Another paper [16] points out that nowadays a large number of different CAE tools are available for the design and analysis of a gear unit and its components, each of which has its own strengths. A major milestone for Industry 4.0 is the establishment of industry–wide standards. The German Research Association for Drive Technology (FVA e.V.), in close cooperation with industry and research, is developing an industry–wide standard for simple data exchange in transmission development under the name REXS (Reusable Engineering EXchange Standard). The REXS initiative pursues the goal of providing a "digital twin" in transmission development and calculation. REXS defines uniform parametric modelling and nomenclature of gear units and their components across standards and industries, based on detailed terminology from FVA's 25 project committees and 50 years of joint industrial research.

This is meant to reduce the number of interfaces involved in the design process. This is the vision of the REXS initiative: a free, nonproprietary, standardized interface for the exchange of transmission data which reduces the complexity of data exchange in the design process significantly (Figure 4).

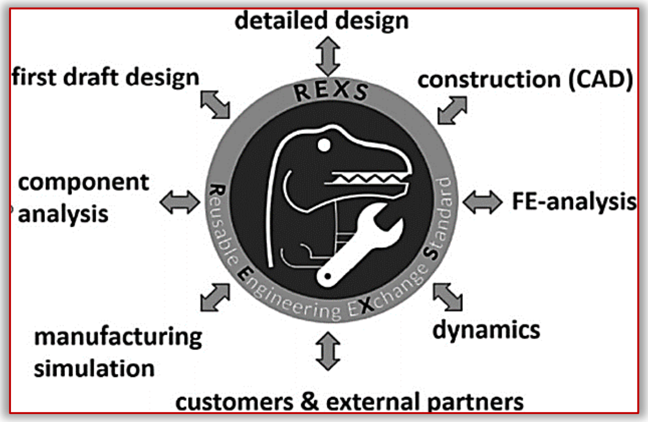

Figure 4. Design process with standardized interface REXS

REXS has the potential to establish itself on a large scale as a standard model for data exchange in the field of gear unit design and analysis. This would result in several advantages for the software manufacturers, for the companies using the tools and for the users:

- Transmission designs and analyses at any level of detail, i.e. from the overall system view via the analysis of individual components to the individual physical phenomena, can always be carried out based on a single data model;
- A simple data exchange between classic analytical gear design programs and universal dynamic, FE and CAD systems would be possible. Expenses for additional, specific modelling could be greatly reduced, etc.

VISION AND UNDERSTANDING OF THE "DIGITAL TWIN"

The following aspects are essential:

- Each part of the machine is represented as a source of information signals;
- The machine units in which it is possible and appropriate to implement the principles of reflexive control are allocated; procedures for the identification of information sources, control objects and reflexive nodes are provided, then their interdependences are determined.

The information model should be designed in such a way as to allow the use of various sources: semantic, structural (logical), parametric (quantitative, mathematical) models; measurement results; expert evaluations; means of simulating the elements and units of the machine (in slow, accelerated and real time scales in relation to the current, retrospective and predicted state).

Thus, the developed methodology anticipated one of the principles of Industry 4.0: the creation and use of an item's digital twin.

The assumption that there are possible conflicts among the subsystems of the machine, endowed with intellectual properties, can be considered as a forecast for the forthcoming Industry 4.0 technologies.

Modern authors' conception is depicted in Figure 5 [17]. This concept is presented in detail below in relation to gears and transmissions.

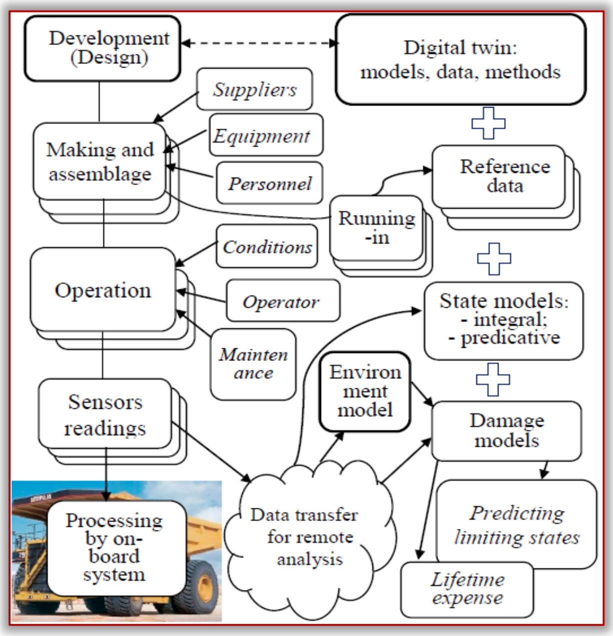

Figure 5. Evolution of the item and its digital twin during life cycle [17]

Fortunately, software tools are rapidly rising to the challenge of concurrently building and integrating digital twins. As the technology evolves, those tools will grow more powerful and sophisticated, and IoT–enabled digital twins will become more tightly integrated into a plant's production processes, and far more capable.

They will also become smarter, using machine learning programs, a type of artificial intelligence, to learn more about a factory's machines and improve the ability of digital twins to simulate and predict their behaviour.

As artificial intelligence systems learn more about specific machines, they will use their digital twins to help engineers run plants more efficiently. If there is some problem with a machine, artificial intelligence can analyze it to see what is wrong. The better the artificial intelligence knows the machine, the more accurately it can predict when that failure is likely to happen. [18]

The growing importance of digital twins in IoT projects today de facto is mainly mentioned in the scope of the manufacturing sector, the bridging of digital and physical worlds in Industry 4.0, the digital transformation of manufacturing and industrial markets overall, including smart supply chain management. As written previously, the usage of the IoT in manufacturing is the highest of all verticals from an IoT technology investment perspective. It's also thanks to IoT that digital twins become affordable and most certainly alter the face of manufacturing technology. [6]

PREDICTIVE MAINTENANCE – INCREASING UPTIME AND REDUCING RISKS

Predictive maintenance always seemed like the perfect use case for the Internet of Things (IoT), more specifically for Industrial IoT (IIoT) and environments where uptime of specific assets is critical and breakdowns can have important consequences for several reasons. Many of the main technologies that are mentioned in the context of the Industry 4.0 play a role in predictive maintenance (Maintenance 4.0, PdM 4.0) and its evolutions: big data, artificial intelligence, machine learning, IoT, cloud computing, data analytics and, increasingly, edge computing and digital twins.

Sensors and actuators are transducers (Figure6). A transducer converts a specific signal which comes in a specific form of energy into another signal in a different form of energy. Sensors convert signals in areas such as heat, humidity, pressure, presence of gases, pressure, acceleration and so forth into a digital signal that gets sent to a control and/or data aggregation systems such as a sensor hub or gateway. They are the start of all IoT data capture and thus must be accurate. The exact types of sensors (there are over a hundred) depend on what should be achieved. In some IoT use cases, projects or devices there are only a few sensors (per connected device), in others there are often thousands.

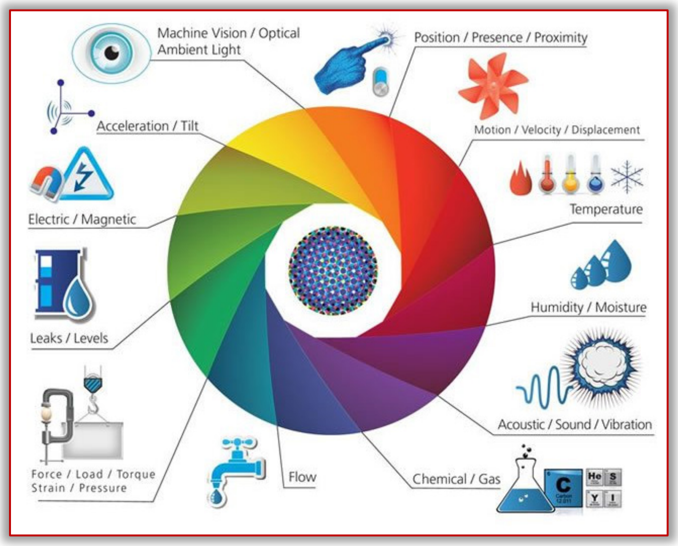

Figure 6. IoT devices – sensors and actuators examples [19]

Transmission systems of vehicles and tractors operate under conditions of varying speeds and loads. In addition to internal factors, external ones (the road surface, car loading, driver skills) influence on the vibration characteristics of transmission units. The main feature of the developed diagnostic method is using conceptual modelling for the oscillating process in the gear drive and the propagation of vibrations in the transmission. It is advisable to apply together integral diagnostic models and predictive ones based on damage accumulation. Such a 'two–coordinate' approach (two points of view) ensures higher veracity of the individual lifetime forecast. [2]

An example is a reducer of a motor wheel of a mining dump truck. The reducer of a motor wheel with installed sensors is shown in Figure 7, and processes in an onboard monitoring system are in Figure 8.

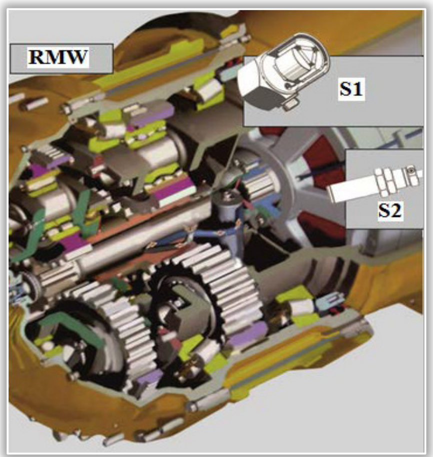

Figure 7. Reducer of a motor wheel with sensors [2]

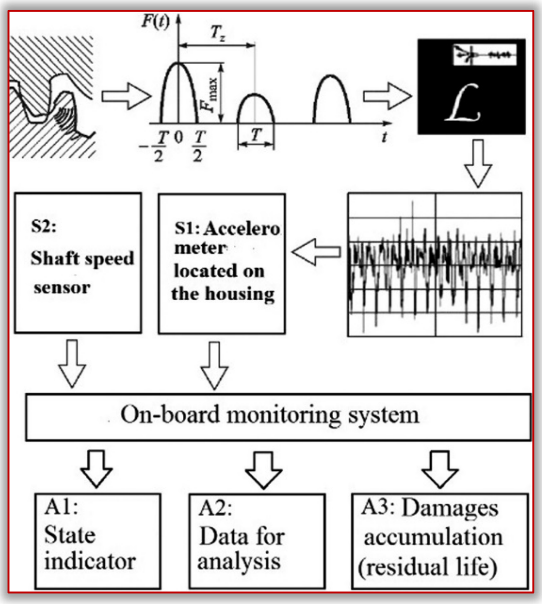

Figure 8. Processes in the RMW and its monitoring system [2]

Industrial IoT, in combination with predictive analytics and machine learning, however, are the main drivers of the more mature stage of predictive maintenance. Actionable, often real–time, data on pre–defined factors are gathered from smart sensors and predictive analytics algorithms are applied to predict when something might occur – and thus proactive maintenance, called predictive in this case, is needed.

The idea of predictive maintenance is simple and attractive enough and is similar to other forms of proactive maintenance with some additional benefits (and disadvantages): unexpected failure of equipment with all related consequences can be avoided, and maintenance can occur before something happens, instead of after the facts (reactive and run–to–failure maintenance), when such is deemed useful and possible. So, predictive maintenance is one of the maintenance methods enabling to do this kind of proactive maintenance and takes the most time and skills to implement. In other words: it's important to use it where it makes true sense.

Typical goal statements of PdM 4.0:

- maximize utilization, minimize costly downtime,
- replace close to failure components only,
- enable just in time estimating order dates,
- discover patterns for problems,
- key performance indicator of asset condition,
- reduce risk.

Predictive maintenance uses machine learning engines with these parameters of the monitored equipment being used as a basis, but the actual difference concerning what the machine learning and predictions say is what is likely to occur within a specific time frame and with a specific probability. Typically, this also means that predictive maintenance uses more data sources and sets than the sensor data from condition monitoring and digitally recorded data from the previous stage, instrument inspection. The difference might seem small, but it's not. Predictive maintenance uses monitoring data, but it uses more and, most importantly, it, indeed, predicts.

Almost all industries require effective tools or systems that help manage large data and use it to infer outcomes based on different situations. IoT technology comprises sensors and advanced gateway connectivity, which derive informed insights for the managers. It enables quick responses and better decision–making.

IoT promotes effective asset management strategies and enhances their performance by sharing valuable information with the managers. This helps reduce their workload of manually operating each task and rather automates the entire industrial processing. Hence, it leads to comparatively lower maintenance of the assets and simplifies the decision–making process. [19]

Keeping equipment in an operational state significantly reduces operating costs, saving the budget for manufacturers. Using sensors, cameras and data analytics, managers in several different product lines are now able to determine when a machine will break down before it stops. IoT–enabled systems can sense warning signs by using data that helps managers create maintenance deadlines and schedule equipment services before any problems occur.

Using real–time data from sensors and actuators, operations managers can quickly access current equipment conditions, recognize warning signs, receive alerts about problems, and get rid of wasting time into scheduling maintenance.

The sensor devices extract information from the assets and transfer the same through the gateway on the connected dashboard. This improves data storage on the cloud–based platform and processes it further in a user–friendly language, allowing effective productivity. The managers find this data easy to analyze and discuss the industrial flaws to encourage improvements in business strategies. [19]

DIRECTING THE DEVELOPMENT OF GEAR TRANSMISSIONS TO THE POSTULATES OF INDUSTRY 4.0

The function of driving systems is realized by the joint action of mechanics, sensors, actuators with appropriate information processing. Mechanics in this context should be understood as all components that directly participate in power transmission. Sensors and actuators also consist of mechanical components, but in this case, they represent the connection between the mechanics and the processor for processing information. With the help of sensors, it is possible to know the quantity of the actual values of individual operating parameters and transfer them to information processing systems. Information processing enables the successful control of power flow and work processes by comparing the actual and set values of the operating parameters of the system, and thus manages the system in order to fulfil its operating function.

Therefore, modern driving systems with these performances are in fact mechatronic systems, which in nowadays conditions of technical development are extremely important. The principle of driving systems operating is usually based on rotational or rotational–translational movement (transport mechanisms, industrial plants).

The power transmission system basically consists of three subsystems: driving engine, power transmission and operating machine. These subsystems consist of mechanical and structural elements. Gears, couplings, shafts, seals and bearings play the most important role in the synthesis of these subsystems.

These three subsystems form one oscillatory system, which is exposed to different influences, i.e. alternating loads. Vibrations negatively affect the successful execution of the system's operational function and can, in some cases lead to the appearance of a resonant state. Therefore, monitoring devices have to be installed in technical systems for monitoring the occurrence of vibrations and critical states of the components of the system.

There is a transmission of power and torque through the transmissions, so different forces occur on its components. In practice, various requirements are required from gear transmission. Thus, for example, in operating conditions, the direction of power flow can be changed, and thus the input and output of power are changed in transmission. There are often cases of branches aggregating or division of power. Particular structural elements often perform several different functions.

In practice, it happens that the constant gear ratio does not meet the working conditions, but it is necessary to bring power to several different places with different operating parameters. There are also cases where a change in both speed rotation and torque value in a wide range is required.

Progress in power electronics has made it possible to regulate speed electronically in some areas (for example a washing machine). Many mechanical couplings are replaced by the use of electronic controls, such as in production systems.

However, in many areas, power transmissions are irreplaceable, because they have many advantages: branching and summation of power, stepwise or continuous change of speed, reliable operation, energy efficiency and compactness of construction.

Driving systems are part of almost all types of machines and devices so the fulfilment of the work function in various areas of the industry depends on their reliable operation. If there is an aspiration to build smart factories, then the priority is the development and creation of smart driving systems. At the same time, it is a usual method not to change the design solution in the initial phase, but to install smart product systems in the existing solution of drive systems.

In this view, the following points should be considered:

- installation of sensors and software that enable full self–monitoring of the state of operating regularity of drive systems;
- installation of systems with integrated logic functions for monitoring the influential parameters of the operating machine and operating environment that affect the operation of drive systems;
- installation of a sensor module for data transmission and communication via IO–link, which as a result has a full connection with Industry 4.0.

For reliable operation of power transmission, it is very important to avoid critical conditions during operation. The risk of damage to the gearbox is reduced if the failures are detected at an early stage. Also, repair costs, as well as losses due to downtime, are avoided. For example, thermal stability and dynamic behaviour play a very important role in the reliable operation of the gear unit. It is the easiest to monitor them through temperature and vibration and to notice the exceeding of boundary conditions promptly through appropriate systems.

DIGITAL TRANSFORMATION OF UNIVERSAL HELICAL GEAR REDUCERS

The digitalization of helical gear reducers is transforming the business models and the manufacturing processes adopted by companies that operate in the industrial automation field. Such companies must meet requirements of more and more flexible production, in small batches, with high customization and short time–to–market, without giving up high technical performances and utmost quality levels. These gear reducer companies should make the effort of shaping a new automation era, more open, interconnected, intuitive and user–friendly. All this, thanks to the development of advanced products and technologies, concretely resulted in an innovative factory concept, called HUMANufacturing. This expression defines its way to Industry 4.0, where robots and the other industrial machines work in strict contact and in full safety with the operator, who remains central in the manufacturing process. [20]

Industry 4.0 has determined the need for a complete rethinking of production models that, from a "make to stock" logic, are evolving towards an "assembly to order" approach. Besides collaborative robots and other innovative products for industrial automation manufacturers have to develop solutions enabling the communication between operators and automation systems through mobile devices, developed according to the Industrial IoT vision. They are completed by preventive and predictive maintenance instruments. Such technologies are inspired by a right–sized automation strategy, aimed at an efficient balancing between machine use and human contribution in the productive context.

INNOVATIVE UNIVERSAL HELICAL GEAR REDUCERS – SENSORS INSTALLATION

In order to be adopted for smart factories, universal helical gear reducer should be expected installation of following sensors:

- Temperature sensor, which will monitor the oil temperature in the gearbox housing and if it reaches a boundary limit value then the sensor will "inform" the main processor. The system will assess whether the temperature rise is due to rising ambient temperature, in which the reducer is located, or due to a higher load of the reducer, which occurred due to a change in the technological process. The system will correct the operation of other components in the system and, if necessary, inform the operator, and in case of reaching a critical value, the processor will shut down the driving and, if necessary, the entire system in which it is installed.
- Oil level sensor, which will monitor the oil level in the gearbox housing. In case of reaching a certain minimum value, the sensor signal will inform the system to add oil, or in complex and responsible systems, register the place of oil loss, and even performed automatic refuelling, and informed the system. In case of reaching a critical oil level value and loss of a large quantity of oil, the sensor would turn off the drive and also inform the system.
- Vibration sensor, which will monitor the vibration level of the gearbox. If the vibration reaches the limit value, the processor would check the condition of other components in the system and check whether the cause of increased vibration is some external sources (some irregularity in the technological process) or an announcement of the forthcoming failure of some gearbox component. In the case the critical vibration value is reached, the sensor would timely prepare the shutdown system and turn off the gearbox and the entire system, if necessary. By applying special systems for vibration spectrum analysis, it would be possible to determine the cause of higher vibrations (bearing damage, gear damage, shaft bending, etc.) in responsible systems, which would speed up the elimination of the causes of elevated vibrations, or, if necessary, timely indicate for the implementation of appropriate activities.
- Rotation sensor, which will monitor the rotation number of the output shaft (or gear). For example, in case the engine is running, and the output shaft does not rotate, the sensor would turn off the drive and immediately notify the system. Of course, this sensor would monitor the actual number of revolutions and in case of a significant change, through the appropriate processor, would conclude the need for a change in the transmission process, or would adjust the number of revolutions to adapt to new ones.
- The operating time sensor, which will monitor the operating time between two oil changes. When it passes the estimated time for replacement, it will notify the system.
- Total operating time sensor, which monitors the total operating time of the gearbox, in order to indicate the performing the service, i.e. mandatory repairing the gearbox or to indicate the period of occurrence of possible gearbox failures.

In the future, motor gearboxes, i.e. their electric motors, will certainly be, even more often than before, equipped with drive control devices (usually frequency regulators) which would automatically adjust the speed of the gearbox output shaft to the requirements of the technological process under full load. Electric motors will be supplied with processors that provide the so–called soft start so that there are no sudden impacts during the start that significantly shorten the service life of the gearbox.

Figure 9. Innovative solution of universal single–stage helical gearbox: (1) solution of company REGAL [21], (2) solution of company STM TEAM [22], solution of company PGR [23]

Despite the fact that the current solutions of universal gear reducers have very good design solutions, their appearance will have to be paid even more attention because all other parameters (quality, price, delivery times, etc.) for most gear manufacturers, will be similar. [24] Therefore, the appearance solution of gears will greatly affect their placement. For example, today the solutions of single–stage motor gearboxes of the company REGAL (Figure9–1) are especially interesting. The design of single–stage gearboxes of companies STM TEAM (Figure9–2) and PGR (Figure9–3) are also interesting. Similar solutions can be expected from other gearbox manufacturers in the future.

Interesting design solutions for two–stage helical gear reducers are solutions of company SESAME (Figure10–1), Stöber (Figure10–2) and BEGE (Figure10–3).

Figure10. Innovative solution of universal two–stage helical gearbox: (1) solution of company SESAME [25], (2) solution of company Stöber [26], (3) solution of company BEGE [27]

Interesting design solutions for three–stage helical gear reducers are solutions of the company Siemens (Figure11–1), Motive (Figure11–2) and Rossi (Figure11–3). Also, there are innovative solutions in other types of gear reducer mounting, for example, shaft–mounted gearbox with axial mounting, but also in other types of gear transmission (bevel, worm, harmonic, etc.).

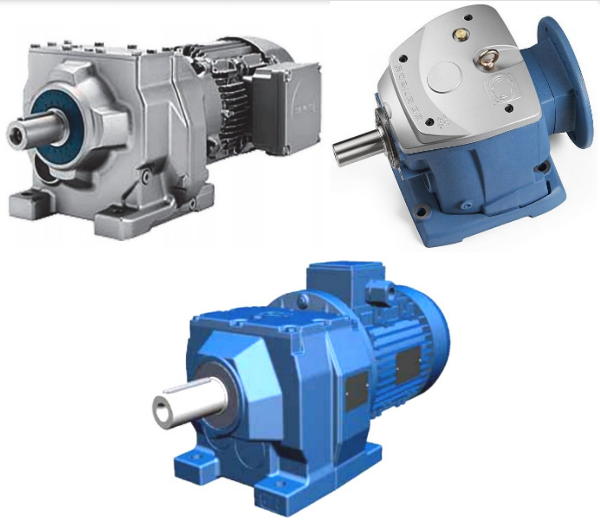

Figure11. Innovative solution of universal three–stage helical gearbox: (1) solution of company SIEMENS [28], (2) solution of company Motive [29], solution of company (3) ROSSI [30]

CONCLUSIONS

The goal of Industry 4.0 is to enable autonomous decision–making processes, monitor assets and processes in real–time, and enable equally real–time connected value creation networks through early involvement of stakeholders, and vertical and horizontal integration.

Industry 4.0 represents the digital transformation of manufacturing. It's most important benefits and potential perspectives are enhancing productivity, automation and the optimization of operational processes, business processes, and manufacturing operations, followed by (predictive) maintenance and smart maintenance services. In order to move to intelligent manufacturing, smart factories, or connected industries, it should bridge things such as real things, people, standards, work processes (man and machine) and more. Moreover, to bridge all that need data and networks. They must all inter–operate and inter–connect. It should bridge IT and OT, have assets such as machines that can connect and communicate thanks to sensors and other equipment and connect people, data, and machines. This is indeed mainly about the Internet of Things and, in a broader perspective the Internet of Services, Internet of People, Services and Things and Internet of Everything.

The digital twin may drive tangible value for companies, create new revenue streams, and help them answer key strategic questions. With new technology capabilities, flexibility, agility, and lower cost, companies may be able to start their journeys to create a digital twin with lower capital investment and shorter time to value than ever before. A digital twin has many applications across the life cycle of a product and may answer questions in real–time that couldn't be answered before, providing kinds of value considered nearly inconceivable just a few years ago. Perhaps the question is not whether one should get started, but where one should start to get the biggest value in the shortest amount of time, and how one can stay ahead of the competition. What will be the first step, and how will it get started? It can be an overwhelming task to get there, but the journey starts with a single step. [10]

The beginning of the period of Industry 4.0 was conditioned by using communication between cyber–physical systems and the internet of things (IoT) and all other parts of the production process. Having all that in mind, it can be concluded that further development of gear transmissions will be aimed at the greater application of artificial intelligence and machine learning, primarily various sensors and processors that will monitor and regulate their work and communication with other segments within the same technological process. These smart gearboxes will have a nice appearance design and high–class technical characteristics, with applied product personalization and customization and a short delivery time.

References

[1] Kuzmanović, S., Miltenović, V., Rackov, M., Innovative design solutions of universal motor gearbox with helical gears, International Scientific Journal Machines. Technologies. Materials., Vol.14 (2020), No.4, pp. 137–141, Publisher: Scientific Technical Union of Mechanical Engineering "Industry–4.0", Sofia, Bulgaria

[2] Algin, V., Ishin, M., Paddubka, S., Starzhinsky, V., Shil'ko, S., Rackov, M., Čavić, M., Development of information model of power transmissions in the light of Industry 4.0, International Scientific Journal Mathematical Modeling, Vol.4 (2020), No.2, pp. 54–63, Publisher: Scientific Technical Union of Mechanical Engineering "Industry–4.0", Sofia, Bulgaria

[3] Miltenović, V., Antić, D.: Inženjering pametnih proizvoda i usluga, Univerzitet u Nišu, Niš, 2020.

[4] Bojan Stanojević, 2016. Industrija 4.0 i budućnost, 2016 [online]. PCpress magazine. Available: https://pcpress.rs/industrija–4–0–i–buducnost/ [accessed 12th April 2022]

[5] CIRP Encyclopedia of Production Engineering. Int. Academy for Production Engineering, Laperriere, Luc, Reinhart, Gunther (Eds.) 2015

[6] https://www.i–scoop.eu/industry–4–0/ [accessed 12th April 2022]

[7] https://www.biz4intellia.com/blog/differentiators–of–industrial–iot–and–iot/ [accessed 12th April 2022]

[8] Marr, Bernard (March 6, 2017). What is Digital Twin Technology – And Why is It so Important?. Forbes.com.

[9] https://www.biz4intellia.com/blog/iot–applications–in–manufacturing/ [accessed 12th April 2022]

[10] https://www2.deloitte.com/us/en/insights/focus/industry–4–0/digital–twin–technology–smart–factory.html [accessed 12th April 2022]

[11] F. Tao [et al.], Digital Twin driven Product Design, Manufacturing and Service with Big Data, International Journal of Advanced Manufacturing Technology. 2017. 1–14

[12] F. Tao [et al.], Digital twin–driven product design framework, International Journal of Production Research. 2018. 1–20

[13] Van der Auweraer, Digital Twin: From Concept to Value Creation across the Product Lifecycle, 15th IFToMM World Congress, 2019, Krakow, Poland.

[14] Meis, J–A., F. Teklote, M. Borowski, Simulation of the tooth root strength under consideration of material quality, finishing process and size effects, International Conference on Gears, Garching, Munich, Germany, September 18–20, 2019. pp. 161–171.

[15] Algin, V. Dependability of technically complicated items in the light of "Industry 4.0", V. Algin, M. Ishin, Topical issues of Mechanical Engineering. 2017. No. 7. pp. 43–54 (in Russian).

[16] Khizhenok, V. Strain–strength characteristics of the polymer heart valve prosthesis, V. Khizhenok, S. Shilko, Russian Journal of Biomechanics. 2006. 10(4). pp. 47—55.

[17] Algin, V. Dependability of technically complicated items in the light of "Industry 4.0", V. Algin, M. Ishin, Topical issues of Mechanical Engineering. 2017. No. 7. pp. 43–54 (in Russian).

[18] https://www.asme.org/topics–resources/content/ identical–twins [accessed 12th April 2022]

[19] https://www.i–scoop.eu/industry–4–0/predictive–maintenance–pdm/[accessed 12th April 2022]

[20] Bonanomi, A., Industry 4.0: Driving Engine of Innovation, Power Transmission World (25 July 2018)

[21] Marathon Gearboxes Inline Coaxial Catalogue, Regal Beloit Australia Pty Ltd (2018)

[22] STM TEAM catalogue, CT17 IGBD 3.1 | ITA – ENG – DEU, 3/2018

[23] PGR Drive Technologies, Catalogue Helical Gear Units, PA/PF series 02/2019

[24] Rackov, M., Kuzmanović, S., Blagojević, M., Đorđević, Z.: Helical motor gear reducer (monography in Serbian), Faculty of Technical Sciences, Novi Sad, 2019.

[25] https://www.sesamemotor.com/en/products/detail/18

[26] SMS/MGS Gearunits, Catalogue 11, STÖBER Antriebstechnik GmbH & Co. KG.

[27] BEGE Power Transmission, Catalogue no. 241704, Helical Gear Motors, Sassenheim, Netherlands

Note: This paper was presented at IRMES 2022 – 10th International Conference on Research and Development of Mechanical Elements and Systems: "Machine design in the context of Industry 4.0 – Intelligent products", organized under the auspices of the Association for Design, Elements and Constructions (ADEKO) and University of Belgrade, Faculty of Mechanical Engineering, Department of General Machine Design, in 26 May 2022, Belgrade (SERBIA).

ISSN: 2067–3809

[1.]Joseph U. OKOKO, [1.]Ubong E. ASSIAN, [1.]Unwana I. UDOUMOH,
[1.]Precious O. EHIOMOGUE, [1.]Akindele F. ALONGE

GLOBAL AND NATIONAL FOOD SECURITY – NEED FOR NOVEL FOODS FORMULATION: A REVIEW

[1.]Department of Agricultural and Food Engineering, University of Uyo, Uyo, 520211, Akwa–Ibom State, NIGERIA

Abstract: Food is a source of livelihood for plants and animals. However, greater emphasis has been on man in this review. An overview of foods, food security (hence, food insecurity) – at global and national levels has been presented. The right to food should be respected and protected as a fundamental human right. Besides, adequate diet is a key to a person's health, hunger fallouts from food uncertainty. There is so much hope on the Sustainable Development Goals (SDG) programme of the United Nations (UN) to bring succour if there are no conscious efforts on the part of governments to provide foods for its citizenry. Governments display loyalty to their citizens by making food security policy. Boosting accessibility to food, making policy statement, improved usage of food with better nutritional status, and a tactical backup for foods already produced are measures that are being used to accomplish food security. The need of formulation of new foods as a panacea to food insecurity has been illuminated. If food security is neglected, the predicted 840 million people will be condemned to near inveterate malnutrition in 2030. Food security, worldwide and coast–to–coast should conspicuously focus on creation of new foods with value addition.
Keywords: global, national, food, security, formulation, sustainable development goals

INTRODUCTION

Food is generally referred to as any material, in any physical state, that is consumed by living organisms in order to put up with life. Of all the necessities of life, the most critical is food. Whoever may be in doubt of this may have to learn from the way of a mad man. The right to food should be seen as being very essential; as much as we see birthright. As birthright? Yes, as that, if we borrow from Christian religious lesson of a man called Esau, who exchanged his birthright for food. In this case, a denial is tantamount to an abuse of someone's right. The right to food – adequate and nutritional food – is an intrinsic component of the fundamental human right; hence the need to respect and protect it. Good nutrition plays a vital role in a person's health, ranging from growth and development to mental health, and the consumption of healthier foods significantly reduces the risk of chronic diseases, such as diabetes and heart disease. Additionally, the immune system improves and delays the aging process. In the United States, good nutrition is expensive nutrition; a luxury many low–income families abandon. Essential expenses– rent, utilities, clothing, and health are priority for many families with limited disposable, and therefore, forgoing the nutritious food option. According to UNCTAD (2017), of the nearly 795 million malnourished people in the world (every ninth person), the majority is living in developing countries and rural areas; and new, existing, and emerging technologies can be applied to address the four dimensions of food security. Adeyeye (2017) has reported that the world is faced with numerous challenges to food security involving under–nutrition, overconsumption, swelling population, increasing prices of foods and diet changes. Other problems also include; ineffective production practices, dangers posed to agricultural production, inefficient supply chains in addition to diminishing venture into research in food systems. Africa generally has the challenges of inadequate novel food processing technologies and appropriate storage equipment. In the light of the report of Adeyeye and Idowu–Adebayo (2019), lately, science and technology are at the front burner globally in transforming agricultural production and food processing with an obvious impression on food, nutrition and family health. Undernourishment and food insecurity are associated with each other. As a matter of fact, food insecurity is significantly correlated with malnutrition (Akerele *et al*., 2013). Where any government fails to arrest the menace of food shortage, such a government is bound to face social glitches such as robbery, civil unrest and increased number of hustlers in the streets *inter alia*. For instance, in Nigeria where the poverty rate is frightening, about 70% of the population is living on less than a dollar per day (Omorogiuwa *et al*., 2014), the wave of criminal activities has been very worrisome. Growing population with attendant rivalry over land and other resources, climate change and other natural misadventures, and inadequate water availability are potential causes of food insecurity. As hydra–headed as the challenge is, it requires a multidimensional and multifaceted approach to solving it. Thus the objectives of this review paper are to give an overview of foods, food security (hence, food insecurity) – at global and national levels, and to identify the place of formulation of new foods as a panacea to food insecurity.

OVERVIEW OF FOOD

Raw food materials can be identified in two broad classes, namely; plant foods and animal foods. Each of these classes can further be subdivided into different types, namely; plant and animal foods/food products.

— PLANT FOODS

Plant foods are those food materials which are obtained from living organisms of the flora kingdom. There are also different types of plant foods that can be identified.

Fruits and Vegetables

Fruits and vegetables are food materials which contain important vitamins, minerals, dietary fibre and plant chemicals. Several varieties of these food materials are available; and there are many ways to prepare, cook and/or serve them. A diet high in fruits and vegetables can help protect someone against devastating diseases as cancer, diabetes, and cardiovascular diseases. Examples of fruits include mango, pineapple, apple and orange, etc.; and vegetables are pumpkin, water–leave, bitter–leave, etc.

Cereals

In the Food Agricultural Organization (FAO) concept; cereals denote crops harvested for dry grain only. For international trade classifications, fresh cereals (other than sweet corn), whether or not suitable for use as fresh vegetables, are classified as cereals (FAO, 1994). Generally, cereals are members of the grass (gramineous) family (*Gramineae*), which include the cereal grains such as wheat, maize, and rice, as well as those of barley, rye, triticale, oats, sorghum and pearl millet. This type of fruit is commonly called a *kernel* or *grain*.

Legumes

Legumes and cereals have played an imperative role in ameliorating the challenges of undernourishment worldwide (Awuchi, 2019). They are rich sources of carbohydrates, protein and lipids and are used as major constituents in the formulation of starch and protein based food. Legumes are members of the bean family, *Fabaceae*, which includes all types of beans and peas as well as soybeans, peanuts, alfalfa and clover. This large, widely distributed family also includes various trees and ornamentals such as black locust, wisteria, lupine and the Texas bluebonnet.

Roots and Tubers

Root and tuber crops, including yam, cassava, potato and sweet potato are the most important food crops for direct human consumption in Africa. They are grown in varied agro–ecologies and production systems ranging from highland densely populated regions to lowland drier areas prone to droughts or floods. These four crops account for about 95% of the total root and tuber crops production in Africa and produce more than 240 million tons annually on 23 million hectares (Sanginga, 2015). The aggregate value of yam, cassava, potato and sweet potato exceeds all other African staple crops, and is much higher than the value of cereal crops (cereals annually producing on average 169 million tons from 108 million ha of land). The major root and tuber crops of the tropics are cassava (*Manihot esculenta* Crantz), yam (*Dioscorea* spp.), sweet potato (*Ipomoea batatas* L.), potato (*Solanum* spp.) and edible aroids (*Colocasia spp.* and *Xanthosoma sagittifolium*). They are widely grown and consumed as subsistence staples in many parts of Africa, Latin America, the Pacific Islands and Asia (FAO, 1977).

Cash / Tree Crops

These are orchards of trees grown for their economic and environmental benefits. Examples include: oil palm, coconut, cashew, rubber, etc.

Oil Crops

These are plants which grown mainly for the oil they produce. They are sometimes called oil–bearing crops. Sunflower, rapeseed and coconut are three examples of oil–bearing crops.

Spices and Herbs

The Geneva–based International Organization for Standardization (ISO) defines spices and condiments as: vegetable products or mixtures thereof, free from extraneous matter, used for flavouring, seasoning and imparting aroma to food. Herbs and spices play a pivotal role in the customary life of mankind as important flavouring agents in foods, beverages and pharmaceuticals and also as ingredients in perfumes and cosmetics (Peter, 2006). They have tremendous importance in the way we live, as ingredients in food, alcoholic beverages, medicine, perfumery, cosmetics, colouring agent and also as garden plants. Ginger, for instance, has been reported to have medicinal value and digestive aid as well as being a spiritual beverage (Bag, 2018). Spices and herbs have antioxidant, antimicrobial, pharmaceutical and nutritional properties (Peter, 2006). In addition to the known direct effects, the use of these plants can also lead to complex secondary effects such as salt and sugar reduction, improvement of texture and prevention of food spoilage. India is known the world over as the 'land of spices' (Peter, 2012). Generally, the leaf of a plant used in cooking may be referred to as a culinary herb, and any other part of the plant, often dried as a spice (Tapsell *et al*., 2006). Examples of spices and herbs include: pepper, aiden fruit, turmeric, garlic, onion, etc.

— ANIMAL FOODS

Animal foods, on the other hand, are those food materials which are obtained from living organisms of the fauna kingdom. There are equally different types of animal foods that can be identified.

Seafoods

These include all products of aquaculture whether natural or man–made. Seafood is any form of sea life regarded as food by humans, prominently fish (tilapia, catfish, sardine, etc.) and shellfish (such as clams, oyster mussels). Seaweeds and some algae plants called sea vegetables.

Dairy Foods

These are types of food produced from the mammary glands of mammals such as cows, goats, buffaloes, etc.). They contain milk. Examples of such products are dried and condensed milk, yoghurt, cheese, etc.

Poultry Products

Poultry are domesticated birds kept by man for their eggs, meat and, in some cases, feathers. Examples include: chicken, turkey, guinea–fowl, to mention but three.

Piggery Products

Piggery involves a branch of animal husbandry that has to do with raising pigs as livestock. It is the ability of the swineherd to manage the farm in such a way that there is a production of maximum number of marketable pigs in the shortest time possible influences the profit he makes over a period of one year (FAO, 2009).

FOOD SECURITY

Food security and nutrition are closely interlinked. It is essential in maintaining an optimum dietary status, and the requirement for nutritious food is fundamental to its definition, which refers not only to sufficient quantities of food (in terms of calories), but also to sufficient quality – in terms of variety and micronutrient content (Ghattas, 2014). Food security is intrinsically important to the ability of human to bloom. According to Barrett (2020), at the 1996 World Food Summit, a unanimous definition was proffered that *food security exists if and only if "all people at all times have physical, social, and economic access to sufficient, safe and nutritious food that meets their dietary needs and food preferences for an active and healthy life"*. The legal right to food has been recognized in treaties, including Article 25 of the 1948 Universal Declaration of Human Rights and Article 11.2 of the 1966 International Covenant on Economic, Social and Cultural Rights, and in the constitutions of countries (Vidar *et al*., 2014). The opposite side of this coin in discourse is food insecurity. It can affect diet quality in different ways, potentially leading to under–nutrition as well as overweight and obesity. Food insecurity can lead to different manifestations of malnutrition (FAO *et al*., 2020). One vital element that explains this connection is the food that people eat; specifically, the quality of their diet. Ensuring access to a healthy diet is a prerequisite for achieving the Sustainable Development Goals (SDG) target of eradicating all forms of malnutrition. Actually, an enough quantity of food has been; and is being produced in the world to feed its entire population. The unfortunate development is that there is a problem of access to the food – whether it be poverty or famine, discrimination, or lack of transportation. In order to ensure human rights as related to adequate standard of living, the creation of an enabling environment that provides for and allows for the procurement of adequate food becomes the mandate of government officials. Food would be adequate when the food is healthy and nutritious in a way our body requires to survival. Consuming nutritious food leads to numerous health benefits including, but not limited to, maintaining a healthy weight, allowing organs and the organ–systems to function optimally, and promoting sleep. For the most part, the good quality foods are on the high–priced side, which leads people to avoid it. Figure 1 shows the number of undernourished people in the world; it continued to increase in 2019. If recent trends are not reversed, the SDG 2.1 zero hunger target will not be met. The SDGs is shown in Table 1.

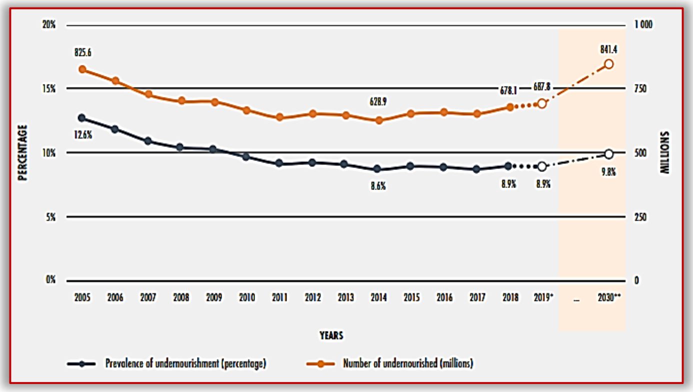

Note: Estimated figures are shown by dotted lines and empty circles. The shaded area signifies predictions for the longer period from 2019 – 2030 target year. The entire sequence was judiciously reviewed to reveal new information readily available.

Figure 1: The number of undernourished people in the world. Source: FAO *et al.* (2020)

Table 1: Sustainable Development Goals (SDGs)

NUMBER	STATEMENT
Goal 1	End poverty in all its forms everywhere.
Goal 2	End hunger, achieve food security and improved nutrition and promote sustainable agriculture.
Goal 3	Ensure healthy lives and promote well–being for all at all ages.
Goal 4	Ensure inclusive and equitable quality education and promote lifelong learning opportunities for all.
Goal 5	Achieve gender equality and empower all women and girls.
Goal 6	Ensure availability and sustainable management of water and sanitation for all.
Goal 7	Ensure access to affordable, reliable, sustainable and modern energy for all.
Goal 8	Promote sustained, inclusive and sustainable economic growth, full and productive employment and decent work for all.
Goal 9	Build resilient infrastructure, promote inclusive and sustainable industrialization and foster innovation.
Goal 10	Reduce inequality within and among countries.
Goal 11	Make cities and human settlements inclusive, safe, resilient and sustainable.
Goal 12	Ensure sustainable consumption and production pattern.
Goal 13	Take urgent action to combat climate change and its impacts.
Goal 14	Conserve and sustainably use the oceans, seas and marine resources for sustainable development.
Goal 15	Protect, restore and promote sustainable use of terrestrial ecosystems, sustainably manage forest, combat desertification, and halt and reverse land degradation and halt biodiversity loss.
Goal 16	Promote peaceful and inclusive societies for sustainable development, provide access to justice for all and build effective, accountable and inclusive institutions at all levels.
Goal 17	Strengthen the means of implementation and revitalize the global partnership for sustainable development.

Source: FAO et al. (2020)

— GLOBAL AND NATIONAL FOOD SECURITY

The world is attempting to be on track to achieve zero hunger by 2030. According to FAO *et al*. (2020), if recent trends continue, the number of people affected by hunger would surpass 840 million by 2030; and food insecurity can worsen diet quality and consequently increase the risk of various forms of malnutrition, potentially leading to under–nutrition as well as overweight and obesity.

GLOBAL FOOD SECURITY

The main concern of the world governments is to end hunger. The programme aims to ensure that at all times all people have physical, social and economic access to sufficient, safe and nutritious food that meets their preferences and dietary needs for an active and healthy life. The government of the United States of America (USA) is in the lead of the international efforts to address the need that people around the world have reliable food supply.

NATIONAL FOOD SECURITY

The government of every country ensures that its citizens and other people taking abode in such country have physical, social and economic access to adequate, safe and healthy food that meets their inclinations and dietary needs for an active and healthy life. Unfortunately, many in African country have fallen short of this laudable pursuit of many countries of the world. Food security becomes a policy when there is a conscious effort on the part of the government of any nation to make and enforce a law that gives the people right to food.

MAIN CONCERN FOR ACCOMPLISHING FOOD SECURITY AND IMPROVED NUTRITION

Augmenting Food Availability

The priorities for increasing the availability of food and the stability of food supplies include: national food production, food imports, and food aid through an additional element relating to ensuring that there is a strategic reserve of grain or other staple foods.

Value–added Access to Food

This has to do with right to utilize food. The priorities established to promote better food utilization and improved nutritional status. Institutional framework for strategy implementation may be achieved through organized governmental bodies to monitor food security and nutrition.

Formulation of Policy Statement

Policy statement formulation that guarantees self–reliance is necessary. The interest of the food security and nutrition strategy should be with food production – both for consumption by the households that produce it and for distribution through the market. As such, the resources dedicated to agricultural research and extension efforts to enhance food and livestock production is an essential element of the path to sustainable food security.

FOOD PRODUCTION

Taking Advantage of all Food Creation Outlooks

This will help address production constraints. In order to realize improvements in general welfare and poverty reduction, the food security of especially developing countries, should increasingly rely on smallholder production. However, this strategy also calls for increased attention to opportunities for production of foods that the country has a comparative advantage in a large scale agricultural enterprise.

Upgrading Post–harvest Handling of Foods

Food availability can be enhanced through increased attention to post–harvest handling. For example, small–scale mechanized cassava value chain provided by private entrepreneurs will in particular, enhance market demand for the country's cassava. Establishment of local, say, rice mills would result in more local rice in the market thereby reducing demand for imported rice. Other approaches to improving processing and reduction of food wastage in storage should be explored.

Diversification of Food Products

The central concern for most developing countries of Africa is the reduction of both hunger and expenditure on food imports. Countries that have heavily depended on food imports until now are looking for new approaches to increase the use of locally grown crops (Abass *et al*., 2016); and research efforts on making gluten–free bread have been increasing rapidly (Masure *et al*., 2015). Strategic attention should be paid to diversification in the food produced domestically in the nations – cereals, legumes, roots and tubers, vegetables, fruits and livestock. The benefits of doing this include: increased diet diversity (associated with improved micronutrient intake) thus reducing micronutrient–deficiency effects; and a more expanded food system which is more resistant to shocks, principally those associated with crop and livestock epidemic – diseases or pest infestations.

Deliberately Safeguarding Key Collective Assets and Incomes

Local production of food is enhanced through the deliberately safeguarding the key assets (such as forests, waters, and other ecosystems that are important for the production of food plants and animals, games and fish) collectively reserved. As government formulates management mechanisms and administers same for these assets, the protection role in contributing to the food security of the communities in their environs and to the nation all together would be guaranteed.

Tactical Food Reserve

Availability of food under all circumstances in any country must be planned. A key element of such planning in many countries in sub–Saharan Africa is the establishment of a strategic backup for staple foods as it is done in Nigeria; though not sufficient for her teeming population. Many of the factors that stimulate the creation of such reserves in some countries are natural disasters such as droughts and other weather–related calamities. Underprivileged access to imported foods may not apply to some other countries. Strengthening strategic food reserve mechanisms, perhaps in part, because the risks of severe disruptions to food systems in the country is necessary. While this system may prove to be adequate, more rigorous analysis of how the country can reliably maintain rapid access to adequate food supply is indispensable. Peradventure it exists; appropriate use of international food assistance should be ensured. However, such food assistance is a potentially useful resource for consolidating social and economic recovery and for development in the country where it applies. Also of critical status are food–based interventions such as nutrition supplements targeted at pregnant and breast–feeding women, infants and school children.

Enhancement of the Access to Use Food

Increasing people's access to food mainly centres on the jurisdictions of increasing opportunities for a reliable source of income. Improving the extant communication and distribution network will boost physical access to food.

Better Food Consumption and Value–added Diets

Disparity in availability of food or access to food does not provide a complete explanation for the key determinants of food security and comprehensive nutritional status. This is evident in the persistent high levels of chronic child under–nutrition, especially in some third–world countries, even when the presence of war is not obvious.

— NEW FOODS FORMULATION & VALUE ADDITION AS PANACEAS FOR GLOBAL & NATIONAL FOOD SECURITY

Igbabul *et al.* (2014) has noted that in some years past, there has been an enhanced inclination towards healthy eating resulting from the development of many novel functional foods together with use of other locally obtainable crops for bread production. In the baking industry, there has been an increasing trend in the usage of non–wheat flours in the manufacture of baked goods such as bread, cake, biscuit, snacks, pasta products and other confectioneries (Oladunmoye *et al.*, 2010). Such products, that have found acceptability worldwide, are used to increase protein intake especially in developing countries (Satin, 1988). Minerals contents and dietary fibre of baked products can be enhanced by composite flours (Karina de Simas *et al.*, 2009). The use of indigenous raw materials in replacement for wheat flour is increasingly necessary (Ajibola and Olapade, 2019). Cassava (*Manihot esculentum* Crantz) is a target for biofortification because of its importance as a staple crop. The Bill and Melinda Gates Foundation has supported a global effort to develop cassava germplasm enriched with bioavailable nutrients since 2005. This initiative is called 'BioCassava Plus', and has 6 major objectives, namely; to increase the: zinc and iron; protein; vitamins A and E as well as to decrease cyanogen content; delay postharvest deterioration; and develop virus–resistant varieties (Montagnac *et al.*, 2009). Figure 2 shows the uses of the derivatives of cassava, a typical case of value addition.

The development of cassava value chains focus on the following top 20 cassava producing countries in Africa (in decreasing order of annual production: Nigeria, Democratic Republic of the Congo, Angola, Ghana, Mozambique, Uganda, Malawi, United Republic of Tanzania, Cameroon, Sierra Leone, Benin, Madagascar, Rwanda, Côte d'Ivoire, Burundi, Congo, Guinea, Kenya, Zambia, Togo (Sanginga, 2015). Abass *et al.* (2016) have suggested that more study is needed to accomplish a sustainable progress in the conversion of raw cassava roots into cassava flour for production of bread.

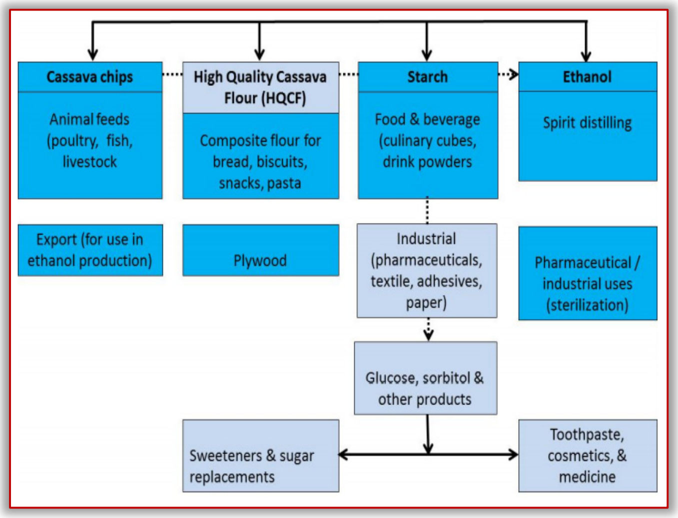

Figure 3: Cassava Derivatives and Their Uses. Source: Sanginga (2015).

The vision for sustainability for African cassava industrialization is expected to create wealth, jobs and promote sector–wide efficiency and productivity growth. It will enhance and meet the demand of emerging industrial needs, traditional products and global demand by reducing production costs and increasing the output of high quality industrial products to strengthen the continent's position in the global context for competition. Five major cassava value chains are proposed for industrialization based on the demand and supply side targets for various African countries and elsewhere as estimated from the FAOSTAT's database: High Quality Cassava Flour (HQCF), starch, chips, high fructose cassava syrup (HFCS) and ethanol (Riley–Mitchell *et al.*, 2012). These value chains offer tremendous potential to fuel the economic growth in the continent as this will create jobs for women and youth, improve food security and generate wealth. Production should be expanded to: (i) meet domestic, industrial demand and export markets through promotion of industrial applications of key value chains (HQCF, livestock feed, starch, ethanol, etc.); (ii) encourage the involvement of large scale farming as a driving force for industrialization; and (iii) encourage private sector investment and engagement. Each country can develop her industry according to her available resources and market opportunities within a globally competitive framework. The limited number of processed forms of yam, poor market linkages and inconsistent policies affecting prices of other cheap energy sources lead to inconsistency in demand or prices of yam tubers for producers. A broader and more diverse range of products will help make the demand for yam more constant and thus reduce risks for yam producers, processors and traders. Increased conversion of fresh ware yams to products with longer shelf life through processing combined with improvements in marketing channels will bring the benefits from the crop to a broader range of consumers and value chain actors. It will reduce the annual postharvest losses; extend the period of availability; increase competitiveness in terms of affordability to increase yam consumption when compared to rice, maize and wheat; and give actors in the yam value chains additional flexibility to respond to market opportunities (seasonally fluctuating market prices). The conversion of fresh ware yams to other products which are more convenient for the rapidly expanding urban populations to handle and prepare into food will cater better to their needs and broaden the range of regular yam consumers. Activities will include:

- study and document the status and potential of manufacturing and marketing of novel yam products;
- conduct workshops to promote opportunities for novel yam products among the value chain actors (producers, processors, traders, transporters, exporters, consumers, policy makers, input suppliers, and research and development agencies);
- organize consultation meetings with value chain actors;
- undertake industrial trials with processors/factories to identify suitable yam varieties;
- develop, and assess consumer acceptability and market potential of novel yam–based products;
- promote consumption of novel and improved traditional yam–based products through social marketing;
- train processors in the preparation of new yam–based products and in improving processing efficiency, nutritional quality, food safety (including avoidance of mycotoxin accumulation), and storage of traditional products;
- adapt, fabricate, and introduce appropriate yam processing equipment for small– and medium–scale processors and train them in their use.

Expected benefits include: (i) increased availability in domestic and export markets, and consumption of diverse new and traditional food products from yam; (ii) yam products meet all established standards of quality, packaging and safety in the relevant markets (e.g. mycotoxin content below the threshold levels); and (iii) entrepreneurs make better evidence–based decisions on models, tools, and technologies for upgrading sweet potato value chains. Process models, technologies, and implementation tools are becoming available for scaling up that support integrating OFSP into multiple value chains, ranging from community–based nutrition/agriculture and school–feeding programs to higher–value urban market chains for bakery products and healthy–choice snack food.

These technical and organizational tools will enable stakeholders to better manage the perishability of sweet potato roots and position it as a healthy food for all in the market place. According the report of Barrett (2020), the 1960s–70s Green Revolution in Asia and Latin America surpassed even the improvement seen earlier in the high–income countries as increased in investment Research and Development drove up the yields of staple crops. This allowed a fast–growing population to consume more calories and protein. The rapid development and diffusion of high–yielding varieties of maize, rice, wheat, and of inorganic fertilizers, irrigation, and machinery, fueled rapid productivity growth. This brought down real food prices sharply, improving calorie and protein access among the poor. It also gave way to the development of new foods. Food concerns would follow from the extensive stress on curbing starvation through calorie and protein supplies increase using starchy staple foods. Given faster growth in staple cereals, roots and tubers, the price of micronutrient–rich fruits, legumes, pulses and vegetables has risen relative to that of staples in many places (Pelletier *et al*., 2020). Food processors, manufacturers, retailers and food service firms should be seeking better ways of presenting their products. Such ways shall include adding more values to, and formulating diverse foods from the existing diets. As the climate predicament is also going faster, changeovers from fossil fuels to renewable energy sources are growing. In the same manner diverse and more nutritious diets should be fabricated. Cassava (*Manihot esculenta crantz*) with improved nutritional value such as pro–vitamin A cassava is currently been used as an aid in reducing the prevalence of dietary Vitamin A deficiency due to its high content of β–carotene . Pro–vitamin A cassava has the potential of providing up to 25% of daily vitamin A requirements of children and women (Aniedu and Omodamiro, 2012). FAOSTAT (2019) has posited that Africa needs more diversification of cassava as food product since her major area of utilization is as food. Starch and protein from cereals, meat, fish and other sources play major roles in providing the desirable characteristics of food. Composite flour technology is being used in developing more nourishing foods globally and nationally. This in effect is important because of the benefit of reducing the economic strangulation due to food importation. In addition, there are the prospects of the utilization of underutilized crops (Ajatta *et al*., 2016). The hospitality industry and the general public have found new healthful products in wheat–cassava composite (Ibrahim and Ukonu, 2016). Some diets have been, and are being formulated to equally have medicinal purposes; a development which has brought about a branch of studies called *Nutraceutics*. As a matter of fact, while bringing colour and taste to the food, some spices have long been considered to possess medicinal value and have been effectively used in the indigenous systems of medicine (Rubio *et al*., 2013). Spices and herbs are common food additions, which over the years, have been used as agents of flavoring, seasoning, and coloring and sometimes as preservative, all over the world for several hundreds of years, especially in India, China, and many other southeastern Asian countries. Herbs and spices have a customary account of usage in the food appreciation, and its links to health (Tapsell *et al*., 2006). However, with the passing of time, spices had become indispensable in the culinary art of cooking to enhance flavour and taste of foods and beverages (Peter, 2012). With the development of procedures for the extraction of spice extracts, spices are extensively used in the perfumery, cosmetics and pharmaceutical industries. The technology of Nutraceutics has led to formulation of gluten–free starchy foods to present a friendly form of foods to coeliac patients. The potential nutraceutical characteristics of starchy products have increased the interest of researchers on this biopolymer (Bello–Perez and Paredes–Lopez, 2009). Nisar *et al*. (2021) developed cookies from wheat flour enriched with powder from apricot pulp so as to improve nutraceutical properties of cookies as well as simultaneous dilution of gluten. Kaur and Bains (2020) have reported the nutraceutical and physiochemical properties, hence the benefits of chia to both humans and nonhumans alike. In the report of Alamu and Mooya (2017), food processing technologies have advanced at unparalleled levels concurrently with the developing global food system both in its degree and in its intricacy. All through the times gone by, humans conquered lack of food and ailments not only by way of harvesting foodstuffs from cultivated lands, but also by dint of processing it through available and sophisticated techniques. The commitment of authorities in Food Science and Technology to making progress in the science of food safeguarding a harmless and abundant food supply in addition to making contributions to healthier people the world over is fundamental to that advancement (Floros *et al*., 2010). Not only those functional foods can be used to solve consumer starvation and provide health needs by having the necessary nutrients, they likewise can be used to prevent diseases which are related to nutrient shortages. In the intervening time, useable bakery products are becoming gradually popular and are normally consumed with some attachments in numerous households, industrial canteens, restaurants and such other places (Rahaie *et al*., 2012).

The food processing industry is one of the largest manufacturing industries universally (Ortega–Rivas, 2010). Researchers are expected to find new models of food development, taking cognizance of the complications intrinsic in the food material. Fito *et al*. (2010) considers “real foods” as multiphasic and multicomponent systems in which the structure plays a key role in product properties – be it physical, nutritional, sensory or safety. Quinn and Bencko (2014) have rightly stated that the public health issues of imbalanced nutrition, scanty access to food and misappropriation of resources – at the governmental and household levels – are presently affecting billions of people globally. Imbalance of food nutrition can be curbed through diversification of food products. In view of the trend of consumption of bakery products among the populace, there need to improve the nutritional value of empty calorie baked products as they are consumed very frequently (Seth and Kochhar, 2017). With increased utilization of indigenous staples, the challenge of limited access to food may be arrested. In many cases of unavailability of food, the root cause may not be less cultivation or yield, but lack of appropriate storage facilities. In the course of new foods formulation and modification, developing food materials with longer storage life automatically falls in. The report of Berry *et al*. (2015) has shown that there has been growing agreement that sustainability is very relevant to food security over the past years. Thus availability of food is not secure if it cannot meet the current needs without jeopardizing the requirements of the succeeding generation. According to Capone *et al*. (2014), humanity, both per person and in absolute terms, is now consuming additional resources than ever. Necessary changes in the consumption and production patterns of societies are crucial for achieving global sustainable development. Since food demand surge is due mainly to changing food consumption patterns and population growth (Berry *et al*., 2015), need therefore arises for re–ordering the consumption patterns by way of presenting assorted and novel foods; perhaps from a combination of two or more food materials. This will make formulation of new foods work like division of labour which lessens task on an individual, yet produces a superb result from synergy of different people. New and diverse foods will have different people with dissimilar inclinations thereby reducing demand pressure on a particular foodstuff.

CONCLUSION & RECOMMENDATION

Food is taken by living plants and animals – man inclusive – in order to be alive. Giving more concern to man, it would be viewed that the right to food is a fundamental human right that has to be respected and protected. Good nutrition is a key to a person’s health. Food products are derivable from plants and animals. Malnutrition is as a result of food insecurity as it can affect diet quality in different ways. The Sustainable Development Goals (SDG) programme of the United Nations is expected to help eliminate all forms of malnutrition. When governments are committed to providing food for the citizens, they make food security a ‘Policy’. Food Security is achieved through boosting accessibility to food, making policy statement, improved usage of food with better nutritional status, and a tactical backup for foods already produced. If the matter of food security is continually lackadaisically handled, the number of people that shall be sentenced to near irredeemable undernourishment may exceed the predicted 840 million before the anticipated time of 2030.

Steps to ensuring food security at global and national levels should prominently centre on creation of new foods with value addition.

References

[1] Abass, A. B., Awoyale, W., Alenkhe, B., Ndavi, M. B., Asiru, W., Manyong, V. and Sanginga, N. : Can food technology innovation change the status of a food security Crop? A review of cassava transformation into “Bread” in Africa, Food Reviews International, 2016.

[2] Adeyeye, S. A. O. : The role of food processing and appropriate storage technologies in ensuring food security and food availability in Africa. Nutrition and Food Science, Vol. 47, No. 1, pp. 122 – 139, 2017.

[3] Adeyeye, S. A. O. and Idowu–Adebayo, F.: Genetically modified and biofortified crops and food security in developing countries: A review. Nutrition and Food Science, Vol.

49 No. 5, pp. 978 – 986, 2019.
[4] Ajatta, M. A., Akinola, S. A. and Osundahunsi, O. F.: Proximate, functional and pasting properties of composite flours made from wheat, breadfruit and cassava starch. Applied Tropical Agriculture, Volume 21, No. 3, pp. 158 – 165, 2016.
[5] Ajibola, G. O. and Olapade, A. A.: Physico–chemical and functional properties of cassava and African yam bean flour blends. Applied Tropical Agriculture, Volume 24, No 1, pp.200 – 207, 2019.
[6] Akerele, D., Momoh, S., Aromolaran, A. B., Oguntona, C. R. B. and Shittu, A. M. : Food insecurity and coping strategies in South–West Nigeria. Springer Science Business Media Dordrecht and International Society for Plant Pathology, pp. 407 – 414, 2013.
[7] Alamu, E. O. and Mooya, A.: Food processing technologies and value addition for improved food safety and security. Smart Technologies for Smallholder Agriculture, pp. 201 – 210, 2017.
[8] Aniedu, C. and Omodamiro, R. M.: Use of newly bred β– carotene cassava in production of value–added products: Implication for food security in Nigeria. Global Journal of Science Frontiers Research, 12, 11 – 16, 2012.
[9] Awuchi, C. G.: Proximate composition and functional properties of different grain flour composites for industrial applications. International Journal of Food Sciences, Vol. 2, Issue 1, No. 4, 43 – 64, 2019.
[10] Bag, B. B.: Ginger processing in India (Zingiber officinale): A review. International Journal of Current Microbiology and Applied Sciences, 7 (04): 1639 – 1651, 2018.
[11] Barrett, C. B.: Overcoming global food security challenges through science and solidarity. American Journal of Agricultural Economics, 00 (00): 1 – 26, 2020.
[12] Bello–Perez, L. A. and Paredes–Lopez, O.: Starches of some food crops, changes during processing and their nutraceutical potential. Food Engineering Review, 1: 50 – 65, 2009.
[13] Berry, E. M., Dernini, S., Burlingame, B., Meybeck, A. and Conforti, P.: Food security and sustainability: Can one exist without the other? Public Health Nutrition, 2015.
[14] Capone, R., Bilali, H. E., Debs, P., Cardone, G., and Driouech, N.: Food system sustainability and food security: Connecting the dots. Journal of Food Security, 2 (1), 13 – 22, 2014.
[15] FAO: Cassava flour and starch: Cassava processing. FAO Plant Production and Protection Series No. 3, 1977.
[16] FAO: Definition and classification of commodities (cereals and cereal products). Food and Agriculture Organization of the United Nations, 1994.
[17] FAO: Farmer's Hand Book on Pig Production. Food and Agriculture Organization of the United Nations; GCP/NEP/065/EC, 2009.
[18] FAO, IFAD, UNICEF, WFP and WHO: The state of food security and nutrition in the world 2020. Transforming food systems for affordable healthy diets. Rome, FAO, 2000.
[19] FAOSTAT: Food and Agriculture Organization (FAO) of the United Nations, Statistics Division, Rome, Italy, 2019.
[20] Fito, P., Le Maguer, M., Aguilera, J. M., Mayor, L., Seguí, L., Betoret, N. and Fito, P. J.: The SAFES methodology: A New Approach for Real–Food Modeling, Optimization, and Process Design. In: Processing Effects on Safety and Quality of Foods. Contemporary Food Engineering Series; 525 – 544, 2010.
[21] Floros, J. D. Newsome, R., Fisher, W., Gustavo, V., C'anovas, B., Hongda, C., Dunne, C. P., Bruce, J. B., Hall, R. L., Heldman, D. R., Karwe, M. V., Knabel, S. J., Labuza, T. P. Lund, D. B., McGloughlin, M. N., Robinson, J. L., Sebranek, J. G., Shewfelt, G. L., Tracy, W. F., Weaver, C. M. and Ziegler, G. R. : Feeding the world today and tomorrow: The importance of food science and technology. Comprehensive Reviews in Food Science and Food Safety, Vol. 9, 572 – 599, 2010.
[22] Ghattas, H.: Food Security and Nutrition in the Context of the Global Nutrition Transition. Food and Agriculture Organization (FAO) of the United Nations Rome, 2014.
[23] Ibrahim, A. and Ukonu, I. C..: Using Composite Flour in Bread Making: Cassava and Wheat Flour. Journal of World Academy of Science, Engineering and Technology International,14 (12), 2016
[24] Igbabul, B. D., Amove, J. and Okoh, A.: Quality evaluation of composite bread produced from wheat, defatted soy and banana flours. International Journal of Nutrition and Food Sciences. Vol. 3, No. 5, pp. 471 – 476, 2014.
[25] Karina de Simas, N., Vieira, L. and Podesta, R.: Effect of king palm (Archontophoenix alexandrae) flour incorporation on physicochemical and textural characteristics of gluten–free cookies. International Journal of Food Science and Technology, 44, 3 – 10, 2009.
[26] Kaur, S. and Bains, K.: Chia (Salvia hispanica L.) – a rediscovered ancient grain, from Aztecs to food laboratories: A review. Nutrition and Food Science, Vol. 50 No. 3, pp. 463 – 479, 2020.
[27] Masure, H. G., Fierens, E. and Delcour, J. A.: Current and forward looking experimental approaches in gluten–free bread making research, Journal of Cereal Science, 2015.
[28] Montagnac, J. A. Davis, C. R. and Tanumihardj, S. A.: Nutritional value of cassava for use as a staple food and recent advances for improvement. Comprehensive Reviews in Food Science and Food Safety, Vol. 8, pp181 – 194, 2009.
[29] Nisar, A., Jan, N., Gull, A., Masoodi, F. A., Amin, T., Bashir, O. and Wani, S.M.: Effect of the incorporation of apricot pulp powder on physicochemical, functional, rheological and nutraceutical properties of wheat flour based cookies. British Food Journal, 2021.
[30] Oladunmoye, O. O., Ojo, A., Akinoso, R. and Akanbi, C. T.: Thermo–physical Properties of Composite Bread Dough with Maize and Cassava Flours. International Journal of Food Science and Technology, 45, 587 – 593, 2010.
[31] Omorogiuwa, O., Zivkovic, J. and Ademoh, F.: The role of agriculture in the economic development of Nigeria. European Scientific Journal, 10: pp.113 – 147, 2014.
[32] Ortega–Rivas, E.: Food Preservation Technologies. In: Processing Effects on Safety and Quality of Foods. Contemporary Food Engineering Series: 3 – 10, 2010.
[33] Pelletier, J., Ngoma, H. Mason, N. M. and Barrett, C. B.: Does smallholder maize intensification reduce deforestation? Evidence from Zambia. Global Environmental Change 63: 102 – 127, 2020.
[34] Peter, K. V.: Herbs and Spices. In: Handbook of Herbs and Spices, Vol. 3, USA, Woodhead Publishing Limited and CRC Press LLC, 2006.
[35] Peter, K. V.: Handbook of Herbs and Spices. Second Edition. Vol. 1, USA, Woodhead Publishing Limited, 2012.
[36] Quinn, J. and Bencko, V.: Food Security, Public Health, Financial Regimes and International Law, 2014.
[37] Rahaie, S., Gharibzahedi, S. M. T., Razavi, S. H. and Jafari, S. M: Recent developments on new formulations based on nutrient–dense ingredients for the production of healthy–functional bread: A review. Journal of Food Science and Technology, 2012.
[38] Riley–Mitchell, D., Badrie, N. and Yarde–Blackman, J.: Cassava (Manihot esculenta Crantz)–wheat flour composite muffins: Effects on quality and sensory characteristics. Tropical Agriculture (Trinidad), Vol. 89, No. 2, 104 – 112, 2012.
[39] Rubio, L., Motilva, M. J. E. and Romero, M. P.: Recent advances in biologically active compounds in herbs and spices: A review of the most effective antioxidant and anti–inflammatory active principles. Critical Reviews in Food Science and Nutrition, 53: 943 – 953, 2013.
[40] Sanginga, N.: Root and Tuber Crops (Cassava, Yam, Potato and Sweet Potato) Background Paper. Feeding Africa Conference, at Abdiou Diof International Conference Centre, Dakar, Senega, October 21 – 23, 2015.
[41] Satin, M.: Bread without wheat. New Scientist, 28, 56 – 59, 1988.
[42] Seth, K. and Kochhar, A.: Formulation and nutritional evaluation of baked products supplemented with partially defatted peanut flour. Nutrition and Food Science, Vol. 47 No. 6, pp. 808 – 816, 2017.
[43] Tapsell, L. C., Hemphill, I., Cobiac, L., Sullivan, D. R., Fenech, M., Patch, C. S., Roodenrys, S., Keogh, J. B., Clifton, P. M., Williams, P. G., Fazio, V. A. and Inge, K. E.: Health benefits of herbs and spices: The past, the present, the future. Medical Journal of Australia, 185 (4), S1 – S24, 2006.
[44] UNCTAD – The United Nations Conference on Trade and Development: The role of science, technology and innovation in ensuring food security by 2030. The United Nations New York and Geneva, 2017.
[45] Vidar, M., Kim, Y. J. and Cruz, L.: Legal Developments in the Progressive Realization of the Right to Adequate Food. FAO Thematic Study 3, 2014.

ISSN: 2067–3809

[1.]Nikhil V. NAIK

COIL BREAKS PREDICTION IN SKIN PASS MILL USING CLASSIFICATION ALGORITHM IN MACHINE LEARNING

[1.] Dept. of Mechanical Engineering. Viva Institute of Technology. Mumbai University, Maharashtra, INDIA

Abstract: Coil breaks are persistent menace for almost every Cold Rolling steel plant. The uncertain demand flow pattern combined with extreme competitive environment has made the steel industry Quality driven. The steel industry consists of processes like Iron Making, Steel Making, Casting, Hot Rolling, Cold rolling, etc. Cold rolling being end process considers defects as wastage of all previous processes, costs, and time invested to achieve the product. Quality defects are considered grave problems for any cold rolling production line. The study aims to predict the formation of coil breaks by use of an artificial neural network at Skin pass mill. The study is conducted at the Tata Steel Cold Rolling Complex (CRC-West) at Tarapur Midc, Boisar. At CRC-W the production lines present are Pickling, 4 hi Rolling mill, Cleaning, Annealing, Skin pass mill, Slitting, Multi blanking line, Cut to length. We are concerning ourselves with the formation of coil breaks at the Skin pass mill. The coil breaks occurs as a result of non-uniform yielding behavior post forming. Typically observed in Deep drawn and extra deep drawn material, however it can also occur in under stabilized IF steel. Prediction of the formation of coil breaks can be done by an artificial neural network program. An ANN is computing system that learns to perform tasks by considering examples and data sets, generally without being programmed with task-specific rules. The appropriate ANN model is to be developed. The input and output parameters of each of these cases have been decided based on criteria as discussed later. With the Input and Output parameters decided, now the dataset can be taken from the tracking software at the Skin pass mill. The Artificial neural network must be trained so as to increase reliability. The trained ANN must now be validated and tested using a program called Python. The ANN will start predicting if coil breaks will occur or not after skin passing using parameters. The accuracy of ANN will increase as size of dataset increases so for further applications; the ANN could be upgraded to include real time monitoring and prediction.

Keywords: coil breaks, skin pass mill, artificial neural network, cold rolled coils, non-uniform yielding, data sets, load, tension, prediction, analysis

INTRODUCTION

The Coil breaks mainly occur due to the material internal defects. The occurrences of coil breaks and their causes have not been studied properly. This dataset is originally from Tata Steel depository. The objective is to predict whether a coil break occurs or not. We use Python to make the artificial neural network. Python is an important language for machine learning as it removes complex operations. Its extensive library and machine learning concepts are very helpful. We use supervised learning, in which datasets and learning is predefined to make the model. The work for project is undergone at Tata Steel, Tarapur which is a cold rolling plant.

Artificial neural network is a structure patterned on the human brain. It contains the compound layers of straightforward processing elements called neuron. Certain of its neighbors with coefficients of connectivity that represent the strengths of these connections are linked to each of the neurons. The overall network learns by adjusting these strengths to output appropriate results. Diagnostic systems, biochemical analysis, image analysis and Internet Algorithm are the various areas where artificial neural network is used successfully. An ANN is a flexible mathematical structure that is capable of identifying complex nonlinear relationships between input and output data sets [1].

In Steel plants systems, normally artificial neural network are used to detect Surface defects. In chemical analysis artificial neural network have been used to analyze Iron and copper samples, track rust levels in pipes and detect conditions such as blowholes. Spots detection on coils, classification of materials according to grades and determination of skeletal age from x-ray images are some of the applications where artificial neural network is being used for image analysis.

Human brain contains (10)^14 tiny cells called Neurons. A neuron is composed of a cell body, a tabular axon and a multitude of hair like dendrites. The dendrites form a very tiny filamentary brush surrounding at the body neuron. The axon is a long, thin tube that splits into branches terminating in little end bulbs that touch the dendrites of other neuron cells. The Synapse is called a small gap between an end bulb and a dendrite. The axon of a single neuron forms synthetic connections with many other neurons. The neuron that produces a signal refers to pre synaptic side of the synapse. The post synaptic side refers in the neuron that receives the signal.

The aim of this this study is to better predict and understand the defect of coil breaks which are formed on the steel coils using the artificial neural network.

LITERATURE REVIEW

The study conducted by authors N. Q. Hung, M. S. Babel, S. Weesakul, and N. K. Tripathi entailed the use of artificial neural network to better forecast rainfall in Bangkok, Thailand. A real world case study was set up in Bangkok ; The ANN models were developed using 4 years of hourly data after 75 rain gauge stations in the area. The developed ANN model is being applied for real time rainfall forecasting and flood management in Bangkok, Thailand. Distinct network types were tested with different kinds of input in-formation targeted at providing forecasts in a near real time schedule,. Preliminary tests showed that a generalized feed-forward ANN model using hyperbolic tangent transfer function achieved the best generalization of rainfall. Especially, the use of a mixture of meteorological parameters (relative humidity, air pressure, wet bulb temperature and cloudiness), the rainfall at the idea of forecasting and rainfall at the neighboring stations, as an input data, advanced ANN model to concern with continuous data containing rainy and non-rainy period, permissible model to subject forecast at any moment [2].

Another study focuses more on simulation and advanced calculations. In this study the focus of author Masoud Bakhtyari Kia is to develop a flood model using various flood causative considerations using ANN techniques and geographic information system (GIS) to modelling and replicate flood-prone areas in the southern part of Peninsular Malaysia. The ANN model for this study was established in MATLAB applying seven flood causative factors. Relevant thematic levels (including rainfall, slope, elevation, flow accumulation, soil, land use, and geology) are generated utilizing GIS, remote sensing data, and field surveys. In the context of objective weight assignments, the ANN is used to directly produce water levels and then the flood map is constructed in GIS [3].

In this particular interesting study author D.A. Fadare used the predictive and simulative abilities of artificial neural network to make a model which shows the solar energy potential in Nigeria. The outcomes show that the correlation coefficients between the ANN forecasts and actual mean monthly global solar radiation intensities for training and testing datasets were higher than 90%, thus suggesting a high dependability of the model for appraisal of solar radioactivity in locations where solar radiation data are not obtainable. The forecasted solar emission values from the prototype were given in form of quarterly maps. The monthly mean solar emission capacity in northern and southern regions ranged from 7.01–5.62 to 5.43–3.54 kWh/m2 day, respectively. A graphical user interface (GUI) was created for the function of the model. The model can be used easily for estimation of solar emission for primary layout of solar applications [4].

PROBLEM DEFINITION

The Problem to be highlighted in the project is the prediction of coil breaks. We are specifically targeting coil breaks formed at Skin pass mill as it is within our scope. There are two types of coil breaks, first is formed at a hot rolling mill and second is formed at Skin pass mill which comes under cold rolling process. As the plant does cold rolling process we can study coil breaks at Skin pass mill. The 80/20 rule is applied and the defects are segregated. We see that the 84.5 % of all the defect tonnages occurs in 3 defects namely coil breaks, rubbing and work roll marks. Nearly 50 % of the tonnages occur in Coil breaks generated at SPM. The defect Coil breaks generated at SPM must be considered and studied as this successful study can help to reduce defect tonnages. The major fact to be considered is that the defect occurs in final stages of overall factory production lines which render all the material cost used before waste.

The problem is severe at plant level as it forms at the skin pass mill which is final process of the cold rolling process and any defect can undermine all the previous work and cost applied to the material. The prediction of the coil breaks is very difficult due to its running condition. So we are training a python run artificial neural network to predict the formation of coil breaks.

DATASET

The dataset contains the 9 attributes in total. The inputs as a whole are of cold rolling coils. The dataset is in two forms namely Data depository and Defect data. The Data depository is very useful to solve the major problems faced at the company due to its availability and storage of data. The Defect data is made available by the Quality department which collects the relevant data regarding all the defects in the company. The month of September is taken as a random month. We first took the coil breaks occurring in the particular month of September. The overall input data contains Average speed of the mill, Rolling force actual average, Elongation Average, Elongation SP average, POR tension average, Recoil tension average, Negative bending, Positive bending, Output in form if coil break occurs or not. Now we will trace which coils have shown coil breaks in the Quality checks. The coils which have coil break will be tagged as “1” for output and the coils which do not have coil breaks will be tagged as “0”.

The skin pass mill has many defects, but the coil breaks are shown to be most persistent one and have nearly 50 % of defect tonnage of all defects at the machine. The skin pass mill is nearly end process for cold rolling process [5]. So any defects at this step would result in the loss of all factors applied for the material. Instability in the plastic flow is generally characterized by the appearance/formation of deformation bands on the material surface at the macroscopic scale. These deformation bands induce surface roughness thereby affecting the surface quality of sheet metal products during metal forming operations such as deep drawing, stamping and also during loading conditions while the component is in service.

METHODOLOGY

The methodology involves the collection of data which can be done by data depository. We have already specified the procedure. The analyzing of the input parameters involves data preprocessing by scaling values in form close to 0 or 1. The scaling of data is important as it helps in the further calculations. The normalizing of the parameters involves making data correlations; it helps for establishing relationships between the data values.

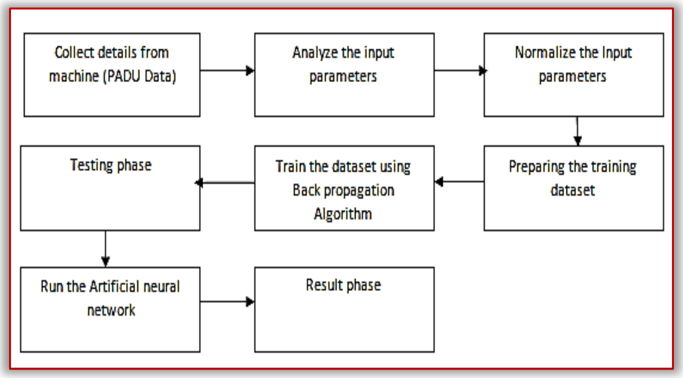

Figure 1. Block diagram for methodology

Around 89 data sets were collected from Tata Steel repository where the data is collected from storage, problem troubleshooting, etc. The primary data involved the total number of coil breaks in month of September. Then the coil number for each was matched with main datasets for the machine. The Data is then portioned in ratio of 80:20. The further process involves the training phase in neural network which would take 80 % of the data set and train it.

The Logistic regression is a predictive analysis module which is used when the output or value takes a form of binary type of data [6]. Here the output is 0 or 1 which is binary. The K neighbor classifier is a statistical recognition module. It is used to determine the nearest value to the given answer. So the issue of the which is nearest 0.6 or 0.4 to 1 can be easily solved. The Gaussian naive Bayes is used as a conditional probability, It assumes all the factors have impact on results and calculates probability accordingly. The Support vector classifier is approximate line which divides two data like coil breaks occur or not on a graph. The Testing step is also an important one as the 20 % of the data testing will enable further increase in accuracy in the model.

The artificial neural network program is now run, we create a fake coil which would be required to input data for which it is to be tested. The input for the coil which is to be checked will involve all the inputs only the coil break input in form of 0 or 1 is not to be input. The artificial neural network will predict this data in array form with 0 or 1 as output.

EXPERIMENTS

The histogram shows the input relationship for individual inputs. The density is high at the Average speed, Elongation average and rolling force average. But the clarity is not seen for the inputs. We have now seen the possible relations in these three inputs on output. Further perfection can be achieved by the program output.

Starting with pair plot we will start exploratory analysis. One thing that we were able to deduce from the pair plot was that all the parameters overlap for the Outcome value, i.e., no matter if coil break occurs or not, you can have the same parameters.

Next in our list was the heat map plot which did give us some insight about the parameters and the relation it has with the other parameters and the Outcome as well.

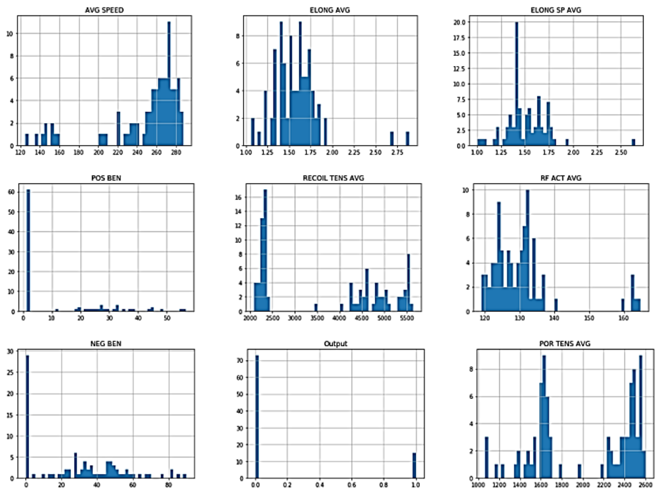

Figure 2. Histogram for all the inputs using Python

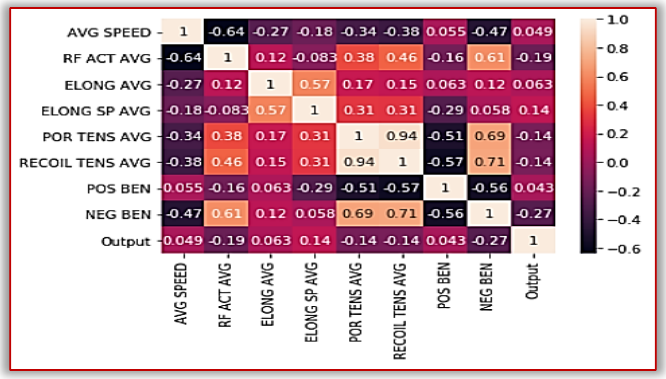

Figure 3. Heat Map for inputs using Python for the model

We find that some pairs have relationship like

- Negative bending and rolling force,
- Elongation average and Elongation SP average,
- POR Tension and recoil tension,
- Negative bending and recoil tension.

This heat map has shown that along with elongation average, POR tension average some factors like Recoil tension average and Negative bending are also significant. Heat map along with histogram has confirmed the effect of Negative bending, elongation average, POR tension, recoil tension on the coil break formation.

So now we make a feature significance plot using the python, it will show all the significant factors after computing the data.

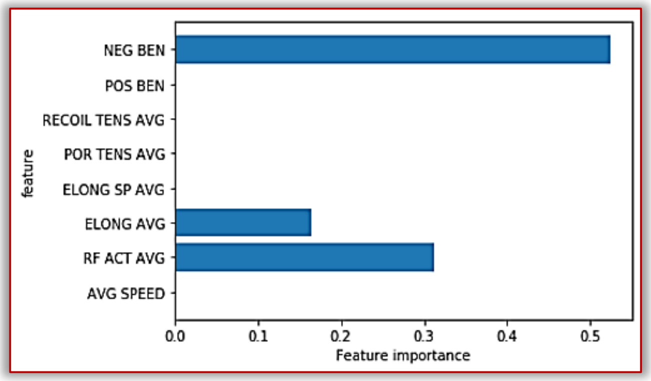

Figure 4. Feature Significance for all inputs on the output using Python

So now we have plot the feature significance for all the inputs. We can see the three inputs Negative bending, Elongation average, rolling force average to be factors which are affecting the output the most. Hence we will further look the feature significance between them.

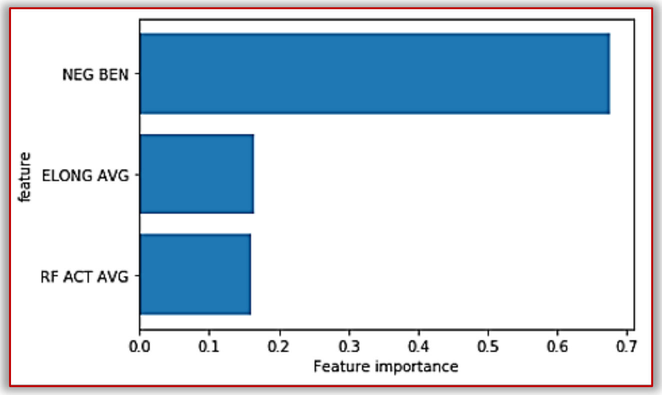

Figure 5. Feature significance for important factors for the model

Parameters used for model are

- Number of unique class labels is 10 for the given neural network, 9 inputs and 1 output.
- Lambda value for L1-regularization is not done so its value will remain 0. This type regularization assigns insignificant value of lambda so as to make the input significance on the outputs similar [7].
- Lambda value for L2-regularization done so the value is 0.1. Regularization is the technique to make program simpler. This also solves over fitting problem as the loss function is penalized [8]. The L2 regularization forces the inputs to act similarly, it does not make the value zero but close to insignificant.
- Number of epochs means number of passes over the training set is 1000.
- The learning rate for the particular neural network is 0.1. Learning rate is an important parameter that helps to decide how much to change model so as to accommodate the error occurred [9].
- The momentum constant is 0.1.

Momentum constant is the factor multiplied with the gradient of the previous epoch t-1 to improve learning speed [10].

w(t) := w(t) - (grad(t) + alpha*grad(t-1))

- The value of decrease constant is 0.00001

Decrease constant shrinks the learning rate after each epoch using the formula [11].

eta / (1 + epoch*decrease_const)

- Shuffles training data every epoch if True to prevent circles. For this neural network the shuffle is kept to true. Shuffling data enables that the model is not biased towards a particular series [12].
- Mini batches means that for efficiency training data is divided into k minibatches. If k=1 it is normal gradient descent learning.
- For this neural network we have set minibatches to 50.

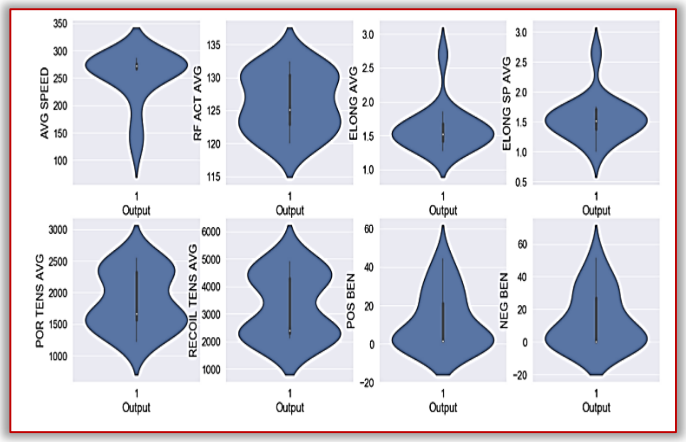

Figure 6. Violin Plot for the outputs in the model

We then wanted to see the distribution of the data points of all the parameters for the entire dataset therefore we plot the violin plots for positive and negative outcome separately.

The violin plots shows quartile ranges properly along with their median and distribution.

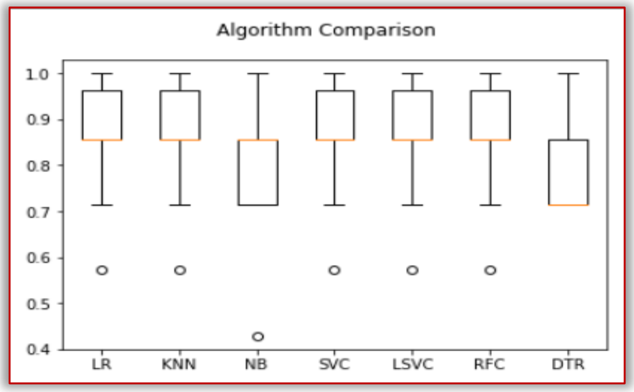

Figure 7. Box Plot using python

We also plot box plot as it along with violin plot will help clarify minute problems. Box plot also works on same ideas violin plot but violin plot is much more detailed as it shows the distribution in form of the shaded area surrounding it [13]. The shaded are around box plot informs the distribution of values. The circles on the graph are called as outliers. The quartiles are of two types for the box plots. The upper quartile is the range which splits 25% of the highest data. The lower quartile is the range that splits 25 % of the lowest data [14].

RESULTS AND DISCUSSIONS

The support vector helped to understand the plot very well. Support vector divides the plot in to two parts and are used for binary data and classification type data [15]. Here the plot is divided into two parts namely 'Blue' means the area where coil break will not occur and 'Red' means area where coil break will occur. We had given 8 inputs to the artificial neural network which will analyze the data and give an output if coil break is formed or not.

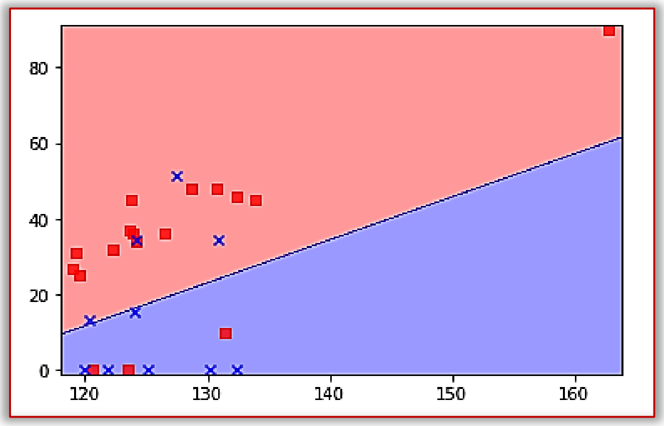

Figure 8. Support Vector for all the outputs

```
# We create a new (fake) coil having the three most correated values high
new_df = pd.DataFrame([[152.05,162.24,1.93,1.4,2449.85,5512.21,1.34,70]])
# We scale those values like the others
new_df_scaled = scaler.transform(new_df)
# We predict the outcome
prediction = svc.predict(new_df_scaled)
# A value of "1" means that coilbreak occurs if "0" does not occur
prediction

array([0], dtype=int64)
```

Figure 9. Output in the python for the model

The above figure shows the working of the predictor in the artificial neural network. The above figure shows the output given by an artificial neural network. The new coil is created where the inputs are given by the user and we could find out if coil break is formed or not. This has effectively created a predictor. In the above example 8 inputs were fed to the predictor, it can be seen that the output is given as array [0]. The value inside array will vary as per the prediction. If the coil break is formed then the array [1] would be seen else the value of array would be array [0]. Here the prediction made is array [0] so we can safely say that the coil break is not formed.

The Defect data will be made available to the Quality department which collects the relevant data regarding all the defects in the company. This will enable the defects are documented and future projects can be undertaken for improvement and quality control.

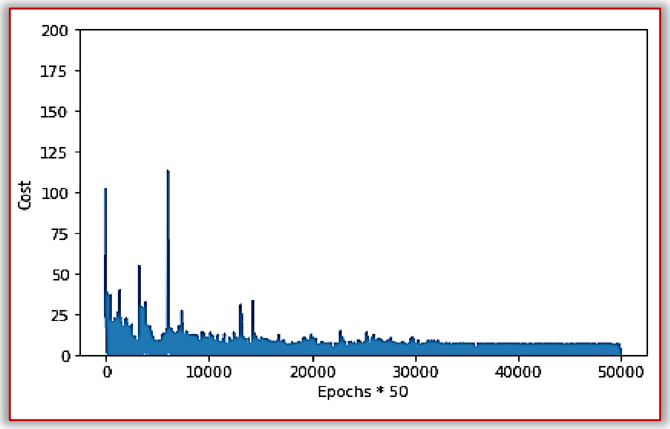

Figure 10. Cost vs epoch graph for the model

The accuracy for training graph is 89.43% which is acceptable and as for testing accuracy it increased to 94.89% accuracy. The model is hence successfully done.

CONCLUSION AND FUTURE SCOPE

Thus we can conclude that after execution of this project the coil breaks which were quite difficult to predict before are now effectively predicted. This will effectively reduce wastage up to a great extent and thus increase the efficiency & availability of the system as well as reducing unnecessary labor fatigue also improving the safety and moral of workers.

The design makes the existing model more accurate and reliable. There are multiple ideas presented in this project and one of them is taken into consideration and elaborated thoroughly to the vision of making its idea clearer. The use of simple yet effective artificial neural network reduces pitfalls and makes the system reliable and quick. Its mechanism along with its operation has been properly elucidated along with its advancement from its early design which is attempted to optimize.

In the future many advance techniques for achieving the above purposes such as provision of cameras for inspection purpose, auto control of loading, bending and other parameters and auto entry of coil in the system with the help of real-time data. This will enable accurate data and further enhance the predictability.

Acknowledgments

- Whenever a work is done successfully, there are many people behind that success. I would wish to take this opportunity to sincerely thank people whom I owe a lot. I feel much delighted in expressing deep sense of gratitude to my respected guide Prof. Niyati Raut for her wholehearted cooperation, encouragement, motivation, valuable suggestions and guidance at every stage of this work leading me to my objectives. I would like to be grateful Mr. Uday Mhatre (Head of Cluster) and Mr. Surendra Chougule (Head of Improvement) for their valuable guidance to my project work. Also my grateful thanks to Mr. Aniket Chatterjee (Manager,SPM Line) for their valuable knowledge about manufacturing given to me during this training period.
- I would also like to thank the whole SPM dept. staff that helped me in solving my difficulties and motivating in my efforts. I am grateful to Principal Dr. Arun Kumar for giving me the opportunity to complete this work.

- The authors declare that the Skin pass mill data supporting the findings of this study are available within the article and its supplementary information files.
- All data generated or analyzed during this study are included in this published article and its supplementary information files attached in the editorial manager system.
- The authors whose names are listed in this paper certify that they have NO affiliations with or involvement in any organization or entity with any financial interest (such as honoraria; educational grants; participation in speakers' bureaus; membership, employment, consultancies, stock ownership, or other equity interest; and expert testimony or patent-licensing arrangements), or non-financial interest (such as personal or professional relationships, affiliations, knowledge or beliefs) in the subject matter or materials discussed in this manuscript.

References

[1] Sajjad Ahmad, An artificial neural network model for generating hydrograph from hydro-meteorological parameters ,Journal of Hydrology,volume 315, 2005, pp 236-251
[2] N. Q. Hung, N. K. Tripathi An artificial neural network model for rainfall forecasting in Bangkok, Thailand, Copernicus Publications, volume 13, 2009,pp 1413–1425,
[3] Masoud Bakhtyari Kia, Saied Pirasteh, An artificial neural network model for flood simulation using GIS: Johor River Basin, Malaysia, Environmental Earth Sciences, volume 67, 2012, pp 251–264.
[4] D.A.Fadare, Modelling of solar energy potential in Nigeria using an artificial neural network model, Elsevier Journal, volume 86, 2009, pp 1410-1422.
[5] Paisan Kittisupakorn, Neural network based model predictive control for a steel pickling process,Elsevier Journal,vol no 19,2009 , pp. 579
[6] Recep Kazan, Prediction of springback in wipe-bending process of sheet metal using neural network,Journal of Materials & design,vol no 30,2009, pp.418.
[7] S.Sohrabkhani,Annual electricity consumption forecasting by neural network in high energy consuming industrial sectors, Elsevier Journal,vol no 49, 2008, pp. 2272
[8] M.Yılmaz,An artificial neural network model for toughness properties in micro alloyed steel in consideration of industrial production conditions,vol no 28, 2007, pp.485
[9] Sh.Mesroghli,Prediction of microbial desulfurization of coal using artificial neural networks,Minerals Engineering Journal,vol no 20, 2007, pp.1285
[10] Liujie Xu,Artificial neural network prediction of retained austenite content and impact toughness of high-vanadium high-speed steel (HVHSS),Materials Science and Engineering Journal,vol no 433,2006,pp.251
[11] M.Wong, Automatic digital modulation recognition using artificial neural network and genetic algorithm, Signal Processing, Vol 84, 2004, pp 351-365
[12] Z Zhang,Artificial neural networks applied to polymer composites, Composites Science and Technology, Vol 63, 2003, Pages 2029-2044
[13] Yichun Sun, Application of artificial neural networks in the design of controlled release drug delivery systems, Advanced Drug Delivery Reviews, Vol 55, 2003, pp 1201-1215
[14] Chienhung Wei, Dynamic Bus Arrival Time Prediction with Artificial Neural Networks ,Journal of Transportation Engineering, Vol 128,2002, pp 224-245
[15] J Kusiak, Modelling of microstructure and mechanical properties of steel using the artificial neural network, Journal of materials processing technology, vol no 127, 2002, pp.115

ACTA TECHNICA CORVINIENSIS
Bulletin of Engineering
ISSN: 2067-3809

ACTA TECHNICA CORVINIENSIS – BULLETIN OF ENGINEERING
TOME XVI [2023] | FASCICULE 2 [APRIL – JUNE]

[1.]Obot Monday OBOT, [2.]Etiette E. UDOMESSIEN, [3.]Edikan M. SAM

ARCHITECTURAL FRAMEWORK FOR THE USE OF EARTHEN ARCHITECTURE IN DEVELOPMENT OF AFFORDABLE HOUSING, IBENO

[1.]Department of Architecture, Faculty of Environmental Studies, University of Uyo, Uyo, NIGERIA
[2.]Directorate of Physical Planning, Akwa Ibom State University, Ikot Akpaden, Akwa Ibom State, NIGERIA
[3.]Department of Geology and Mining Technology, University of Port Harcourt, Port Harcourt, NIGERIA

Abstract: Housing is a very critical basic need of man and constitutes the third necessity of life. The choice of material for housing construction determines the overall cost of a project. High cost of conventional building materials in Nigeria and its non–sustainability warrant the search for other sources of building materials locally in order to meet the housing needs of low income citizens. These lead to need to promote the utilization of earth as a material/construction technique for the designing and development of affordable and sustainable housing need of the local population. In this study, literature and case studies were carried out to find out the construction process employed. From the findings, affordable housing can be provided without compromising durability and strength through the use of modern earthen architecture technique. Therefore, a site was proposed; several analyses, architectural and structural designs of the components of the proposed building were presented using ArchiCAD 16. There is need for its implementation through government projects and housing to create a role model for people to see and adopt the method.
Keywords: Architectural Framework, Earth, Development, Sustainable Housing, Construction

INTRODUCTION

Nigerian population is estimated to be about 167 million with rural areas harbouring over 52.22% of her population. About 112 million Nigerians (representing 67.1%) of the population live below poverty level(NBS, 2016). The phenomenal rise in population over the past few years has manifested in the acsute shortage of housing in terms of both quantitative (short supply) in the urban areas and qualitative (low quality) in rural areas (Abimaje*et al.*,2014).The total housing needs of the country were put at 8 million units by the year 2000 by Federal Ministry of Works and Housing, and 12–14 million units in 2007 (Akeju, 2007). A more recent estimate puts the figure even higher at 16–17 million units, meaning that at an average cost of N2.5 million Naira per housing unit is envisaged. Nigeria will require N35 trillion Naira to fund the housing deficit of 17 million housing units (Onyike, 2007). Qualitative housing is particularly acute in the rural areas of Nigeria, resulting in the manifestation of such housing problems as habitability problem, substandard housing, durability problem and poor aesthetic houses. Traditional housing, which constitutes approximately 70% of rural dwellings in the north and 17% in the south of Nigeria, is constructed by individual households using locally available building materials. These traditional and makeshift housing in the areas are generally susceptible to damage, lack of durability and conditions for comfort as well as strength and stability (Amasuomo and Amasuomo, 2014). These buildings are constructed with thatch or zinc roofs, bamboo pole, mud or locally sawn and untreated timber walls; and mud floors that are usually damp especially during the rainy seasons. Because, the building materials are of organic origin (Parry, 1980), they are not durable, deteriorate quickly with an expected durability period of between 1 and 5 years (Osasona, 2007; Parry, 1980). Therefore, they require frequent replacement than modern building materials (Obande, 1990). According to Walker and McGregor (1996), earth is the most basic and the most ubiquitous building material known to man. In order to meet the supply gap of 23 million units by 2023, 2.6 million homes will have to be constructed annually. However, optimistic estimates suggest that only around 200,000 units a year are currently being built, hence earthen architecture perhaps offers the most likely practical prospect for bridging the housing deficit gap in that not only is earth available in abundance, cheap and eco–friendly; it also saves manufacturing cost, time and energy. Already, the environmental benefits of earthen architecture over the conventional buildings are a major advantage as the world is going green. The addition of minimal modern technology to the timeless wisdom of traditional building techniques with earth can create excellent hybrid structures that have greatly improved strength and durability (Joseph, 2017). Several literature searches and case studies have been made to affirm usability, durability and strength of earthen architecture (Morgan, 2008; Auroville Earth Institute, 2017; Filemio, 2009; Adam and Agib, 2001; Minke, 2006; Morris, 2012; Ahmmed, 2005).Hence, the major objective of this study was to create a design that would serve as model for affordable, durable, aesthetically pleasing and sustainable housing in Ibeno Local Government of Akwa Ibom State through the use of earth as the main construction material which has its ecological footprint within the study area.

MATERIALS AND METHODS

— Area of Study

Ibeno Local Government Area was chosen for the location of the proposed project. It is located at the southern part ofAkwa Ibom Stateon coordinates 4.568693°N, 7.976396°E, occupying a vast coastal area of over 1,200 sq. km. Ibeno town lies on the eastern side of the QuaIboe River about 3 kilometres (1.9 mi) from the river mouth, and is one of the largest fishing settlements on the Nigerian coast. It has an estimated population of 75,380 people. However, the project site is located along IwoachangAdorokuku Road, in Ibeno Local Government Area as shown in Figure 2.

Figure 1: Ibeno on the map of Akwa Ibom State
Source:www.akwaibomstategov.com(2017)

Figure 2: Google imagery
Source: Google Earth (2017)

— Design Criteria

The location is expected to be:

- convenient for health facility, shops, bank or ATM boot, park, public transport, leisure and sport facilities,
- integrated with surrounding area with close proximity to existing facilities and infrastructures,
- aesthetically compatible,
- clear delineation of public, communal and private spaces,
- free from excessive noise / industrial pollution,
- vehicular access essential,
- well secured with essential surveillance and adequately drainage system due to high rainfall.

— Materials / Equipment

Materials / equipment used in this study included surveying kits with its equipment, Architectural design software application (ArchiCAD 16), etc.

— Methodology

Both environmental and infrastructural analyses were conducted for the proposed building construction. Environmental analysis was carried out using the data collected from GIS Department, University of Calabar, Calabar (Table 1).Besides, a trial pit soil test and building orientation were conducted to ascertain its soil bearing capacity and direction that would be subjected to sunlight, respectively. Infrastructural analysis included accessibility to proposed site location, large–scale public systems services e.g. power and water supplies, public transportation, telecommunications, roads and schools.

Table 1: Summary of environmental data collected from GIS Department, University of Calabar,

S/N	Parameters	Mean	Range / Description
1.	Relative humidity	80%	65% – 96%
2.	Air Temperature	29^{0}C	Day: 28 – 30^{0}C daily
		20^{0}C	Night: 18 – 22^{0}C daily
3.	Sunshine	1450 hours/ year	1400 – 1500 hours /year
4.	Rainfall		Very high between May – October (2000 – 3000 mm)
5.	Wind		South –west wind prevalent between April – October.
			North east trade wind prevalent between December – January
6.	Vegetation		Swamp forest that allows the growth of trees, shrubs and vast greeneries.
7.	Topography		Slight slope towards thewest

Source: GIS, University of Calabar (2017).

Besides, comparative analysis of different blocks worksin terms of cost of production such as compressed stabilized interlocking earth block (CSIEB) masonry (5% cement stabilization), sun–dried mud block, burned clay brick, stabilized soil block and concrete masonry unit was also carried out. The site was surveyed and marked out for low, middle and high income earners apartments. The architectural design software application was used to generate ground, first and second floors, roof plan, sectional views and elevations for low, middle and high income earners apartments. Details for floor plan, channel design, sections, staircase design and exterior views of three different apartments were also generated.

RESULTS AND DISCUSSION

— Site Analysis

The result of site analysis is shown in Figure 3. The site is easily accessible. It is a part of the landscape of the main Airport layout; hence it is well positioned to allow for easy drainage of rainwater. It slopes towards the west. This would be harnessed during construction. The soil type is loamy clay which makes it good for water to drain off easily and also a material for construction. Existing services are electricity, pipe borne water and telecommunication network. However, the design for orientation is a fundamental step to ensure that buildings work with the passage of the sun across the sky.

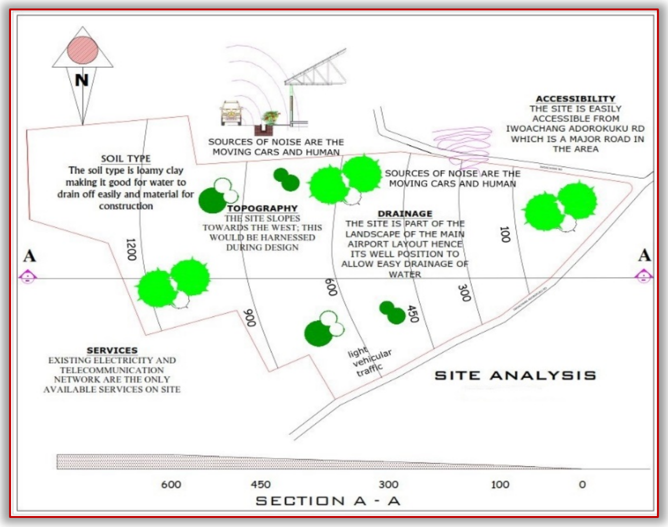

Figure 3: Site analysis

The proposed project should be oriented along or close to the East–West axis such that the shorter facades are subjected to the sun for the greater part of the day as shown in Figure 4.

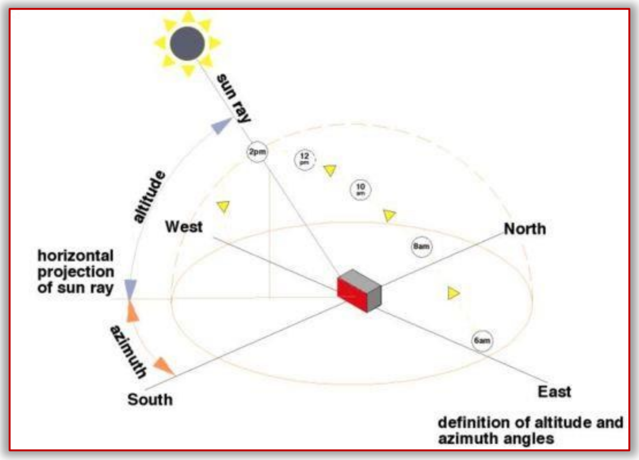

Figure 4: Building orientation

— Comparative Analysis of Different Block Works

The results of comparative analysis of different block works are presented in Appendices 1– 3. Based on block and wall appearances, dimensions, weight, texture, number of blocks needed to make up a square meter; wet compression strength, thermal conductivity and density, stabilized soil block and interlocking stabilized soil block were suggested for use. Though, no performance test was conducted, they were selected based on texture (smooth and flat). However, it takes total of N 3,120.00 andN2, 463.63 for the production of 150 mm sand–crete block and compressed stabilized block, respectively, in making a square meter wall. The compressed stabilized block seems to be a better option in this regards.

— Site Layout

The site layout is presented in Figure 5. The blue, yellow, purple and light green legends represent public facility, high, middle and low income earners, respectively. Different facilities are indicated with alphabets A to L.

Figure 5: Site layout

— Architectural Drawings for Low, Middle and High Income Earners Apartment Buildings – Low, Middle and High Income Earners' Apartment Buildings

Figure 6 to 21 are the ground, 1st and 2nd floor plans, roof plan and sectional views for low, middle and high income earners' apartment buildings.

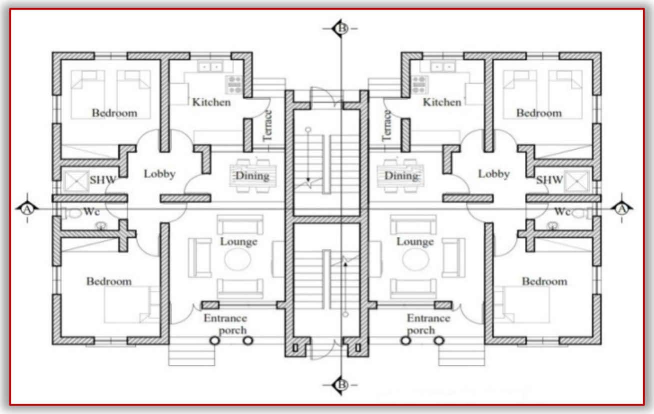

Figure 6: Ground floor plan for low income earners' apartment building

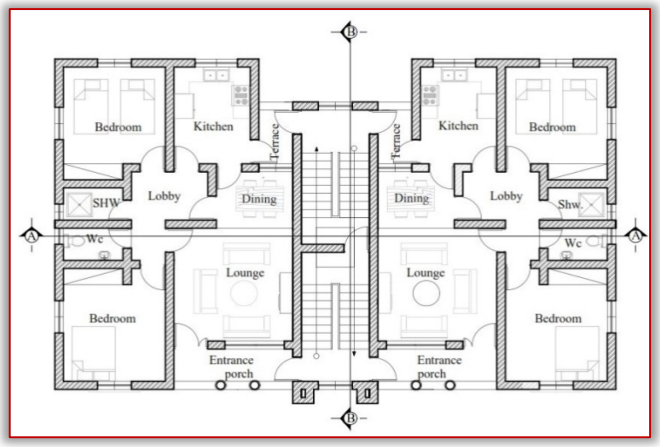

Figure 7: 1st and 2nd floor plans for low income earners' apartment building

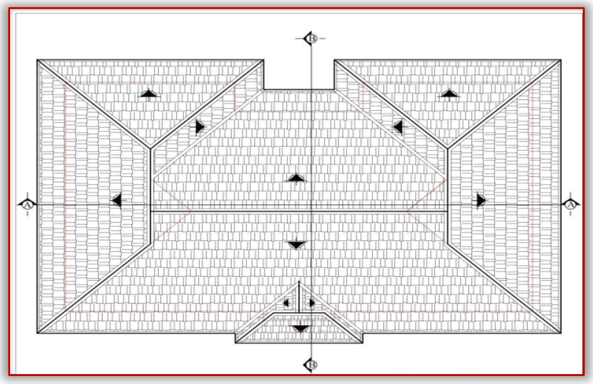

Figure 8: Roof plan for low income earners' apartment building

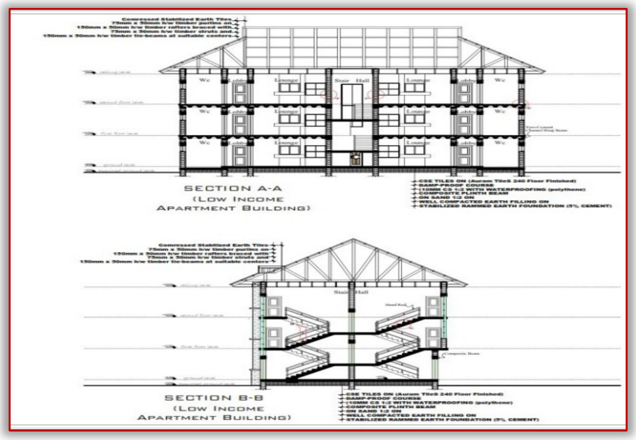

Figure 9: Sectional views for low income earners' apartment building

Figure 10: Front and right elevations of low income earners' apartment building

Figure 11: Rear and left elevations of low income earners' apartment building

Figure 12: Ground and 1st floor plan for middle income earners' apartment building

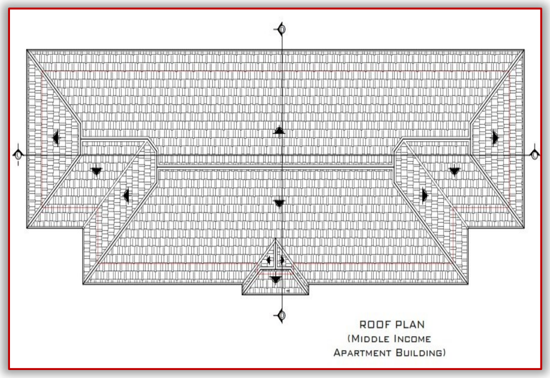

Figure 13: Roof plan for middle income earners' apartment building

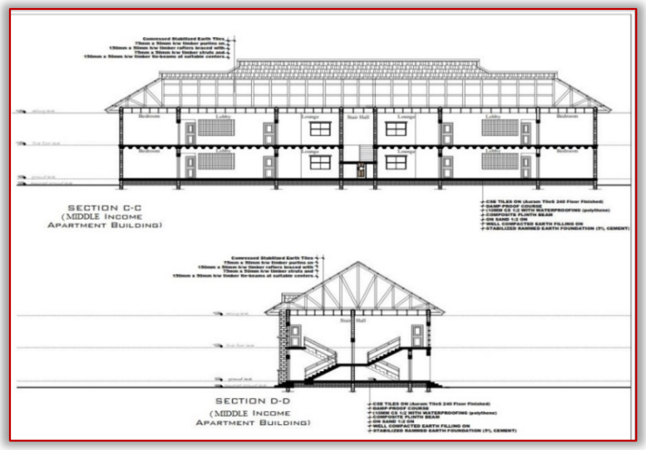

Figure 14: Sectional views of middle income earners' apartment building

Figure 15: Front and right elevations of middle income earners' apartment building

Figure 16: Rear and left elevations of middle income earners' apartment building

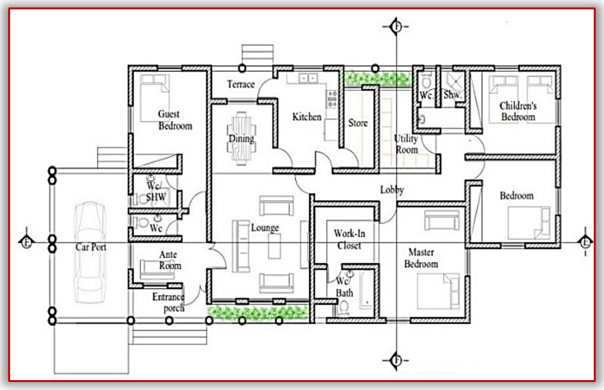

Figure 17: Floor plan for high income earners' apartment building

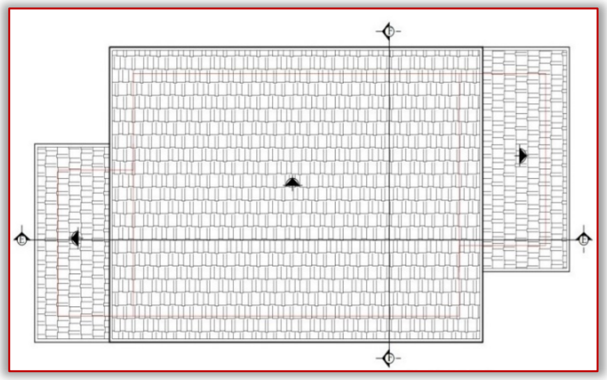

Figure 18: Roof plan for high income earners' apartment building

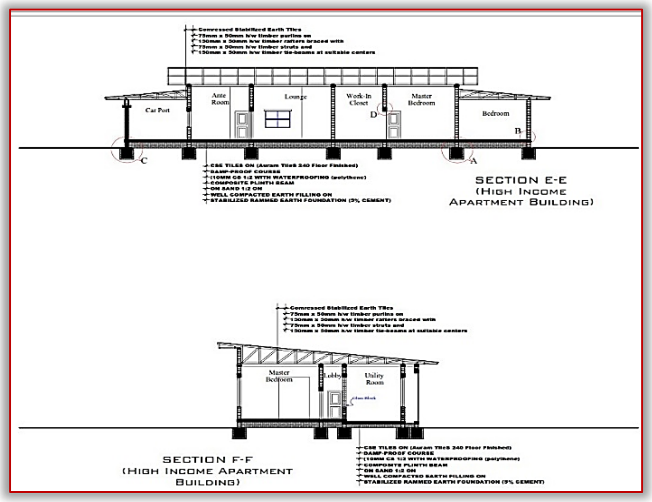

Figure 19: Sectional views of high income earners' apartment building

Figure 20: Front and right elevations of high income earners' apartment building

Figure 21: Rear and left elevations of high income earners' apartment building

Typically, the ground floor, 1st and 2nd floor plans of the proposed building structure for low income earners' apartment has 2–bedroom flat on each arm (Figures 6 and 7). The ground and 1st floor plans for middle income earners' apartment has a 3–bedroom flat on each arm (Figure 12), while the floor plan for high income earners' apartment is a 4–bedroom flat (i.e., consisting of children, extra, guest and master bedroom) with a car port (Figure 17). The roof plan for all categories of income earners is designed to allow for easy running down of rainwater (Figures 8, 13 and 18). The sectional views of the proposed building for low income earners' apartment represent a 2–storey building (Figure 9); that of middle income earners' apartment represents1–storey building (Figure 14) while that ofhigh income earners' apartment is to be a bungalow (Figure 19).The sections (A–A and B–B; CC and DD; and E–E and F–F) are meant to give the details of the interior components and how they are to be built. The elevations of all categories of income earners apartments (front and right, and rear and left elevations) depict the aesthetic views of the proposed building.

— Proposed Building Components, Materials and Construction Techniques

The proposed building components, materials and construction techniques are tabulated in Table 2.

Table 2: Building components, materials and construction techniques

Building Components	Materials and Construction Techniques
Foundations	Stabilized rammed earth foundations (5% cement stabilization).
Plinth Units	Composite plinth – step plinth with CSEB, plinth beam with reinforced concrete cast in U shaped CSEB.
Walls	Compressed stabilized interlocking earth block (CSIEB), masonry (5% cement stabilization).
Floor Slab	Ground floor: Stabilized rammed earth finished with AURAM tiles 240. Upper floors: Floor with hourdi blocks placed on ferrocement channels.
Columns	Composite columns with AURAM round hollow blocks 240 and RCC
Beams	Composite lintel, single height, with AURAM U blocks 240 and RCC
Roof	Energy serving clay tiles.
Doors	Wooden doors and frames made from trees cut on site
Windows	Glass
Finishing	Lime stabilized earth plasters for mortar and plastering.
Internal finish	Smooth cement finish or stone for bathrooms will be preferred to energy intensive ceramic tiles.
Ceiling	Bamboo mat
Water Proofing	Wallswith bitumen paint on a stabilized earth plaster. Floor with a layer of pebbles.

— Space Analysis

Thus, the following functional spaces are required for the proposed building (Table 3).

Table 3: Space and floor area requirement for a single unit

Living room	19.8 m^2
Visitors WC	1.82 m^2
Dining	14.0m^2
Kitchen	9.0m^2
Store	4.0m^2
Master bedroom	20.0m^2
Twin bedroom (children)	14.0 m^2
Toilets	3.0 m^2
Verandahs	6.0m^2
TOTAL	140.62m^2
Add 20% circulation space for lobby and walls	28.20m^2
GROSS TOTAL	136.82 m^2

— Detail of Structural Design of the Building Components – Ferro Cement Channels

Figures 22 and 23 show the layout of ferro cement channels and its floor details, respectively.

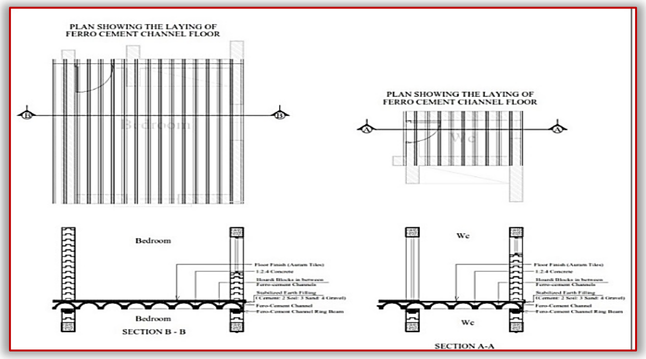

Figure 22: Floor plan showing the laying of ferro cement channels

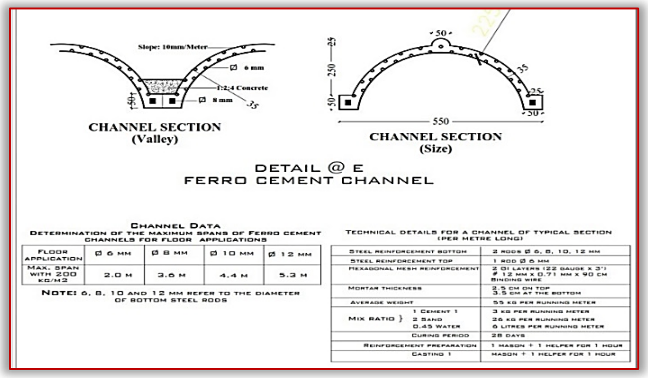

Figure 23: Detail of ferro cement channel

As seen in Figures 22 and 23, different floor applications require certain span of ferro cement channel. It should be noted that 6, 8, 10 and 12 mm represent the diameter of bottom steel rods. The maximum spans with 200 kg/m^2 are 2.0, 3.0, 4.4 and 5.3, respectively. The technical details for a channel of typical section must include steel reinforcement.

— Compressed Stabilized Earth Foundation, Composite Plinth Beam, Floor Slab, Floor Finishes and Column Composite Designs

The designs of compressed stabilized earth foundation, composite plinth beam, floor slab, floor finishes and column composite designs are presented in Figures 24, 25 and 26.

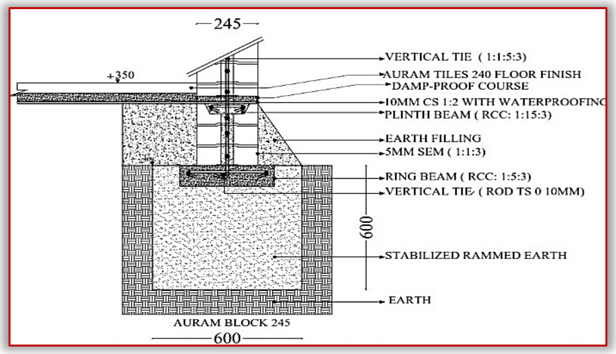

Figure 24: Compressed stabilized earth foundation and composite plinth beam

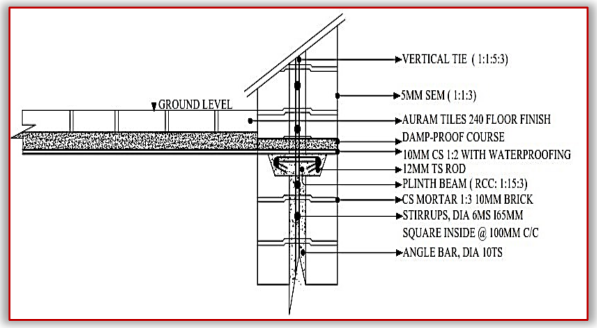

Figure 25: Floor slab design and floor finishes

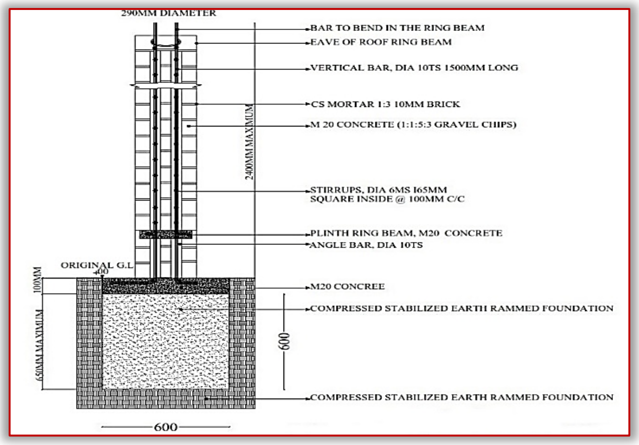

Figure 26: Column composite design

The construction of compressed stabilized earth foundation and composite plinth beamshall involve trench digging, soil levelling, water–cement addition (200 litre of water with 1 bag of cement), and ramming; and the construction of floor slab design and floor finishes shall be according the method described by Auroville Earth Institute (2017). For column composite, vertical reinforcements should be ø10 mm for the blocks 290; stirrups must be ø 6 mm and placed every 20 cm c/c. The holes, where reinforcement, are inserted cast with concrete 1 cement: 2 sand: 4 (chips gravel).The columns 290 can be linked only on 1 side of the building (through a beam or ring beam) (Auroville Earth Institute, 2017).

— Beam and Staircase Designs

The design ofbeam and staircase are presented in Figure 27 and 28.

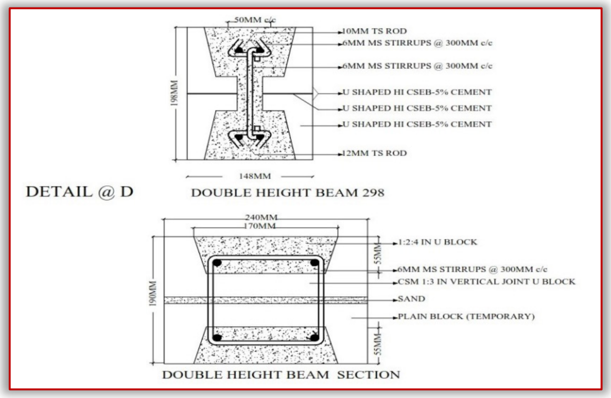

Figure 27: Beam design

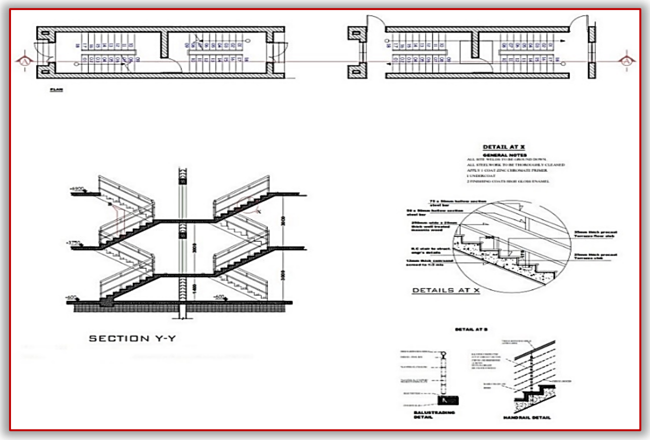

Figure 28: Staircase design

The bottom of the double height beam (Figure 27) is cast first in a reversed position and after 1 month it should be returned. Either on the ground or the top part is precast in other U blocks or the incomplete beam is lifted with care and the concrete is cast in situ into other U blocks. Staircase construction shall be built using modern conventional techniques.

— Models of Exterior Views of Low, Middle and High Income Earners' Apartment Buildings

The models of exterior views of low, middle and high income earners' apartment buildings are presented in Figure 29 to 31.

Figure 29: Model of exterior view of low income earners' apartment building

Figure 30: Model of exterior view of middle income earners' apartment building

Figure 31: Model of exterior view of high income earners' apartment building

CONCLUSION

Based on the literatures search and case studies conducted on the evolution and principles of earthen architecture, it was observed from the findings, that the earthen architecture has been improved upon. This innovation is the utmost expressions of earthen architecture since they allow the material to be used to its very best advantage. Hence, earthen architecture was proposed for building of housing scheme where all architectural and structural designs were spelled out and could be managed by public private partnership (PPP).

APPENDICES

Appendix 1: Comparative Analysis of ISSB

Properties	Interlocking Stabilised Soil Block	Sun-dried Mud Block	Burned Clay Brick	Stabilised Soil Block	Concrete Masonry Unit
General Info					
Block Appearance					
Wall Apperance (not rendered)					
Dimension (L x W x H) (mm)	265 x 140 x 100 mm	250 x 150 x 70 mm to 400 x 200 x150mm	200 x 100 x 100 mm	290 x 140 x 115 mm	400 x 200 x 200 mm
Weight (kg)	8-10 kg	5-18 kg	4-5 kg	8-10 kg	12-14 kg
Texture	Smooth and fl at	Rough and powdery	Rough and powdery	Smooth and fl at	Coarse and fl at
Blocks needed to make up a sq.m.	40	10 to 30	30	21	10
Performance					
Wet Compressive Strength (mps)	1 - 4	0 - 5	0.5 - 6	1 - 4	0.7 - 5
Thermal Insulation (W/m C)	0.8 - 1.4	0.4 - 0.8	0.7 - 1.3	0.8 - 1.4	1 - 1.7
Density (kg/m3)	1700 - 2200	1200 - 1700	1400 - 2400	1700 - 2200	1700 - 2200

Appendix 2: Cost Analysis of Sand Crete Block

	Material	Quantity	Calculation	Cost (₦)
1 unit 225mm Sandcrete block	Cement	1 bag		2550
	Sharp sand	18 head pans	@ 200 each	3600
	225mm block	25 blocks		6150
	Sandcrete block	1 unit	$\frac{6150}{25}$	250
	Assume 10% for labour		$\frac{10 \times 250}{100}$	25
	Assume 20% for plants and others.		$\frac{20 \times 250}{100}$	50
	Total cost FOR 1 unit 225mm sandcrete block 250 + 25 +50			=325
The cost per sqm of 225mm Sandcrete block	10 sandcrete blocks cover one square metre = 10 X 325 Assume 10% for cost of mortar for laying the blocks Assume 10% for labour for laying the blocks Total cost per square metre for 225mm sandcrete blocks			3250 = 250 = 250 =3750
1 unit 150mm Sandcrete block	150mm block	30 blocks		6150
	Sandcrete block	1 unit	$\frac{6150}{30}$	200
	Assume 10% for labour		$\frac{10 \times 200}{100}$	20
	Assume 20% for plants and others.		$\frac{20 \times 200}{100}$	40
	Total cost FOR1 unit 150mm sandcrete block 200 + 20 +40			=260
The cost per sqm of 150mm Sandcrete block	10 sandcrete blocks cover one square metre = 10 X 260 Assume 10% for cost of mortar for laying the blocks Assume 10% for labour for laying the blocks Total cost per square metre for 150mm sandcrete blocks			2600 = 260 = 260 =3120

Notes: The unit cost of the Sandcrete hollow blocks was computed based on the following assumptions:
Mix Ratio = 1:9 (that is; one headpan of Ordinary Portland Cement to nine head pans of sharp sand). This translates to one bag of ordinary Portland cement to eighteen headpans of sand, since there are two headpans in a bag of cement.

Appendix 3: Cost Analysis of Compressed Stabilized Block

Material	Quantity	Calculation	Cost (₦)
Laterite	1 cement Bag		550
Cement	1 bag		2550
Laterite	One 4Litre container	$\frac{550}{8}$	68.75
Cement	One 4Litre container	$\frac{2550}{8}$	318.75
Laterite	19 parts	19 parts @ 68.75 each	1,306.25
Cement	1 part	1 part @ 318.75 each	318.75
Polythene sheet for curing	1	318.75	318.75
CSB	40No of CSB	1,306.25+318.75 +318.75	1943.75
Unit of cost 1 CSB block	1N o	$\frac{1,943.25}{40}$	48.59
Labour	10% of unit cost of block	$\frac{48.59 \times 10}{100}$	4.86
Plants and others (water)	20% of unit cost of block	$\frac{48.59 \times 20}{100}$	9.72
Total cost 1 unit Compressed Stabilised Blocks 48.59 + 4.86+9.72			= 63.17
The cost per sqm	39 CSEB cover one square metre = 39 X 63.17 = 2463.63 No mortar required Assume 15% for labour (more blocks involved) = 7.28 Total cost per square metre = 24.70		

Note: The unit cost of the CSBs was computed based on the following assumptions:
- Mix Ratio = 1:19 (that is, one part of Ordinary Portland Cement to nineteen parts of laterite by volume)
- A 4 litre container was used as the gauge in measuring the composition of Compressed Stabilised Block.
- 4No containers (each 4litre capacity) = 1 head pan.
- 2No head pans = 1 bag of cement,
- 8No containers (each 4litre capacity) = 1 bag of cement.
- Cost of labour is 10% of a unit cost of block
- Cost of Plants and Others (water) is 20% of a unit cost of block

References

[1] Abimaje, J.,Akingbohungbe, D. O. and Baba, A. N. (2014).Housing Affordability in Nigerian Towns: A Case of Idah, Nigeria. International Journal of Civil Engineering, Construction and Estate Management,Vol.1,No.2,pp.31–38,
[2] Adam, E.A and Agib, A.R.A. (2001). Compressed Stabilised Earth Block Manufacture in Sudan. United Nations Educational. Scientific and Cultural Organization 7 Place de Fontenoy, 75352 Paris 07 SP, France Paris.
[3] Ahmed, K. I. (2005). Handbook on Design and Construction of Housing for Flood Prone Rural Areas of Bangladesh, Published by Asian Disaster Preparedness Centre (ADPC) in partnership with Bangladesh Disaster Preparedness Centre, CARE–Bangladesh, Bangladesh Ministry of Food and Disaster Management and BRAC University with support from United States Agency for International Development.
[4] Akeju, A. (2007). Challenges to Providing Affordable Housing in Nigeria, Paper Presented at the 2nd Emerging Urban Africa International Conference On Urban Housing Finance in Nigeria, Held at ShehuYar'adua Centre Abuja, October 17–19, 2007.
[5] Amasuomo, T.T. and Amasuomo, J.O. (2014). Improving Durability of Rural Buildings in Riverine Niger Delta Region: A Case Study on Need to Utilize Appropriate Technology. International Journal of African Society, Cultures and Traditions, 4(1), 17–43.
[6] Auroville Earth Institute (2017). Earth Building Works Available Online http://www.earth– auroville.co
[7] Filemio, V. (2009) The Architecture and Mechanics of Earthen Structures. Proceedings of the Third International Congress on Construction History. May, Cottbus, Germany. pp. 579B586.
[8] GIS, University of Calabar (2017). Department of Geographical Information System, University of Calabar, Calabar, Nigeria
[9] Joseph, F. K. (2017). An Overview of Natural Building Techniques. Online at http://www.networkearth.org/naturalbuilding/overview.html
[10] Morgan, W.N. (2008). Earth Architecture from Ancient to Modern. University Press of Florida, USA.
[11] Morris, H.W. (2012).Natural Disasters and Earth Buildings: Resistant Design and Construction. Modern Earth Buildings, Materials, Engineering, Construction and Applications. Ed Woodhead Publishing Limited, United Kingdom.
[12] Minke, G.(2006). Building with earth, design and technology of a sustainable architecture. Birkhauser Publishers for Architecture. Basel, Berlin, Boston
[13] National Bureau of Statistics [NBS] (2016). Nigerian population. Online at https://www.nigerianstat.gov.ng/ (Accessed on 3rd Jan., 2017)
[14] Obande, M. O. (1990). BlockLaying and Concreting, Longman, Nigeria Ltd, Ikeja–Lagos.
[15] Onyike, J. (2007). An Assessment of Affordability of Housing by Public Servants in Owerri, Nigeria, Journal of Land Use and Development Studies, 3: 21–34.
[16] Osasona, C.O. (2007). From Traditional Residential Architecture to the Vernacular: The Nigerian Experience.
[17] Parry, J. M. P. (1980). Building Materials and Components in Appropriate Industrial Technology for Construction and Building Materials. Monograph, No. 12. Vienna: UNIDO.
[18] Walker, B. and McGregor, C. (1996) Building with Earth in Scotland: Innovative Design and Sustainability. Edinburgh: Scottish Executive Central Research Unit.

ISSN: 2067–3809

[1.]Miklós SZABÓ, [1.]Zoltán András NAGY, [1.]Tamás HARTVÁNYI

RANDOM ALLOCATION EFFECT ON STORAGE PERFORMANCE

[1.] Széchenyi István University, Győr, HUNGARY

Abstract: Todays not the products race with products, but supply–chains with supply–chains, also every chain is so strong as the weakest part of it. It is essential to show high–performance on market, not just in production, but in logistic process too. A compact rack–system has one of the best area utilization, but it is afraid of less dynamic capacity. The authors started find a solution, how to utilize area for logistic process next to fast material handling. In this paper we publish a simulation that shows out the effect of random allocation on storage performance in a compact rack–system that opens new ways for research.
Keywords: Storage Location Assaignment Problem (SLAP), simulation, compact rack–system

INTRODUCTION

The inventories have two main criteria: static– and dynamic capacity. Static capacity defines the amount of materials could be hold at the same time, dynamic capacity defines the amount of materials could be handled in time–period. Most cases companies use conventional pallet rack system that seems to be the most effective in dynamic capacity, because every pallet is available without moving other pallets, but many times inventories has limited area to use and high amount of materials to handle. In that reason companies have to use other rack systems that are more effective in area utility.

According to Pareto thesis most of the handled materials came from a few Stock Keeping Units (SKUs), while the other small part of materials is many. Because of that the compact rack–system is more logic choice than the conventional one in aspect of SKUs.

We think that compact rack–system can be dynamic too. With compact rack systems less travel–distance has to be done. The question is how to minimize the material–handling. In this paper we make a case study simulation to determine how to set up a warehouse in this situation and what can be reached by that way.

We have two options, how to influence the material–handling performance, first we can say how to allocate materials in a warehouse. By other words: the required time for a list of tasks is depends on, how the warehouse was look like, when the work was started. The second method is to say, what to do, the incoming materials where should be placed and which one should be given out first.

In this paper we present simulations of the warehouse behavior for random allocations compared to the scientific ABC organized solution. The second method will be covered in other time.

LITERATURE REVIEW

Before the simulations we have to pay attention for state of art, because the Storage Location Assignment Problem (SLAP) is an NP–hard problem and researched by many others. Juan José Rojas Reyes, Elyn Lizeth Solano–Charris and Jairo Rafael Montoya–Torres collected 71 representative papers published in the theme between 2005 and 2017 [6].

The problem is often inspected with Genetic Algorithm (GA), for example it is discussed end enveloped by Changkyu Park & Junyong Seo in [11] and [12] or Jing Xie, Yi Mei, Andreas T. Ernst, Xiaodong Li & Andy Song in [7] and [8]. GA makes generally many computations and last long time. In our simulation it is solved much faster aware of could be less effective. Our research could be a good base for GA computations too.

Other approaches collected by Behnam Bahrami, Hemen Piri & El–Houssaine Aghezzaf in [3]. Problem could be solved by classifying the stored materials that is presented by Ren–Qian Zhang, Meng Wang & XingPan in [5] or R.Micale, C. M. La Fata, G. La Scalia in [4]. In our research ABC analysis is compared to total random allocations.

Our results could be utilized not just in the modelled warehouse, but in many other field where compacted storage systems are preferred, for example in works of Sacramento Quintanilla, Ángeles Pérez, Francisco Ballestín & Pilar Lino [9] or in maritime terminals as shown in works of Xiaoyuan Hu, Chengji Lianga, Daofang Chang & Yue Zhang [2] or Lu Chen & Zhiqiang Lu [10].

SIMULATIONS

— System Description

To solve SLAP we have planned many simulations, they help choose between the solutions. In this paper we represent the first simulations, in what we created with random arrangements for a real situation's reduced model.

Our case study based on data of a factory's raw material inventory. In our model all the materials stored on pallets and use the same size of store location. The FIFO is not a requirement that could be anywhere, if the materials counted in bound of big series and a new serial means a new material number.

The entrance of the warehouse is in opposite of the exit, so the materials' flow has straight line shape, every material moves across the warehouse to production and none of them comes back, so there is no rest material in our model. In real life the materials have buffing area in production, it is unnecessary to move them back, they can be hold there for later production, if it is more than the actual serial required. The finished goods stored in other inventory.

We kept the shape of the rack system that was a drive–in system with 6 pallets deep width and 3 levels height. Materials moved by a forklift and locations are available if there are no other materials in the lane closer to the corridor, but it does not matter on which height it stands. There are two block of racks on the left and right side of the corridor. In each block there are 18 lanes so the maximal static capacity of the model is 648 pallets.

The model inherited the volume ratio of materials in the original inventory. The amount of SKUs is reduced to 100 by selecting every 19th material for simulation, but their volume ratio is almost equal to volume of original inventory's SKU percent volume ratio. That can be seen in Figure 1, how well the Pareto thesis is represented in simulations.

There are 557 materials to starts with. We have to say how to range these items in the warehouse to influence the performance. We don't know what will be, we know only chance what will be a task, so the system is stochastic as randomness of reality, not a deterministic model.

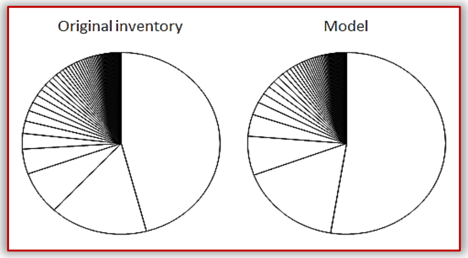

Figure 1. Volume ratio of SKUs

To count the dynamic capacity, we created a table where it is recorded, how many time is needed to move in and out of the rack to or from that exact location. If a needed material is blocked by other materials in the lane, then the others have to be moved on the corridor, then move out the searched one and then move back the others without change the order, just shift a bit deeper. It is not allowed to leave an empty location blocked in any lane. The time needed to make a location free is calculated in table too, depending on the location coordinates and the blocking locations before that.

To evaluate the efficiency of storage location assignment we made simulations with 100 task–lists, each list contains 2000 tasks. Every task could be either get in or a give out. The task lists were build up in aspect of the past and it tries to get the inventory fulfilment about 80% and never ask a material that is not stored in yet. When the task–lists were built, there was higher chance to store in the lower fulfilment and low chance to get something out, and there was lower chance to store in something in higher fulfilment and higher chance to get something out.

We kept the circulate habit of the materials, rate of materials and amount of items should store in and given out, so for example if a material used to come in on 20 pallets, then it generated 20 tasks of the same material to store in followed by each other, before another task were generated.

Each task–list is independent to others, but each were generated by the same chances. The task–lists were recorded to keep it in every simulation, in that case they are comparable.

The exact location is chosen by greedy algorithm: when a unit has to be placed in, the system chooses the shortest way in time to deploy if that is a valid location, and when a unit has to be given out, the system chooses the fastest available unit to give out. There is no restriction between materials and locations every material could be placed on any location.

The value of solutions was calculated with the following formula:

$$v = \frac{\sqrt{\frac{\sum_{i=1}^{n}\left(\sum_{j=1}^{m} t_{ij}\right)^2}{n}}}{m} \qquad (1)$$

where v means the value of a simulation, m is the amount of tasks in a task–list, n is the amount of task–lists and t_{ij} is the time required to do the j task in i task–list. With this formula a weighted average is given for time required to do a task. Behind the weighting stands the same theory a behind the average distance to mean value and deviation. If a solution solved the task–lists with the same average time required in another solution, but it has less deviation, than it get a better value. Of course the aim of the simulations is to minimize v value.

— First run

We generated total random arranges to see, how it can impact the performance of warehouse. The first 1000 solutions were ranged from 90.7 to 101.3 as it is shown in Figure 2.

The ABC analytic solution was 94.4, so the 26% of random arranges were better than this. We made hundred tusk–lists to avoid getting solutions around one exact situation – that could be easily defined by the given order, we wanted to get an approximately good solution for any stochastic–possible situations. For a similar reason it is important to have many tasks in every task–lists, and that helps find solutions for long time.

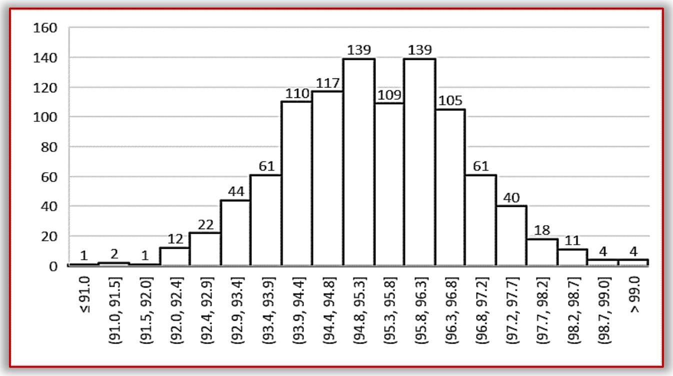

Figure 2. Histogram of simulations by the first 1000 arrangements

The required time for a task could be less than 30 seconds if it could be done near to the corridor, but if a material is deeply covered and 15 positions have to be empty before it and later move the materials from there back, then it could take almost a half–hour. The question is how many times they will occur.

The average operation–time is changing during the list – it could be seen in Figure 3, where we display it for the best, the worst and the median solution. The ABC analytic solution is indicated with red line.

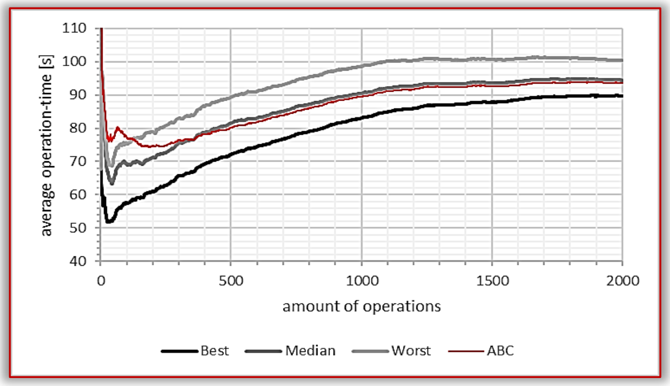

Figure 3. Average operation–time in simulation depending on amount of operations

The first 300–400 tasks' average operation–time is varying a lot, from here to 1100–1600 it is increasing constantly and in the final part it is converging to one value. In the first part they can be judged well, but in the followings every line is going parallel to each other and lastly no big changes are expected, it seems unnecessary to have longer task–lists.

— Validation

To prove the simulations are good to test the effectiveness of arranges after the first thousand simulations we created a new hundred task–lists with 2000 tasks in each as it was written earlier. The simulations' *v* value in the original and the newly generated validating data have to be near to each other. If the result is the same, then the arrange optimization would be independent to task lists, but if the differences are high, then the result is task–list specific.

The new values of the solutions were luckily only 0.32% different from the first run. The biggest difference 1.34% was at the Case 334, as it can be seen between some of the two values are sampled in Figure 4. The vertical axis is for the *v* values and the horizontal axis shows the identification number of cases. The values of the whole 1000 members range are on average 0.20% higher than the original ones.

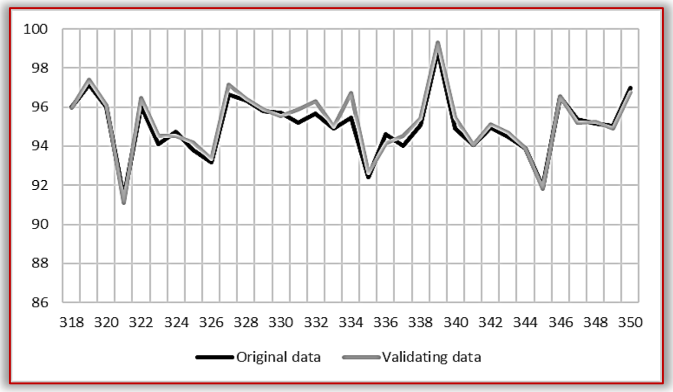

Figure 4. The value of original and validating data around the biggest differences (Case 334)

With this small differences, the method seems to be right, the simulations could be continued for a bigger research with the original task–list.

— Result of ten–thousand simulations

After the validation of the method, we continued the simulations to extend the case–numbers to ten–thousand. The mean value changed from 95.32 to 95.30, the best value was reduced from 90.70 to 90.54, but there was no worse than in the first thousand case, so the worst value didn't change from 101.29.

As it was shown in Fig. 3 for the first thousand simulations, we present the average operation–time changing during the task–lists by the best, the worst and the median solution in Fig. 5 for the extended range.

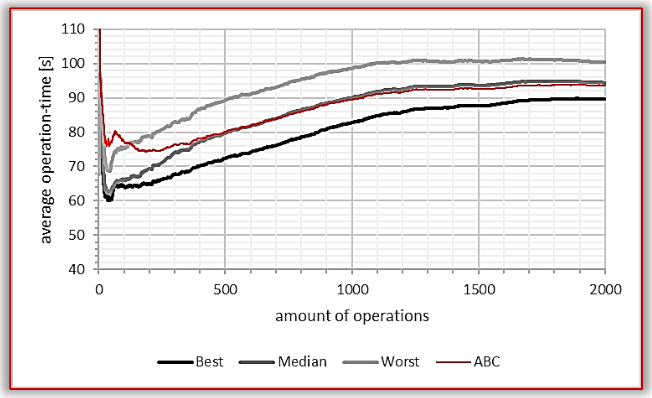

Figure 5. Average operation–time in simulation depending on amount of operations

The three parts are on the same period, the behavior of the lines are also the same, but the best solution comes from much higher value, so it started from a worse position, but the final value becomes better.

The median line goes in the opposite way, it started from a much better first period, but become the same as in case of the first runs, they different only after the 5th digit: the *v* value changed from 95.28212 to 95.28211. These changes make us sure, we had to make all the 2000 tasks in all task–lists.

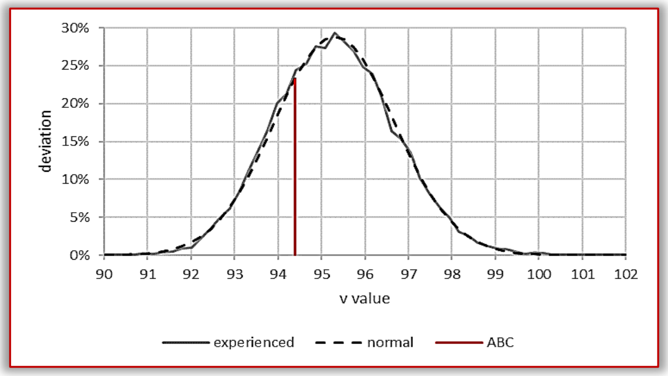

Figure 6. Experienced deviation of simulations' *v* value and normal distribution

The result of the simulations is well described by a normal distribution. According to Kolmogorov–Smirnov test, it has 61% confidence, because the biggest difference between normal and experienced distribution is 0.0090 around 44%. The experienced deviation is indicated with it in Fig. 6. A red line shows, where the ABC is analytic solution and all the solutions on left to it are better. The best experienced solution makes it about 4% better.

CONCLUSION AND FUTURE WORK

We presented the Pareto thesis' impact to utility of rack–systems efficiency in warehouses, collected methods and to SLAP, developed a simulation system for an exact problem, to show out, how important is to pay attention on materials arrangements, validated the method and made 10 000 simulations.

We don't think, that our best random arrangement for the problem is good enough, but this experience proved that it is worth to looking for better solutions. The presented simulations could be a good base to start GA population or could be used for a neural net building.

There are many questions that we would like to answer in the future:

- We would like to build a general model, to make simulations with other rack–systems, other shapes and constructions to optimize the area–utility. What shapes is ideal for a situation and what influence it?
- How many racks should be compact and many conventional ones should be used to optimize area–utility? How deep and how high they should be?
- How would impact the result if the temporary storage on the corridor is prohibited?
- What can we reach if the selection in model would be changed from greedy algorithm to something else?
- What we have to do if we can see further for example ten or twenty tasks and not just one?
- How to arrange the inventory if we would have better solutions in short terms?
- When is it worth to make the calculations for a new arrangement and rearrange the warehouse? Could it be done by new dynamic process?

When we answer these questions, then the supply chains could be better served by the warehouses.

References

[1] Trindade, M. A. M., Sousa, P. S. A. & Moreira, M. R. A., "Ramping up a heuristic procedure for storage location assignment problem with precedence constraints." in Flex Serv Manuf J, 2021
[2] Xiaoyuan Hu, Chengji Lianga, Daofang Chang & Yue Zhang, "Container storage space assignment problem in two terminals with the consideration of yard sharing", in Advanced Engineering Informatics Volume 47, 2021
[3] Behnam Bahrami, Hemen Piri & El–Houssaine Aghezzaf, "Class–based Storage Location Assignment: An Overview of the Literature", Proceedings of the 16th International Conference on Informatics in Control, Automation and Robotics – Volume 1: ICINCO, pp. 390–397, 2019
[4] R. Micale, C. M. La Fata, G. La Scalia, "A combined interval–valued ELECTRE TRI and TOPSIS approach for solving the storage location assignment problem" in Computers & Industrial Engineering Volume 135, pp. 199–210, 2019
[5] Ren–Qian Zhang, Meng Wang & XingPan, "New model of the storage location assignment problem considering demand correlation pattern" in Computers & Industrial Engineering Volume 129 pp. 210–219, 2019
[6] Juan José Rojas Reyes, Elyn Lizeth Solano–Charris & Jairo Rafael Montoya–Torres, "The storage location assignment problem: A literature review" in International Journal of Industrial Engineering Computations 10 pp. 199–224, 2019
[7] Jing Xie, Yi Mei, Andreas T. Ernst, Xiaodong Li & Andy Song, "Scaling Up Solutions to Storage Location Assignment Problems by Genetic Programming" in Asia–Pacific Conference on Simulated Evolution and Learning SEAL 2014: Simulated Evolution and Learning pp. 691–702, 2014
[8] Jing Xie, Yi Mei, Andreas T. Ernst, Xiaodong Li & Andy Song "A Genetic Programming–based Hyper–heuristic Approach for Storage Location Assignment Problem" in 2014 IEEE Congress on Evolutionary Computation (CEC) July 6–11, 2014, Beijing, China
[9] Sacramento Quintanilla, Ángeles Pérez, Francisco Ballestín & Pilar Lino, "Heuristic algorithms for a storage location assignment problem in a chaotic warehouse" in Engeneering Optimization Volume 47 – Issue 10 pp. 1405–1422, 2014
[10] Lu Chen & Zhiqiang Lu, "The storage location assignment problem for outbound containers in a maritime terminal" in International Journal of Production Economics Volume 135, Issue 1, pp. 73–80, 2012
[11] Changkyu Park & Junyong Seo, "Comparing heuristic algorithms of the planar storage location assignment problem" in Transportation Research Part E: Logistics and Transportation Review Volume 46, Issue 1 pp. 171–185, 2010
[12] Changkyu Park & Junyong Seo, "Mathematical modeling and solving procedure of the planar storage location assignment problem" in Computers & Industrial Engineering Volume 57, Issue 3 pp.1062–1071, October 2009

ACTA TECHNICA CORVINIENSIS
Bulletin of Engineering
ISSN: 2067–3809

[1.]Bogdan–Dorel CIOROAGĂ, [2.]Emanoil LINUL, [1.]Vasile George CIOATĂ

EFFECT OF WELDING CURRENT INTENSITY ON TENSILE STRENGTH OF PRESSURE VESSEL STEEL SUBMERGED WELDED JOINTS

[1.]Politehnica University Timișoara, Faculty of Engineering in Hunedoara, Str. Revolutiei nr. 5, Hunedoara, ROMANIA
[2.]Politehnica University of Timisoara, Blvd. M. Viteazu, No. 1, Timisoara, ROMANIA

Abstract: The quality of welded pressure vessels joints consists in using an optimal welding regime, a parameter that has a high influence in submerged arc welding is the welding current intensity. Increasing the welding current intensity correlated with an optimal welding speed and working voltage may result in increasing productivity. This paper deals with aspects of the effect of changing only the welding current intensity parameter within a welding regime that has the rest of the parameter's constant. The study presents how the welding current intensity affects the tensile strength of the welded joints from pressure vessel steel. The main aspects that are considered: the yield strength, breaking force and breaking stress occurred in stretching of the welded joints. The test specimens were created by using the welding process realized by using a semiautomatic industrial submerged arc welding machine. The base material used is a pressure vessel steel identified under the coding P355 N.

Keywords: welding, arc, parameter, stress, strain, intensity, amperage

INTRODUCTION

Pressure vessels are industrial machines that work in pneumatic or hydraulic circuits, a fact that requires the construction conditions of these products to ensure good tightness, resistance to high pressures and temperatures. As well the presence of mechanical fatigue must also be considered to which they can be subjected in exploitations with dynamic operating regimes, this means repeated pressure and temperature variations as well as sudden changes in the flow regimes of the fluids they store. [1]

In industrial applications that do not require a high standard of hygiene, such as the chemical or food industry, pressure vessels made of laminated steel sheets are used. The material of the semi–finished product is a carbon steel with a fine granular structure called pressure vessel steel, this material has good plastic properties and has a high mechanical resistance in high temperature conditions, also having a very good weldability. [2]

In order to ensure optimal operating conditions, it is essential that pressure vessels have welded joints that are as tight and durable as possible. The method used to assemble pressure vessels by submerged electric arc welding, the welding regime of this method is defined by a set of parameters that can be controlled by the welder operator. One of these parameters is the intensity of the welding current, which directly influences the strength of the welded seam, the geometry of the welded seams and their homogeneity. There are also several factors that are specific to welding processes that are influenced by this parameter such as:

- the degree of penetration of the additive material into the base material
- the size of the heat affected zone
- the deposition rate of the additive material

It is known that there are certain correlations between certain welding defects and parameters of the welding regime, which in the case of the intensity of the electric welding current can be found defects such as:

- cracks appeared during cooling welded seams
- over–elevation of welded seams due to too high a deposition rate
- pronounced thermally embrittled zone due to the too high temperatures developed in the area of the welding arc
- leaks at the root of the weld formed from the base material due to a high deposition rate and a high degree of dilution [3]

Regarding the submerged arc welding method, it should be mentioned that is used on a large scale for the mass production of pressure vessels. There are 2 consumables that are used during submerged arc welding processes such as: the electrode wire that is wound on a drum being similar to that of MIG/MAG welding and the flux layer which is a granular powder.

During the submerged arc welding process, the burning of the arc takes place under the layer of flux deposited over the welded seam, acting as a protective environment isolating the electric arc from the atmosphere and enriching the welding pool with beneficial alloying elements. Figure 1 shows the principle underlying the submerged electric arc welding process. [4]

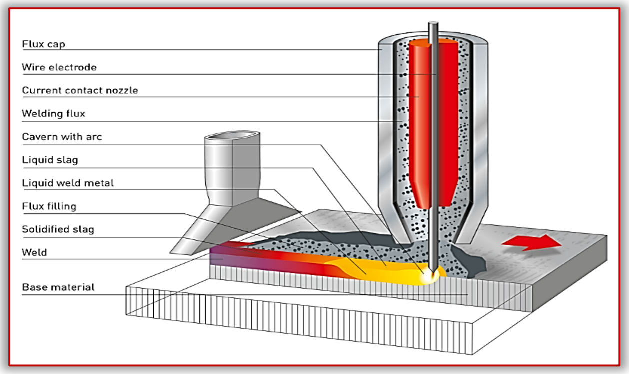

Figure 1. The process of submerged arc welding [5]

The method of depositing the flux can be through the electrode holder torch as in figure 1 or through a tube that deposits the flux layer in advance, later it is sucked by a flux collection system, it being recirculated to reduce losses of flow material.

The entire system of equipment used to make welds for pressure vessels is a complex one, there are auxiliary equipment for handling the cylindrical semi–finished product and auxiliary equipment for supporting the welding system. The connection and operation of the welding equipment is shown in figure 2, were also is exemplified the technique of external welding of a cylindrical vessel is presented. [6]

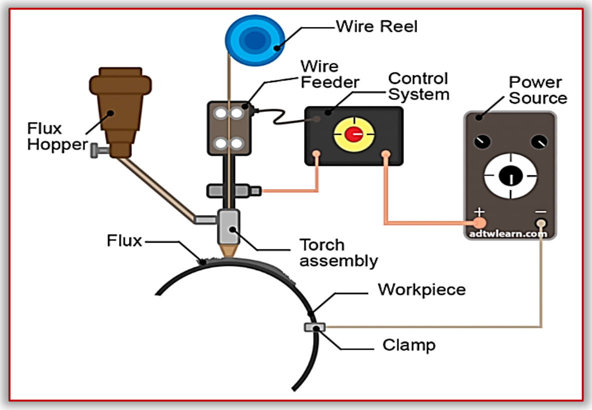

Figure 2. Submerged arc welding equipment [7]

In order to study the strength of welded joints with different intensities of the electric arc, a set of tensile test specimens was made for 3 different intensities of the welding arc current. Each set consisting of 4 specimens welded with the same regime. After testing the samples, stress–strain curves result, they provide a clear picture of the behaviour of welded joints during exploitation, the stretching being present during the operation of pressure vessels.

RESEARCH METHODOLOGY

The first stage of the experiments consisted in defining the welding process, for these the following welding process characteristics were established:

- Base Material: Carbon steel for pressure vessels P355 N (SR EN 10216–3:2003) [8]
- Filler material: Circular section wire 3.2 mm from molybdenum–alloyed copper for welding non–alloy and low–alloy steels under a flux layer, OK Autrod 12.24. [6]
- Protective environment of the electric arc: Flux the layer deposited in a layer with a thickness of 25 mm, OK flux 10.47 [6]
- Welding process feature:
  - Welding under flux with wire electrode (121), EN ISO 4063 [9]
  - Butt welding with full penetration (BW), SR EN 287–1
  - Welding with root support (mb), SR EN 287–1
  - One–pass welding (sl), SR EN 287–1 [10]
  - Horizontal (PA), SR EN ISO 6947:2011 [11]

Figure 4 shows the submerged welding process of two plate–type semi–finished products to create a welded sample, where it can be seen that the welding installation has a torch that has two roles: to manipulate the electrode and to deposit the flux layer in the welding area. The torch is followed by a system for collecting the flux left after welding. There is also a laser indicator that follows the welding direction for the correct orientation of the electrode.

Figure 4. Welding process of sample

From each welded sample, a set of 4 specimens were extracted for tensile testing in accordance with the standard BS EN 895:1995, having the main dimensions:

- sample length: 250 mm
- sample width: 37 mm
- the width in the breaking area: 25 mm
- the radius of passage between the brea king zone and the width of the sample: 26 mm
- sample thickness: 6 mm
- length in the grip area: 78 mm

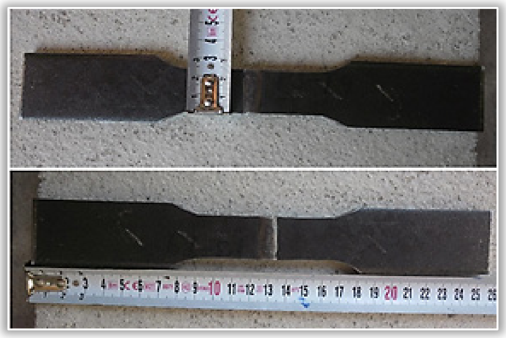

Figure 6. Tensile test specimen

The production of the specimens for the tensile test was carried out only by mechanical processing with cooling in order not to thermally influence the material, in figure 6 it can be observed the final tensile test specimen used.[12]

EXPERIMENTAL RESULTS

The obtained results are the stress–strain curves from which a series of strength indicators can be extracted for determination the strength of welded joints executed with welding regimes of 300A, 400A and 500A. Figure 8 shows the representative stress–strain curves for each set of specimens tested by applying a stretching force with progressive magnitude until the specimen completely breaks. The stretching speed at which the samples were tested is 50 MPa/s. [13]

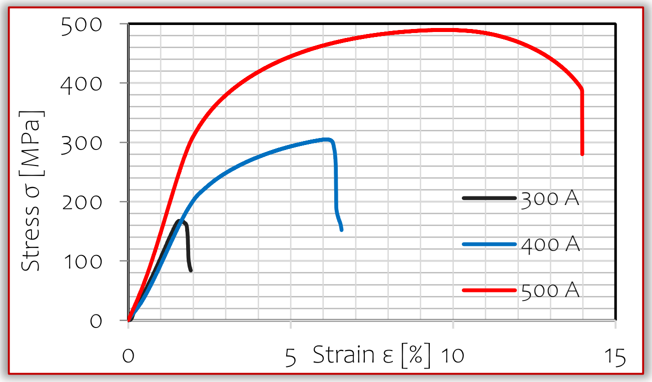

Figure 8. Stress–strain curves

A clear tendency to increase the resilience of welded joints is observed, directly proportional to the increase in the intensity of the welding current. The stress–strain curves increasing in gauge both on the tension axis and on the displacement axis denote the fact that the increase in the intensity of the welding current has a beneficial effect on the increase in the resistance of the welded seam. The ceiling of the increase in tensile strength of the welded joints occurs in the samples welded with 500 A where the sample fracture occurs through the base material. The other samples welded with lower amperages showed fractures through the weld bead, a fact that indicates poor penetration and a low deposition rate of the filler material.

Figure 9 shows graphs that reflect the evolution of the most important resistance indicators. An increasing evolution of both indicators is observed, the indicated values are averages of the data collected from the curves resulting from the test of the 12 specimens divided into three sets, 4 for each welding regime separately.

A more pronounced capping tendency is observed for the parameter average maximum stretching force compared to the average maximum stress, this predicts a fact that indicates that the existence of a set of samples executed with a more pronounced welding regime in terms of the intensity of the welding current would have presented a maximum stretching force not far from the value of 85.1 kN associated with the welding regime with 500 A.

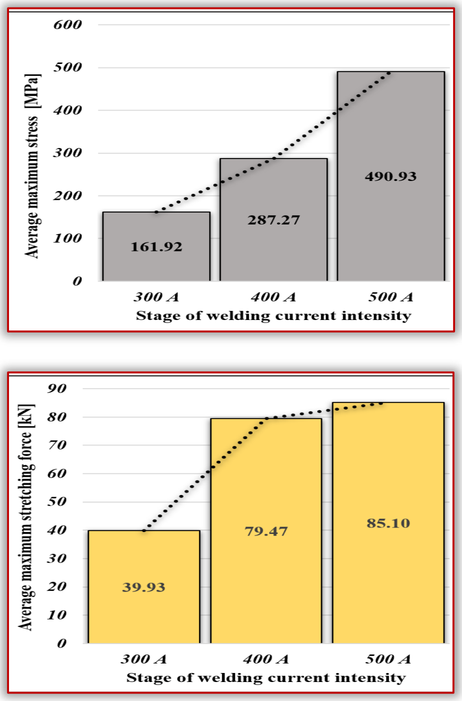

Figure 9. Stress–strain curves

Regarding the tendency of the stress increase in the breaking section of the samples, it can be mentioned that it increases by approximately 74% for each increase in the welding current by 100 A.

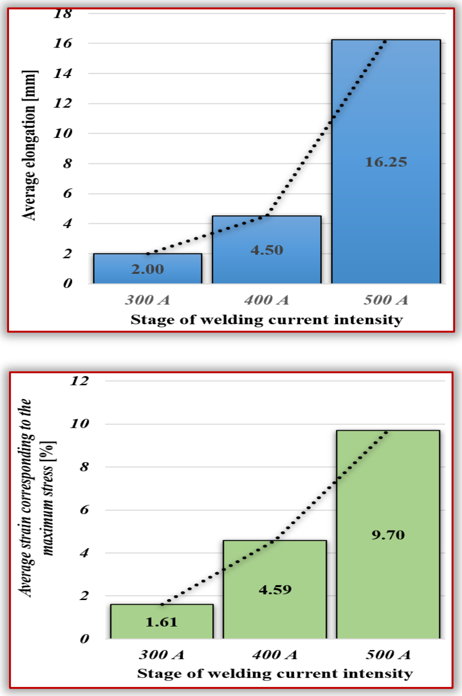

Figure 10. Stress–strain curves

Figure 10 shows graphs that reflect the situation of the indicators specific to the aspects that deal with the deformation of the welded joint under stretching loads. The average elongation chart presents a situation that indicates an increase in ductility for the welded joints by applying an increasing welding amperage. The samples welded with the lowest amperage of 300 A show a very high fragility when breaking and those welded by using with a current intensity of 500 A show a clear tendency to cap the ductility specific to an average elongation of 16.25 mm.

Regarding the average strain corresponding to the maximum stress this shows an increasing trend with the increase in the intensity of the welding current which respects a pattern of 148% increase for every 100A.

There are also other indicators resulting from the tests that can be analysed, they are presented in table 1, all the values are averages of the indicators and not all of them respect a clear increasing tendency with respect to the increasing of the welding current intensity.

Table 1. Average strength indicators resulted from strain test results.

Average strain test results	Welding current intensity			
	300 [A]	400 [A]	500 [A]	U.M.
Breaking stress	83.97	152.04	279.96	MPa
The strain corresponding to the breaking stress	1.92	6.56	13.97	%
Yield tensile stress	130.74	102.18	300.51	MPa
The strain corresponding to the yield tensile stress	1.2	1.08	1.9	%
Modulus of elasticity	105250	118550	314540	MPa
Strain energy	180.55	1416.34	5694.70	kJ

The indicators listed in table 1 that show a clear upward trend are:

- the breaking stress, with a constant average growth of 83% for every increase of the welding amperage with 100 A.
- The strain corresponding to the breaking stress, with a sudden increase of 241% followed by a lower increase of 112% indicating the capping trend.
- Modulus of elasticity, with an increase of 12,6% followed by a sudden increase of 165%.
- Strain energy, with a sudden increase of 684% followed by a lower increase of 320% indicating the capping trend.

CONCLUSIONS

After analysing the indicators resulting from the stress–strain curves obtained after testing the samples, it can be said that the increasing of welding current intensity has a benefice effect of increasing the mechanical properties of the pressure vessel steel welded joints. The main aspect observed is that with the increase in the intensity of the electric welding current there is a better penetration of the filler material into the base material, which favours the increase of the mechanical resistance of the welded joint. Also, the submerged electric arc welding process has a much more pronounced deposition and dilution rate of the filler material with the increase in the intensity of the welding current.

The strength indicators collected from the stress–strain curves, that show pronounced jumps with a clear ceiling trend are:

- The Strain energy, at the ceiling value of 5694,70 kJ
- The strain corresponding to the breaking stress, at the ceiling value of 13,97%
- The elongation, at the ceiling value of 16,25 mm
- The maximum stretching force, at the ceiling value of 85,1 kN

References

[1] Ghanbari G, Liaghat M A, A. Sadeghian, Mahootchi A, Sokouti I, Heidary R, Mohammadi M H, Ansarifard A, Seraj M, Pressure Vessel Design – Guides&Procedure, ISBN 13: 9786001921377, Navid Shiraz Publication, 2011.
[2] *** European standard EN 10027–1:2005, Designation systems for steels – Part 1: Steel names.
[3] Harsh S, Balram R, Rudra P S, A review paper on effect of input welding process parameters on structure and properties of weld in submerged arc welding process, Materials today proceedings, Volume 26, Part 2, 2020, Pages 1931–1935
[4] BODEA Marius, Sudare şi procedee conexe, ISBN: 978–606–737–143–7, Editura UTPRESS, Cluj–Napoca, 2016.
[5] *** https://www.kjellberg.de/submerged–arc–welding–2.html
[6] ESAB – Technical Handbook, Submerged Arc Welding – Fluxes and wires for joining non and low–alloyed Steels, stainless steels and nickel–base alloys.
[7] https://adtwlearn.com/welding–processes/submerged–arc–welding
[8] *** European standard EN 10216–3:2003, Seamless steel tubes for pressure purposes. Technical delivery conditions Alloy fine grain steel tubes.
[9] *** European standard EN ISO 4063:2009, Welding and allied processes — Nomenclature of processes and reference numbers.
[10] *** European standard SR EN 287–1:2011, Qualification test of welders – Fusion welding Part 1: Steels.
[11] *** European standard SR EN ISO 6947:2011, Welding and allied processes — Welding positions
[12] *** Standard BS EN 895:1995, Destructive tests on welds in metallic materials – transverse tensile test.
[13] Patnaik S N, Hopkins D A, Strength of Material: A New Unified Theory for the 21st Century, ISBN 0–7506–7402–4, Elsevier Butterworth Heinemann, 2004.

ISSN: 2067–3809

Faculty of Engineering Hunedoara,
5, Revolutiei, 331128, Hunedoara, ROMANIA
http://acta.fih.upt.ro

ACTA TECHNICA CORVINIENSIS – BULLETIN OF ENGINEERING
TOME XVI [2023] | FASCICULE 2 [APRIL – JUNE]

[1.] Oluranti Adetunji ABIOLA, [2.] Adekola Olayinka OKE, [2.] Dare Aderibigbe ADETAN

THE EFFECT OF FIRING TEMPERATURE ON SOME PHYSICAL PROPERTIES OF OSUN STATE CERAMIC TILES

[1.] Elizade University, Department of Automotive Engineering, Ilara–Mokin, NIGERIA
[2.] Obafemi Awolowo University, Department of Mechanical Engineering, Ile–Ife, NIGERIA

Abstract: The work evaluates the effect of firing temperature on the physical properties of ceramic tiles. This was with the view to determine the optimum processing condition for Osun State ceramic tiles. Ceramic raw materials collected from Osun State were batched using clay–feldspar–silica sand blending ratio of 5:4:1, 5:3:2, 5:2:3, 5:1:4, 6:3:1, 6:2:2, 6:1:3, 7:2:1, 7:1:2 and 8:1:1 by weight; and homogeneously mixed. Three replica samples were molded by dry forming and fired at 1200, 1300 and 1400°C and subjected to water absorption, apparent porosity, apparent relative density and bulk density tests in line with the ISO 10545–3 (1996) standard. The results showed that water absorption, apparent porosity, apparent relative density, and bulk density were within the range 10.43 to 15.02%, 22.77 to 30.20%, 2.26 to 3.09 and 1.34 to 1.45 g/cm3 respectively, while the Figures revealed that sample with 60% clay, 30% feldspar and 10% silica sand fired at 1320°C will exhibit the best physical properties. In conclusion, ceramic raw materials collected from Osun State are viable for ceramic tile production.
Keywords: clay feldspar, silica sand, triaxial blend, physical properties, ceramic tiles

INTRODUCTION

Ceramic tiles are tiles made of a triaxial clay–based combination that are frequently used to cover walls and floors in buildings (Irabor *et al*., 2014; El Nouhy, 2013; Martin–Marquez *et al*., 2008; Iqbal and Lee, 2000; Abiola *et al*., 2021). It is essentially a hygienic item with a porous body and a thick layer of white or colorful glaze that is widely used in living rooms, bathrooms, kitchens, hospitals, labs, schools, public restrooms, and shopping centers (El Nouhy, 2013). According to Iyasara *et al*. (2014) The three silicate clay minerals clay, silica sand, and feldspar are combined to create ceramics, which are inorganic compounds that react with one another at the right high temperature. They can survive extremely high temperatures as well as chemical erosion, which many other materials are susceptible to (Carter and Norton, 2007; European Commission, 2007; Jung, 2008).

Ceramic tiles are characterized by low water absorption, usually between 3.3% and 11.1% (Amoros *et al*., 2007; Griese, 2007; Bryne, 2008; ISO 10545, 1996). Water absorption is commonly referred to as an indicator of porosity for wall and floor tiles (Chukwudi *et al*., 2012). Amount, size and distribution of porosity are among the important factors which affect the physical and mechanical properties of ceramic tiles. Tiles with the lowest apparent porosity have the lowest water absorption, high bulk density and high compressive strength (Soni *et al*., 2015). The porosity is connected to the liquid phase during firing and is affected by the transformations that occur during sintering (Ozturk and Ay, 2014).

Meanwhile, the properties of any ceramic body are dependent on the properties of the raw material and firing temperature (Choudhury *et al*., 2012). Several researchers have reported different triaxial blends as well as diverse optimum firing temperatures for ceramic tiles production. Braganca and Bargmann (2004) reported 1340°C; Amoros *et al*. (2007) and Idowu, (2014), between 1190 and 1220°C; for El–fadaly (2015) it was between 1190 and 1230°C; The American Ceramic Society (2005) stated 1400°C as the maximum firing temperature; while Mathew and Fatile (2014) reported 1218°C as suitable firing temperature.

According to ISO standard 10545 (1996), the physical properties of any ceramic tile (water absorption, apparent porosity, apparent relative density and bulk density) depend mostly on the amount, size and distribution of particles; material composition; and firing temperature (Ozturk and Ay, 2014; Lin and Lan, 2013). Since studies have provided several processing methods for ceramic tiles, it has become imperative to study the effect of material blending ratio and firing temperature on the physical properties of ceramic tiles produced from raw materials collected from Osun State.

MATERIALS AND METHODS

The kaolinite clay utilized in this study was gathered from Ipetumodu, the administrative center of the Ife North Local Government region of Osun State, Nigeria (Oke and Omidiji, 2016). Silica sand was gathered at the Isasa River in Osun State, Nigeria, which divides the local governments of Ayedaade and Ife North. Feldspar was gotten at Osogbo, the capital of Nigeria's Osun State. The three raw materials collected were beneficiated separately as specified by Abiola *et al.*, (2019).

— Preparation of materials

The ceramic raw materials were prepared as described by Abiola *et al.* (2021). Clay, silica sand, and feldspar were thoroughly combined to create a more chemically and physically homogenous substance for producing tiles. Due to many discrepancies regarding the ideal mixing ratio for ceramic materials, the mixing ratios for the raw materials were varied (Braganca and Bargmann, 2004; Amoros *et al.*, 2007; El–Fadaly 2015; Martín–Márquez *et al.*, 2010; Idowu, 2014).

To predict the mixing ratio of ceramic ingredients, Norsker and Danisch's (1993) 10–step tri–axial blending chart was used. Only the ceramic blends with clay–feldspar–silica sand ratios of 5:4:1, 5:3:2, 5:2:3, 5:1:4, 6:3:1, 6:2:2, 6:1:3, 7:2:1, 7:1:2, and 8:1:1 and designated as blends A, B, C, up to J were chosen from the chart's potential sixty–six combinations. Due of the fact that ceramic is referred to as a triaxial blend product, thirty blends that contain fewer than three materials were disregarded (Teo *et al.*, 2016; Idowu, 2014; Irabor *et al.*, 2014; Iyasrara *et al.*, 2014; Soni *et al.*, 2015; El Fadaly, 2015). Since clay is the main component used in the creation of ceramic tiles, 26 additional blends with less than 50% clay percentage were also disregarded (Solanki and Shah, 2016; Soni *et al.*, 2015; Irabor *et al.*, 2014; Adindu *et al.*, 2014; El Ouahabi *et al.*, 2014; El Nouhy, 2013; Misra *et al.*, 2013; Manfredini and Hanuskova, 2012; Murray 1999).

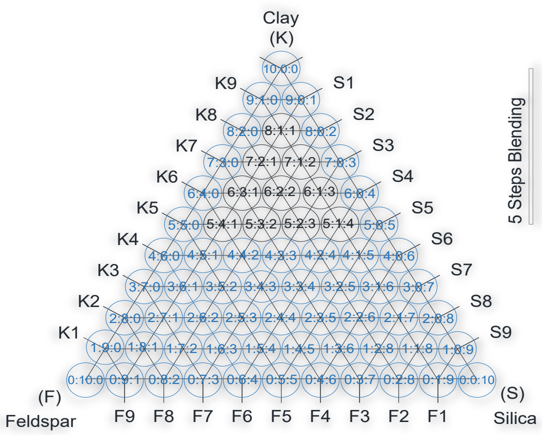

Figure 1: 10 steps triaxial blending chart

Each blend of the ceramic materials, A through J, was compacted to the recommended size for the physical property test sample, 50 x 15 x 15 mm, according to the instructions provided by Bresciani et al. (2004). After forming, the samples were dried by convection in an open laboratory drying oven (model DHG–9101–2A manufactured by Searchtech Instrument) where heated air was circulated around the ceramic samples. Since water should evaporate from a ceramic combination below 100°C, the air around the samples was held at 95°C to remove any water content. The materials were maintained in this condition for 20 hours using the Br.MSME–DI technique (2011). It is anticipated that this drying procedure will stop the final product's eventual differential shrinkage, warping, cracking, and deformation.

According to Br.MSME–DI (2011) recommendation, the ceramic samples were heat–treated in the laboratory drying oven at 300°C before firing in order to provide additional drying, vaporize or decompose organic additives and other impurities, as well as remove leftover, crystalline, and chemically bound water. According to the plan put forth by Br.MSME–DI (2011), the ceramic samples were kept in the kiln for 20 hours at a constant temperature of 300°C. The ceramic samples were removed from the kiln after this time, allowed to naturally cool at room temperature, then fired in a furnace (model XD–1700M manufactured by Zhengzhou Brother Furnace Company, China). The fire temperatures employed for the experiment were 1200, 1300, and 1400°C. These temperatures were used because Martn–Márquez et al. (2008) claimed that firing ceramic tile above the vitrification range will result in a drastic fall in the physical properties due to the forced expulsion of trapped gases, resulting in bloating and blisters and Abiola and Oke (2017) claimed that Ipetumodu clay begins to disintegrate at 1450°C. Additionally, as the American Ceramic Society (2005) states that the highest sintering temperature for the manufacture of ceramic tiles is 1400°C, which value was chosen as the maximum firing temperature as well. To assess the behavior of the local tiles made below the recommended maximum firing temperature for ceramic products, lower temperatures (1200°C and 1300°C) were necessary. This was because many researchers had suggested sintering temperatures ranging from 1190 to 1340°C. (Braganca and Bargmann 2004; Amoros et al., 2007; Idowu, 2014; Mathew and Fatile, 2014; El–fadaly, 2015). To guarantee that the samples' cross–sections were heated to the same temperature, the samples were kept at the appropriate firing temperatures for around an hour (Abeid and Park, 2018; Ashby, 2005). Following that, the samples were held in the kiln for a cycle of at least 18 hours where it was cooled, in line with Br. MSME–DI (2011).

— Physical properties test

The ceramic tiles were removed from the kiln after cooling and tested for water absorption, apparent porosity, and apparent relative density in accordance with the recommendations of Abiola et al. (2021) and ISO 10545–3 (1996).

The water absorption was calculated from equation (1):

$$A_w = \frac{m_2 - m_1}{m_1} \text{ x } 100\% \qquad (1)$$

where A_w is water absorption (%); m_1 is the average mass of the dry samples in gram (g); and m_2 is the average mass of the wet samples in gram (g) (ISO 10545–3, 1996).

Apparent porosity was calculated from equation (2) as:

$$P_a = \frac{m_2 - m_1}{m_2 - m_3} \text{ x } 100\% \qquad (2)$$

where P_a is the apparent porosity (%); m_1 is the average mass of the dry samples in gram (g); m_2 is the average mass of the wet samples in gram (g); and m_3 is the average mass of the suspended samples impregnated by boiling water in gram (g) (ISO 10545–3, 1996).

Meanwhile, apparent relative density was calculated using equation (3) (ISO 10545–3, 1996) as:

$$RD_a = \frac{m_1}{m_1 - m_3} \qquad (3)$$

where RD_a is the apparent relative density; m_1 and m_3 are the same as in equation (2) (ISO 10545–3, 1996).

Bulk density was determined using equation (4) as:

$$BD = \frac{m_1}{V} \qquad (4)$$

where BD is the bulk density, in g/cm^3; m_1 is the average mass of the dry samples in gram (g); and V is the exterior volume of the sample, in cm^3 (ISO 10545–3, 1996).

— Experimental design

The experiment was created using Design Expert 6.0.8 Portable using the surface response approach. In order to determine the impact of firing temperatures (1200 oC, 1300 oC, and 1400 oC) and triaxial blend ratios (5:4:1, 5:3:2, 6:2:2, 6:1:3, 7:2:1, 7:1:2, and 8:1:1) on the physical properties (water absorption, apparent porosity, apparent relative density, and bulk density) of ceramic tiles, a two–factor design matrix linear model was used. Design matrix of sixty (60) experiments design for two factors were used on each combination of firing temperature and blending ratio for physical properties.

RESULTS AND DISCUSSION

— Water absorption

The results of the physical properties tests are as seen in Figure 2. Water absorption decreased with increased temperature and later reduced with continued increase in temperature.

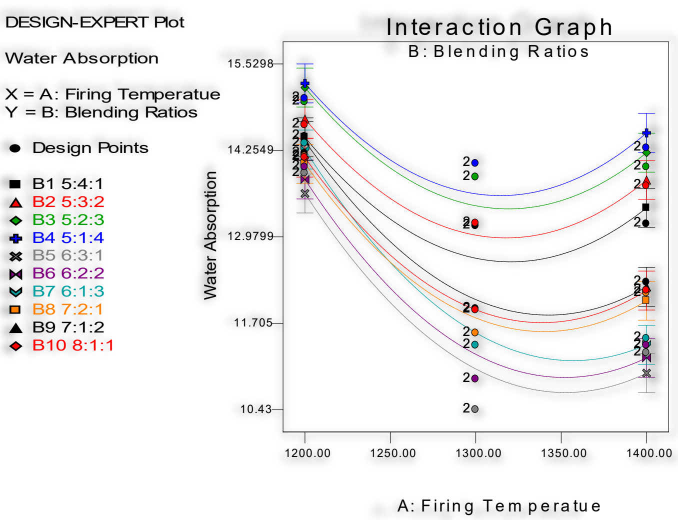

Figure 2: Water absorption of the ceramic tile samples fired at different temperatures

The reduced water absorption with increased temperature could be due to the liquid phase formation at high temperature and densification as the sample cools to room temperature (Alves *et al.*, 2015; Kimambo *et al.*, 2014). The liquid phase that is formed fills the pores and decreased the porosity (Viruthagiri *et al.*, 2009). Thus, increased temperature reduces or eliminates pores within the ceramic article, thereby, reducing the article's porosity and its tendency to absorb water. (Soni *et al.*, 2015).

The general increase in water absorption for all samples as firing temperature rises from 1300°C to 1400°C may be due to bloating which takes place as a result of the expansion of gases enclosed in the pores; this causes the increase in porosity (Kimambo *et al.*, 2014; Hettiarachchil *et al.*, 2014). In addition, the high firing temperature can cause mullite crystals to become coarse and decrease densification and hence increase water absorption (Kimambo *et al.*, 2014).

Ceramic tiles, characterized by low water absorption between 3.3% and 11.1% is the most important physical property for ceramic tiles mostly used as floor tiles (Amoros *et al.*, 2007; Bryne, 2008; ISO 10545, 1996). According to technical standards, the tiles with water absorption higher than 10% can be used as wall tiles and the majority of standard wall tiles have glazed porous bodies with water absorption between 10% and 20% (Kimambo *et al.*, 2014). Thus, the tiles produced in this study (with water absorption in the range 15.02–10.43%) are suitable wall tiles.

Figure 2 shows that only the ceramic samples "E" and "F" fired at temperature 1300°C have water absorption 10.43% and 10.88% respectively which falls within the ISO standard and 15.02% been the maximum recorded for sample D fired at 1200°C. Meanwhile Idowu (2014) recorded a much higher water absorption of 20% with ceramic tiles produced from clay, silica sand and feldspar collected from Ifon, Igbokoda and Ijero respectively while Mathew and Fatile (2014) recorded a much better water absorption of between 0.2% to 0.38% with material collected from Ijero, Ajaokuta and Okpella. Ogundare *et al.*, (2015) alighted a similar result (water absorption: 0.9%– 3.9%) with porcelain tiles produced materials collected form Ijero and Okpella. The water absorption of 5.61% to 17.12% was recorded in the study of Chukwudi *et al.*, (2012) while Soni et al., (2015) recorded 0.9% to 5.9% in its study. El–Nouhy (2013) collected 14 different ceramic tile samples produced in Egypt and found all the samples to have water absorption ranging from 8.5% to 16.0%.

— Apparent porosity

The results in Figure 3 show that the behaviour of apparent porosity is similar to water absorption (Soni *et al.*, 2015) as they both generally decreased with increased temperature and later increased with continued increase in temperature. The reduced apparent porosity with increased temperature could also be due to the liquid phase formation at high temperature and densification as the sample cools to room temperature (Alves *et al.*, 2015; Kimambo *et al.*, 2014) as explained for water absorption.

Figure 3 shows the minimum and maximum apparent porosity recorded as 22.77% for sample E fired at 1300°C and 30.20% for sample D fired at 1200°C respectively. The result is similar to the findings of Chukwudi *et al.*, (2012); Ogundare *et al.*, (2015); and Soni *et al.*, (2015) which recording apparent porosity of 11.29% to 31.32%; 11% to 16%; and 5% to 26% for samples fired at 1200°C; 1250°C; and 1350°C respectively. The apparent porosity established by El–Nouhy (2013) in his study ranged from 17.5% to 27.5%.

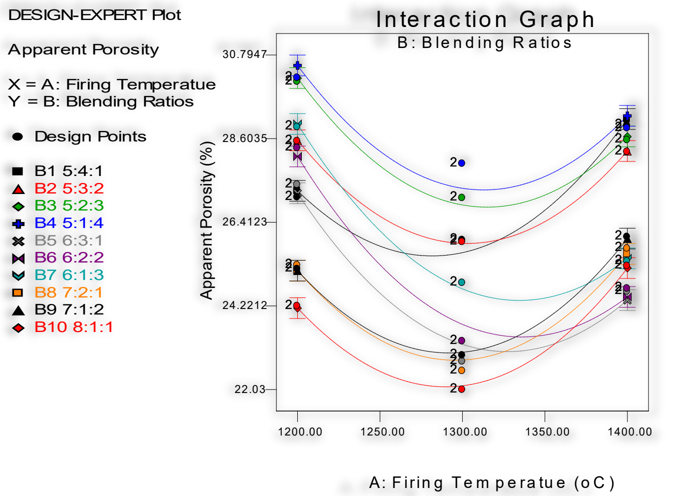

Figure 3: Apparent porosity of the ceramic tile samples fired at different temperatures

The values of the apparent porosity of all the ceramic samples were found to decrease with an increase in firing temperature and later increase with further increase in temperature as shown in Figure 3. The increase in apparent porosity at higher firing temperature is believed to be caused by bloating which takes place as gas is expelled from the matrixes, thereby resulting in increased apparent porosity (Kimambo *et al*., 2014; Matin–Marquez *et al*., 2008). The increase in the apparent porosity with further increase in firing temperature from 1300°C to 1400°C may be due to increase in fluxing oxides, Na_2O and K_2O and feldspar content in the tiles (Kimambo *et al*., 2014; El Nouhy, 2013; Matin–Marquez *et al*., 2008).

— Apparent relative density

The apparent relative density for samples A, E, G, H, I and J shown in Figure 4 increased as firing temperature increases.

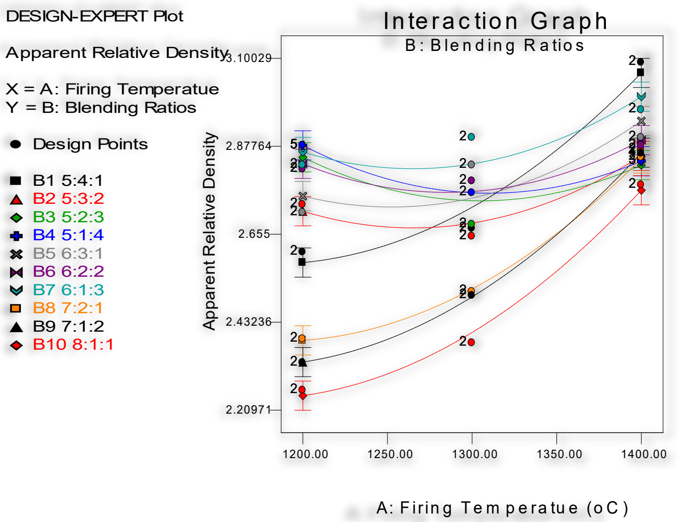

Figure 4: Apparent relative density of the ceramic tile samples fired at different temperatures

This is similar to the submission of Choudhury *et al*., (2012) and Zabotto *et al*., (2012). It could be seen with the samples that feldspar has a direct relationship with the apparent relative density as increased feldspar result in increased apparent relative density. This is in line with the result of Chao *et al*., (2010) and could be due to bloating in the matrixes. The increase in the apparent relative density of the ceramic samples with increased firing temperature could also be an indication that cation concentration is increased as increased cation within the matrix will cause increase apparent relative density (Zabotto *et al*., 2012).

— Bulk density

The bulk density of ceramic samples reduced with increased firing temperature as shown in Figure 5. The lower bulk density at higher firing temperature may be attributed to bloating which takes place as gasses are expelled from the matrices to cause the increase in porosity (Kimambo *et al*., 2014). Sample D fired at 1400°C has the least bulk density when compared to the rest of the samples. This is because the bulk density of any ceramic article decreases with a decrease in the feldspar content. The feldspar which is a fluxing oxide helps in the production of liquid phases which fill the pores and increase the bulk density of the ceramic body (El Nouhy, 2013). The bulk density of the ceramic body attains its maximum level when the available liquid phase is enough to block the open pores (Kimambo *et al*., 2014).

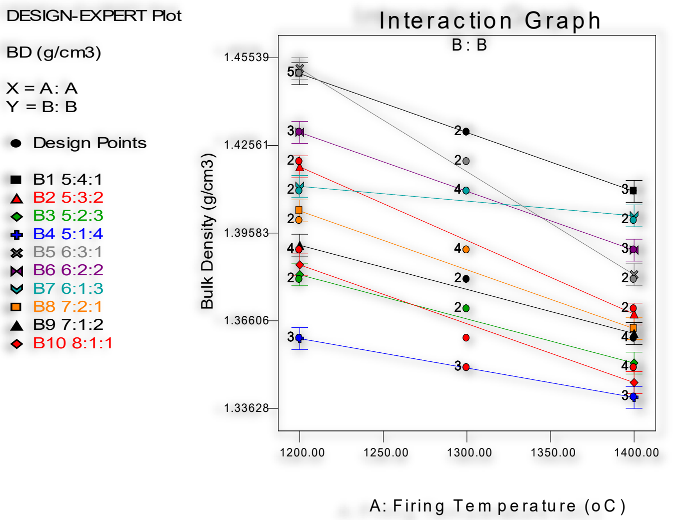

Figure 5: Bulk density of the ceramic tile samples fired at different temperatures

CONCLUSION

There is appreciation in the physical properties of ceramic tiles as firing temperature increases from 1200°C to just above 1300°C and these properties deteriorate with a further increase in temperature. Therefore, the ceramic sample will attain the best physical properties at about 1320°C (as can be deduced from the Figures).

The ceramic sample produced from Osun State raw materials in this study will be suitable for wall tiles since the water absorption is between 10% and 15%.

References

[1] Abeid, S. and Park, S.E.: Suitability of vermiculite and rice husk ash as raw materials for production of ceramic tiles. International Journal of Materials Science and Applications, 7 (2), 39–48, 2018.

[2] Abiola, O.A. and Oke, A.O.: Carbonised palm kernel shell effect on the physico–chemical properties of clay–sand mixture. Journal of Applied Science, Engineering and Technology, 17 (1), 17–23, 2017.
[3] Abiola, O.A.; Oke, A.O.; Omidiji, B.V. and Adetan, D.A.: The effect of beneficiation on some properties of Osun State ceramic raw materials. Journal of Casting & Materials Engineering, 3 (3), 62–66, 2019.
[4] Abiola, O.A.; Oke, A.O.; Omidiji, B.V. and Adetan, D.A.: The effect of raw materials on some properties of Osun State ceramic tiles. Journal of Engineering studies and Research, 27 (1), 7–12, 2019.
[5] Adindu, C.I.; Moses, J.; Thaddeus, C.A. and Tse, D.T.: Exploring ceramic raw materials in Nigeria and their contribution to nation's development. American Journal of Engineering Research, 3 (9), 127–134, 2014.
[7] Alves, H.J.; Melchiades, F.G. and Boschi, A.O.: Effect of feldspar particle size on the porous microstructure and stain resistance of polished porcelain tiles. Journal of the European Ceramic Society, 32, 2095–2102, 2012.
[8] Amoros, J.L.; Orts, M.J.; Garcıa–Ten, J.; Gozalbo, A. and Sanchez, E.: Effect of the green porous texture on porcelain tile properties. Journal of the European Ceramic Society, 27, 2295–2301, 2007.
[9] Ashby, M.F.: Materials selection in mechanical design, Third Edition, Pergamon Press, Butterworth–Heinemann Linacre House, Jordan Hill, Oxford, 2005.
[10] Braganca, S.R. and Bergmann, C.P.: Traditional and glass powder porcelain: Technical and microstructure analysis. Journal European Ceramic Society, 24 (8), 2383–2388, 2004.
[11] Bresciani, A.; Ricci, C. and Imola S.: Innovative process for ceramic tile manufacturing by double pressing with continuous precompaction. Castlelon, p. 49–60, 2004.
[12] Br. MSME–DI: Ceramic glazed wall tiles, small scale production enterprise. W.B.S.I.D.C Industrial Estate, J.P. Avenue, Durgapur–12, p. 1–18, 2011.
[13] Bryne, M. F.: Properties of Ceramic Tile, 2008. http://www.thetileryatp.com/assets/files/press/A6_Tile_Properties.pdf.
[14] Carter, C.B. and Norton, M.G.: Ceramic materials: Science and engineering. First Edition, Springer–Verlag, New York. p. 3 – 4, 2007.
[15] Chao, S.; Petrovsky, V. and Dogan, F.: Effects of sintering temperature on the microstructure and dielectric properties of titanium dioxide ceramics. Material Science, 45, 6685–6693, 2010.
[16] Choudhury, S.; Bhuiyan, M.A and Hoque, S.M.: Effect of sintering temperature on apparent density and transport properties of NiFe2O4: Synthesized from nano size powder of NiO and Fe2O3. Int. Nano Lett. 1 (2), 111–116, 2012.
[17] Chukwudi, B.C.; Ademusuru, P.O. and Okorie, B.A.: Characterization of sintered ceramic tiles produced from steel slag. Journal of Minerals and Materials Characterization and Engineering, 11, 863–868, 2012.
[18] El–Fadaly, E.: Characterization of porcelain stoneware tiles based on solid ceramic wastes. International Journal of Science and Research, 4 (1), 602–608, 2015.
[19] El Nouhy, H.A.: Assessment of some locally produced Egyptian ceramic wall tiles. Housing and Building National Research Center Journal, 9, 201–209, 2013.
[20] El Ouahabi1, M.; Daoudi, L.; De Vleeschouwer, F.; Bindler, R. and Fagel, N.: Potentiality of clay raw materials from northern Morocco in ceramic industry: Tetouan and Meknes areas. Journal of Minerals and Materials Characterization and Engineering, 2 (3), 145–159, 2014.
[21] European Commission: Reference document on best available techniques in the ceramic manufacturing industry, 2007. http://eippcb.jrc.es.
[22] Griese, B.: Porcelain in the ceramic tile industry. Tilt Council of North America's Product Performance Testing Laboratory, p. 70–73, 2007. https://www.tcnatile.com/images/pdfs/Porcelain%20in%20the%20Ceramic%20Tile% 20Industry.pdf.
[23] Hettiarachchi1, P.; Wickramasinghearachchi, R.C. and Pitawala H.M.T.G.A.: A comparison of fluxing effects of granite and feldspar on red clay body composition. Journal of Geological Society of Sri Lanka, 16, 101–108, 2014.
[24] Idowu, I.O.: Production of vitrified porcelain tiles using local raw materials from southwestern Nigeria. Journal of Emerging Trends in Engineering and Applied Sciences, 5 (6), 421– 428, 2014.
[25] Iqbal, Y. and Lee, W.E.: Microstructural evolution in triaxial porcelain. Journal of American Ceramic Society, 83 (12), 3121–3127, 2000.
[26] Irabor, P.S.A.; Jimoh, S.O, and Omowumi, O.J.: Ceramic raw materials development in Nigeria. International Journal of Scientific and Technological Research, 3 (9), 275–287, 2014.
[27] ISO 10545: EN ISO norms for ceramic tiles – Testing methods, 1996. www.norfloor.no/media/ wysiwyg/DIY/ISO_10545–2.pdf.
[28] Iyasara, A.C.; Joseph, M. and Azubuike, T.C.: The use of local ceramic materials for the production of dental porcelain. American Journal of Engineering Research, 3 (9), 135–139, 2014.
[29] Jung, P.: Quality Control: Preparation of Samples for XRF Analysis. The article was written for Retsch Inc., Newtown, PA. p. 23–27, 2008.
[30] Kimambo, V.; Philip, J.Y.N. and Lugwisha, E.H.: Suitability of Tanzanian kaolin, quartz and feldspar as raw materials for the production of porcelain tiles. International Journal of Science Technology and Society, 2 (6), 201–209, 2014.
[31] Lin, K.L. and Lan, J.Y.: Water retention characteristics of porous ceramics produced from waste diatomite and coal fly ash. Journal of Clean Energy Technologies, 1 (3), 211–215, 2013.
[32] Manfredini, T. and Hanuskova, M.: Natural raw materials in "traditional" ceramic manufacturing. Journal of the University of Chemical Technology and Metallurgy, 47 (4): 465–470, 2012.
[33] Martín–Márquez, J.; Rincón, J. Ma. and Romero, M.: Effect of firing temperature on sintering of porcelain stoneware tiles. Ceramics International, 34, 1867–1873, 2008.
[34] Martín–Márquez, J.; Rincon, J. Ma. and Romero, M.: Mullite development on firing in porcelain stoneware bodies. Journal of the European Ceramic Society, 30 (7), 1599–1607, 2010.
[35] Mathew, G.O. and Fatile, B.O.: Characterization of vitrified porcelain tiles using feldspar from three selected deposits in Nigeria. Research Journal of Recent Sciences, 3 (9), 67–72, 2014.
[36] Misra, S.N.; Machhoya, B.B. and Savsani, R.M.: Thermo physical characteristics of vitrified tile polishing waste for use in traditional ceramics–an initiative of CGCRI, Naroda centre. International Conference on Ceramics, Bikaner, India. International Journal of Modern Physics: Conference Series, 22, 118–133, 2013.
[37] Murray, H.H.: Applied clay mineralogy today and tomorrow. Clay Minerals, 34, 39 – 49, 1999.
[38] Norsker and Danisch: Glazed for the self–reliant potter. Publication of the Deutsches Zentrum für Entwicklungstechnologien, Germany, 1993.
[39] Ogundare, T.; Fatile, O. and Ajayi, O.: Development and characterization of parian bodies using feldspar from two selected deposits. Leonardo Electronic Journal of Practices and Technologies, 27, 147–156, 2015.
[40] Oke, A.O and Omidiji, B.V.: Investigation of same moulding properties of a Nigeria clay–bonded sand. Archives of Foundry Engineering, 16 (3), 71–76, 2016.
[41] Ozturk, Z.B. and Ay, N.: Investigation of porosity of ceramic tiles by means of image analysis method. Journal of Ceramic Processing Research, 15 (6), 393–397, 2014.

[42] Solanki, K.M. and Shah, S.R.: Analysis of drying process in ceramic tiles industries. International Journal of Advance Research and Innovative Ideas in Education, 2 (3), 409–418, 2016.
[43] Soni, A.; Mathur, R. and Kumar, K.: Study on particle size distribution and its effects on shrinkage, porosity and bulk density of tri–axial porcelain tiles. Indian Journal of Research, 4 (5), 58–60, 2015.
[44] Teo, P.T.; Seman, A.A.; Basu P. and Sharif N.M.: Characterization of EAF steel slag waste: the potential green resource for ceramic tile production. 5th International Conference on Recent Advances in Materials, Minerals and Environment (RAMM) & 2nd International Postgraduate Conference on Materials, Mineral and Polymer (MAMIP), 4–6 August 2015. Elsevier, Procedia Chemistry, 19, 842 – 846, 2016.
[45] The American Ceramic Society: Kiln firing chart: Pottery making illustration, 2005. http://www.ceramicartdaily.net/PMI/KilnFiringChart.pdf. (Accessed September 13, 2016).
[46] Viruthagiri, G.; Gobi, R. and Rajamannan, B.: Mechanical properties related to the use of Glass waste as a raw material in porcelain stoneware tile mixtures. Recent Research in Science and Technology, 1 (2), 52–57, 2009.
[47] Zabotto, F.L.; Gualdi, A.J. and Eiras, J.A.: Influence of the sintering temperature on the magnetic and electric properties of $NiFe_2O_4$ ferrites. Materials Research, 15(3), 428–433, 2012.

ISSN: 2067–3809

1.Adnan RAMAKIĆ, 2.Dusanka BUNDALO, 3.Zlatko BUNDALO

AN APPROACH TO GAIT RECOGNITION USING DEEP NEURAL NETWORK

1. Technical Faculty, University of Bihać, Bihać, BOSNIA & HERZEGOVINA
2. Faculty of Philosophy, University of Banja Luka, Banja Luka, BOSNIA & HERZEGOVINA
3. Faculty of Electrical Engineering, University of Banja Luka, Banja Luka, BOSNIA & HERZEGOVINA

Abstract: In this paper, an analysis was performed in the context of gait recognition. Gait recognition is an approach for people identification based on the gait characteristics of a person. Gait recognition methods essentially belong to the behavioral biometric methods. While walking, each person creates different patterns that may be used for the purpose of identification. For this reason, many gait recognition methods have been presented in recent years that use gait in different ways for the purpose of identification. Some of the presented methods were based on the silhouettes of a person, while others used different models based, for example, on different measurements of the human body. Following the above, the approach of gait recognition was analyzed, focusing on some important aspects of this type of identification. In addition, the use of a Deep Neural Network (DNN) for gait recognition was investigated.

Keywords: Biometric Methods, Deep Neural Network (DNN), Gait Energy Image (GEI), Gait Recognition, People Identification

INTRODUCTION

People identification is an important process in many aspects of human life. Most people are confronted with some kind of identification in the course of their lives, e.g., at airports, when crossing borders, with various security systems, e.g., to gain access to various facilities, etc. For this reason, different systems of identification have been introduced, using different methods for the purpose of identification. The mentioned methods are usually based on features related to and extracted from human body characteristics, i.e., physiological characteristics. In addition, behavioral characteristics of individuals are also used. The methods based on the mentioned characteristics (the so-called biometric characteristics) and the features extracted from them are called biometric methods. Accordingly, there are physiological and behavioral biometric methods.

Some examples of physiological biometric methods are fingerprint, methods based on eye features extracted from parts of the eye such as the iris and retina, methods using facial features, hand features, etc. Some examples of behavioral biometric methods are methods that use a person's voice, methods based on gait analysis, methods based on keystroke dynamics, signatures, etc. It is important to note that some methods are more reliable than others. For example, a method based on iris features is more reliable than a method based on keystroke dynamics. In general, the use of a particular biometric characteristic depends on the application. Each of the mentioned biometric characteristics has advantages and disadvantages, and it is not possible that one biometric characteristic satisfy all applications [9].

In this paper, gait recognition for people identification was analyzed. Gait recognition is a method based on the analysis of a person's gait. Gait is a behavioral biometric characteristic of a person, and various features and methods based on them have been presented in recent years. In the following chapters of this work, different aspects of gait recognition and some well-known gait recognition methods have been analyzed. Also, three experiments were conducted using Deep Neural Network (DNN) and results were presented.

GAIT RECOGNITION

Gait recognition is a method for people identification based on gait analysis. When walking, each person creates different patterns that may be used for identification. For this reason, two approaches to gait recognition are in use: the appearance-based approach and the model-based approach. An appearance-based approach usually uses the silhouettes of people or parts of them, i.e. different representations of the silhouettes. A model-based approach is usually based on a model that uses different measurements of the human body, e.g., the length of the legs or arms [18].

With the introduction of the Kinect device by Microsoft in 2010 [14], more attention began to be paid to gait recognition as a method for people identification. Microsoft Kinect is a device that can be used in conjunction with Microsoft's Xbox console for interaction without the need to use an intermediate device, such as a controller. It contains an RGB (Red, Green, Blue) camera, depth sensor, and microphone array. It makes it possible to obtain RGB and depth images, as well as additional features such as skeleton information. Later, Microsoft also introduced a version of Kinect for Windows with a corresponding software development kit (SDK). After that, Microsoft introduced the second generation of Kinect, but today the production of Kinect is not continued. It has been replaced by Azure Kinect. Microsoft Kinect for Xbox 360 console is shown in Figure 1.

This makes the Kinect device well suited for gait recognition tasks, as it is possible to implement methods based on both approaches to gait recognition, model-based and appearance-based. Using the skeleton feature provided by Kinect, many model-based gait recognition methods have been implemented, while with the availability of RGB and depth images, many appearance-based gait recognition methods have been implemented because the person silhouettes required for appearance-based approaches can be obtained from RGB and depth images. Figure 2 shows an example of the steps involved in implementing a gait recognition system and this can be realized as follows.

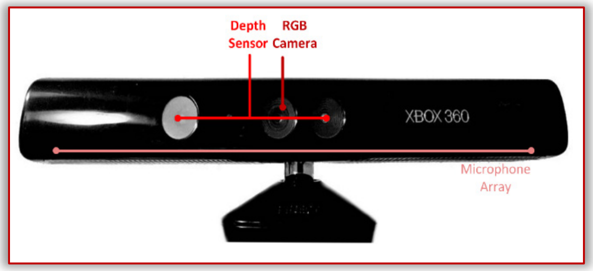

Figure 1. Microsoft Kinect for Xbox 360 Console

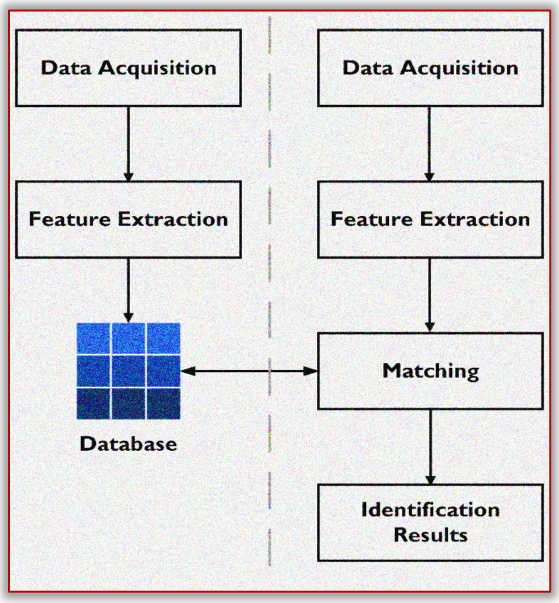

Figure 2. Gait Recognition System (Steps)

Some gait recognition system can be roughly divided into two parts. The first part is the creation of a database, and the second part is an identification part. This is illustrated in Figure 2, where the left side of the figure is related to the creation of a database, while the right part of the figure is an identification part. In the first part, features extracted from silhouette images, for example, must be stored for each person. In Figure 2 *Data Acquisition* refers to the acquisition of RGB or depth images, e.g., with Microsoft Kinect. Also, in Figure 2 may be added some additional steps between *Data Acquisition* and *Feature Extraction* related to data preparation, image processing, etc., but broadly the same as in Figure 2. *Feature Extraction* refers to the process of extracting features related to each person. This depends on the implementation and the defined type of features to be used in the gait recognition system. The database (*Database*) contains the features defined and extracted for each person.

The second part is the identification part (Figure 2, the right side of the figure), which consists of the data acquisition (*Data Acquisition*), the feature extraction (*Feature Extraction*), the matching of the features (*Matching*) and at the end the results of the matching, i.e. the identification results (*Identification Results*). An identification process works as follows. If there is a person to be identified, it is necessary to capture RGB or depth images with a device such as, e.g., Kinect. Depending on the implemented method, the features should be extracted, for example, from the silhouettes of a person. An example of the extracted silhouettes (unprocessed) from the RGB images for one person is shown in Figure 3. After the features are extracted, they should be matched with the features stored in the database. The best match between the extracted features and the features stored in the database results in the identified person.

Figure 3. The Extracted Silhouettes for One Person

In the previous text, an example scenario was described in which the system and the implemented method for gait recognition work with the silhouette of the person (the appearance-based approach). Similarly, can be implemented and some other system that uses some other elements for obtaining the features, for example, some measurements from the human body (the model-based approach). The steps shown in Figure 2 are essentially the similar for the most gait recognition systems.

Today, most gait recognition systems are implemented using machine learning and deep learning, where a model is created and trained using a deep neural network or some type of classifier. In recent years, many methods for gait recognition have been presented. The presented methods were based on either a model-based or an appearance-based approach. One of the most popular methods is the Gait Energy Image (GEI) [6]. GEI was defined as an image containing the silhouettes of a person over a gait cycle, normalized, aligned, and temporally averaged. Based on GEI, some other methods such as Backfilled Gait Energy Image (BGEI) [22] have also been developed. BGEI is similar to GEI, where silhouettes are filled from the foremost pixels to the back of the image. Also, other interesting presented methods are HGEI-i and HGEI-f [12] [20], where fusion of the information between GEI features and height of a person feature has been done. Gait Gaussian Image (GGI) [1] is a period-based gait recognition method intended for feature extraction from gait images over a gait cycle. An interesting approach presented in [8] divides the human body image into areas and then extracts features for each area. Gait Energy Volume (GEV) [21] extends the concept of GEI to 3D. Some other interesting methods for gait recognition can be found in [7] [3] [17] [19] [11].

The main advantage of gait recognition as a method of person identification is the possibility of person identification at a long distance. A stereo camera with a long range can be used for this purpose. Also, no interaction with a person to be identified is required. This means that a particular person can be identified without knowing that the identification process is in progress. It is important to note that gait is not as unique a human characteristic as, for example, fingerprint or iris, so the use of gait recognition methods often requires some additional features along with gait features. This makes implementation more complex and harder to implement.

EXPERIMENTAL SETUP

Three experiments were performed using a well-known gait recognition method called Gait Energy Image, or as it is acronym GEI. GEI was introduced by authors Han and Bhanu [6] and represents an image with multiple silhouettes of a person over a gait cycle that are normalized, aligned, and temporally averaged. Casia Dataset B [24] [23] [15] was used for experimental evaluation. Casia Dataset B is a gait database that contains 124 subjects with gait data obtained from 11 views and with three variations - viewing angle, clothing, and carrying condition changes [15]. Some examples of GEI images from Casia Dataset B [24] [23] [15] are shown in Figure 4. For all three experiments, 100 subjects were used.

(a) Normal gait (90 degrees viewing angle)

(b) Clothing changes (90 degrees viewing angle)

(c)Carrying changes (90 degrees viewing angle)

(d) Normal gait (180 degrees viewing angle)

Figure 4. Examples of GEI images from Casia Dataset B [24] [23] [15]

In the first experiment, GEI images with a viewing angle of 90 degrees were used for each of the 100 persons. In total, there were only six images in normal gait for each person. Thus, a total of 600 images. In the second experiment, GEI images with the viewing angle of 90 degrees were used for each of the 100 persons. In total, there were 10 images for each person (six images with the person in normal gait, two images with carrying condition changes, and two images with clothing changes). Thus, a total of 1.000 images. In the third experiment, GEI images with different viewing angle, carrying condition changes, and clothing changes were used for each of the 100 person. For each person, there were 110 GEI images (66 images with the person in normal gait, 22 images with carrying condition changes, and 22 images with clothing changes). A total of 11.000 images.

For the experiments, a deep neural network in Matlab was created. The neural network created consists of seven layers, the first layer being the feature input layer (*featureInputLayer*). Mentioned layers are *featureInputLayer*, *fullyConnectedLayer*, *batchNormalizationLayer*, *reluLayer*, *fullyConnectedLayer*, *softmaxLayer*, and *classificationLayer*.

Since the neural network works with features, it is necessary to obtain features from defined GEI images for each person. For this purpose, a bag of visual words (*bagOfFeatures* in Matlab, with parameters *VocabularySize* (500) and *PointSelection* as *Detector*) [4] [13] was used, where the visual vocabulary is created by default from Speeded-Up Robust Features (SURF) [2]. The features obtained were stored in a table.

Feature data were divided into a training and a test part in a ratio of 85% for training and 15% for testing. Other training options include 30 epochs, an initial learning rate of 0.01 (the first and second experiment) and 0,001 (the third experiment). And the Adaptive Moment Estimation Optimizer (Adam) [10] was used.

In addition to the Deep Neural Network, two classifiers were also used. The classifiers mentioned are Support Vector Machines (SVM) [5] and k-Nearest Neighbors (kNN) [16]. The same features, as in case of Deep Neural Network, were used for SVM and kNN classifiers, in the same ratio of 85% for training and 15% for testing.

RESULTS AND DISCUSSION

With certain experimental settings, the following results were obtained. In the first experiment, the accuracy was 90% in the case of the Deep Neural Network, using 600 images (six images for each person). For the two classifiers, the accuracy was 94.1% in the case of SVM and 84.9% in the case of kNN. Table 1 and Figure 5 show the results of the first experiment.

Table 1. The Obtained Results for the First Experiment

THE FIRST EXPERIMENT	
The Method Used	Accuracy
Deep Neural Network	90%
SVM Classifier	94.1%
kNN Classifier	84.9%

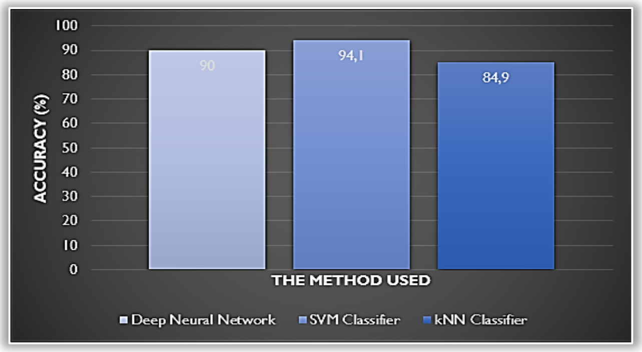

Figure 5. The Obtained Results for the Methods Used (The First Experiment)

In the case of the Deep Neural Network and the defined settings for the second experiment, the accuracy was 84.7%. In the second experiment, there were 1.000 images, for each of 100 subjects 10 GEI images. For the classifiers used, the accuracy was about 74.8% in the case of SVM and 67.4% in the case of kNN. The obtained results, in terms of accuracy, for the second experiment are shown in Table 2 and Figure 6.

Table 2. The Obtained Results for the Second Experiment

THE SECOND EXPERIMENT	
The Method Used	Accuracy
Deep Neural Network	84.7%
SVM Classifier	74.8%
kNN Classifier	67.4%

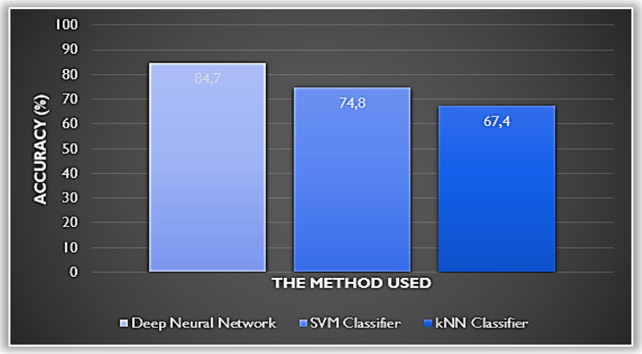

Figure 6. The Obtained Results for the Methods Used (The Second Experiment)

In the third experiment, slightly different settings were used and the learning rate was 0,001 instead of 0.01 as in the first and second experiment. The reason for changing the settings was better overall results. Also, in the third experiment, there were 11.000 images, 110 GEI images for each of the 100 subjects. In the case of the Deep Neural Network, the results in terms of accuracy were 54.7%. For the classifiers used, the accuracy was 54.2% for SVM and 48.8% for kNN. The obtained results, in terms of accuracy, for the third experiment are shown in Table 3 and Figure 7.

Table 3. The Obtained Results for the Third Experiment

THE THIRD EXPERIMENT	
The Method Used	Accuracy
Deep Neural Network	54,7%
SVM Classifier	54,2%
kNN Classifier	48,8%

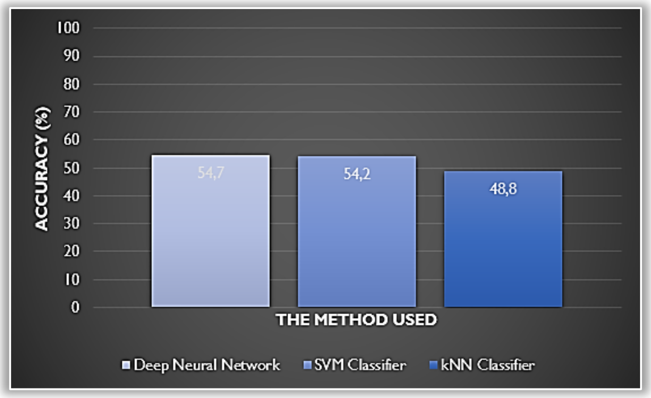

Figure 7. The Obtained Results for the Methods Used (The Third Experiment)

The comparison of the obtained results for the three performed experiments is shown in Figure 8.

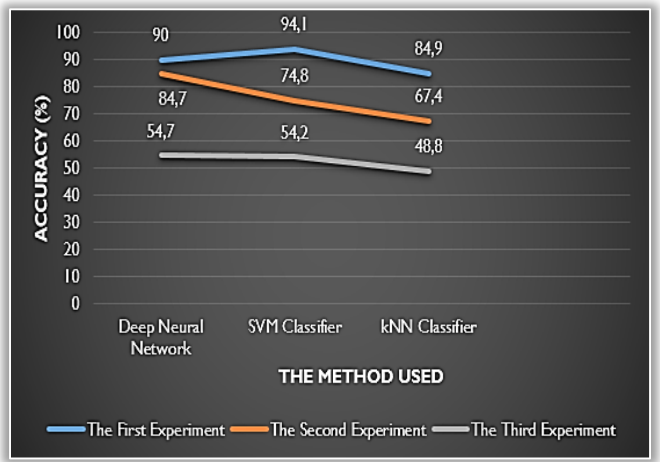

Figure 8. Comparison of the Results for the Performed Experiments

In the first experiment, the Deep Neural Network achieved the second highest result (accuracy) of 90% for defined experimental settings and the learning rate of 0,01. The SVM classifier achieved the highest result of 94.1%. Somewhat lower was the result for kNN with 84.9%. In the second experiment, the Deep Neural Network had the highest accuracy of 84.7%. This was achieved with defined experimental settings where the learning rate was 0.01. Compared to the Deep Neural Network, SVM and kNN classifiers had lower accuracy of 74.8% and 67.4%, respectively. In the third experiment, the Deep Neural Network achieved the highest results of 54.7% with learning rate of 0,001. Also, the two classifiers used achieved 54.2% in the case of SVM and 48.8% in the case of kNN.

In two out of three experiments, the Deep Neural Network achieved the best results compared to the classifiers used. In the experiment with a smaller number of images (the first experiment), the SVM classifier achieved better results. With increasing number of images for each subject and overall, the Deep Neural Network achieved the best results. It is important to note that the duration of the training process for the Deep Neural Network was several minutes, using standard laptop, in the case of the third experiment, where a large number of images were used.

The GEI images were also used as input instead of features. Instead of the feature input layer (*featureInputLayer*), image input layer (*imageInputLayer*) with customized options was used. More specifically, a Convolutional Neural Network (CNN) was created and used. The settings for the experiments with CNN were similar to those in the case of using extracted features (for the three experiments described above), with 85% of the images used for training and 15% for testing. In this case (for used GEI images), the results for defined experiments were significantly lower in terms of accuracy and the duration of the training process was much longer (several hours in the case of the third experiment).

It is important to note that besides SVM and kNN classifiers, other classifiers were also used (such as Tree) and the results obtained were lower compared to SVM and kNN classifiers and also compared to Depp Neural Network.

CONCLUSION

In this paper, it was analyzed gait recognition for people identification. Gait recognition is one of the behavioral biometric methods that analyze the features of gait and use them for purpose of identification, re-identification etc. During a gait cycle, each person forms certain patterns that can be utilized in purpose of identification. In recent years, different methods have been presented that rely on a model-based or appearance-based approach, meaning that are based on some model or on some person's silhouettes representation.

In this paper, a deep neural network was developed for use with a well-known gait recognition method called Gait Energy Image or GEI. Also, the Casia Dataset B for experimental evaluation was used. Three experiments were defined using 100 subjects from the Casia Dataset B in different ways. An accuracy of about 90% was achieved in certain settings. Also, two classifiers, kNN and SVM, were used for comparison with created Deep Neural Network, which achieved slightly lower results in the two out of three experiments.

References

[1] Arora, P. and Srivastava, S. (2015). Gait Recognition Using Gait Gaussian Image. In: 2nd International Conference on Signal Processing and Integrated Networks (SPIN), 791-794. IEEE.
[2] Bay, H., Ess, A., Tuytelaars, T. and Van Gool, L. (2008). Speeded-Up Robust Features (SURF). Computer Vision and Image Understanding, 110(3), 346-359. Elsevier.
[3] Chattopadhyay, P., Roy, A., Sural, S. and Mukhopadhyay, J. (2014). Pose Depth Volume Extraction from RGB-D Streams for Frontal Gait Recognition. Journal of Visual Communication and Image Representation, 25(1), 53-63. Elsevier.
[4] Csurka, G., Dance, C., Fan, L., Willamowski, J. and Bray, C. (2004). Visual Categorization with Bags of Keypoints. In: Workshop on Statistical Learning in Computer Vision (ECCV), 1-2.

[5] Gunn, S. R. (1998). Support Vector Machines for Classification and Regression. ISIS Technical Report, 14(1), 5-16.
[6] Han, J. and Bhanu, B. (2005). Individual Recognition Using Gait Energy Image. IEEE Transactions on Pattern Analysis and Machine Intelligence, 28(2), 316-322. IEEE.
[7] Hofmann, M., Bachmann, S. and Rigoll, G. (2012). 2.5D Gait Biometrics Using the Depth Gradient Histogram Energy Image. In: 5th International Conference on Biometrics: Theory, Applications and Systems (BTAS), 399-403. IEEE.
[8] Iwashita, Y., Uchino, K. and Kurazume, R. (2013). Gait-based Person Identification Robust to Changes in Appearance. Sensors, 13(6), 7884-7901. MDPI.
[9] Jain, A. K., Ross, A. and Prabhakar, S. (2004). An Introduction to Biometric Recognition. IEEE Transactions on Circuits and Systems for Video Technology, 14(1), 4-20. IEEE.
[10] Kingma, D. P. and Ba, J. (2014). Adam: A Method for Stochastic Optimization. arXiv preprint arXiv:1412.6980.
[11] Kumar, M. N. and Babu, R. V. (2012). Human Gait Recognition Using Depth Camera: A Covariance Based Approach. In: Proceedings of the 8th Indian Conference on Computer Vision, Graphics and Image Processing, 1-6.
[12] Lenac, K., Sušanj, D., Ramakić, A. and Pinčić, D. (2019). Extending Appearance Based Gait Recognition with Depth Data. Applied Sciences, 9(24), 5529. MDPI.
[13] Nister, D. and Stewenius, H. (2006). Scalable Recognition with a Vocabulary Tree. In: Computer Society Conference on Computer Vision and Pattern Recognition (CVPR), 2161-2168. IEEE.
[14] Official Web Page of Microsoft - Kinect Device. Link: https://learn.microsoft.com/en-us/windows/apps/design/devices/kinect-for-windows [Accessed 05/1/2023]
[15] Official Web Page of the Institute of Automation, Chinese Academy of Sciences. Link: http://www.cbsr.ia.ac.cn/english/Gait\%20Databases.asp [Accessed 05/1/2023]
[16] Peterson, L. E. (2009). K-Nearest Neighbor. Scholarpedia, 4(2), 1883.
[17] Preis, J., Kessel, M., Werner, M. and Linnhoff-Popien, C. (2012). Gait Recognition with Kinect. In: 1st International Workshop on Kinect in Pervasive Computing, 1-4. New Castle, UK.
[18] Ramakić, A. and Bundalo, Z. (2023). Gait Recognition as an Approach for People Identification. In: International Symposium on Innovative and Interdisciplinary Applications of Advanced Technologies, 717-726. Springer.
[19] Ramakić, A., Bundalo, Z. and Bundalo, D. (2020). A Method for Human Gait Recognition from Video Streams Using Silhouette, Height and Step Length. Journal of Circuits, Systems and Computers, 29(7), 2050101. World Scientific.
[20] Ramakić, A., Sušanj, D., Lenac, K. and Budalo, Z. (2020). Depth-based Real-time Gait Recognition. Journal of Circuits, Systems and Computers, 29(16), 2050266. World Scientific.
[21] Sivapalan, S., Chen, D., Denman, S., Sridharan, S. and Fookes, C. (2011). Gait Energy Volumes and Frontal Gait Recognition Using Depth Images. In: International Joint Conference on Biometrics (IJCB), 1-6. IEEE.
[22] Sivapalan, S., Chen, D., Denman, S., Sridharan, S. and Fookes, C. (2012). The Backfilled GEI-A Cross-capture Modality Gait Feature for Frontal and Side-view Gait Recognition. In: International Conference on Digital Image Computing Techniques and Applications (DICTA), 1-8. IEEE.
[23] Yu, S., Tan, D. and Tan, T. (2006). A Framework for Evaluating the Effect of View Angle, Clothing and Carying Condition on Gait Recognition. In: 18th International Conference on Pattern Recognition (ICPR), 441-444. IEEE.
[24] Zheng, S., Zhang, J., Huang, K., He, R. and Tan, T. (2011). Robust View Transformation Model for Gait Recognition. In: 18th International Conference on Image Processing, 2073-2076. IEEE.

ACTA TECHNICA CORVINIENSIS
Bulletin of Engineering
ISSN: 2067-3809

[1.]Dušan JOVANIĆ, [1.]Valentina MLADENOVIĆ, [1.]Dragan HALAS

HARDNESS TEST OF 3D PRINTED WORK PIECE FROM PLA PLASTIC

[1.] Technical College of Applied Sciences, Zrenjanin, SERBIA

Abstract: The paper presents a hardness test of a 3D printed workpiece with a filament of polymeric material – polylactide (PLA) by Shore A scale method. One of the disadvantages of 3D printing is that the parts have much weaker mechanical characteristics and need to be tested to determine the functionality of the working part. Hardness testing of plastic materials is defined by the standard SRPS EN ISO 868: 2015 – Plastics and ebonite – Determination of hardness by indentation using a durometer (Shore hardness) and was performed with an analog durometer – hardness tester.
Keywords: Hardness testing, Additive production, 3D printing, Polylactic acid (PLA)

INTRODUCTION

Due to the lower quality of the processed surface and weaker mechanical characteristics of polylactide (PLA) parts obtained by 3D printing, it is necessary to determine the mechanical characteristics: hardness, tensile strength, impact strength, compressive strength, bending strength, fatigue strength, creep, aging, friction coefficient, resistance to shear and crack propagation according to SRPS ISO 17296–3: Additive technologies – General principles – Part 3: Main characteristics and corresponding test methods. In addition, it also defines test categories for metal parts, plastic parts and ceramic parts and classifies them into three groups: group H (tests of functional parts that are highly safety–critical), group M (tests of functional parts that are not safety–critical) and group L: testing parts during construction or prototype parts. Hardness testing is provided for all these groups of plastic parts.

The goal of this work is to determine the hardness of the workpiece made of PLA plastic depending on the height of the applied layer in the shell and infill. In addition, it is necessary to determine the hardness for different filling methods (linear, zigzag and concentric) at the same layer height.

The hypotheses of the research are that the highest hardness of the workpiece made of PLA plastic is achieved at the lowest layer height both in the casing and in the filling, and that the hardness is the same for the same layer height, and different ways of filling.

ADDITIVE MANUFACTURING

Additive manufacturing can be divided according to SRPS ISO 17296–2:2017: Additive technologies – General principles – Part 2: Overview of process categories and filling, into: Bath photopolymerization – laser stereolithography (SLA) and full–layer illumination–based stereolithography (DLP – SLA, LCD –SLA), Powder substrate fusion – procedures using laser (SLS, SLM, DMLS) and procedures using electron beam (EBM), Material extrusion (FFF – Fused filament fabrication), direct printing (PolyJet, PolyJet Matrix) , Bonding printing (3D Print, 3D Print with suspension application), Lamination of foils (LOM – Laminated object manufacturing, PSL) and Deposition of materials using directed energy (DED – Directed energy deposition).

An overview of the types of additive manufacturing standards is shown in Figure 1 [10].

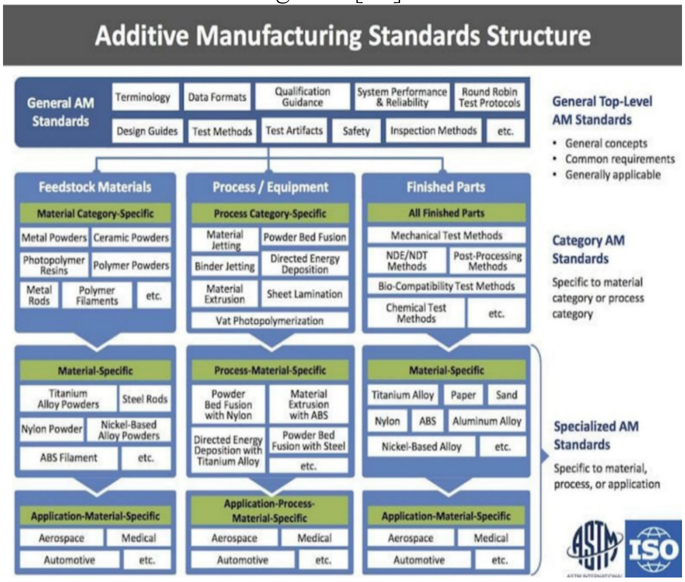

Figure 1. Overview of types of additive manufacturing standards according to ISO/TC 261 and ASTM F42

THE PROCESS OF EXTRUDING MATERIALS

The process of material extrusion (FFF – Fused filament fabrication or FDM – Fused Deposition Modeling, the trade name of the company Stratasys [11], uses solid thermoplastic material – filament, which is pushed through a heated nozzle, the temperature of which depends on the type of polymer, and in a doughy–melted state it is applied to a heated or unheated build plate, after which it hardens and forms the desired piece layer by layer.

The most important parameters that can be adjusted with a 3D printer for the process of extruding materials – FFF are: manufacturing speed, extrusion speed, the height of the applied layer in the shell and infill and the temperature of the nozzle and build plate.

POLYMERS – POLYLACTIC ACID (PLA)

There are a large number of polymers with different mechanical, physical, chemical, electrical, thermal and other characteristics, which have a wide range of applications.

PLA is a thermoplastic biodegradable plastic obtained from organic sources (corn starch, sugar cane or beet) – by fermentation of plant starch and has similar characteristics as polypropylene (PP), polyethylene (PE) or polystyrene (PS). It is used to produce food containers, foils and medical implants and has a high surface energy that makes it ideal for 3D printing. The disadvantages of PLA are low heat resistance and relatively low strength. The characteristics of PLA are given in Table 1 [8].

Table 1. Characteristics of polylactide acid – PLA

The parameters	Values
Heat Deflection Temparature– EN ISO 75	52 °C
Density	1,24 g/cm^3
Tensile Strength EN ISO 527–1	50 MPa
Flexural Strength EN ISO 178	80 MPa
Impact Strength (IZOD) – EN ISO 180	96,1 (J/m)
Shrinkage rates	0,37–0,41%

The chemical formula of polylactide acid is H–[OCH(CH3)CO]n–OH, and the PLA polymer for this type of 3D printing is in filament form.

EXPERIMENTAL PART

In a series of experiments, a blind flange was used as a working object. These elements are used, during the construction of pipelines, to close the ends of pipelines or forks, as well as when testing pipe closures. They are connected with screws and nuts to pipeline flanges, forks or pipe closures with a mandatory seal between the elements. The blind flange, whose structural shape and dimensions were used in this work, was made according to the EN 1092–1 Type 11 / DIN 2632 PN6 standard. The outer dimensions of the flange are Φ 80 x 12 and it has four M10 holes spaced on a Φ 55 diameter.

The 3D model of the flange (Figure 2) was realized in the software package SOLIDWORKS 2016, and then it was formed into a suitable STL file with the maximum resolution allowed by the software.

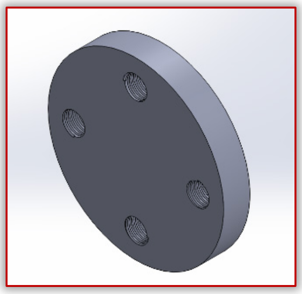

Figure 2. 3D CAD model of blind flange

The STL file of the flange was imported via Ultimaker open source Cura software and is shown in Figure 3.

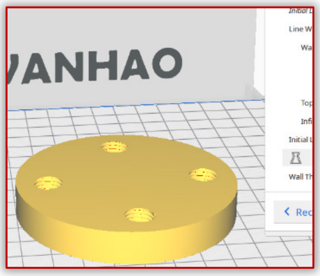

Figure 3. Imported STL file of blind flange

After that, the corresponding parameters were varied according to the experimental plan and a series of flanges with the same external appearance (Figure 4) but different characteristics was produced.

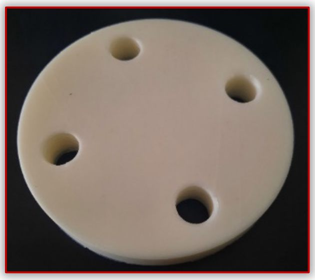

Figure 4. Appearance of the 3D printed object

As measuring instrumentation, a durometer – hardness meter (hardness meter) BAREISS, Germany, according to Shore, scale A with a conical shape of the needle at an angle of 350, shown in Figure 5, with a minimum sample thickness of 4 mm and an accuracy of 0.5 HS A [6].

Figure 5. Device for measuring the hardness of PLA parts

The characteristics of Wanhao PLA filament are shown in Table 2.

Table 2. Features of Wanhao PLA filament

The parameters	Values
Filament type	PLA
Diameter (mm)	1.75
Melting point (°C)	190 – 210
Build plate temperature (°C)	0 – 60

In Figure 6 is shown the 3D printer Wanhao Duplicator 6 on which the elements for the experiment were printed, and its technical characteristics are given in Table 3 [7].

Table 3. Wanhao Duplicator 6 3D Printer Technical Features

The parameters	Values
Additive technology	Material extrusion (FFF)
Materials	PVA, PLA, ABS, PEVA, HIPS
Max. part dimensions (mm)	200 x 200 x 180
Layer thickness (μm)	20 – 200
Filament diameter (mm)	1.75
Nozzle outlet diameter (mm)	0.4
3D printing speed (mm/s)	30 – 150
Working temperature (°C)	180 – 260
Build plate temperature (°C)	50 – 100

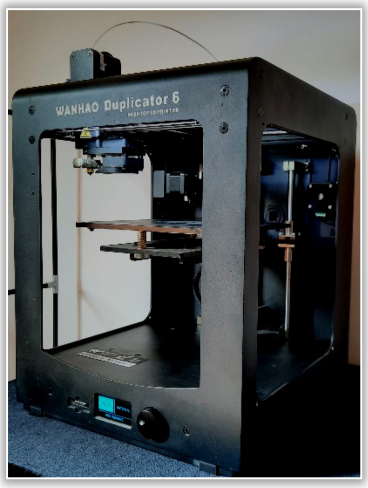

Figure 6. 3D printer Wanhao Duplicator 6

RESULTS AND DISCUSSION

The surface quality of the workpiece made of PLA plastic depends on the height of the applied layer in the shell and infill. The lower the height of the applied layer, the higher the quality of the object and the greater the ability to perform details, but the production time is nonlinearly longer.

The hardness values depending on the height of the applied layer and the type of filling, as well as the temperature of the build plate, are shown in Table 4, and the hardness values for different types of filling (pattern), with an unheated work plate, are shown in Table 5.

Table 4. Hardness values for different heights of the applied layer and heating of the build plate at the same linear filling

Pattern	Build plate temperature (°C)	Layer height (mm)	Hardness HS (A)
Lines	55	0.1	98
	20	0.1	99
	20	0.2	98
	20	0.4	96

Table 5. Hardness values for different types of fillings (patterns)

Pattern	The length of the filament used (m)	Layer height (mm)	Build time (min)	Hardness HS (A)
Lines	0.52	0.1	13	99
Zig Zag	0.52	0.1	13	99
Concentric	0.52	0.1	12	99

Macroscopic images of PLA objects with a layer height of 100, 200 and 400 microns at x5 magnification are shown in Figure7.

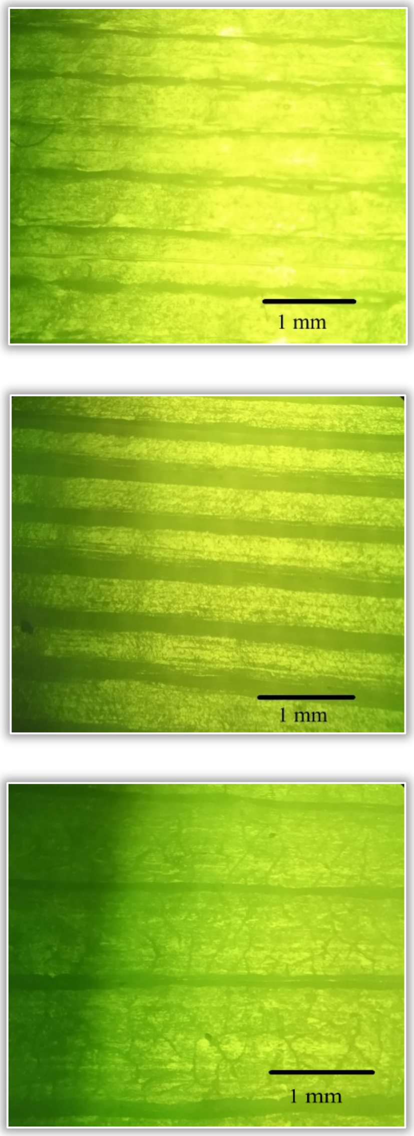

a)

b)

c)

Figure 7. Macroscopic image of a PLA object with a layer of 100, 200 and 400 microns high at x5 magnification and a cross–section of a layer with a layer height of 100 microns

In Figure 7a, the darker lines represent the furrows between the layers, which are places of stress concentration, and the wider they are, the rougher the surface. Macroscopic inspection revealed that the width of the applied layer (layer) is the largest at the highest height of the applied layer (Figure 7c) and that it is twice as large in relation to the height of the applied layer of 0.2 mm (Figure 7b). It can also be seen that the width of the groove (unfilled), almost twice as large at the height of the applied layer of 0.2 mm (Figure 7b) compared to the height of the applied layer of 0.1 mm (Figure 7a).

A cross section of flange and the number of layers for an application height of 0.1 mm is shown in Figure8.

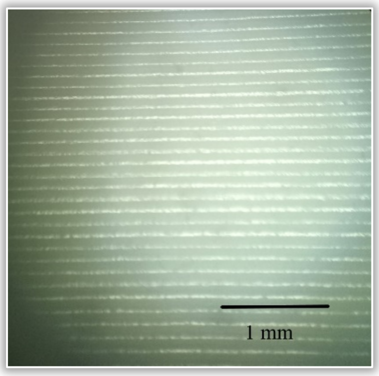

Figure 8. A cross–section of a layer with a layer height of 100 microns

The hardness (HS–A) of the PLA plastic part depending on the height of the applied layer (h) is shown in Figure 8.

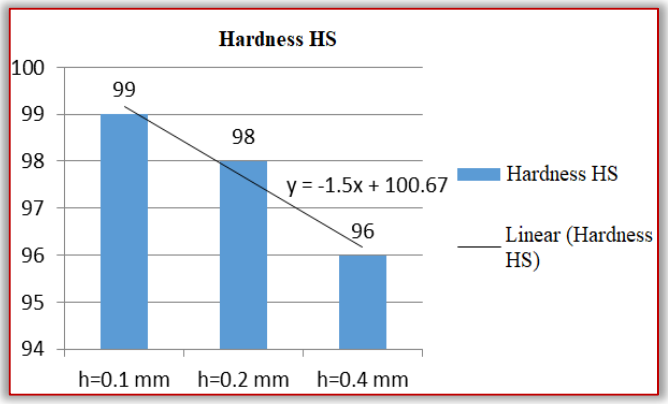

Figure 9. Hardness depending on the height of the applied layer

The hardness of PLA samples made by 3D printing with FFF technology depends on the height of the applied layer, so that it is maximum for the smallest height and decreases almost linearly according to the smallest hardness to the largest height during linear filling.

The heating of the board at the same filling and height of the applied layer has a slight effect, so that the hardness is lower by 1%.

The hardness is the same for the same layer height, with different filling methods (linear, zigzag and concentric).

CONCLUSION

3D printing with the process of extruding material with FFF technology has a low quality of the processed surface, and from the point of view of hardness, the hypotheses is confirmed that the highest hardness of the workpiece made of PLA plastic is achieved at the lowest layer height of 0.1 mm, with complete filling in the shell and filling (infill) and decreases almost linearly according to the lowest hardness for the highest height at linear filling.

The filling (pattern) does not significantly affect the hardness values because for all three types of filling (linear, zigzag and concentric) the hardness value is the same.

At the same filling and height of the applied layer, the heating of the plate only slightly affects the hardness of the workpiece, reducing it by 1%.

References

[1] Redwood, B; Schöffer, F.; Garret, B.: The 3D printing handbook: technologies, design and applications, 3D Hubs, 2017.

[2] SRPS EN ISO 868:2015– Plastične mase i ebonit — Određivanje tvrdoće utiskivanjem pomoću durometra (tvrdoća po Šoru)

[3] SRPS EN ISO/ASTM 52900:2017 Aditivne tehnologije – Opšti principi – Terminologija

[4] SRPS ISO 17296–2:2017: Aditivne tehnologije – Opšti principi – Deo 2: Pregled kategorija procesa i punjenje

[5] SRPS ISO 17296–3: Aditivne tehnologije – Opšti principi – Deo 3: Glavne karakteristike i odgovarajuće metode ispitivanja.

[6] Internet source: www.bareiss–testing.com/product/analog–durometers–hp–series/

[7] Internet source: www.wanhao3dprinter.com

[8] Internet source: https://www.twi–global.com/technical–knowledge/faqs/what–is–pla

[9] Luis Quiles–Carrillo, Nestor Montanes, Fede Pineiro, Amparo Jorda–Vilaplana, Sergio Torres–Giner: Ductility and Toughness Improvement of Injection–Molded Compostable Pieces of Polylactide by Melt Blending with Poly(ε–caprolactone) and Thermoplastic Starch, Materials (Basel), 2018 Oct 30;11(11):2138

[10] Internet source: https://committee.iso.org/sites/tc261/home/projects.html

[11] Internet source: https://www.stratasys.com/en/fdm–systems

Note: This paper was presented at IIZS 2022 – The XII International Conference on Industrial Engineering and Environmental Protection, organized by Department of Mechanical Engineering and Department of Environmental Protection of the Technical Faculty "Mihajlo Pupin" Zrenjanin, from the University of Novi Sad, in cooperation with partners – University Politehnica Timisoara, Faculty of Engineering, Hunedoara (ROMANIA), University "St. Kliment Ohridski", Technical Faculty, Bitola (MACEDONIA), "Aurel Vlaicu" University of Arad, Faculty Of Engineering, Arad (ROMANIA), University of East Sarajevo, Faculty of Mechanical Engineering East Sarajevo, Sarajevo (BOSNIA & HERZEGOVINA) and University of Giresun, Faculty of Engineering, Giresun (TURKEY) – in Zrenjanin, SERBIA, in 06–07 October, 2022.

ACTA TECHNICA CORVINIENSIS
Bulletin of Engineering

ISSN: 2067–3809

ACTA TECHNICA CORVINIENSIS – BULLETIN OF ENGINEERING
TOME XVI [2023] | FASCICULE 2 [APRIL – JUNE]

[1.]Gergely DEZSŐ, [1.]Ferenc SZIGETI

INVESTIGATION OF SHAPE ACCURACY OF SELECTIVE LASER MELTED Ti6Al4V LATTICE STRUCTURE BY COMPUTER TOMOGRAPHY

[1.]University of Nyíregyháza, Institute of Engineering and Agriculture, Department of Physics and Production Engineering, Nyíregyháza, HUNGARY

Abstract: Selective laser melting is a widely applied additive manufacturing technology for metals, especially Ti6Al4V alloy today. Manufacturing of lattice structures stands in focus of scientific research, because of special technological advantages of those, like production of lightweight parts, opportunity of combination with other materials utilizing pores, biomedical applications, several scenarios of production resulting in tuned mechanical properties. In our experiments tensile test specimens were produced with periodic trabecular structure. Pore size of structure were varied. Shape accuracy of test specimens were measured by computer tomography. Size accuracy of the total specimen, size and shape accuracy of pores, places of material defects and excesses were identified and described quantitatively. Our experiments showed that most part of test specimens were precise enough. However special areas were identified with high inaccuracies. Moreover most dangerous errors, material absence and cracks also observed.

Keywords: lattice structure, Ti6Al4V, selective laser melting, shape accuracy, dimensional accuracy

INTRODUCTION

In 20th century manufacturing technologies went through the most extraordinary advancement in history of mankind [1–3]. Beside several areas of technological development additive manufacturing (AM) brought a revolutionary change opening up new doors of integration of production with other systems of economy like remanufacturing, informatics, robotics [4], logistics [5], commerce, construction [6] and medicine [7–9]. Flexibility of AM strongly contributes to mass customization production emerging in the frame of industry 4.0 [10]. Number of research publications related to AM increase exponentially since 2000 [11]. AM with its new opportunities and challenges [12] also transforms even way of thinking in engineering design [13–15]. AM today is applicable for composing new materials with designed and tuned properties, like composites [16, 17] and special microscopic-level mixtures [18].

Standard ISO/ASTM 52900 introduces a nomenclature for AM technologies and concepts connected with AM [19]. This standard specifies seven class of AM technologies: binder jetting (BJT), directed energy deposition (DED), material extrusion (MEX), material jetting (MJT), powder bed fusion (PBF), sheet lamination (SHL) and vat photo polymerization (VPP).

Distinctive feature of PBF technology is that during the process thermal energy fuses a part of a powder bed. PBF technologies can be applied to many different materials, most frequent ones are plastics and metals. In the followings we deal with metals

Fusion comes true in two main ways, sintering and melting. The process is called sintering if original powder particles do not completely melt. When all powder particles are melted, it is called melting. Source of thermal energy is usually laser beam or electron beam.

Selective laser melting (SLM) is a PBF method which uses laser beam for full melting of material to be fused [20]. When it is applied for metals it is often called direct metal selective laser melting (DMSLM). This paper presents result of DMSLM applied on Ti6Al4V material, and we refer to this briefly as SLM, because there is no risk of ambiguity.

Feedstock material of SLM is metal powder. Such kind of powders differ from base materials of powder metallurgy. Today a complete industrial background exists to supply AM market with powders of several metals and alloys. Most important properties of AM metal powders are particle size distribution, average size, particle shape, nominal chemical composition, and level of accuracy of chemical composition. Quality of metallic parts produced by AM depends of quality of metal powder which it is made of [21, 22].

SLM is a production method with several process parameters. Significant part of scientific literature treats how properties of parts produced depends of SLM process parameters [23–26].

Dimensional and shape accuracy are also dependent from SLM process parameters [27–32].

AM technologies in themselves are rarely able to produce ready to use parts. Commonly so-called postprocessing methods are used to achieve required quality of the product. Aims of postprocessing are surface modification in order to improve shape accuracy , wear resistance [33, 34], surface roughness [35–37].

Computer tomography first gained ground in biomedicine is a cost and expertise demanding method, at the same time it is increasingly applied also in other fields of industry for three-dimensional imaging of complex structures. This is especially true for inspection of additively manufactured lattice structures which form a new and promising class of parts [38, 39].

In this paper we introduce an experimental study on shape and size accuracy of a lattice structure produced by SLM from Ti6Al4V alloy. Since a lattice structure has numerous details inside, where those can not be observed by optical methods, computer tomography (CT) has been applied as imaging procedure. Aim of this study was to show out dimensional and shape deviations, material excess and lack, as well as cracks and fractures originated from manufacturing procedure.

MATERIAL AND METHODS

— Material Ti6Al4V

Samples were produced from Ti6Al4V ELI powder by SLM. Ti6Al4V is known as a widely applied metal alloy in industry, which is also intensively studied in science. In our experiments we used a special form of Ti6Al4V containing extra low interstitials (ELI). Chemical composition of Ti6Al4V ELI in weight% is 5.5-6.75% Al, 3.5-4.5% V, C ≤ 0.08%, O ≤ 0.2%, N ≤ 0.05%, H ≤ 0.015%, Fe ≤ 0.4%. All other elements must be present in less than 0.1%, and total amount of other elements must be less than 0.4% [40].

This metal alloy has remarkable advantages like low mass density, good mass-strength ratio, chemical endurance and biocompatibility. It is applied in biomedical, pharmaceutical, vehicle, nuclear industries and several other fields [41, 42].

— Sample production

The shape of the sample is identical to a standard tensile test specimen with rectangular cross section expected that active zone (which part is used to break away) of it has lattice structure. Lattice is periodical. Unit cell is cubic with 2.5 mm edge length. Figure 1 shows overall shape of the test specimen and middle part with lattice structure magnified.

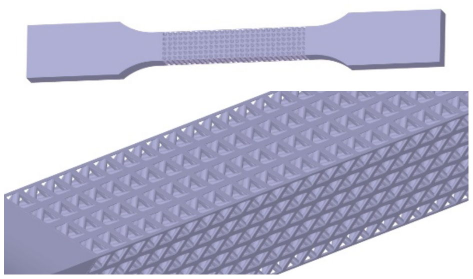

Figure 1. A standard tensile test specimen with modified active zone. It has lattice structure built up from cubic unit cells

This sample was produced in horizontal orientation with its smallest faces down as left side of Figure 1 sows. Manufacturing machine was an EOS M290 400W. Production parameters were set to default values.

— Computer tomography

Computer tomography is often applied for inspection of additively manufactured metallic parts [38] [39].

Computer tomography may be known for most people from medical practice. Aim of such a measurement is to gain a 3D representation of internal structure of a body, which is not observable by optical methods. In industry aim is the same. Difference from medical machines is that specimen rotates and X-ray source stands, and usually it applies stronger X-ray for inspection.

A computer tomograph uses X-ray to radiograph the sample. By this way a projection of internal structure is captured like a shadowed plane image. As the sample rotates several such an image are taken. Spatial representation of internal structure is gained by numerical mathematical methods in digital form, usually as an STL (standard triangulation/tessellation language) model. Resolution is characterized with so-called voxel size, which depends on acceleration voltage, size of sample and distance of sample and source.

In our experiment a Werth industrial computer tomograph (CT) machine was applied with maximum 225 kV accelerating voltage.

In this study shape of the lattice was imaged, which is really the surface of the solid body. Now microstructure inside the material was not revealed.

RESULTS AND DISCUSSION

After CT measurement we had two electronic body representation of the specimen in STL format. First is the CAD body model which was the base of manufacturing. This is the ideal shape of the specimen. Second body model was resulted from CT inspection by processing software of the measurement system. This represents the realized shape of the body. The two STL file were compared with each other.

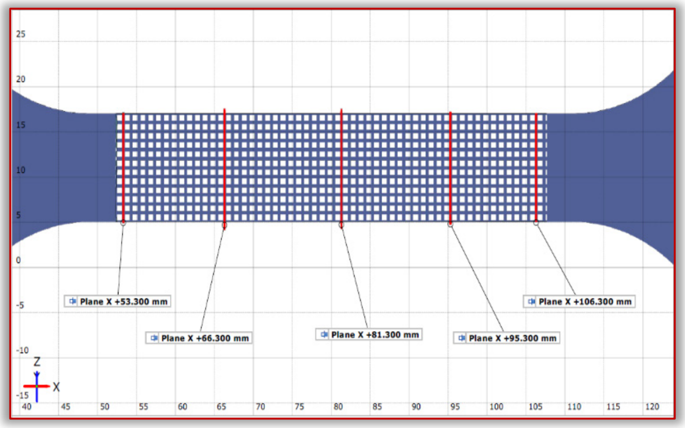

Figure 2. Section planes of CT generated STL body model for measurements and observations

Figure 2 shows planes in which measured STL file was sliced and digital dimensional measurements and observations was taken.

Two STL files were fit to each other by least squares method. Figure 3 shows deviations of measured shape from designed (ideal) shape. This image represent absolute value of deviations with color code. It is observable that maximum deviation on the flags is +0.213 mm. Compared to classical manufacturing technologies this is a bad value. However we must not forget that there are biomedical applications where this accuracy is sufficient. For example a bone implant needs not higher accuracy since bone grows around it.

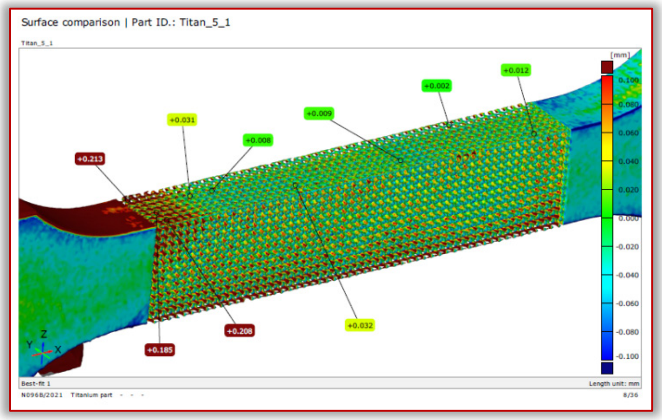

Figure 3. Deviations of measured shape from ideal shape of test specimen. On this image z coordinate is represented in mm units

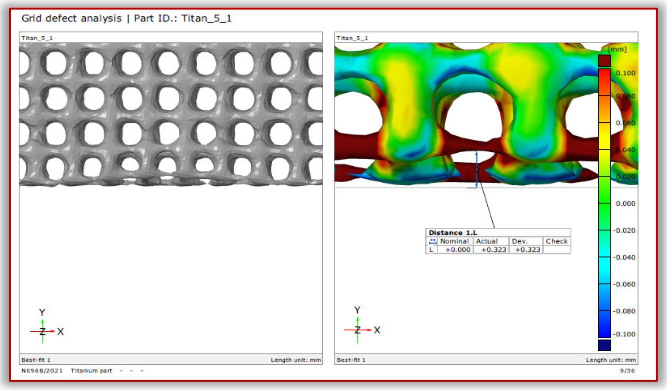

Figure 4. Pores of the lattice structure, and deviation from designed shape by color code

On Figure 4 we can see a highly important phenomenon. Original designed shape is rectangular with plane faces and sharp corners. In contrast to it, manufactured (realized) shape is quite rounded. This follows from principle of SLM. When particles of metal powder are melted those moves as fluid drops and their movement is determined by two factors: surface tension and wetting the underneath not melted metal part. Both effects makes the material arrange along rounded shapes and will never form either sharp corners or plane faces. Manufactured shape seems as it was designed from unit cells with spherical holes. SLM will never create sharp corners in micro scale.

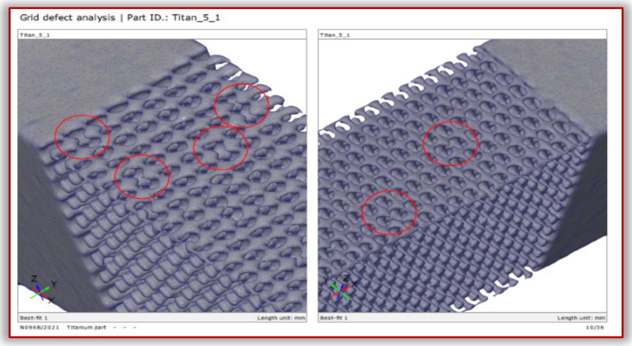

Figure 5. Red circles show material defects and excesses

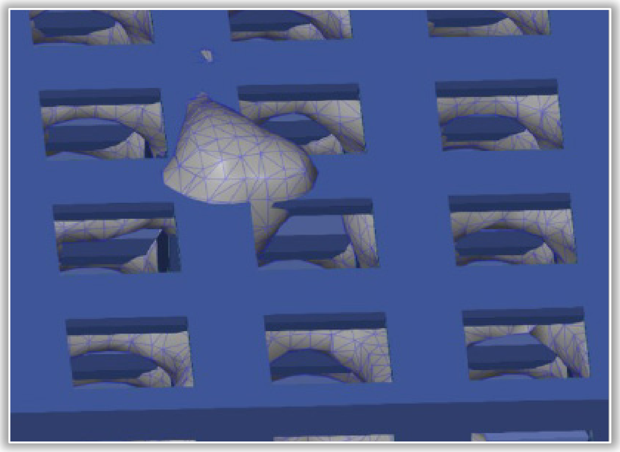

Figure 6. A special region with material excess. Blue color shows designed ideal shape, and measured shape is visible in grey

On Figure 5 several material defects are demonstrated. This may come from contractile effect of surface tension. The higher is the temperature the stronger is this effect. It means that overheating is to be considered and corrected if we can see high number of such material defects.

Figure 6 shows a material excess. This may come from uneven powder spreading or splatter phenomena, which is similar to what is well known in case of welding.

SUMMARY AND CONCLUSIONS

In this study a tensile test specimen with lattice structure in the middle was investigated. The test specimen was produced by SLM in horizontal direction. Material of the specimen is Ti6Al4V. Shape and dimensional accuracy of the specimen was studied by CT inspection. Both designed and measured shape was available in STL files. Two body model were fit to each other and deviations were visualized and characterized numerically.

The following conclusions can be stated:

- Largest dimensional deviation of manufactured specimen from designed shape is in the magnitude of 0.2-0.3 mm. This is not sufficient in most mechanical engineering applications, but may be eligible for biomedical purposes.
- In macro scale the shape of the specimen stands close to the design.
- In micro scale shape of lattice details are rounded even if the original design was rectangular, brick-like with

plane faces and sharp corners. Shape of pores is not cubic, indeed spherical or circular.

- Material defects can be observed at several locations of the model in the lattice structure. Thin rod-like fractions and fine details tend to be rounded by fluid behavior during the SLM process. This is valid for details with size under 1 mm.
- Material excess can also be observed. This may come from inaccuracies of powder spreading of splatter.

Acknowledgements

This work was supported by project entitled "Research of osteosynthesis of implants and development trabecular structure using additive manufacturing", and with identification number: GINOP-2.2.1-15-2017-00055. Test specimens were manufactured at the Biomechanical Laboratory at University of Debrecen, Hungary within the research work of the project. This project was supported by the Scientific Council of the University of Nyíregyháza.

References

[1] B. Esmaeilian, S. Behdad, and B. Wang, 'The evolution and future of manufacturing: A review', J. Manuf. Syst., vol. 39, pp. 79–100, 2016.
[2] J. J. Beaman, D. L. Bourell, C. C. Seepersad, and D. Kovar, 'Additive Manufacturing Review: Early Past to Current Practice', J. Manuf. Sci. Eng., vol. 142, no. 11, 2020.
[3] N. K. Katiyar, G. Goel, S. Hawi, and S. Goel, 'Nature-inspired materials: Emerging trends and prospects', NPG Asia Mater., vol. 13, no. 1, Art. no. 1, Jul. 2021.
[4] T. J. Wallin, J. Pikul, and R. F. Shepherd, '3D printing of soft robotic systems', Nat. Rev. Mater., vol. 3, no. 6, Art. no. 6, 2018.
[5] J. Kern, 'Additive Manufacturing: Shaping the Supply Chain Revolution?', in The Digital Transformation of Logistics, 1st ed., M. Sullivan and J. Kern, Eds. Wiley, 2021, pp. 41–60.
[6] A. Paolini, S. Kollmannsberger, and E. Rank, 'Additive manufacturing in construction: A review on processes, applications, and digital planning methods', Addit. Manuf., vol. 30, p. 100894, 2019.
[7] B. Bhaskaran and J. R.S., 'Additive Manufacturing: A Review', pp. 2349–3976, 2022.
[8] P. Bindiganavile Anand, N. Lokesh, A. Buradi, and S. N., 'A comprehensive review of emerging additive manufacturing (3D printing technology): Methods, materials, applications, challenges, trends and future potential', Mater. Today Proc., vol. 52, 2021.
[9] A. Rajic, E. Desnica, I. Palinkaš, D. Nedelcu, and L. Vulicevic, '3D Printing Technology with Plastic Materials for Hip Implant Master Patterns Manufacturing', Mater. Plast., vol. 56, pp. 882–890, 2019.
[10] M. Sanguedolce, G. Rotella, M. R. Saffioti, and L. Filice, 'Functionalized additively manufactured parts for the manufacturing of the future', Procedia Comput. Sci., vol. 180, pp. 358–365, 2021.
[11] B. Durakovic, 'Design for additive manufacturing: Benefits, trends and challenges', Period. Eng. Nat. Sci. PEN, vol. 6, no. 2, Art. no. 2, 2018.
[12] L. E. J. Thomas-Seale, J. C. Kirkman-Brown, M. M. Attallah, D. M. Espino, and D. E. T. Shepherd, 'The barriers to the progression of additive manufacture: Perspectives from UK industry', Int. J. Prod. Econ., vol. 198, pp. 104–118, 2018.
[13] M. Dotcheva, J. Favrot, K. Dotchev, and J. Zekonyte, 'Planning for Metal Additive Manufacturing', Procedia Manuf., vol. 51, pp. 710–716, 2020.
[14] A. Wiberg, J. Persson, and J. Ölvander, 'Design for additive manufacturing – a review of available design methods and software', Rapid Prototyp. J., vol. 25, no. 6, pp. 1080–1094, 2019.
[15] I. Knežević et al., 'Application of 3D Printed Fixtures for Welding', vol. 22, pp. 15–18, 2019.
[16] V. Monfared, H. R. Bakhsheshi-Rad, S. Ramakrishna, M. Razzaghi, and F. Berto, 'A Brief Review on Additive Manufacturing of Polymeric Composites and Nanocomposites', Micromachines, vol. 12, no. 6, Art. no. 6, 2021.
[17] J. Sun et al., 'A review on additive manufacturing of ceramic matrix composites', J. Mater. Sci. Technol., 2022.
[18] T. Zhang et al., 'In situ design of advanced titanium alloy with concentration modulations by additive manufacturing', Science, vol. 374, no. 6566, pp. 478–482, 2021.
[19] 'ISO/ASTM 52900:2021(en), Additive manufacturing — General principles — Fundamentals and vocabulary'. https://www.iso.org/obp/ui#iso:std:iso-astm:52900:ed-2:v1:en (accessed Sep. 07, 2022).
[20] C. Y. Yap et al., 'Review of selective laser melting: Materials and applications', Appl. Phys. Rev., vol. 2, no. 4, p. 041101, 2015, doi: 10.1063/1.4935926.
[21] A. Khorasani, I. Gibson, J. Kozhuthala Veetil, and A. Ghasemi, 'A review of technological improvements in laser-based powder bed fusion of metal printers', Int. J. Adv. Manuf. Technol., vol. 108, pp. 1–19, 2020.
[22] A. H. Maamoun, Y. F. Xue, M. A. Elbestawi, and S. C. Veldhuis, 'Effect of Selective Laser Melting Process Parameters on the Quality of Al Alloy Parts: Powder Characterization, Density, Surface Roughness, and Dimensional Accuracy', Materials, vol. 11, no. 12, Art. no. 12, 2018.
[23] A. Khorasani, I. Gibson, U. S. Awan, and A. Ghaderi, 'The effect of SLM process parameters on density, hardness, tensile strength and surface quality of Ti-6Al-4V', Addit. Manuf., vol. 25, pp. 176–186, 2019.
[24] W. Shi, J. Li, Y. Jing, Y. Liu, Y. Lin, and Y. Han, 'Combination of Scanning Strategies and Optimization Experiments for Laser Beam Powder Bed Fusion of Ti-6Al-4V Titanium Alloys', Appl. Sci., vol. 12, no. 13, Art. no. 13, 2022.
[25] H. Shipley et al., 'Optimisation of process parameters to address fundamental challenges during selective laser melting of Ti-6Al-4V: A review', Int. J. Mach. Tools Manuf., vol. 128, pp. 1–20, 2018.
[26] G. R. Buican, G. Oancea, C. Lancea, and M. A. Pop, 'Influence of Layer Thickness on Internal Structure of Parts Manufactured from 316-L Steel Using SLM Technology', Appl. Mech. Mater., vol. 809–810, pp. 369–374, 2015.
[27] F. Bartolomeu et al., 'Predicting the output dimensions, porosity and elastic modulus of additive manufactured biomaterial structures targeting orthopedic implants', J. Mech. Behav. Biomed. Mater., vol. 99, pp. 104–117, 2019.
[28] G. Dezső and P. Kósa, 'Dimensional and shape accuracy of cylindrical and paralellepiped-like parts made by selective laser melting technology', vol. XVIII, no. 1, pp. 39–45, 2020.
[29] G. Miranda, S. Faria, F. Bartolomeu, E. Pinto, N. Alves, and F. Silva, 'The Influence of Laser Power and Scan Speed on the Dimensional Accuracy of Ti6Al4V Thin-Walled Parts Manufactured by Selective Laser Melting', Metals, vol. 12, p. 1226, 2022
[30] S. Pal, V. Kokol, N. Gubeljak, M. Hadzistevic, R. Hudak, and I. Drstvensek, 'Dimensional errors in selective laser melting products related to different orientations and processing parameters', Mater. Tehnol., vol. 53, no. 4, pp. 551–558, 2019.
[31] L. Zhang, S. Zhang, H. Zhu, Z. Hu, G. Wang, and X. Zeng, 'Horizontal dimensional accuracy prediction of selective laser melting', Mater. Des., vol. 160, pp. 9–20, 2018.
[32] D. Michal, R. Hrušecký, P. Košťál, and I. Molnár, 'Analysis of Shape and Dimensional Deformation of the Model with a Precision Circular Hole Produced by Digital Light Processing (DLP) Additive Technology', Mater. Sci. Forum, vol. 994, pp. 213–220, 2020.
[33] H. Kato, H. Ueki, K. Yamamoto, and K. Yasunaga, 'Wear Resistance Improvement by Nanostructured Surface Layer Produced by Burnishing', Mater. Sci. Forum, vol. 917, pp. 231–235, 2018

[34] G. D. Revankar, R. Shetty, S. S. Rao, and V. N. Gaitonde, 'Wear resistance enhancement of titanium alloy (Ti–6Al–4V) by ball burnishing process', J. Mater. Res. Technol., vol. 6, no. 1, pp. 13–32, 2017
[35] N. S. Qu, X. L. Fang, Y. D. Zhang, and D. Zhu, 'Enhancement of surface roughness in electrochemical machining of Ti6Al4V by pulsating electrolyte', Int. J. Adv. Manuf. Technol., vol. 69, no. 9–12, Art. no. 9–12, 2013
[36] C. Cosma, N. Balc, M. Moldovan, L. Morovic, P. Gogola, and C. Borzan, 'Post-processing of customized implants made by laser beam melting from pure Titanium', J. Optoelectron. Adv. Mater., vol. 19, pp. 738–747, 2017.
[37] G. Varga, G. Dezső, and F. Szigeti, 'Surface Roughness Improvement by Sliding Friction Burnishing of Parts Produced by Selective Laser Melting of Ti6Al4V Titanium Alloy', Machines, vol. 10, no. 5, Art. no. 5, 2022.
[38] P. Sperling, A. du Plessis, and G. Schwaderer, 'Challenges and Approaches for Metrology of Additive Manufactured Lattice Structures by Industrial X-Ray Computed Tomography', Adv. Mater. Res., vol. 1161, pp. 131–136, 2021.
[39] C. Sen, G. Dursun, A. Orhangul, and G. Akbulut, 'Assessment of Additive Manufacturing Surfaces Using X-ray Computed Tomography', Procedia CIRP, vol. 108, pp. 501–506, 2022
[40] 'Titanium Alloy: Ti-6Al-4V'. http://www.metalspiping.com/titanium-alloy-ti-6al-4v.html (accessed Aug. 15, 2022).
[41] M. Fousová, D. Vojtěch, J. Kubásek, E. Jablonská, and J. Fojt, 'Promising characteristics of gradient porosity Ti-6Al-4V alloy prepared by SLM process', J. Mech. Behav. Biomed. Mater., vol. 69, pp. 368–376, 2017.
[42] S. Liu and Y. C. Shin, 'Additive manufacturing of Ti6Al4V alloy: A review', Mater. Des., vol. 164, p. 107552, 2019.

Note: This paper was presented at IIZS 2022 – The XII International Conference on Industrial Engineering and Environmental Protection, organized by Department of Mechanical Engineering and Department of Environmental Protection of the Technical Faculty "Mihajlo Pupin" Zrenjanin, from the University of Novi Sad, in cooperation with partners – University Politehnica Timisoara, Faculty of Engineering, Hunedoara (ROMANIA), University "St. Kliment Ohridski", Technical Faculty, Bitola (MACEDONIA), "Aurel Vlaicu" University of Arad, Faculty Of Engineering, Arad (ROMANIA), University of East Sarajevo, Faculty of Mechanical Engineering East Sarajevo, Sarajevo (BOSNIA & HERZEGOVINA) and University of Giresun, Faculty of Engineering, Giresun (TURKEY) – in Zrenjanin, SERBIA, in 06–07 October, 2022.

ISSN: 2067-3809

Fascicule 2
[April – June]
tome XVI [2023]

ACTA Technica CORVINIENSIS
BULLETIN OF ENGINEERING

ISSN: 2067-3809

ACTA TECHNICA CORVINIENSIS – BULLETIN OF ENGINEERING
TOME XVI [2023] | FASCICULE 2 [APRIL – JUNE]

1.Ivan GRGIĆ, 1.Jure MARIJIĆ, 1.Marko VILIĆ, 1.Mirko KARAKAŠIĆ, 2.Eleonora DESNICA, 3.Jurica SEMENIĆ

DESIGN PROCESS, OPTIMIZATION, AND LIFE-CYCLE ASSESSMENT OF THE MULTIPURPOSE BAG CLIP

1.University of Slavonski Brod, Mechanical Engineering Faculty in Slavonski Brod, Slavonski Brod, CROATIA
2.University of Novi Sad, Technical Faculty "Mihajlo Pupin", Zrenjanin, SERBIA
3.University North, University Center Varaždin, Varaždin, CROATIA

Abstract: With the aim to preserve food freshness and prevent it from further microbial contamination after bag opening, the multipurpose bag clips were designed and various designs of the bag clips can be found on the market. Once the plastic bag is open, it is not possible to close it again without an additional tool. A review of the market and available literature has identified the potential for the redesign of the existed bag clip in terms of geometry optimization concerning the technological design guidelines of polymers and recyclability and to show the design process of such products. Applying the design theory guidelines, Autodesk Fusion 360 and SolidWorks as tools, and product life cycle assessment (LCA), a polymeric multi-purpose bag clip was designed to the level of a functional prototype. The bag clip consists of four parts, two frames, an insert, and a closure. It is intended for closing and opening candy bags, snacks, and freezer bags. The prototype of the bag clip was 3D printed and functionality was successfully tested. The final product has a mass of 32% less than the initial and it is fully recyclable. According to the LCA, the disadvantage of the proposed bag clip is the high energy consumption for its production.
Keywords: bag clip, design theory, life-cycle assessment, optimization, 3D printing

INTRODUCTION

Polymers are ubiquitous materials in everyday human life. There are various types of polymer products such as various plastic parts in cars, aircraft, insulation materials, various packaging, various medical aids, parts of electrical devices, etc. [1]

Closures belong to the group of packaging, and their main function is food and beverage safety and reducing food and beverage waste. The most commonly used closures are bottle closures, as shown in Figure 1 [2].

Figure 1. Plastic closures

Polymer products are usually produced in large quantities, ie in serial or mass production. This method of production requires a minimum amount of waste, maximum productivity, minimum production time, optimal production conditions, and ultimately full product functionality. The design process can have a significant impact on all of these conditions. Concerning the design process of products from non-plastic materials, the design of polymer products has certain specifics. It is important to provide basic information about the type of material before starting the process to help determine the right guidelines for the design. The choice of material is often based on the mechanical properties of the material. Such information is commonly available in the material specifications provided by the material manufacturers. Polymer closures are made by injection molding, which is also the most common production process by which polymer products are made. Injection molding of polymeric materials is the injection of polymeric substances of certain shear viscosity from the preparation unit (the funnel) in a tempered mold cavity. Injection molding produces a mold that, after the cooling, can be removed from the mold cavity, whereby the mold takes the shape of mold cavities. In the process of polymer products design, it is important to pay attention to the basic strategies of molding, and these are:

- Maximum functionality
- Optimal material
- Minimum mass

Having in mind the maximum functionality, one of the goals of polymer products design is to eliminate as many assemblies and parts as possible by combining components and at the same time achieving as many functions of construction as possible [4]. In this paper, the construction is represented by a bag clip. An analysis of the available literature did not show any work on this topic, however, an analysis of the products available on the market showed that there are different designs of bag clips. The idea for the design came from the polymer bag clip shown in Figure 2. [5]. A 3D model of the bag clip was generated, respecting the set of the requirements and the process of technological design of polymer products. Numerical analysis, optimization, and life-cycle assessment of the newly created product were performed, and the functionality was analyzed using a prototype made by 3D printing.

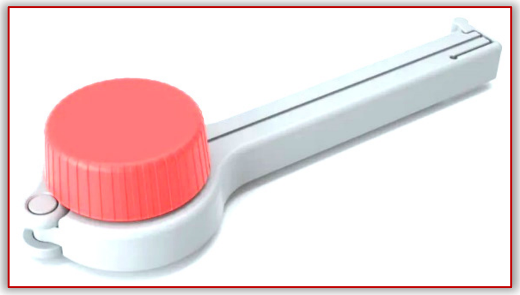

Figure 2. Plastic bag clip

MATERIAL AND METHODS

— Conceptual design of the multipurpose bag clip

After setting the list of requirements and creating a morphological matrix and combining different principles of the solution to perform partial functions for a multipurpose polymer bag clip, four variants were selected. The evaluation procedure determined the optimal solution shown in Figure 3. It should be mentioned that all solutions meet the requirements prescribed in the requirements list.

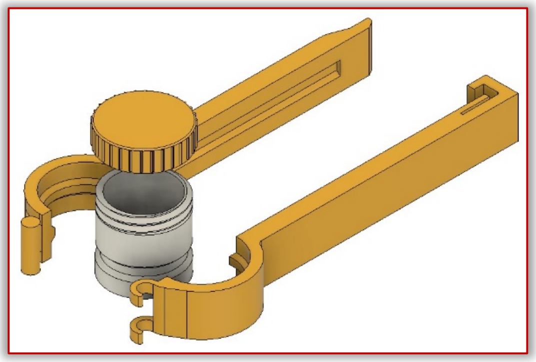

Figure 3. Optimal conceptual design

— Technological design of the multipurpose bag clip

The application of basic design strategies also has a significant impact on the technological design of the mold and these are the maximum molding functionality, optimal material, and the minimum weight. Polypropylene(PP) was selected as the optimal material in accordance with the requirements list. It must be polymeric, recyclable, safe for use in the food industry, have a low density, corrosion-resistant, and deformable. Furthermore, the different color shades of the selected material are welcome.

The review of the design characteristics is given in below:

- The wall thickness of the parts of the bag clip was kept in the range of 1 to 3 mm (Figure 4.).
- The transitions between different wall thicknesses are shaped in a way to prevent the formation of stress concentrations.
- Accumulation of masses on all parts of the structure was avoided
- The optimal value of the radius is set to be 0.5 mm
- The parts of the structure are shaped so that they are symmetrical on at least one axis (Figure 5.)
- A buttress thread SP400-M-8 was chosen as the optimal solution which allows high thread loading forces, while also providing fewer capability deformations during mold cooling.

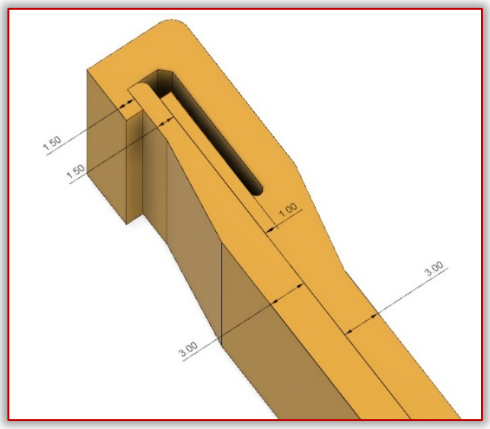

Figure 4. Wall thickness

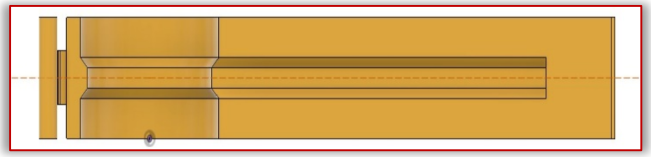

Figure 5. The symmetry of the part

— Numerical analysis of critical points

First of all, it is necessary to simplify the design to facilitate the creation of the initial stress and displacement calculations of the structure. It is assumed that the critical place of the construction is on the first part of the frame in the area on the inside of the buckle. Namely, in order to open the bag clip frame, it is necessary to move the buckle with a finger, which can be physically described as the action of the force of the finger at the beginning of the buckle (Figure 6.) whereby the buckle deformation of the part occurs.

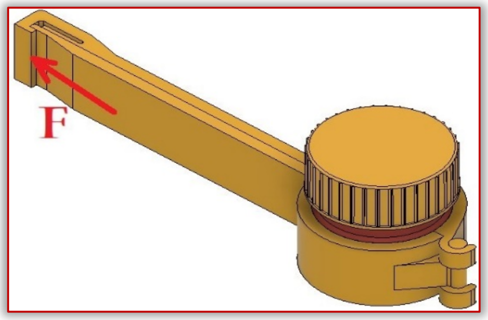

Figure 6. The acting force of the finger

Due to easier analysis, part of the construction has been simplified according to Figure 7., where only the longitudinal part of the frame with the hinged buckle and the rounded part for the insert was taken into account. Furthermore, it was assumed that the part of the frame with the buckle is fixed, and on the part where the buckle acts the finger force of 25 N [6] was applied.

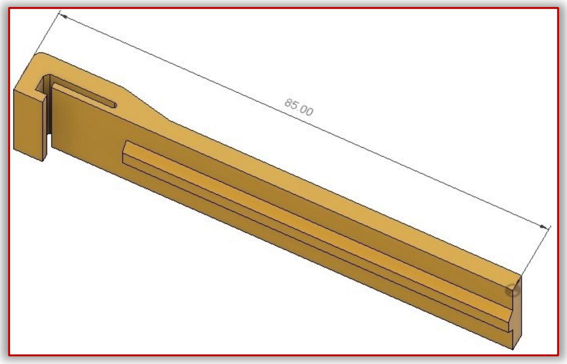

Figure 7. The simplified structure

The main parameters of the numerical analysis are given in Table 1. The finite element mesh is presented in Figure 8. The fine mesh was set on the critical side of the part.

Table 1. Parameters of the numerical analysis

The parameters	Values
Mesh type (element)	tetrahedron
Force	25 N
Material	Polypropylene
Element size (fine mesh)	0,6 mm
Element size (coars mesh)	1,7 mm
Nodes	25.781
Elements	24.285
Boundary condition	Fixed support

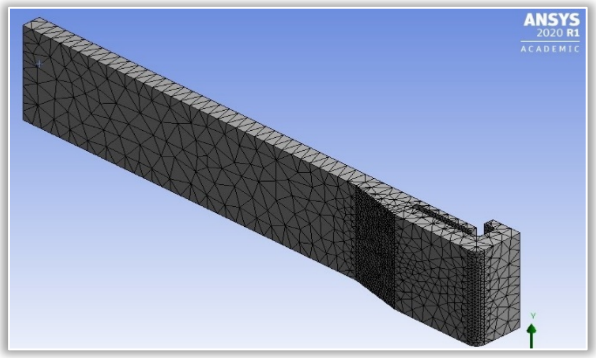

Figure 8. Tetrahedron mesh (fine and coarse)

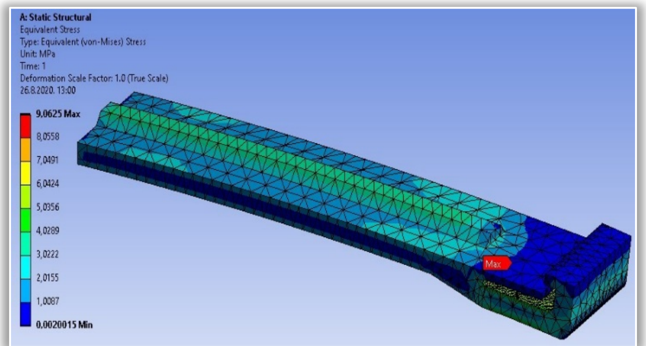

Figure 9. The Von-Mises Stress distribution

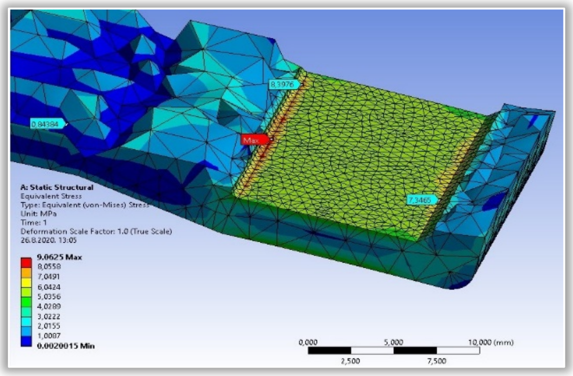

Figure 10. The Von-Mises Stress distribution

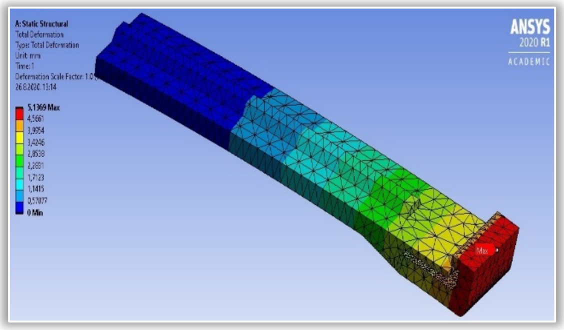

Figure 11. The total deformation on the inside of the buckle

The results of the numerical calculation are satisfactory. The criterion according to which the value of the maximum equivalent stress must be less than the allowable stress value of the material, which in this case is 9,0625 MPa < 26,2 MPa is satisfied. A total displacement of 5,1369 mm is acceptable for polypropylene polymer construction. In comparison with steel structures, this is a significant shift, however, the modulus of elasticity of selected polypropylene is 200 times smaller than the modulus of elasticity of steel which provides it a significantly higher possibility of deformation. The results of this calculation confirmed that this construction can take over the set load within the specified limits of allowable stress and displacement. In other words, during the opening, the frame will not break or permanently deform. The mass of the whole construction is 0,022502 kg or 22,502 g, while the mass of the simplified part for calculation is 0,0051473 kg or 5,1473 g.

— Bag clip optimization

The production of polymer products is unprofitable for small batches due to high mold prices. It was assumed that hundreds of thousands of pieces will be produced. Therefore it is necessary to minimize production costs as much as possible. Since the costs can be directly associated with the surface of the product, it is reasonable to minimize the amount of material required for its production. Hence, it is necessary to determine the minimum mass of the product with optimization compliance with the set of the limits, and then according to the obtained results (optimized parameters) proceed with the final design of the entire multipurpose bag clip.

The geometry consists of four parts, namely frame, buckle, frame amplification, and groove. The frame is the biggest part whose dimensions of the rectangular profile (width and height) will be optimized. The second part is the buckle, looking at the profile of the buckle the width remains fixed (1,5 mm) and the height of the profile was optimized. The value of the buckle height is equal to the height of the frame profile. The third is a fixed part of the amplification of the frame that was not optimized but the length of that part is equal to the height of the profile.

The fourth part is a groove that has fixed dimensions and has not changed during the optimization.

In Figure 12 an overview of the input and output optimization parameters is given. Input parameters were the width of the rectangular frame profile (3 mm) and the height of the profile (18 mm). The output parameters were the mass (5,1473 g), maximum equivalent stress (9,0625 MPa), and total displacement (5.1369 mm). The constraints of the input parameters (Figure 13.) for this structure are geometric and arise from a profile of the structure which is rectangular. The width (thickness) of the structure must not be less than 1 mm and more than 3 mm according to Figure 4., therefore, a profile width limit of 1 to 3 mm was set. The profile height limit is in the range of 10 to 20 mm. Furthermore, Figure 14 shows the optimization constraints related to the equivalent stress and total deformation. For the process of direct optimization to optimize the bag clip, the software was selected to generate 100 different samples according to given constraints. Then, from these samples, select the three most acceptable results in accordance with the objective function (minimum mass) and set limits.

Outline of All Parameters

	A	B	C	D
1	ID	Parameter Name	Value	Unit
2	Input Parameters			
3	Static Structural (A1)			
4	P11	profile_height	18	mm
5	P15	profile_width	3	mm
*	New input parameter	New name	New expression	
7	Output Parameters			
8	Static Structural (A1)			
9	P6	Geometry Mass	0,0051473	kg
10	P13	Equivalent Stress Maximum	9,0625	MPa
11	P14	Total Deformation Maximum	5,1369	mm
*	New output parameter		New expression	
13	Charts			

Figure 12. Outline of the parameters

Table of Schematic B2: Optimization

	A	B	C	D
1	Input Parameters			
2	Name	Lower Bound	Upper Bound	
3	P11 - profile_height (mm)	10	20	
4	P15 - profile_width (mm)	1	3	
5	Parameter Relationships			
6	Name	Left Expression	Operator	Right Expression
*	New Parameter Relationship	New Expression	<=	New Expression

Figure 13. The constraints of input parameters

Table of Schematic B2: Optimization

	A	B	C	D	E	F	G
1	Name	Parameter	Objective		Constraint		
2			Type	Target	Type	Lower Bound	Upper Bound
3	Minimize P6	P6 - Geometry Mass	Minimize		No Constraint		
4	P13 <= 26,2 MPa	P13 - Equivalent Stress Maximum	No Objective		Values <= Upper Bound		26,2
5	P14 <= 10 mm	P14 - Total Deformation Maximum	No Objective		Values <= Upper Bound		10
*		Select a Parameter					

Figure 14. Stress and deformation constraints

In Figure 15, the change of the goal function during the optimization process is shown, the diagram shows that the mass of the structure gradually increases as the values of input parameters grow. Thus, by increasing the geometric parameters of the structure, the mass of the structure grows, and the values of the maximum equivalent stresses and the total displacement are declining. The results of the optimization process are given in Figure 16.

Out of all one hundred generated samples, the software singled out the three best solutions characteristics shown in Figure 17. According to the goal function (mass reduction), the first solution is the best, it gives the smallest mass. However, the first solution has the maximum value of the maximum equivalent stress and the total displacement. The third solution has a maximum mass and total displacement. Out of the three offered solutions, the variant under number two was chosen as the optimal solution. Although the chosen variant does not have the least mass concerning other solutions, due to the acceptable weight of the structure and the lowest values of stress and a total displacement of all the offered variants, this solution was chosen. The function of the optimization goal is fulfilled, the initial mass was reduced from 5,1473 g to 3,1268 g which is a 40% reduction in weight! A ton of polypropylene whose price is approx. € 1400, there is approx. € 560 in savings. The final design of a bag clip is shown in Figure 18.

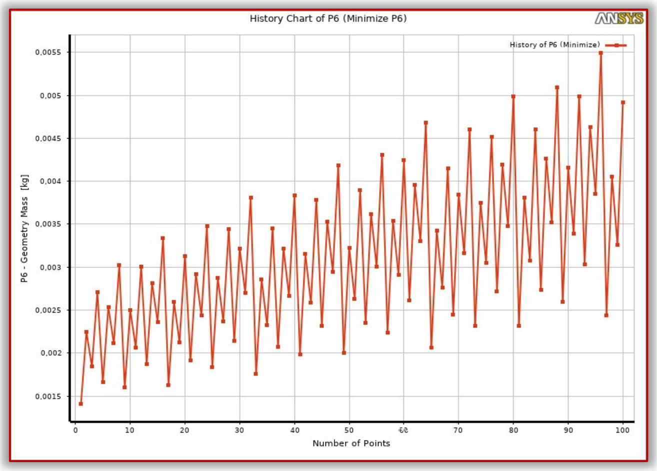

Figure 15. The mass change

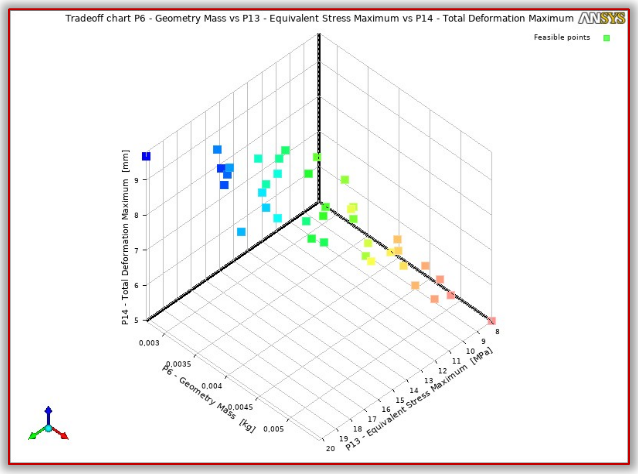

Figure 16. The results of the optimization

Candidate Points	Candidate Point 1	Candidate Point 2	Candidate Point 3
P11 - profile_height (mm)	10,35	11,95	13,75
P15 - profile_width (mm)	2,51	2,5725	2,2913
P6 - Geometry Mass (kg)	0,0027089	0,0031268	0,0032151
P13 - Equivalent Stress Maximum (MPa)	20,203	16,284	17,354
P14 - Total Deformation Maximum (mm)	9,6827	8,5966	9,714

Figure 17. The three best solutions

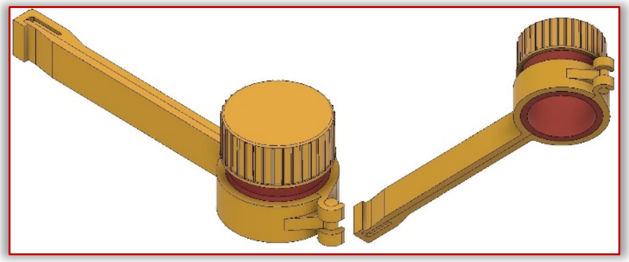

Figure 18. The final optimal design of the bag clip

To test the product functionality, the bag clip prototype was 3D printed using the hobby-grade 3D printer Creality Ender 3. No functionality issues were found.

— Qualitative life-cycle assessment of the bag clip

ECODESIGN Assistant Pilot [7] was used only for qualitative LCA analysis due to the extensiveness of quantitative analysis, i.e. collection and processing of large amounts of data. The purpose of the qualitative analysis was to show the environmental impact of this polymeric bag clip during its life cycle.

The LCA analysis aimed to:
- determine the type of product (A-E)
- suggest at least 3 proposed strategies to increase sustainability

Table 2 presents the set of estimated parameters used for the LCA analysis. The results can be divided into two parts, product classification, and recommendations for strategic improvements. The results of the analysis (Figure 19) show that the multipurpose bag clip is a B type of product. These are the products that require high production requirements, and they are characterized by the following [8]:
- production requires large amounts of energy,
- parts are transported over long distances,
- the product is difficult to repair, i.e. it requires new production.

Table 2. Parameters of the numerical analysis

The parameters	Values
Product Life Time	5 years
Material	Polypropylene
Energy input	50 kWh
Waste per unit	5% of the mass
Production per year	100.000
Means of transportation (Truck)	1.000 km
Frequency of use	300 uses/year

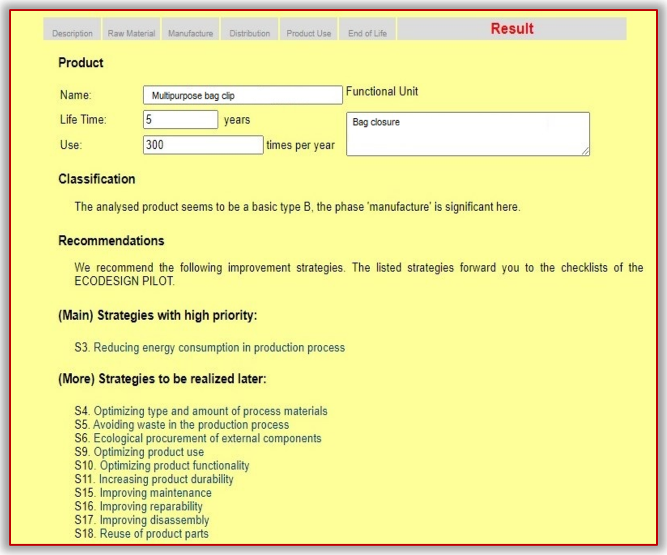

Figure 19. The recommendations and strategies for bag clip improvement

CONCLUSIONS

The construction of polymer products has its specifics. First of all, it is important to pay attention to the basic design strategies of molding: maximum functionality, optimal material, and minimum weight. The basic rules of technological design are also important, e.g. design as thin walls as possible, anticipate bevels, avoid undercuts, etc. Applying design recommendations for assembly (DFA) for polymer products can significantly reduce the cost of materials, mold making, etc. Namely, due to increasing competition in the market and the development of the technology, the application of the DFA principles is not a possibility but a need. Due to the reduction of plastic waste generation, already in the process of construction of polymer products, it is important to take into account the method of reuse of plastic waste. LCA analysis has shown that the selected material ensures the reuse of the product, which means that at the end of exploitation does not end up in nature as garbage but is completely recycled and used for the new processing. Finally, the initial mass of a product was reduced by 32 %. In the case of the production process, the high priority should be to reduce energy consumption.

References

[1] A European Strategy for Plastics in a Circular Economy 2018, Available at https://eur-lex.europa.eu/legal-content/
[2] PLASTICS TODAY, Available at https://www.plasticstoday.com/plastics-gaining-more-acceptance-closures-market
[3] Šercer, M., Križan, B., Basan, R.: Konstruiranje polimernih proizvoda, University of Zagreb, Zagreb, 2009.
[4] Erhard, G.: Designing with Plastics, Carl Hanser Verlag GmbH & Co, Munich, 2006.
[5] Cults, Available at https://cults3d.com/en/3d-model/home/bag-clip-with-screw
[6] Hu, D., Ren, L., Howard, D., Zong, C. Biomechancial Analysis of Force Distribution in Human Finger Extensor Mechanism, BioMed Research International, Vol. 2014, ID 743460, 2014.
[7] ECODESIGN, Available at http://pilot.ecodesign.at/assist/assistent?lang=en
[8] Veliki, T.: Ekološki i energetski aspekt proizvoda P4, Ekološki i energetski dizajn proizvoda, University North, Varaždin, 2019.

Note: This paper was presented at IIZS 2022 – The XII International Conference on Industrial Engineering and Environmental Protection, organized by Department of Mechanical Engineering and Department of Environmental Protection of the Technical Faculty "Mihajlo Pupin" Zrenjanin, from the University of Novi Sad, in cooperation with partners – University Politehnica Timisoara, Faculty of Engineering, Hunedoara (ROMANIA), University "St. Kliment Ohridski", Technical Faculty, Bitola (MACEDONIA), "Aurel Vlaicu" University of Arad, Faculty Of Engineering, Arad (ROMANIA), University of East Sarajevo, Faculty of Mechanical Engineering East Sarajevo, Sarajevo (BOSNIA & HERZEGOVINA) and University of Giresun, Faculty of Engineering, Giresun (TURKEY) – in Zrenjanin, SERBIA, in 06–07 October, 2022.

ISSN: 2067-3809

ACTA TECHNICA CORVINIENSIS – BULLETIN OF ENGINEERING
TOME XVI [2023] | FASCICULE 2 [APRIL – JUNE]

[1.]Cristian CIOBANU, [2.]Gheorghe VOICU, [2.]Irina–Aura ISTRATE, [2.]Paula VOICU, [2.]Mariana–Gabriela MUNTEANU

VARIATION OF ENERGY CONSUMPTION AND SPECIFIC SURFACE BLAINE RESULTING FROM SIMULATION OF CLINKER GRINDING IN A CEMENT MILL

[1.]CEPROCIM SA, ROMANIA
[2.]University Polytechnic of Bucharest, ROMANIA

Abstract: Given the technological importance of the grinding processes and the energy implications they bring, the present work sought to deepen the physics of these processes, namely: the determination of the energy consumption of the laboratory mill, the determination of the Blaine Specific Surface Area (SSA) and the variation between them. This work aimed to optimize large clinker grinding plants in the cement industry, by measuring in a laboratory mill with a rotating horizontal drum, the energy consumption, and the Blaine specific surface area. For example, clinker grinding in a laboratory ball mill was simulated by a professional simulation program EDEM 2022.0. To carry out the experiments, clinker material from a cement factory in Romania marked Clincher A was used. To carry out the experimental research, the CEPROCIM process was applied, which is based on the grinding of a batch of material in a laboratory mill with a rotating horizontal drum.
Keywords: grinding, specific surface, porosity, the average diameter

INTRODUCTION

The grinding processes in the technological flow represent the main consumer of electricity in the cement industry, having a share of over 95% of the energy consumption for the whole of the grinding operations and over 70% of the total electricity consumption of this industry, (Opris, S., 1994).

The specific energy consumption of the grinding operations is accentuated by the increased resistance of the granules to the crushing efforts. Grain breakage begins in areas where cracks or other microstructural defects are found, where the material yields more easily.

As the particle sizes decrease, the probability of structural defects inside the granules also decreases, so the required efforts increase as the grinding process progresses:

- increasing the weight of elastic deformations of the material;
- the formation of secondary microcracks, which do not propagate, closing after the action of crushing efforts ceases;
- heating the shredded material;
- agglomeration of fine particles: this last phenomenon is harmful, because it consumes energy, having an effect opposite to breakage, reducing the specific surface of the product;
- sticking the fine material on the grinding organs, which dampens the shocks and reduces the grinding efforts;
- too advanced shredding of a part of the material.

The particles resulting from the crushing of the initial granules with different characteristics do not simultaneously reach sizes smaller than the prescribed limit. The need to prolong the grinding operation until all the granules have the appropriate size also implies the appearance of fractions with too high fineness, especially in the case of high reduction ratios, such as those that are achieved in grinding processes, thus amplifying the effects of the phenomena listed above.

Given the technological importance of the grinding processes and the energy implications they bring, the present work sought to deepen the physics of these processes, namely: the determination of the energy consumption of the laboratory mill, the determination of the Blaine Specific Surface Area (SSA) and the variation between them.

MATERIALS AND METHODS

To carry out the experiments, clinker material from a cement factory in Romania marked Clincher A was used. At the initial moment of the determinations, the sample was chemically characterized according to the requirements of SR EN 196–2:2013 – Test methods of cement. Part 2: For the chemical analysis of cement (Romanian Standard, 2013), the final clinker used to produce cement was type: CEM I 42.5 R, which is a Portland cement with high initial strength. The main constituents are Portland clinker (K) (95 %) and minor components (0–5%), (Holcim, 2021).

To carry out the experimental research, the CEPROCIM process was applied, which is based on the grinding of a batch of material in a laboratory mill with a rotating horizontal drum (Figure1) in two stages:

- the first stage with ball loading, (Figure 2);
- the second stage with a load of biconical bodies, (Figure 3).

The fineness of the material was periodically determined by the R009 residue and Blaine specific surface area (SSA). The first stage was considered completed when R009 is ~35% residue (R009 – residue on the 90 μm sieve). The energy consumption between the moments when the fineness of the material is determined was identified with the help of a wattmeter (the consumption was read directly from the meter). These consumptions were accumulated from the beginning of the determination and related to the mass of the batch (20 kg of clinker), calculating the specific energy consumption w_{li}, in the predetermined time unit of 10 minutes.

$$\text{Energy consumption} = \frac{\text{counter difference}}{\text{batch mass}} \quad \frac{[\text{KWh}]}{[\text{kg}]} \tag{1}$$

The curves R009 = f(w_{li}) and s = f(w_{li}) were plotted. The grindability index is the specific energy consumption w_1 corresponding to a reference fineness, (Opriș S., 1994). It can be evaluated by the specific Blaine surface and by sieving on a sieve of 009 mm (4900 mesh/cm² according to SR EN 196–6).

$$c_1 = \frac{w}{w_1} \tag{2}$$

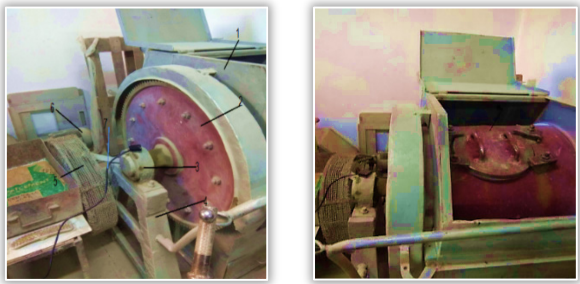

a)

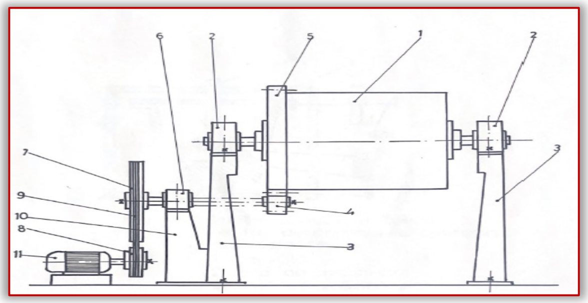

b)

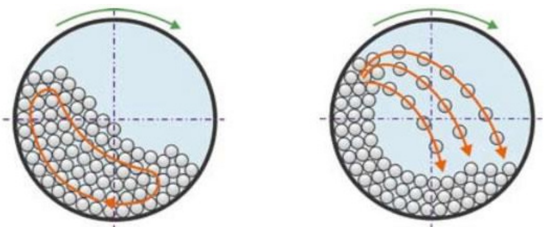

I. II.

Figure 1 – Laboratory ball mill. a) principle diagram of the ball mill: 1 – mill body; 2– mill bearings; 3 – mill supports; 4– attack pinion; 5 – toothed crown; 6– attack pinion bearing; 7,8– wheels for trapezoidal belts; 9 – trapezoidal belts; 10 – bearing support for the attack pinion; 11 – engine. b) operating regimes of ball mills, (Hanan Sankay Industrial Co., Ltd, 2022; Ene G. et al., 2005);
I – cascade operation mode; II – cataract operation mode

The specific Blaine surface area was calculated according to relation (3) and is conventionally expressed in cm²/g, as:

$$S = \frac{K}{\rho} \cdot \frac{\sqrt{e^3}}{(1-e)} \cdot \frac{\sqrt{t}}{\sqrt{10 \cdot \eta}} \qquad \frac{[\text{cm}^2]}{[\text{g}]} \tag{3}$$

where: K – device constant; e – porosity of the layer; t – measured time, in (s); ρ – cement density, in (g/cm³); η – air viscosity at the test temperature, in (Pa· s).

$$K = \frac{s_0 \rho_0 (1-e)\sqrt{10 \cdot \eta}}{\sqrt{e^3 \sqrt{t_0}}} \tag{4}$$

where: S_0 – the specific surface of the reference cement, (cm²/g); ρ_0 – volume mass of the reference cement, (g/cm³); t_0 – the average of three timed values of time, (s); η_0 – air viscosity corresponding to the average of three temperatures, in (Pa·s).

According to the CEPROCIM method, the load with grinding bodies, for the first experiment in the first phase of grinding (coarse) was according to the data presented in table 1:

Table 1. Load grinding bodies

Ø[mm] grinding balls	65–75	55–65	45–55	Total
G[kg] grinding balls	76,90	38,55	28.85	~144.3

Figure 2 – Grinding balls of different sizes

The final grinding (second phase – the fine one) was done with an equivalent load of bicones of ~144.3 kg. The bicones have the size of Ø 25 X 30 mm, in the laboratory ball mill. Grinding with bicones started in the ball mill, according to the CEPROCIM methodology, when the material residue on the 90 μm sieve (R90μm) reached around 30% (grinding balls were removed and bicones were inserted).

Figure 3 – Bicones

The same laboratory ball mill was used to simulate clinker grinding. Table 2 shows the properties of the materials used for the simulation and table 3 the parameters used for the simulation in the case of the previously mentioned ball mill. Clinker powder distribution, ball distribution, and wear were modeled using DEM. Dry grinding simulations were performed using a standard coefficient of restitution of 0.3 and a coefficient of friction of 0.75 (ball–ball and ball–material collisions), (Cleary, P.W., 2001). The charge consisted of powders and balls with a filling of 40% of the charge (by volume). The specific gravity of the support is equal to 2.7 kg/m^3.

Table 2. Properties of materials used for simulation

Parameters	Value
Poisson ratio	0,3
Young modulus(N/m^2)	$1{,}8\cdot10^{11}$
Density (kg /m^3)	7800

Table 3. Ball mill parameters used for simulation

Parameters	Value
Motor shaft power (kW)	0,37
Angular speed (rpm)	250
Effective disc diameter (mm)	140
Mill filling (%)	40
Mill speed (% critical speed)	10–100
Time step(s)	$1{,}1*10^{-4}$
Ball density (kg/m^3)	7800
Ball size (mm)	60
Mill internal length (mm)	535
Internal diameter of the mill (mm)	540
Weight of grinding balls (kg)	144,3

RESULTS

The stages of the experiment presented in this article, are:

- Clinker A (20kg) was sieved on the Ø =7 mm sieve, then the material remaining on the sieve was crushed in the jaw crusher Retsch BB100 to shred the clinker to pass it completely through the 7 mm sieve (Figure 4).

Figure 4 – Retsch BB 100 jaw crusher

- The content obtained was homogenized and subjected to sieving on particle size fractions (table 4), through a set of standardized sieves, according to SR EN 933–2 – 1998 (Romanian Standard, 1998), and later the particle size curve from Figure 5.

Table 4. The amount of material (pass percentage) rejected on the site of different sizes – clinker A

Sieve [mm]	Material remaining on the sieve [g], [%]		T [%]	R[%]
	p[g]	p[%]		
5	122,90	10,22	89,78	10,22
3	228,27	18,98	70,8	29,2
1	246,28	20,48	50,32	49,68
≤1	605,31	50,32	100	100
Total material	1202,76		–	

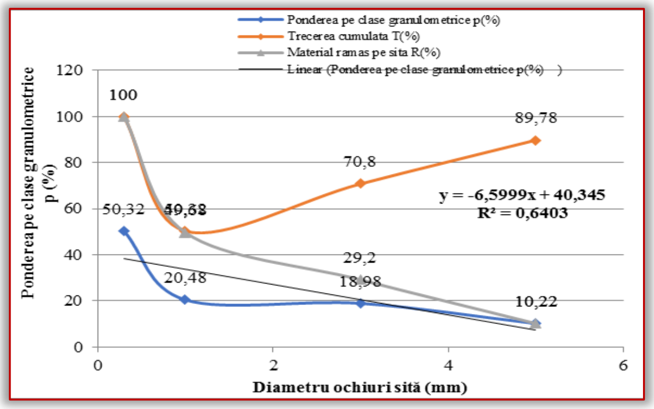

Figure 5 – Granulometric curve related to the amount of material–clinker A

- Experimental determinations regarding energy consumption when crushing clinker A

Clinker A (20 kg) was ground resulting in 10 samples (2 ball samples and 8 bicone samples). When the material residue on the 90 μm sieve (R90μm) reached around 30%, the grinding balls were removed and bicones were inserted. Thus, according to relation (1), the values presented in table 5 were obtained.

Table 5. Energy consumption related to grinding time – clinker A

No.crt.	Grinding time [min]	Counter display [kWh]	Counter difference [kWh] in time steps	Grinding bodies
0	0	7350421	0	Grinding balls
1	10	7350661	240	
2	20	7350882	221	
3	30	7351096	214	Bicones
4	40	7351314	218	
5	50	7351526	212	
6	60	7351746	220	
7	70	7351968	222	
8	80	7352196	228	
9	90	7352417	221	
10	100	7352642	225	

Table 6. Consumurile de energie raportat la timpul de măcinare – clincher A

No.crt.	Grinding time [min]	Resulting energy consumption [kWh/kg]	Cumulative energy consumption [kWh/kg]
1	10	10,7	10,7
2	20	10,9	21,6
3	30	10,6	32,2
4	40	11	43,2
5	50	11,1	54,3
6	60	11,4	65,7
7	70	11,05	76,75
8	80	11,25	88,00

After determining the energy consumption resulting from the grinding of clinker A, the variation of the specific crushing energy in the unit of time is shown in Figure 6.

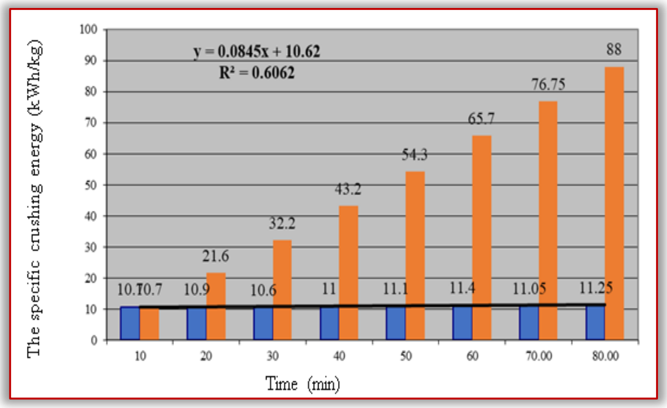

Figure 6 – Variation of specific clinker crushing energy A

Experimental determinations regarding the specific surface area when grinding clinker

To determine the Blaine Specific Surface Area (SSA) for different grinding times and different degrees of loading with balls and material, the calculation was made according to relation (3).

The equipment constant, K, was calculated according to relation (4), for a specific porosity value e = 0.50, and the test temperature t = 20±2°C.

Thus, in table 7 the Blaine Specific Surfaces (SSA) resulting from the calculation were noted.

Table 7. SSA values and power consumption per unit of time

No.crt.	Grinding time [min]	Consumption meter indicator [kWh]	Grinding bodies	$R_{90\mu m}$ bile [%]	SSA bicones [cm^2/g]
0	0	0	0	0	0
1	10	240	Grinding balls	51.68 %	–
2	20	221		33.6%	–
3	30	214	Bicones	–	2250
4	40	218		–	2650
5	50	212		–	2830
6	60	220		–	3180
7	70	222		–	3520
8	80	228		–	3590
9	90	221		–	3700
10	100	225		–	3870

After determining the energy consumption when grinding type A clinker, the variation of the specific Blaine surface area (SSA) in the time unit was graphically represented (Figure 7).

A linear increasing variation of SSA with a slope of 228.7 $cm^2/g/min$ is found.

Determination of the grinding ability index which is represented by the specific energy consumption w1 corresponding to a reference fineness.

Based on the results obtained and noted in table 8, the correlation coefficient diagram was drawn, figure 8, with the industrial mills (c_1) in which the specific energy consumption of the industrial mill was noted with w, in the assumption of action through the pinion–crown final group gear and speed reducer.

According to the value calculated by the cement factory $W_{consumption\ industrial\ mill}$ is 32.92 kWh/t. This results in the following values for the correlation coefficient c1 (from formula 2) for the experimental determinations made

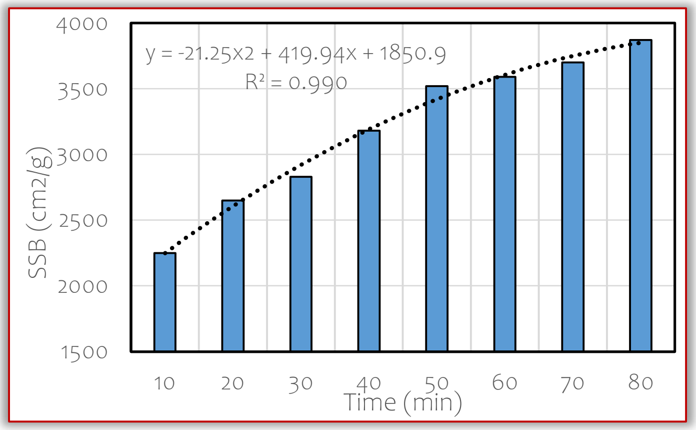

Figure 7 – Variation of blaine specific surface area when grinding clinker a with bicones mill

Table 8. Values of correlation coefficients c1 and energy consumption for clinker A

No.crt.	Grinding time [min]	Experimental result energy consumption [kWh/t] clinker A	Correlation coefficient c1 clinker A
1	10	10.7	3.08
2	20	10.9	3.02
3	30	10.6	3.11
4	40	11	2.99
5	50	11.1	2.97
6	60	11.4	2.89
7	70	11.05	2.98
8	80	11.25	2.93

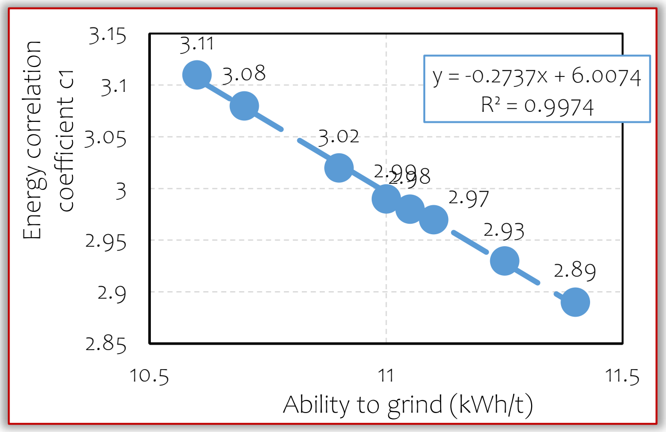

Figure 8 – Correlation of coefficient with industrial clinker mills A with grinding ability

Modeling assumptions are described starting from material identification (contact law), mill geometry and fill, and description of simulation and post–processing. During the simulation, all particles are considered and represented as spherical element. The stages of building a model are:

- cleaning the geometry (adding the components that will be simulated with their characteristics: balls, clinker), importing geometry;
- setting the dynamics of the model elements;
- setting the parameters of the model elements;
- setting the parameters of bulk materials.

Furthermore, the computer–aided design (CAD) geometry used for the DEM simulations is shown in Figure 9.

The geometry shows the characteristic regions of charge motion and the stochastic variability of the particle flow pattern. Thus, the particles are colored according to their speed. Figure10 illustrates the different stages of particle breaking. The particle size distribution is mainly concentrated near the mill wall due to the high centrifugal accelerations caused by the drum motion.

With an increase in speed, the powders occupy almost the entire volume of the mill space. In addition, smaller particles, which receive a large amount of impact energy, travel in closed trajectories near the mill wall due to gravity.

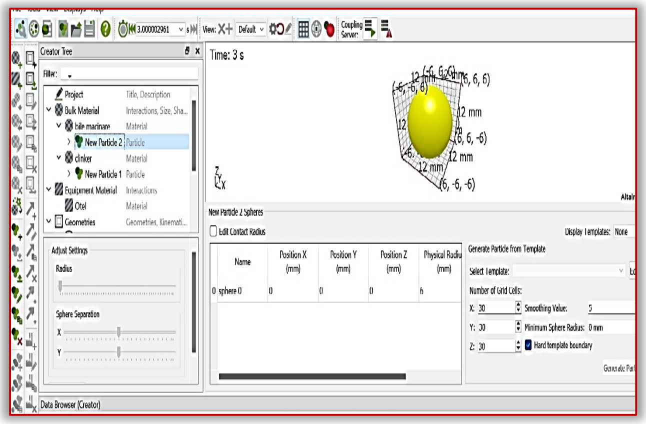

Figure 9 – Geometria de proiectare asistată de computer

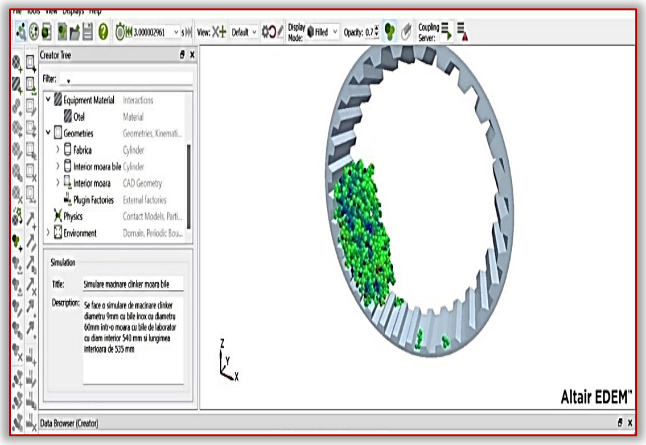

Figure 10 – Diferitele etape ale spargerii particulelor

Thus, the simulation results are consistent with those obtained by Hirosawa et. al. (2021). Furthermore, the velocity provides information about the charge movement. In the beginning (Figure10), it seems that all the particles are uniformly distributed inside the load. As the mill speed increases (Figure10), the particles concentrate near the wall and are launched higher from the edge of the charge.

However, it means that the particles and balls are well mixed. Figure11 shows particles moving at high speed, which produces high energy impacts during the grinding process. This can be explained by the fact that the flow of finer powder particles through the grinding media (mill walls–shields and balls). The number of collisions was also found to decrease with increasing energy per collision (Daraio, D., et al, 2020).

The variation of collision frequency with energy loss for different types of collisions (ball–particle–die, ball–ball, and ball–particle), collected from the DEM simulation, is shown in Figure11. A reduction in the number of collisions and an increase in their magnitude can be observed.

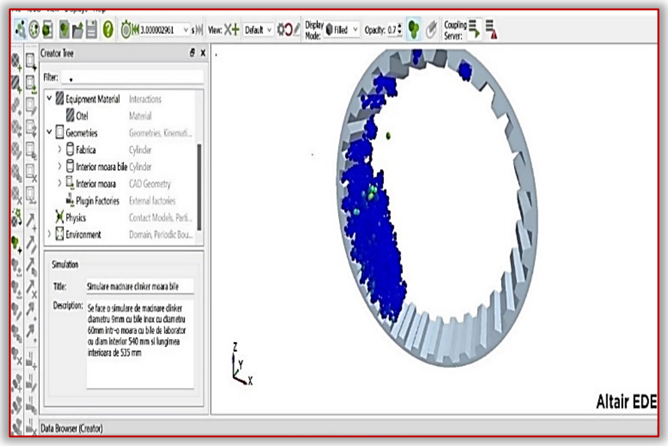

Figure 11 – Reducerea numărului de coliziuni

CONCLUSIONS

After finishing the grinding, the clinker fell within the norms for the production of cement type CEM I 42.5 R. (having the Blaine specific surface around 3800 cm^2/g), and the energy consumption is about 100 KWh/t.

The determination of the specific surface area (SSA) of the crushed material using the Blaine permeameter method is applicable for all cements defined in the EN 196–6: 2018 standard.

The simulation can be applied to calculate collision rates and impact energy spectra of industrial–scale ball mills and to understand particle behavior inside the mill

Raw material grinding plants in the cement industry are complex plants inside which, in addition to mechanical grinding processes, and thermo–technological processes through their drying take place. The major difficulty in the design, management, and optimization of the installation derives from the fact that in most cases the values of the input quantities and/or the environmental parameters register strong disturbances in a short time interval compared to the calculated values. For this reason, an analytical approach that covers all possible situations is not possible.

Acknowledgement

This research was supported, among others, by Executive Unit for Financing Higher Education, Research, Development and Innovation, UEFSCDI, under the PNCDI III – Programme 2, sub–programme 2.1., as follows partially from: submission code PN–III–P2–2.1–PTE–2019–0446, funding contract no. 53PTE/23.09.2020, project title "Hydrophilic auto–chassis for high energy efficiency operation of interchangeable equipment intended for performing public utility work", acronym ASHEUP, research direction 3.Econano–technologies and advanced materials, subdomain Advanced materials and submission code PN–III–P2–2.1–PED–2019–4123, funding contract no. 380PED/23.10.2020, project title "Multifunctional hexa–rotors tricopter for precision farming", acronym 4.0–MHRT, project domain 1.Bioeconomics, subdomain 1.1.

References

[1] Cleary, P.W. (2001). Charge Behaviour and Power Consumption in Ball Mills: Sensitivity to Mill, Operating Conditions, Liner Geometry and Charge Composition. International Journal of Mineral Processing, Vol. 63, 79–114. https://doi.org/10.1016/S0301–7516(01)00037–0
[2] Daraio, D., Villoria, J., Ingram, A., Alexiadis, A., Stitt, E.H., Munnoch, A.L. and Marigo, M. (2020). Using Discrete Element Method (DEM) Simulations to Reveal the Differences in the γ–Al2O3 to α–Al2O3 Mechanically Induced Phase Transformation between a Planetary Ball Mill and an Attritor Mill. Minerals Engineering, 155, Article ID: 106374, https://doi.org/10.1016/j.mineng.2020.106374
[3] Ene, G., Tomescu, Gh., Dobra, S. G. (2005). Machines for shredding solid materials. Design guidelines, Publisher: MatrixROM, ISBN: 973–685–868–5
[4] Hirosawa, F., Iwasaki, T. & Iwata, M. (2021). Particle Impact Energy Variation with the Size and Number of Particles in a Planetary Ball Mill. MATEC Web of Conferences, 333, 1–5. https://doi.org/10.1051/matecconf/202133302016
[5] Opris, S. (1994). Cement Industry Engineer's Handbook/ Manualul inginerului din industria cimentului, Vol. I, Technical Publishing House, Cement National Institute CEPROCIM S.A./Institutul National de ciment CEPROCIM SA
[6] *** Hanan Sankay Industrial Co.,Ltd (2022). http://ro.sk–rockcrusher.com/grinding–mill/ball–mill.html
[7] *** Holcim, (2021). https://www.holcim.ro/ro/produse–si–servicii/produse/ciment/cem–i–425–r
[8] *** Romanian Standard (1998). Tests to determine the geometric characteristics of the aggregates. Part 2: Particle size analysis – control sieve, nominal mesh sizes
[9] *** Romanian Standard. (2013). Cement test methods. Part 2: Chemical analysis of cement (SR EN 196–2:2013). https://magazin.asro.ro/ro/standard/111291

Note: This paper was presented at ISB–INMA TEH' 2022 – International Symposium on Technologies and Technical Systems in Agriculture, Food Industry and Environment, organized by University "POLITEHNICA" of Bucuresti, Faculty of Biotechnical Systems Engineering, National Institute for Research–Development of Machines and Installations designed for Agriculture and Food Industry (INMA Bucuresti), National Research & Development Institute for Food Bioresources (IBA Bucuresti), University of Agronomic Sciences and Veterinary Medicine of Bucuresti (UASVMB), Research–Development Institute for Plant Protection – (ICDPP Bucuresti), Research and Development Institute for Processing and Marketing of the Horticultural Products (HORTING), Hydraulics and Pneumatics Research Institute (INOE 2000 IHP) and Romanian Agricultural Mechanical Engineers Society (SIMAR), in Bucuresti, ROMANIA, in 6–7 October, 2022.

ACTA TECHNICA CORVINIENSIS
Bulletin of Engineering

ISSN: 2067–3809

ACTA TECHNICA CORVINIENSIS – BULLETIN OF ENGINEERING
TOME XVI [2023] | FASCICULE 2 [APRIL – JUNE]

[1–4.]Yelizaveta CHERNYSH, [5.]Mykola KHARYTONOV, [1,2.]Viktoriia CHUBUR, [4.]Vladimir SHTEPA, [2.]Hynek ROUBIK

APPLICATION OF BIOCHAR OF DIFFERENT GENESIS: APPLIED ASPECTS OF ACTIVATION

[1.]Sumy State University, Sumy, UKRAINE
[2.]Czech University of Life Sciences Prague, Prague, CZECH REPUBLIC
[3.]T. G. Masaryk Water Research Institute, Prague, CZECH REPUBLIC
[4.]International Innovation and Applied Center "Aquatic Artery", Sumy, UKRAINE
[5.]Dnipro State Agrarian and Economic University, Dnipro, UKRAINE

Abstract: The paper considers various biochar activation processes in bioprocesses, particularly in anaerobic digestion, to intensify the production of biogas and biofertilizer. Based on the literature research study, the applied aspects of biochar activation processes in the agricultural and bioenergy sectors were analyzed, with small–scale laboratory experiments to verify theoretical hypotheses. Ultrasonic pretreatment was performed with a power of 200 W and a frequency of 30 kHz. The biochar was also subjected to microscopy. After ultrasound treatment, changes in the structure of biochars of different genesis were detected, which is also consistent with changes in the ORP values of activated biochars. A comparative thermogravimetric analysis of biochar samples was carried out.
Keywords: biochar, activation, biogas, biofertilizer, ultrasonic pretreatment

INTRODUCTION

Today, the use of biochar in various spheres of human economic activity has become increasingly widespread. Biochar is a solid material containing carbon with a large amount of hard–mineralized aromatic structures, obtained by carbonization of renewable organic biomass at high temperatures and without oxygen access (pyrolysis) (*Edinburgh Research Explorer Biochar Quality Mandate (BQM) Version 1.0*, n.d.).

Periodically, the term "biochar" is associated with the term "charcoal," which is obtained in the process of producing lumpy charcoal, which does not correspond to the definition of biochar. Biochar is also a plant–derived charcoal with a carbon content of 93–99% and the absence of harmful and toxic impurities. Due to its main properties – purity and absence of impurities, as well as high carbon saturation, biochar can be used in agriculture – both in animal husbandry and in the agricultural sector (*Kamarudin et al., 2022*) (*Kamarudin et al., 2022*).

Biochar as an additive in agriculture has the following advantages (*Biochar, the benefits of using natural soil fertilisers – Proposition, 2020*):

- speeds up plant growth and development as the soil is constantly heated;
- removes residues from the soil of chemicals that were applied earlier (herbicides, pesticides, and other pesticides);
- promotes the functioning of microorganisms in the soil, which have a positive effect on crop yields;
- increases soil porosity, provides oxygen access to plant roots, and air circulation;
- improves the composition of infertile soils (alumina, sandy ,loam and sandy soils);
- neutralize soils with increased acidity;
- protects soil from some pests (nematodes, wireworm);
- prevents purulent processes;
- preserves and supports nutrients and necessary microelements in the soil, and eliminates the problem of their leaching.

It also serves as a raw material for the production of activated carbon, is used for drinking water and wastewater treatment, for the elimination of toxins and disinfection, and is used in segments of industry where there is a need for pure carbon. For example, in Germany, biochar is actively used in agriculture as ready–to–use mail mixed and as a soil substrate. It is also used as a food additive for cattle, birds and pets. Biochar is a high–value–added processed product with a very broad testing potential; its production solves the current problem of waste recycling, contributes to the introduction of "green technology" and the production of bioenergy (*Biochar And The Biomass Recycling Industry | BioCycle, 2011*).

Of particular importance in some biochemical processes is the high resistance to the chemical reaction and resistance to swelling of adsorbents. In this aspect, carbon adsorbents compare favorably with mineral– and polymer–basedĂ adsorbents, which opens up wide opportunities for their practical use. In this direction, we can also consider biochars, and there are electrochemical features of biochars, which are now actively investigated and can be applied in biogas technologies.

Regarding the activation of coals of different nature, a number of works (*Bisaria et al., 2022; Peter et al., 2019, 2020; Y. Wu et al., 2016*) studied the effect of the type of processing (mechanical, ultrasonic) on the degree of dispersion, density of carbon powders, and their morphology;

samples of "carbon powders" with sieve properties obtained by different methods determined their structural characteristics (*Stavitskaya, 2009*).

Ultrasound treatment is a means of active influence on various structures of substances (*Moskalenko & Danilov, 2009*):

- on the course of heat and mass exchange processes in substances;
- on the structure of solids and processes of their contact interaction.

The use of ultrasonic sound in technological processes of production and processing of materials and substances allows (*Kamarudin et al., 2022; L. Wu et al., 2022; Moskalenko & Danilov, 2009*):

- reduce the cost of a process or product;
- obtain new products or improve the quality of existing ones;
- to intensify traditional technological processes or stimulate the implementation of new ones.

In this regard, the problem of identifying the nature of the specific effects of acoustic ultrasonic vibrations on the processes of deep processing of raw materials is relevant. The idea of the implementation of combined processes in obtaining active coals of different genesis, including biochar, has been developed in a number of studies (*Kizito et al., 2022; Kobayashi & Kuramochi, 2022; Liu et al., 2022; Zhang et al., 2022; Zhao et al., 2022*). The technology for obtaining charcoal by combined pyrolysis–vapor–gas activation using alternating electric current has been proposed. Ways of directed regulation of the porous structure parameters and adsorption properties of wood active carbons have been investigated. Processes of activation of coals at processing by a constant electrolytic field by a voltage in a diapason 1.5–30 V lead to the reception of hydrogen–activated charcoal. When used in aqueous solutions, this charcoal is negatively charged, sending hydrogen ions into the solution and attracting cations, which intensifies the purification process (*Belyaev, 2000*).

Rapid pyrolysis of biomass pretreated with mineral acid produces high–quality biofuels, but the biochar resulting from this process has not been characterized, and its effectiveness as an additive for aanaerobic digestion (AD) is unknown. This study reports the effect of the physicochemical properties of two different biochars on AD of urban sludge: one was produced by pyrolysis of raw corn cobs (BC–1) and the other was produced by pretreatment of the same corn cobs with sulfuric acid (BC–2). BC–1 had higher carbon content, alkalinity and specific surface area, but lower ash and sulfur content than BC–2. Both biochars contained volatile fatty acids and residual sugars that serve as substrates for anaerobic bacteria to improve biogas / methane production. When biochars were added to AD, their effect on biogas production showed opposite trends. In general, the results showed that the effect of biochar on AD depends on the properties of the biochar, and the choice of a suitable biochar is important to ensure higher biogas production and to maintain a stable process (*Zhou et al., 2020*).

A study (*Wambugu et al., 2019*) evaluated the effect of biochar addition on anaerobic digestion (AD) of food waste. Of the five biochar tested, Fe, Co, Ni, and Mn leached in very small amounts (<10 mg/kg), while treated wood waste and willow pyrochar leached large amounts of K (1,510 and 1,969 mg/kg), respectively. AD experiments were carried out in a 1:1 inoculum:substrate ratio, at 30°C and under stirring conditions. The results showed that the volume of biogas produced by treatment with hydrosugar from brewery residues and pyrosugar from treated wood was lower than that produced by a control that used only food waste. Food waste supplemented with 1.5 ml of micronutrients produced the highest amount of biogas, 588 ml/g COD (CH_4 content 48%). In addition, two identical upflow anaerobic sludge reactors (UASB), that is, the control reactor and the biochar supplemented reactor, operated at 30°C, with organic loading rates (OLR) ranging from 3.4 to 7.8 g COD/L per day. The average COD removal efficiency in the control reactor and the biochar–added reactor was 47% and 77% at OLRs of 6.9 to 7.8 g COD/L. per day, respectively. The results clearly show that the type of biochar and its trace element concentration play a key role in determining its effectiveness in improving the production of biogas from food waste (*Wambugu et al., 2019*).

Biochar can receive and give out electrons, as in microbial fuel cells, where biochar can be activated and used as an anode and cathode (*Patwardhan et al., 2022*). However, the electrical conductivity of biochar is not based on a continuous flow of electrons, as in copper wire; it is based on continuous electron hopping, which is important for the functioning of biochar as a microbial electron mediator or so–called electron boat, which facilitates even inter–species transfers. Because of the relatively large size of the biochar particles, the electron transfer capacity of the biochar carbon matrices can lead to the exchange of electrons over considerable distances, allowing greater access to alternative acceptors, such as those of minerals, for oxygen–free microbial respiration. We assume that it can also be used effectively in electrolysis processes of the substrate to intensify anaerobic digestion, which requires experimental studies.

Thus, the purpose of this work is to study the possible applied use of biochar in anaerobic digestion with an experimental study of the effect of ultrasonic treatment on the properties of biochar.

MATERIALS AND METHODS

Ultrasonic pretreatment was performed in a stainless steel tube section with a total working volume of 250 ml. Ultrasonic equipment, consisting of 3 transducers, with a power of 200 W and a frequency of 30 kHz was placed in the section.

Figure 1 shows the laboratory experimental installation of ultrasonic treatment.

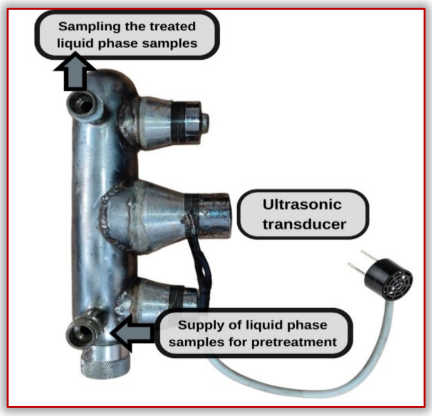

Figure 1 – Laboratory device for ultrasonic treatment

The ultrasonic treatment unit works as follows: The treated liquid enters the treatment tank through special holes in which the solution is poured manually, which provides uniform distribution over the entire cross–sectional area of the chamber. Ultrasonic vibrations are formed in the process. The direction of propagation of the ultrasonic vibrations is perpendicular to the surfaces of the smooth transitions. Thus, the ultrasonic field with the intensity necessary and sufficient for the formation and maintenance of the developed cavitation mode is created in the entire space between the walls of the unit and the surface of the radiator in the internal volume of the tank.

Temperature mode – 35 ^{0}C. Processing time: 1 min. Light microcopying was used to identify changes in the structure of the samples using a biological XS–5520 microscope with a video camera.

A comparative thermogravimetric analysis of biochar samples made from wood residues and corn stalks was carried out to obtain information about their thermal stability using the derivatograph Q–1500D of the "F. Paulik–J. Paulik–L. Erdey" system. Differential mass loss and heating effects were recorded. The measurements results were processed with the software package supplied with the device. Samples of wood and bark biomass were dynamically analyzed at a heating rate of 10°C/min in the air atmosphere. The weight of the samples was 100 mg. Aluminum oxide was used as the reference substance.

RESULTS

— Results of ultrasound treatment of biochars of different genesis

In the study, two types of biochar were taken: one produced from corn residues, the other by pyrolysis of wood residues from the furniture industry (Figure 2).

Table 1 shows the pH and ORP values before and after ultrasonic treatment of biochars of different genesis.

Microcopying of the biochars was also performed. It should be noted that the initial high porosity of biochar (b), compared to biochar (a) (Figure 3).

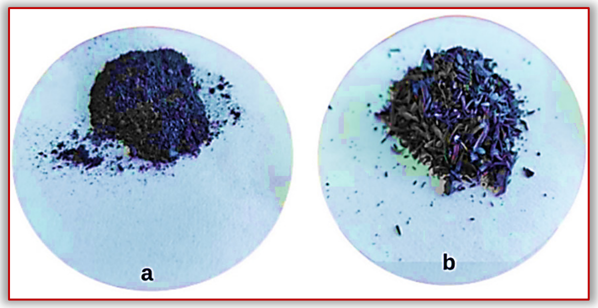

Figure 2 – Biochars:
a – from plant residues (corn); b – from wood residues from the furniture industry.

Table 1. Changes in the parameters of the treated liquid phase with biochar

Composition	Volume of water	Sonication treatment	TDS	pH	ORP
2.5 g biochar (a)	250 ml	before treatment	363	10.5	−49
		after treatment	457	10.5	−20
2.5 g biochar (b)		before treatment	844	11.3	−50
		after treatment	746	11.22	−50

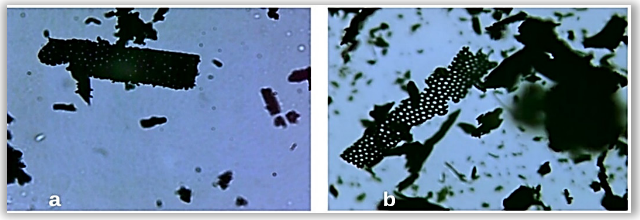

Figure 3 – Biochars before treatment, microscopy, 40x magnification:
a – from plant residues (corn); b – from wood residues from the furniture industry

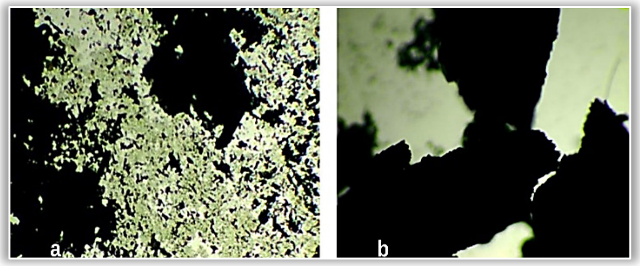

Figure 4 – Biochars after treatment, microscopy, 4x magnification:
a – from plant residues (corn); b – from wood residues from the furniture industry

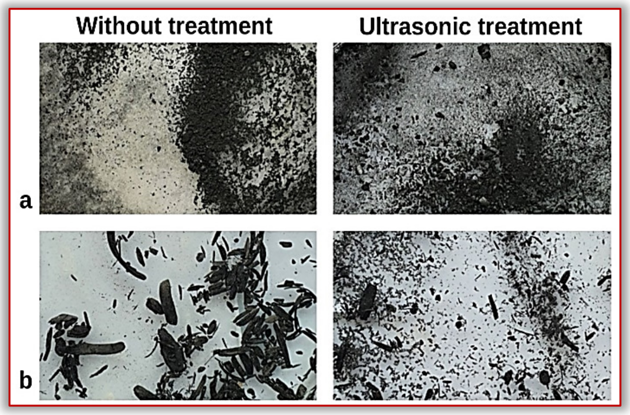

Figure 5 – Comparison before and after ultrasonic treatment:
a – from plant residues (corn); b – from wood residues from the furniture industry

After ultrasound treatment, more influence was revealed on biochar (a) during microscopy, which is also consistent with the change in its ORP values (it increased from –49 to –20 mV). The structure of biochar (a) became much more homogeneous with high fine fraction content, when drying preparations for microscopy of biochar (a) it sorbed water better compared to biochar (b) (Figure 4 and 5).

The TG and DTG combustion curves were analyzed for thermal stability of the two types of biochar made from wood residues and corn stalk (Figure6).

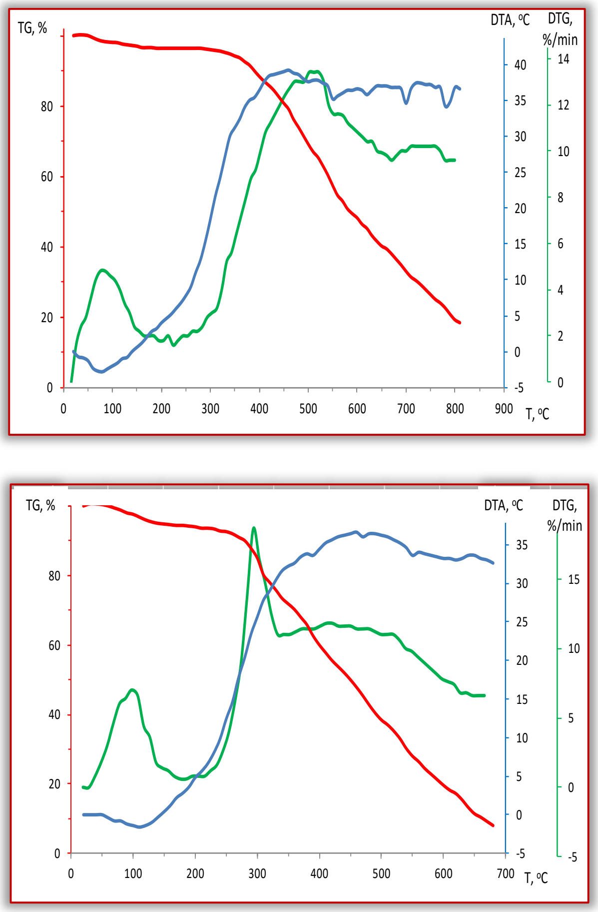

(a)

(b)

Figure 6 – TG, DTA and DTG of biochar produced from:
a – wood residues; b – corn biomass

According to the DTG curves the first thermal peaks that occurred within 75 – 100°C. As visible in Figure 6, the moisture of the biochars produced was retained after the preliminary pyrolysis procedure, which is consistent with the findings of Li and Chen (2018). . Thus, these types of biochar can be used as water sorbents to improve moisture retention in the soil. The thermal peaks at 200 – 400 °C are associated with the loss of hemicellulose and cellulose, whereas the peaks at 370 – 550°C are associated with the thermal decomposition of lignin. The sharp peak fixed at 300 – 480°C fixed for biochar from corn biomass can be explained as a result of the autocatalytic reaction of hemicellulosic, cellulosic, and lignocellulosic components (*Yang et al., 2007*). Thus, the pyrolysis process was a reason for the formation of more thermostable substances in the tested biochar samples.

Formalization of the direction of use of biochar together with digestate in soil bioremediation processes

Anaerobic digestion is an effective method for processing raw materials of organic origin. The passage of raw material and its composition is one of the key points of processing. Anaerobic digestion can be successful even with heavy metal contaminated raw materials provided that biochar is added as an additive. Accordingly, the study (*Wang et al. 2021*), although the environmental risk of heavy metals (HM) in digestate can potentially increase during anaerobic digestion of contaminated feedstock, states that biochar contributes to the passivation of heavy metals in the process.

Furthermore, HM passivation by (*Wang et al. 2021*) also obtained the result of increased biogas productivity in an example of contaminated pig manure. The methane yield increased up to 26% with the addition of additives up to 7% biochar (on a dry weight basis). Different groups of heavy metals were also found to passivate faster at different concentrations of biochar (5% and 7%).

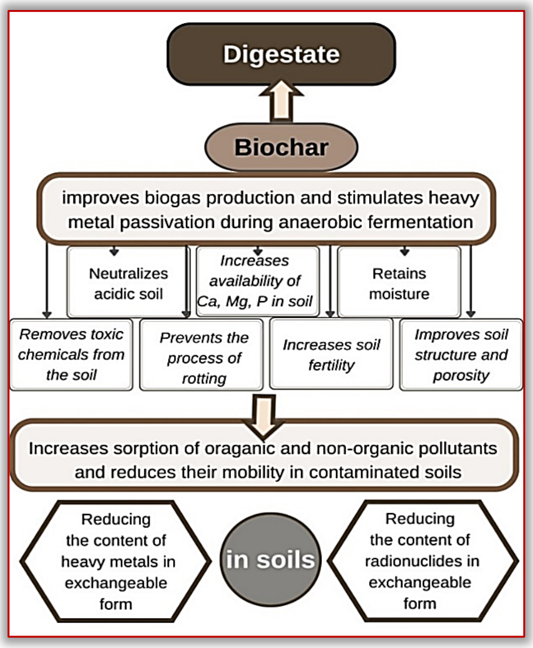

Figure 7 – Impact of biochar on the soil structure

Figure 7 shows the main characteristics of biochar conditioning a successful combination with digestate for soil remediation applications. In the process of obtaining the target product of biofuel, digestate is formed, which is an important product for the restoration of soil quality. To maintain the normal functioning of the soil–biota system of soils contaminated with HMs and radionuclides, a comprehensive approach to cleaning and increasing productivity is necessary. Biochar and digestate independently of each other have properties to reduce the concentration of heavy metals in soil solution. A study (*van Poucke et al., 2020*) compares the potential of biochar in different raw materials and digestate applications to highlight the potential to immobilize metals in soil and aquatic systems, reducing phytotoxicity.

Biochar and products based on it as agents for the immobilization of toxic substances, including HM contained in the soil, can be an environmentally friendly solution for soil remediation.

The use of biochar helps solve the problem of the bioavailability of heavy metals as a result of the direct application of its mixture to rigid digestate. (*Xue et al., 2021*) conducted an experiment using fruit biochar and porcine digestate to clean cadmium–contaminated greenhouse soil. The advantages of co–application were the ability to maintain a more stable pH and electrical conductivity and to effectively improve the properties of organic matter of soil with a reduction in the activity of a particular group of heavy metals. It was shown that the bioavailability of heavy metals and enzyme activity are related to the proportion of biochar–digestate mixing.

Research by *Anae et al. (2021*) also looked at the microbiological characteristics of the combination, where the study showed the promising potential of digestate as a source of nutrients and bacteria for soil bioremediation. In summary, biochar–digestate can be engineered by bioengineering to contain selected microbial consortiums that will incorporate a biochemical system that will facilitate remediation of contaminated soil beyond conventional methods. A related study Šimanský et al. (2022) demonstrates different effects of a biochar–based composite application, depending on soil texture, cation exchange capacity, organic carbon content, and stability of the humic substance.

The work found that for productive, fertile, and alkaline soils uncontaminated with HM, changes in macronutrient regime after the application of biochar–based composite are insignificant but can be influenced by soil texture. However, the application of such composites with fertilizers leads to changes in the physical and chemical properties of the soil and a variety of benefits in sandy and loamy soils. It was traced the dependence after the application of composites that the immobilization of heavy metals is caused by the higher content of organic carbon and fulvic acids in sandy soils,soils, while in loamy soil their elimination depended on the higher content of available phosphorus.

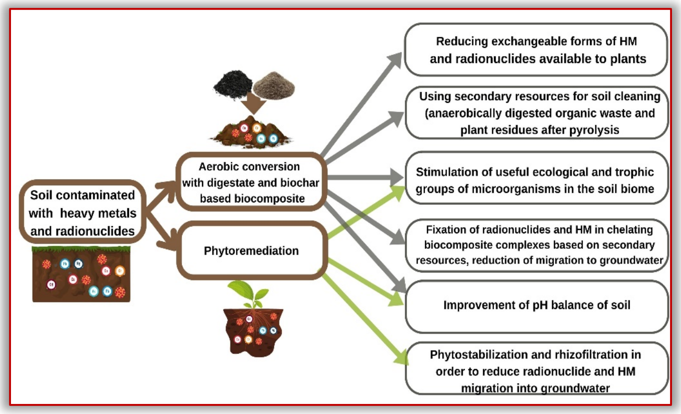

Figure 8 – Impact of remediation methods for soils contaminated with heavy metals and radionuclides

Based on these and previous studies, we have developed a scheme (Figure 8) that positively influenced the use of biocomposite based on digestate and biochar in combination with phytoremediation.

Furthermore, digestate pyrolysis to produce biochar has been investigated in recent years (*Ayaz et al., 2022; Chen et al., 2019; N. Wang et al., 2022; Zuo et al., 2020*), as pyrolysis can stabilize the metals in biochar.

The potential applications of biochar derived from high moisture digestate could be as an adsorbent to remove contaminants, as a soil amendment to enhance plant growth, and as a catalyst to improve bioprocessing (*N. Wang et al., 2022*).

Although conventional technologies exist to address contaminated soils, the use of biochar–based biocomposite as an effective recoverable adsorbent for enhanced bioremediation is considered by many researchers to be a promising strategy to mitigate the effects of co–contamination of soils with HM and radionuclides.

CONCLUSIONS

Biochar is an effective adsorbent with a wide range of applications in terms of its physicochemical characteristics. The activation of biochar affects the morphological structure of the particles and leads to a certain change in the physicochemical parameters of the substance with the biochar compound. Furthermore, an opportunity to use biochar in biogas technology in various combinations is considered.

However, combinations of biochar and digestate as an effective soil improver for the remediation of soils contaminated with heavy metals and radionuclides are recommended to be the focus of further research. Biocomposites based on digestate and biochar have the advantage of cleaning and improving soil conditions and plant growth and can be found in different combinations.

Acknowledgement

This research project was carried out as planned research projects of the Department of Ecology and Environmental Protection Technologies of Sumy State University, related to the topics "Assessment of the technogenic load of the region with changes in industrial infrastructure" according to the scientific and technical program of the Ministry of Education and Science of Ukraine (state registration No 0121U114478); Joint Ukrainian–Czech R&D project "Bioenergy innovations in waste recycling and natural resource management", 2021–2022.

We are thankful to the Czech government support provided by the Ministry of Foreign Affairs of the Czech Republic, which allowed this scientific cooperation to start within the project "AgriSciences Platform for Scientific Enhancement of HEIs in Ukraine.

References

[1] Anae, J., Ahmad, N., Kumar, V., Thakur, V. K., Gutierrez, T., Yang, X. J., Cai, C., Yang, Z., & Coulon, F. (2021). Recent advances in biochar engineering for soil contaminated with complex chemical mixtures: Remediation strategies and future perspectives. Science of The Total Environment, 767, 144351
[2] Ayaz, M., Stulpinaite, U., Feiziene, D., Tilvikiene, V., Akthar, K., Baltrėnaitė-Gedienė, E., Striugas, N., Rehmani, U., Alam, S., Iqbal, R., Toleikiene, M., & Doyeni, M. (2022). Pig manure digestate-derived biochar for soil management and crop cultivation in heavy metals contaminated soil. Soil Use and Management, 38(2), 1307–1321
[3] Biochar And The Biomass Recycling Industry | BioCycle. (n.d.). Retrieved July 7, 2022, from https://www.biocycle.net/biochar–and–the–biomass–recycling–industry/

[4] Bisaria, K., Singh, R., Gupta, M., Mathur, A., & Dixit, A. (2022). Novel acoustic–activated alkali–functionalized Trapa bispinosa peel biochar for green immobilization of chlorpyrifos from wastewater: artificial intelligence modelling and experimental validation. Biomass Conversion and Biorefinery
[5] Chen, H., Osman, A. I., Mangwandi, C., & Rooney, D. (2019). Upcycling food waste digestate for energy and heavy metal remediation applications. Resources, Conservation & Recycling: X, 3, 100015
[6] Edinburgh Research Explorer Biochar Quality Mandate (BQM) version 1.0. (n.d.).
[7] Kamarudin, N. S., Dahalan, F. A., Hasan, M., An, O. S., Parmin, N. A., Ibrahim, N., Hamdzah, M., Zain, N. A. M., Muda, K., & Wikurendra, E. A. (2022). Biochar: A review of its history, characteristics, factors that influence its yield, methods of production, application in wastewater treatment and recent development. Biointerface Research in Applied Chemistry, 12(6), 7914–7926
[8] Kizito, S., Jjagwe, J., Mdondo, S. W., Nagawa, C. B., Bah, H., & Tumutegyereize, P. (2022). Synergetic effects of biochar addition on mesophilic and high total solids anaerobic digestion of chicken manure. Journal of Environmental Management, 315
[9] Kobayashi, T., & Kuramochi, H. (2022). Optimized production conditions and activation of biochar for effective promotion of long–chain fatty acid degradation in anaerobic digestion. Bioresource Technology, 358
[10] Liu, Y., Jiang, Z., Fu, J., Ao, W., Ali Siyal, A., Zhou, C., Liu, C., Dai, J., Yu, M., Zhang, Y., Jin, Y., Yuan, Y., & Zhang, C. (2022). Iron–biochar production from oily sludge pyrolysis and its application for organic dyes removal. Chemosphere, 301
[11] Patwardhan, S. B., Pandit, S., Kumar Gupta, P., Kumar Jha, N., Rawat, J., Joshi, H. C., Priya, K., Gupta, M., Lahiri, D., Nag, M., Kumar Thakur, V., & Kumar Kesari, K. (2022). Recent advances in the application of biochar in microbial electrochemical cells. Fuel, 311
[12] Peter, A., Chabot, B., & Loranger, E. (2019). Enhancing Surface Properties of Softwood Biochar by Ultrasound Assisted Slow Pyrolysis. IEEE International Ultrasonics Symposium, IUS, 2019–October, 2477–2480
[13] Peter, A., Chabot, B., & Loranger, E. (2020). The influence of ultrasonic pre–treatments on metal adsorption properties of softwood–derived biochar. Bioresource Technology Reports, 11
[14] Šimanský, V., Jonczak, J., Chlpík, J., & Polláková, N. (2022). The status of heavy metals in arable soils of contrasting texture treated by biochar – an experiment from Slovakia. Journal of Environmental Science and Health, Part A, 57(1), 1–17
[15] van Poucke, R., Egene, C. E., Allaert, S., Lebrun, M., Bourgerie, S., Morabito, D., Ok, Y. S., Ronsse, F., Meers, E., & Tack, F. M. G. (2020). Application of biochars and solid fraction of digestate to decrease soil solution Cd, Pb and Zn concentrations in contaminated sandy soils. Environmental Geochemistry and Health, 42(6), 1589–1600
[16] Wambugu, C. W., Rene, E. R., van de Vossenberg, J., Dupont, C., & van Hullebusch, E. D. (2019). Role of Biochar in Anaerobic Digestion Based Biorefinery for Food Waste. Frontiers in Energy Research, 7
[17] Wang, J., Hao, X., Liu, Z., Guo, Z., Zhu, L., Xiong, B., Jiang, D., Shen, L., Li, M., Kang, B., Tang, G., & Bai, L. (2021). Biochar improves heavy metal passivation during wet anaerobic digestion of pig manure. Environmental Science and Pollution Research, 28(1), 635–644
[18] Wang, N., Chen, Q., Zhang, C., Dong, Z., & Xu, Q. (2022). Improvement in the physicochemical characteristics of biochar derived from solid digestate of food waste with different moisture contents. Science of The Total Environment, 819, 153100
[19] Wu, L., Zhao, X., & Bi, E. (2022). Predicting the effect of dissolved humic acid on sorption of benzotriazole to biochar. Biochar, 4(1)
[20] Wu, Y., Zhang, P., Zhang, H., Zeng, G., Liu, J., Ye, J., Fang, W., & Gou, X. (2016). Possibility of sludge conditioning and dewatering with rice husk biochar modified by ferric chloride. Bioresource Technology, 205, 258–263
[21] Xue, S., Chen, F., Wang, Y., Shao, Z., Zhang, C., Qiu, L., Ran, Y., & He, L. (2021). Effects of Co–Applications of Biochar and Solid Digestate on Enzyme Activities and Heavy Metals Bioavailability in Cd–Polluted Greenhouse Soil. Water, Air, & Soil Pollution, 232(4), 140
[22] Zhang, Y., Jeyakumar, P., Xia, C., Lam, S. S., Jiang, J., Sun, H., & Shi, W. (2022). Being applied at rice or wheat season impacts biochar's effect on gaseous nitrogen pollutants from the wheat growth cycle. Environmental Pollution, 306
[23] Zhao, X., Xu, K., Wang, J., Wang, Z., Pan, R., Wang, Q., Li, S., Kumar, S., Zhang, Z., & Li, R. (2022). Potential of biochar integrated manganese sulfate for promoting pig manure compost humification and its biological mechanism. Bioresource Technology, 357
[24] Zhou, H., Brown, R. C., & Wen, Z. (2020). Biochar as an Additive in Anaerobic Digestion of Municipal Sludge: Biochar Properties and Their Effects on the Digestion Performance. ACS Sustainable Chemistry & Engineering, 8(16), 6391–6401
[25] Zuo, L., Lin, R., Shi, Q., & Xu, S. (2020). Evaluation of the Bioavailability of Heavy Metals and Phosphorus in Biochar Derived from Manure and Manure Digestate. Water, Air, & Soil Pollution, 231(11), 553
[26] Belyaev Ye. Yu. (2000). Production and application of activated charcoal for environmental purposes. Chemistry of Plant Raw Materials, 2, 5–15.
[27] Biochar, the benefits of using natural soil fertilisers – Proposition. Retrieved July 7, 2022, from https://propozitsiya.com/ru/gidrotermalnaya–karbonizaciya–biomassy–put–k–resheniyu–ekologicheskih–problem
[28] Moskalenko T.V. & Danilov O.S. (2009). Influence of ultrasound on the degree of extraction of humic acids from the Kangalassky lignite deposit. Science and Education, 1, 43–45. Stavitskaya G.G..(2009). Uniformly Porous Nanosize Carbon Materials of Aerogel Type with Molecular–Sieve Properties. Nanosystems, Nanomaterials, Nanotechnologies, 7(3), 683–699.

Note: This paper was presented at ISB–INMA TEH' 2022 – International Symposium on Technologies and Technical Systems in Agriculture, Food Industry and Environment, organized by University "POLITEHNICA" of Bucuresti, Faculty of Biotechnical Systems Engineering, National Institute for Research–Development of Machines and Installations designed for Agriculture and Food Industry (INMA Bucuresti), National Research & Development Institute for Food Bioresources (IBA Bucuresti), University of Agronomic Sciences and Veterinary Medicine of Bucuresti (UASVMB), Research–Development Institute for Plant Protection – (ICDPP Bucuresti), Research and Development Institute for Processing and Marketing of the Horticultural Products (HORTING), Hydraulics and Pneumatics Research Institute (INOE 2000 IHP) and Romanian Agricultural Mechanical Engineers Society (SIMAR), in Bucuresti, ROMANIA, in 6–7 October, 2022.

ISSN: 2067-3809

ACTA TECHNICA CORVINIENSIS – BULLETIN OF ENGINEERING
TOME XVI [2023] | FASCICULE 2 [APRIL – JUNE]

[1.]Andreea MATACHE, [1.]Mihai MATACHE, [1.]Mariana EPURE, [1.]Nicoleta VANGHELE, [1.]Ancuţa–Alexandra PETRE, [2.]Andreea ENEA

DIGITALIZATION OF THE FOOD SYSTEM AS A MEANS TO PROMOTE FOOD AND NUTRITION SECURITY– A REVIEW

[1]INMA Bucharest, ROMANIA
[2.]Agricultural Research and Development Station Secuieni, Neamt County, ROMANIA

Abstract: Recently, digitization has become a topic of maximum interest in specialized literature. This is due to current trends and attention to socio–economic issues and population development. As a result, in the agri–food industry as well, digitization is expected to significantly contribute to solving various challenges such as the increasing demand for products and the use of resources. Alternatively, supporting food security is already a global requirement. The food industry is complex and involves various industrial activities such as production, processing, preparation, preservation, packaging and distribution. To maintain food security and ensure products for the ever–growing population, the solution would be the sustainability of agriculture and the food industry. Artificial intelligence–based systems are applicable in almost all stages of automation technology in the agri–food industry, thus ensuring high–quality products. In this paper, we will present digitization solutions in preservation, packaging and distribution processes/technologies in the food industry with the help of artificial intelligence (AI).
Keywords: food safety, internet of things (IoT), digitization in agriculture, artificial intelligence (AI)

INTRODUCTION

Recently, the food industry has faced various challenges related to the ever–changing demands of both customers and suppliers. As a result, new technological methods were implemented in the production systems. These solutions aim to exploit the high economic and innovative potential resulting from the continuous impact of the rapidly advancing information and communication technology (ICT). (*Xi X et al., 2021*). Artificial intelligence (AI), such as methods in machine learning, is increasingly being used in health and healthcare to provide accurate and productive information (*Kamel M.N. et al., 2019*). As food safety increasingly uses digital tools, it is becoming increasingly clear that access to the real–world data that is needed for model development and parameter estimation is a major challenge. Extensive testing of raw materials, processing plants, and finished products for various pathogens and/or indicator organisms may represent an additional cost. The application of the obtained data can be enhanced with digital tools such as agent–based models (ABM) and machine learning (ML) algorithms, which are designed to improve food safety in an establishment (*Marvin H. J. P. et al., 2017*).

The production process in the agri–food industry contains multiple stages, such as harvesting, processing, distribution and storage. These processes have witnessed remarkable changes with the application of science and technology. The first industrial revolution in the early 19th century had a remarkable impact on agriculture and food processing. Demand for labor was increasing, and companies made profits by adding value to local foods, which were often packed, stored and distributed over long distances. Applying the relationship between digital technology and the effectiveness of food safety oversight contributes to a better understanding of the role of digital technology in food safety oversight and how to maximize its influence. In this process, the higher the knowledge level of consumers, the greater the positive promotion effect of digital technology (*Xi et al., 2021*). According to the World Health Organization, approximately 600 million people are affected by foodborne illness each year, of which 420,000 die, resulting in the loss of 33 million years of healthy life (*Scharff et al., 2015*). An appropriate compliance mechanism must be established so that local governments, manufacturers and regulatory bodies understand the importance of their collaboration in achieving high quality and safe products. By applying digital technology, monitoring food safety is made much easier (*Xi et al., 2021*).The development of cross–border infrastructures for digitization supports the global food system by helping find innovative and safe food products. Food manufacturers and processors must adapt to customer demands while maintaining food safety (*Raheem et al., 2019*).

MATERIALS AND METHODS

The continuous development of digital technology is forcing companies in the food industry to restructure their business models. Artificial intelligence is being applied to more and more of the production stages and especially in food safety risk assessment and management. With the adoption of new digital technologies, questions arise regarding the ownership, use, privacy and transparency of the data obtained.

Systems used in modern factories, such as supervisory control and data acquisition (SCADA), manufacturing execution systems (MES), and enterprise resource planning (ERP) create digital models of manufacturing operations. In addition to making the entire production chain more efficient, the data obtained can be applied to improve food safety (*World Food System Centre, 2018*). The industrial revolution in the Internet of Things (IoT) will exploit data collection from precision agriculture, connected factories/logistics and precision food safety to improve microbial risk management. Alternatively, the interaction of public health databases, e–commerce tools, social networks and technologies such as blockchain will improve traceability for food case management (*Donaghy J.A. et al., 2021*). Current global trends will have particular challenges for future global food safety, food security and nutrition. Change will occur from innovation in food production and productivity, the structural and socio–economic impacts on food supply chains to the adaptation of quality and food safety management systems (*King T. Et al., 2017*).

The application of smart agriculture tools and data analysis platforms can significantly increase food security with a low environmental impact (*Garnett T.et al., 2013*). Digitizing the food systems applies innovative technology to optimize harvesting, processing, distribution and storage operations along the agri–food value chain. Mechanization at the beginning of the 19th century, automation in the 1970s and the development of the Internet in recent decades have had a significant impact on our activities and implicitly on the agri–food chain. The World Food System Center anticipated that "the dynamics of the entire food value chain are changing, and unintended consequences are entering the economic landscape through digitization¨ (*World Food System Centre, 2018*).

In the food industry, product quality is essential because defects and contamination can be harmful to human health. Digitization with accurate input and output data of the entire process will help guarantee safety and traceability. In a foretold scenario, technological advances emerging from the fourth industrial revolution (Industry 4.0) will benefit the current food system by becoming greener and more sustainable (*Struebi P., 2016*). The application of digital technologies such as artificial intelligence (AI), machine learning, Internet of Things (IoT) and blockchain in supply chain management a phenomenon that has led innovators and practitioners to analyze and make decisions corresponding to customer requirements and organizations in the system. Agri–food supply chains (AFSC) link the point of production and the point of consumption of food products and supply chain management refers to "managing the relationship between the supply of raw materials for agriculture, production, processing and logistics and distribution of products (*Amentae T.K. et al., 2021*).

RESULTS

With increasing customer demands, global health and the environmental crisis, there has been an accelerated need to develop technologies that are as sustainable as possible. All these aspects have led to obtaining new advanced techniques, such as those with stem cells, 3D printing. The agri–food industry is in continuous evolution and the best results are expected (*Ojo O.O. et al.,2018; Jambrak A.R. et al., 2021*). Digitization is expanding in all areas of industry, and the food industry is no exception. The new industrial revolution is often titled with phrases like Industry 4.0 (I4.0), Cyber–Physical Systems (CPS), Internet of Things (IoT), Cloud Computing and so on (*Zimmer M. et al., 2019; Baurina S.B. et al., 2022*). The digitized food industry involves the use of new technologies in all stages of agro–industrial production, from production to processing, marketing and storage of products. Their implementation depends not only on the degree of computerization, but also on the level of use of systems, devices and mechanisms that allow the possibility of autonomy, use (without human intervention) (*Baurina S.B. et al., 2022; Prause L. et al., 2021*). With the help of artificial intelligence, maintaining quality at the same cost has become much easier (*Sharma S. et al., 2021*).

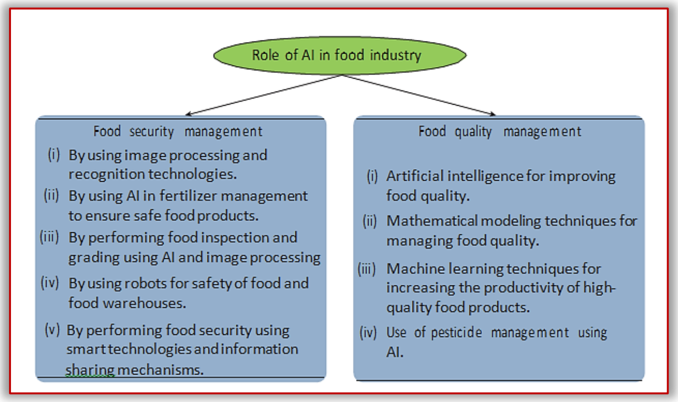

Figure 1 – Role of AI in the food industry (Kumar I. et al., 2021).

Artificial intelligence–based or autonomous systems are applied in almost all stages of technology. They enable the world to efficiently optimize problems, computerize the food industry and transform food products (*Soltani–Fesaghandis G. et al., 2018*). But the use of AI is not only limited to these things, it can be useful in food processing, storage and delivery of food products. Smart gadgets like robotics and smart drones can also play an essential and significant role in reducing packaging costs. It will help deliver food products, performing the task in hazardous environments and providing excellent quality products (*Bera S., 2021*).

— Digitization solutions in preservation processes/technologies

Companies are employing digital technology to collect more data about their workflow operations and to assure safety and quality in food processing, packaging, and distribution (*Cardei P. et al., 2021; Mircea F., et al., 2022*). Food preservation must be carried out in line with international food safety standards. Pasteurization is an essential step in the food industry because it prevents the product from spoiling, keeping its quality at the highest possible level (*Panchal H. et al., 2018*). To adapt digitization technologies to the pasteurization process, it is necessary to investigate consumer products with appropriate sensors and data analysis. Several European projects in the field of food safety have emphasized the need for stronger and more in–depth education and collaboration as solutions to the field concerns, which include funding problems, professional education and technical competitiveness (*Nenciu F., et al., 2020*). Near–infrared diffuse reflectance (NIR) spectroscopy along with multivariate data analysis (MVDA) was applied to discriminate different fruit and vegetable products. Foods were preserved in glass containers, which are commonly used for pasteurizing fruit and vegetable products. The samples were placed on top of a specially designed and 3D printed sample holder, improving the reproducibility of the measurements (*Zimmer M. et al., 2019*).

The results of the investigation represent progress toward a fully automated and autonomous pasteurization process using NIR and MVDA as the main data recording and processing unit (*Zimmer M. et al., 2019*). Chilling and freezing are methods used to preserve food. Conventional cooling and freezing techniques are ineffective in predisposing food to spoilage. To increase the effectiveness of traditional preservation methods, efforts have been made to discover new solutions to ensure high–quality food. Particular interest has been given to pressure–related techniques such as vacuum cooling (VC), vacuum film cooling (VFC), vacuum spray cooling (VSC), isochoric freezing (ICF) and pressure swing freezing (PSF). Research results show that pressure–related cooling and freezing techniques are effective in improving product quality and have real potential in the food industry, as shown in figure 2 (*Zhiwei Z. et al., 2020*).

ICF is a technique that maintains product integrity without causing structural damage to the protein content. Its operation took a different approach by integrating the locality–sensitive hashing (LSH) technique, to achieve a secure and reliable data publication. Experimental results using the real–world QoS dataset, i.e., WS–DREAM, show the competitiveness of the ICFLSH approach in terms of time cost and accuracy (*Chao Y. et al., 2018; Năstase G. et al., 2017*). Drying is the most common method of preserving agricultural crops. This preservation method is simple and affordable, but time–consuming and affects the quality of the final product.

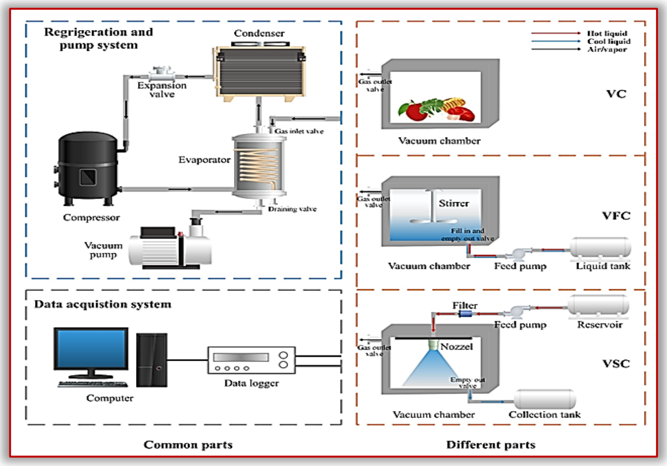

Figure 2 – Schematic of the experimental setup for pressure–related cooling techniques. The red and blue arrows indicate the liquid before and after cooling, and the black arrow indicates air or vapor from the vacuum chamber. VC: vacuum cooling; VFC: vacuum film cooling; VSC: vacuum spray cooling *(Zhiwei Z. et al., 2020)*.

The potential of using a CV imaging system along with a laser diode in monitoring and predicting the quality properties of sweet potato during drying was investigated. Overall, this innovative quality inspection method could provide a solid basis for current trends in non–destructive monitoring of the drying process of agricultural crops. The results obtained for sweet potato can also serve as a basis for other tropical tuber crops, as well as in other post–harvest processing and plant disease detection. The digital imaging system is shown in figure 3 (*Onwudea D.et al., 2018*).

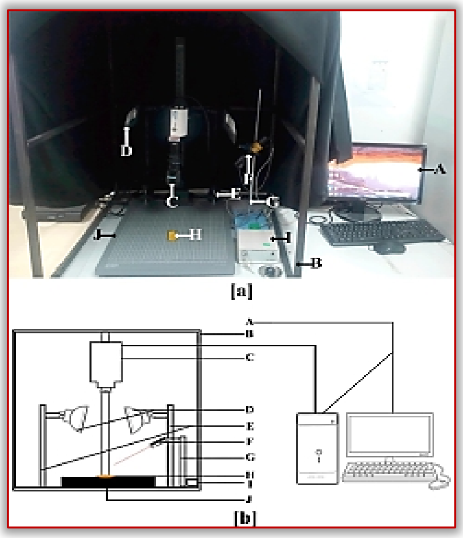

Figure 3 – [a] RGB digital and backscattering imaging system; [b] Schematics of combined RGB digital and backscattering imaging system (A = computer system; B = supporting frame; C = CCD camera; D = halogen lamps; E = Lamp holders; F = laser light emitter; G = laser light emitter's holder; H = sweet potato sample; I = laser diode control box; J = sample capturing platform (*Onwudea D.et al., 2018*).

— Digitization solutions in food packaging

Food packaging is a stage in the food industry that is increasingly facing the demand from consumers and government organizations. This stage must solve the problems related to theft and counterfeiting, food quality and safety, but also the reuse and recycling of packages (*Vanderroost M. et al., 2017*). The global smart packaging market is in continuous development. Growth in 2017/2018 was estimated at USD 44.3 billion and is expected to reach USD 26.7 billion by 2024. Figure 6 shows the estimated growth rate of the global market by 2026 (*Schaefera D. et al., 2018*).

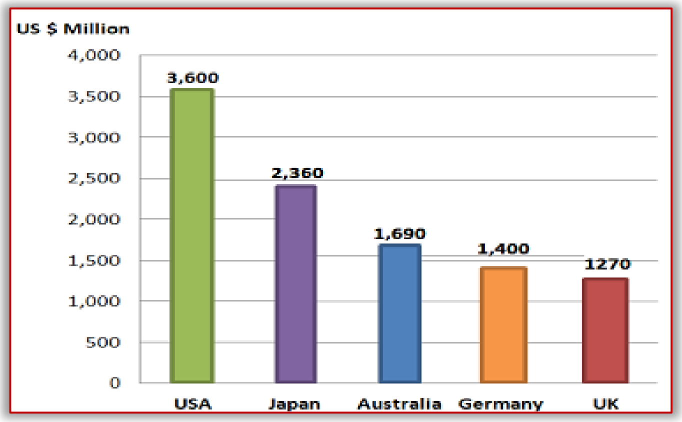

Figure 4 – Predicted global market growth rate *(Schaefera D. et al., 2018).*

The potential of digitizing the life cycle of a food package was studied, and can be used as a model for future research. The creation of new, innovative and quality food packages is inherently linked to uncertainty and risk. Packaging functions and their interrelationships realized with the help of various computer systems are presented schematically in figure 5 (*Vanderroost M. et al., 2017*).

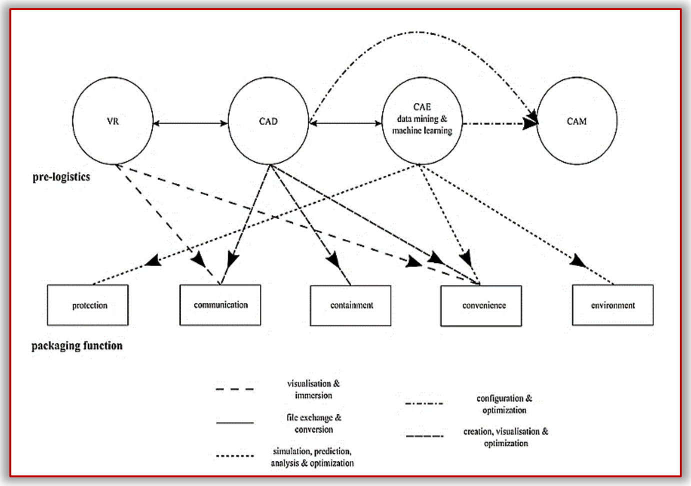

Figure 5 – The scheme of the different computer systems applied in the research, design and production stage, their role in the realization of the different packaging functions and their interrelationships *(Vanderroost M. et al., 2017).*

In the specialized literature, the existing challenges in research and the technical problems that reduce the efficiency of logistics operations regarding food packaging and their interaction with consumers, the reuse or recycling of food packages are exposed. Connecting smart food packaging to the IoE, of course, requires the development of new–cyber–physical systems (CPS) that automate, control and optimize operations related to logistics and the sale and consumption stage of the life cycle of a food package (*Vanderroost M. et al., 2017*). Due to its versatile applications, the Internet of Things (IoT) and blockchain are also gaining attention in the food industry and can help automate tasks and save time (*Waqas Khan P. et al., 2020; Zhang J. et al., 2020*). FoodSQRBlock, a blockchain–based framework that digitizes food production information and makes it more accessible, traceable and verifiable by consumers and producers by using QR codes to embed the information, was studied. Integrated FoodSQRBlock into Google Cloud Platform to replicate a real food production scenario using pumpkins and milk as examples of products from real UK farms. Experimental analysis demonstrates the feasibility and scalability of deploying the FoodSQRBlock in the cloud. To design the BT framework, a three–layer and multi–level system is presented, the architecture of which is represented in Figure 6 (*Dey S. et al., 2021*).

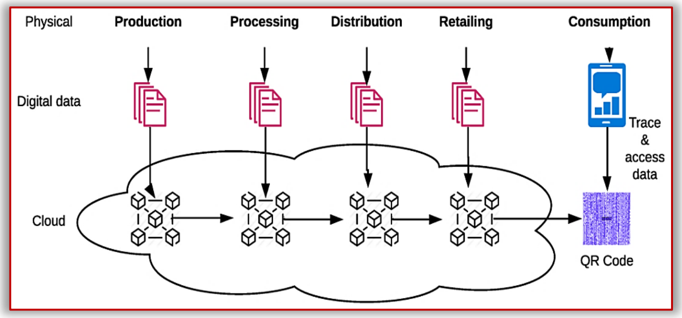

Figure 6 – Overview of the system architecture of the Food Safety Quick Response Block (FoodSQRBlock) based on the farm–to–fork supply chain

The conceptual design procedure of packaging with customized and adapted geometries based on the digitization of fresh food, in this case, apples, was analyzed. Through 3D scanning techniques, reliable digital elements were obtained that could be used in advanced technologies. In this sense, it was possible to define a procedure for reverse engineering different types of food, detailing the specific parameters according to size and finish. After analyzing the results, it can be said that the final solution obtained is positive. The parameterized design was made possible by the virtual evaluation of the digitized fruits, as exhibited in figure 7 (Rodríguez–Parada L. et al., 2019).

The production of high–quality packaging in accordance with today's requirements is necessary. Digital packaging is characterized by the advantages of digital printing in packaging (*Velichka M., 2021*). An example of food machines in Industry 4.0 is vacuum processing machines (figure 8) that produce food products. The vacuum processing system combines homogenization technology, the highest reproducibility, short batch times and high profitability with ease of use (*Afam I.O. Jideani et al., 2020*).

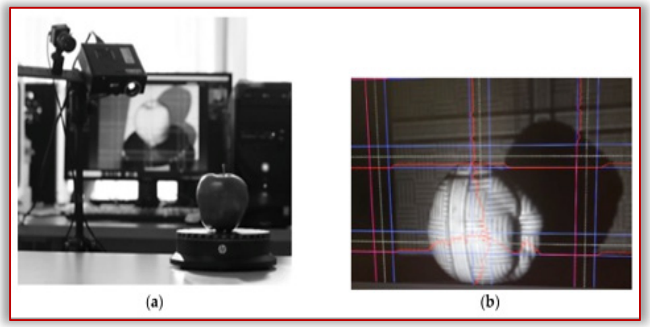

Figure 7 – (a) Scanning procedure using the SLS–1 David® V5 scanner, (b) Visualization of the apple through the software (HP 3D Scan David®, version Pro V5, HP inc., Palo Alto, CA, US)

Figure 8 – A Maxx vacuum processing machine

Unlike the human factor, robotic software can run rule–based steps in a fraction of the time it takes a human to do so. RPA software can record multiple steps between multiple systems. SMI is a software application that was developed according to the principles of Industry 4.0 and IoT. The SWM supervisor is based on a modular web portal that can be customized for any application domain. Thanks to this innovative SMI system, the main causes of bottling or packaging line downtime are easily identified order to improve the entire line. Implementing RPA in the industrial brewing process has resulted in significant cost savings (*Hradecká M., 2019*).

— Digitization during storage

AI in the food industry enables analysis of needs and requirements and focuses on creating high–quality packaging with better shelf life (*Raghavendra G.S. et al., 2022*). During storage, heating and cooling processes make food more prone to microbial spoilage by bacteria or fungi, thus affecting microbial stability (*Tomašević I. et al., 2021*). To maintain as much as possible the quality of food products, it is essential to implement a storage environment monitoring system. In this sense, the use of different sensors with the help of IoT is presented as a viable solution for reducing product losses and increasing food safety (*Si–Wen G. et al., 2021*). The use of the IBM SPSS software platform was analyzed, which provides an easy–to–use interface and a robust set of functions that allows the rapid extraction of useful information (*Raghavendra G.S. et. al., 2022*). The IBM SPSS platform was applied to assess the quality during storage of Nile tilapia filets after ozonated water treatment. The obtained results showed that pretreatment of ozonated water partially improves the quality and extends the shelf life of tilapia filets (*Yongqiang Z. et al., 2015*).

In the literature, the analysis of data obtained using IBM SPSS indicates that the influence of workaholism on food waste (eg food reuse, food storage, etc.) by consumers has a positive influence. The conceptual framework used is presented in figure 9 (*Cantaragiu, R.E. et al., 2020*).

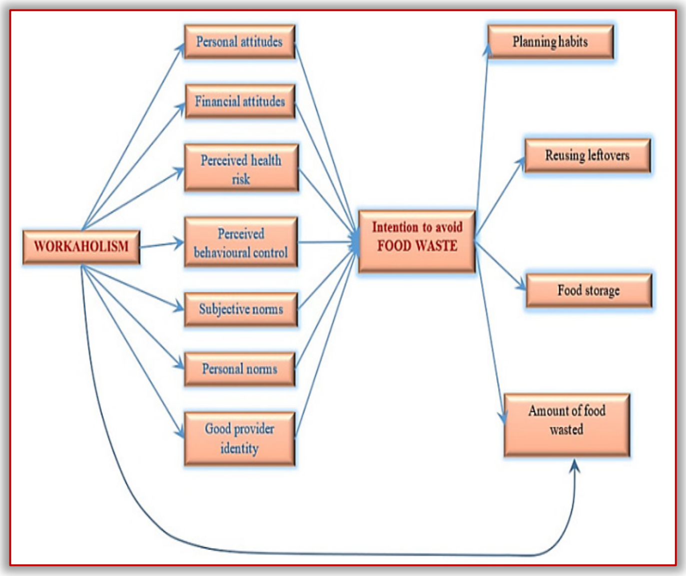

Figure 9 – The conceptual framework *(Cantaragiu, R.E. et al., 2020)*.

IBM SPSS software was also used to identify hygienic practices for the storage of cooked food among school food vendors in Nigeria. Hypothesis testing established that the health education intervention had a positive influence on hygiene practices ($p<0.05$) (*Odikpo L. et al., 2020*).

— Palletizing digitization solutions

In today's society, one cannot understand the mass production of a product without the use of artificial intelligence, as is the case with palletizing. Robots are used in various fields of activity (agriculture, transport, food production, packaging and delivery) (*Hamann E., 2020*). Automated systems can be controlled and monitored remotely, which benefits food packaging and palletizing processes where speed and consistency are needed. Even more so, in the context of food safety, where human interaction with food is desirable. Examples of robots used in palletizing are shown in figures 10 and 11.

Figure 10 – A robot palletizing eggs (Walker J., 2019)

Figure11 – Robots performing the process of palletizing (Shriya S. et al., 2021)

— Key Technologies– Beverage Distribution Software

Like the other steps in the food industry, distribution knows a continuous development and must be adapted to the current requirements related to volume, speed and handling in food safe conditions. Technologies offered by Bastian Solution help increase system capacity, efficiency and order flow. Gain better visibility of orders and inventory and increase storage capacity and eliminate the use of offsite warehouses.

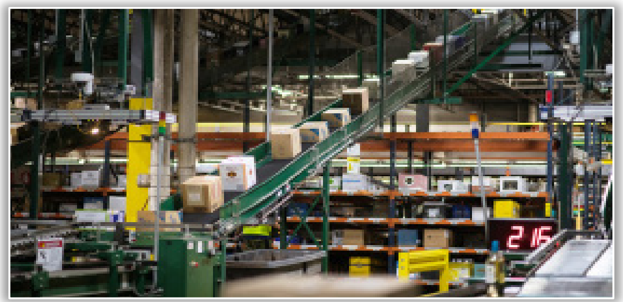

Figure12 – Wine and Spirits Distribution Center Southern Glazer's Wine and Spirits of America

Figure13 – Exacta software provides complete, real–time visibility of orders throughout the system

ExactaBev beverage distribution software features 4–part ordering and automatic order routing. Exacta software provides complete, real–time visibility of orders throughout the system. This technology is used by the world's largest wine and spirits distribution center Southern Glazer's Wine and Spirits of America which has operations in 44 states (figures 12 and 13).

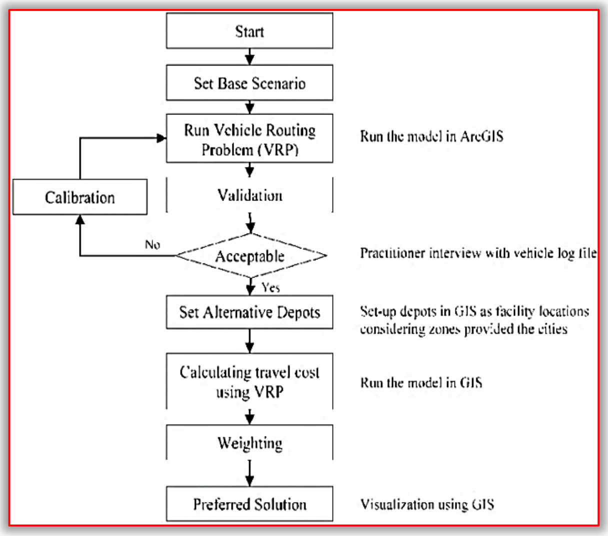

Figure 14 – The research framework of the study (EunSu L. Et al., 2015).

Another method that can be easily applied to distribution companies for long–term and medium–term strategic planning is described in figure 14 (*EunSu L. Et al., 2015*).

CONCLUSIONS

There is an urgent need to have a change in our food system that encourages food security and sovereignty. The technology foundation behind digitization, as described in this paper, when clearly aligned to the food industry, can revolutionize the industry. Digitization in the food system will positively affect food safety and security, thereby ensuring human security. Cross–border collaboration at the regional level that encourages sustainability, transparency and efficient resource management will improve with digitization.

In the current scenario, the food industry is using the basic level of artificial intelligence. Every day, the role of AI becomes vital due to its ability to escalate hygiene, food protection and waste management systems. In the future, AI will transform the food processing industry because it has so much potential to drive reasonable and healthier productivity for customers and employees.

Acknowledgements

This work was supported by a grant offered by the Romanian Minister of Research as Intermediate Body for the Competitiveness Operational Program 2014–2020, called POC/78/1/2/, project number SMIS2014 + 136213, acronym METROFOOD–RO;

This work was supported by Ministry of Research, Innovation and Digitalization through Program 1–Development of the national research–development system, Subprogram 1.2 – Institutional performance – Projects for financing excellence in RDI, Contract no. 1PFE/30.12.2021.

References

[1] Amentae T.K., Gebresenbet G. (2021), Digitalization, and Future Agro–Food Supply Chain Management: Literature–Based Implications. Sustainability 2021, 13, 12181;
[2] Baurina S.B., Khudyakov S.V., Uchirova M.Y. (2022), Digital Mainstream in the Promotion of Food Industry Products, IOP Conf. Series: Earth and Environmental Science, 988, 052041;
[3] Bera S. (2021), "An application of operational analytics: for predicting sales revenue of restaurant," in Machine Learning Algorithms for Industrial Applications, pp. 209–235;
[4] Cantaragiu R.E. and Ghinea V.M. (2020), The Impact of Workaholism on Consumer Food Waste. Amfiteatru Economic, 22(Special Issue No. 14), pp. 1140–1158;
[5] Cardei, P., Nenciu, F., Ungureanu, N., Pruteanu, M.A., Vlăduţ, V., Cujbescu, D., Găgeanu, I., Cristea, O.D. (2021), Using Statistical Modeling for Assessing Lettuce Crops Contaminated with Zn, Correlating Plants Growth Characteristics with the Soil Contamination Levels. Appl. Sci. 11, 8261;
[6] Dey S., Saha S., Kumar Singh A. and McDonald–Maier K. (2021), FoodSQRBlock: Digitizing Food Production and the Supply Chain with Blockchain and QR Code in the Cloud, Sustainability, 13(6), 3486;
[7] Donaghy J.A., Danyluk M.D., Ross T., Krishna B., Farber J. (2021), Big Data Impacting Dynamic Food Safety Risk Management in the Food Chain. Front Microbiol.,12:668196;
[8] EunSu Lee, Alan D. Dybing and Sumadhur Shakya (2015), Facility Location Problem of Beverage Distribution Considering Time Window and Land Use Plan Using GIS, Beverages,1(2), pp.55–69;
[9] Evert O., Odikpo L.C, Ehiemere I. et al. (2019), Effect of health education on food hygiene practices and personal hygiene practices of food vendors in public secondary schools at Oshimili south local government area, Intern. Journ. of Med. Res. & Health Scie., Vol.8;
[10] Garnett T., Appleby M. C., Balmford A., Bateman I. J., Benton T. G., Bloomer P., et al. (2013), Sustainable intensification in agriculture: premises and policies, Science, 341, 33–34;
[11] Guo S.–W., Mohammad Asif Ikabl (2021), Smart Agriculture, and Food Storage System for Asia Continent: A Step Towards Food Security, International Journal of Agricultural and Environmental Information Systems, Vol.12, Issue 1;
[12] Hamann E. (2020), Amid rising costs and limited availability, farmers struggle to find enough workers, Sacramento Business Journal, p. Food and Lifestyle;
[13] Hradecká M., (2019), Robotic Internal Audit – Control Methods in the Selected Company, Agris on–line Papers in Economics and Informatics, Vol. XI, Nr. 2;
[14] Jambrak A.R., Nutrizio M., Djekić I., Pleslić, S., Chemat F. (2021), The Internet of Nonthermal Food Processing Technologies (Iontp): Food Industry 4.0 and Sustainability, Aplic. Sci., 11, 686;
[15] Jideani A., Mutshinyani A.,.Maluleke N. et al. (2020), Impact of Industrial Revolutions on Food Machinery – An Overview, Journal of Food Research; Vol. 9, No. 5;
[16] Jingyu Zhang, Siqi Zhong, Tian Wang, Han–Chieh Chao, Jin Wang (2020), Blockchain–based Systems and Applications: A Survey, Journal of Internet Technology Vol. 21, No.1;
[17] Kamel Boulos, M.N., Peng, G. & VoPham, T. (2019), An overview of GeoAI applications in health and healthcare. Int J Health Geogr 18, 7;
[18] King T., Cole M., Farber J. M., Eisenbrand G., Zabaras D., Fox E. M., et al. (2017), Food safety for food security: relationship between global megatrends and developments in food safety, Trends Food Sci. Technol., 68, 160–175;
[19] Kumar I., Rawat J., Mohd N., and Husain S. (2021), Opportunities of Artificial Intelligence and Machine Learning in the Food Industry, Hindawi Journal of Food Quality, Vol. 2021, 4535567;
[20] Marvin H. J. P., Janssen E. M., Bouzembrak Y., Hendriksen P. J. M., Staats M. (2017), Big data in food safety: an overview, Crit. Rev. Food Sci. Nutr. 57, 2286–2295;
[21] Mircea, C., Nenciu, F., Vlăduţ, V., Voicu, G., Cujbescu, D., Gageanu, I., Voicea, I. (2020), Increasing the performance of cylindrical separators for cereal cleaning, by using an inner helical coil. INMATEH Agric. Eng. 62, 249–258;
[22] Năstase G., Lyu C., Ukpai G., Serban A., Rubinsky B. (2017), Isochoric, and isobaric freezing of fish muscle, Biochem. Biophys. Res. Commun., 485, 279–283;
[23] Nenciu F., Oprescu M.R., Biris S.–S. (2022), Improve the Constructive Design of a Furrow Diking Rotor Aimed at Increasing Water Consumption Efficiency in Sunflower Farming Systems. Agriculture 12, 846
[24] Ojo O.O., Shah S., Coutroubis A., Jimenez M.T., Ocana Y.M. (2018), The potential impact of industry 4.0 in the sustainable environment of the food supply chain, Proceedings of IEEE 2018 IEEE International Conference on Technology Management, Operations and Decisions (ICTMOD), 172–177;
[25] Onwudea D., Hashim N., Abdan K. et al. (2018), Combination of computer vision and backscattering imaging for predicting the moisture content and colour changes of sweet potato (Ipomoea batatas L.) during drying, Computers and Electronics in Agriculture, Vol. 150, pp. 178–187;
[26] Panchal H., Patel R., Chaudhary S., Patel D.K., Sathyamurthy R. & Arunkumar T. (2018), Solar energy usage for milk pasteurization:A comprehens.review, Renew.and Sustain. Energy Reviews, 92,1–8;
[27] Prause L., Hackfort S., Lindgren M. (2021), Digitalization, and the third food regime, Agriculture and Human Values, 38:641–655;
[28] Privacy–Aware Data Publishing and Integration for Collaborative Service Recommendation, Chao Y., Xinchun C. Lianyong Q., Xiaolong X. and Xuyun Z. (2018), Special Section on Security and Trusted Computing for Industrial Internet of Things, vol. 6;
[29] Raghavendra G.S., Shyni Carmel Mary, Purnendu Bikash Acharjee et al. (2022), An Empirical Investigation in Analysing the Critical Factors of Artificial Intelligence in Influencing the Food Processing Industry: A Multivariate Analysis of Variance (MANOVA) Approach, Artificial Intelligence in Food Quality Improvement, Article ID 2197717;
[30] Raheem D., Shishaev, M., Dikovitsky V. (2019), Food System Digitalization as a Means to Promote Food and Nutrition Security in the Barents Region, Agriculture 2019, 9,168;
[31] Rodríguez–Parada L., Mayuet P. and Gáme A. (2019), Custom Design of Packaging through Advanced Technologies: A Case Study Applied to Apples, Materials, 12(3), 467;
[32] Schaefera D. and Cheung W. (2018), Smart Packaging: Opportunities and Challenges, Procedia CIRP 72, pp.1022–1027;
[33] Scharff R.L.S. (2015), State estimates for the annual cost of food borne illness. J Food Protect. 78:1064;
[34] Sharma S., Bisoyee P., Jathar J. (2021), Food Quality Assurance using Artificial Intelligence: A Review Paper, International Research Journal of Engineering and Technology (IRJET), 8, pp.1841–1847;
[35] Shriya S., Pallavee B., Jayant J. (2021), I Food Quality Assurance using Artificial Intelligence: A Review Paper, international Research Journal of Engineering and Technology (IRJET), 8, pp.1841–1847;
[36] Soltani–Fesaghandis G. and Pooya, A. (2018), "Design of an artificial intelligence system for predicting success of new product development and selecting proper market–product strategy in the food industry," International Food and Agribusiness Management Review, vol. 21, no. 7, pp. 847–864;

[37] Struebi P. (2016), How the Fourth Industrial Revolution can radically Improve Our Food Supply Chain. Huffington Post. New York, NY, USA;
[38] Tomašević I., Putnik P., Valjak F., Pavlić B., Šojić B., Bebek Markovinović A., & Bursać Kovačević D. (2021), 3D printing as novel tool for fruit–based functional food production, Current Opinion in Food Science, 41, 138–145;
[39] Vanderroost M., Ragaert P., Verwaeren J. et al. (2017), The digitization of a food package's life cycle: Existing and emerging computer systems in the pre–logistics phase, Computers in Industry, Vol. 87, pp.1–14;
[40] Vanderroost M., Ragaerta P., Verwaeren J.et al. (2017), The digitization of a food package's life cycle: Existing and emerging computer systems in the logistics and post–logistics phase, Computers in Industry 87, pp.15–30;
[41] Velichka Marinova (2021), Trends in Packaging Sector Chief., Economic Sciences Series, vol.10, Nr.1;Walker J., 2019, Fast Food Robots, Kiosks, and AI Use Cases from 6 Restaurant Chain Giants. Emerc., 22, p. Unknown;
[42] Waqas Khan P., Byun Y. and Park N. (2020), IoT–Blockchain Enabled Optimized Provenance System for Food Industry 4.0 Using Advanced Deep Learning, Sensors, 20;
[43] World Food System Centre (2018);
[44] Xi X., Wei, S., Lin, K.L., Zhou H., Wang K., Zhou H., Li Z., Nan N., Qiu L., Hu F., Tsai F.S., Chen D. (2021), Digital Technology, Knowledge Level, and Food Safety Governance: Implications for National Healthcare System. Front Public Health, 25;9:753950;
[45] Yongqiang Zhao, Xianqing Yang, Laihao LI, et al. (2015), Different Chemical, Microbiological, Color and Textural Changes in Nile Tilapia (Oreochromis Niloticus) Fillets Sterilized by Ozonated Water Pretreatment During Frozen Storage, Journal of Food Processing and Preservation;
[46] Zhiwei Zhu, Tian Li & Da–Wen Sun (2020), Pressure–related cooling and freezing techniques for the food industry: fundamentals and applications, Critical Reviews in Food Science and Nutrition;
[47] Zimmer M, Schneider J. (2019), Near–infrared diffuse reflectance spectroscopy for discriminating fruit and vegetable products preserved in glass containers, Croat. J. Food Sci. Technol., 11 (1), 104–112;
[48] https://www.mdpi.com/sustainability/sustainability–1303486/article_deploy/html/images/sustainability–13–03486–g003.png;
[49] https://www.mdpi.com/materials/materials1200467/article_deploy/html/images/materials–12–00467–g001.png;
[50] https://pfrymakoruma.com/ww–en/machinedetails/;
[51] https://www.ibm.com/products/spss–statistics;
[52] https://www.bastiansolutions.com/assets/1/6/;

Note: This paper was presented at ISB–INMA TEH' 2022 – International Symposium on Technologies and Technical Systems in Agriculture, Food Industry and Environment, organized by University "POLITEHNICA" of Bucuresti, Faculty of Biotechnical Systems Engineering, National Institute for Research–Development of Machines and Installations designed for Agriculture and Food Industry (INMA Bucuresti), National Research & Development Institute for Food Bioresources (IBA Bucuresti), University of Agronomic Sciences and Veterinary Medicine of Bucuresti (UASVMB), Research–Development Institute for Plant Protection – (ICDPP Bucuresti), Research and Development Institute for Processing and Marketing of the Horticultural Products (HORTING), Hydraulics and Pneumatics Research Institute (INOE 2000 IHP) and Romanian Agricultural Mechanical Engineers Society (SIMAR), in Bucuresti, ROMANIA, in 6–7 October, 2022.

ISSN: 2067–3809

[1.]Igor KOVAČEV, [1.]Mateja GRUBOR, [1.]Karlo ŠPELIC, [1.]Stjepan PLIESTIĆ, [1.]Stjepan SITO, [1.]Nikola BILANDŽIJA

EFFECT OF USING A SOYBEAN OIL AND DIESEL FUEL MIXTURE ON THE POWER AND EXHAUST EMISSIONS OF A TRACTORS DIESEL ENGINE

[1.] University of Zagreb Faculty of Agriculture, Zagreb, CROATIA

Abstract: Aim of paper is to determine the impact of the mixing of crude soybean oil in mineral diesel fuel on the performance of an internal combustion diesel engine in a tractor. Laboratory testing has determined the impact of the use of such a fuel mixture on the rated engine power and exhaust emissions (CO, CO_2, HC and NO_x). For the purposes of the test, four types of fuel were used, diesel fuel, and mixtures of diesel fuel and soybean degummed oil in concentrations of 5% (S5), 10% (S10) and 20% (S20). Power measurement revealed an increase in average engine power and torque. Hourly fuel consumption was almost the same for all types of fuel. Measurement of exhaust emissions showed an increase in CO, HC and NO_x emissions with the addition of soybean oil to diesel fuel
Keywords: engine power, fuel consumption, tractor performance, alternative fuel

INTRODUCTION

Energy is an important input for economic growth and improving the quality of life, and fossil fuels are still the main conventional source of energy. Most countries import crude oil to meet the increasing demand for energy, and in order to achieve partial independence, various alternative fuels are introduced (*Sahoo, P. K., Das, L. M., Babu, M. K. G et al., 2009*). Based on the above, biodiesel has received considerable attention considering the possibility of its use as a renewable alternative fuel and as an addition to existing petroleum–based fuels (*Barnwal, B. K., Sharma, M. P., 2004*).

Fossil diesel is formed by hundreds of different chains of carbohydrates with residual sulfur and residual crude oil, and even low–sulfur and low–aromatic fossil diesel fuels contain 20–24% aromatics (benzene, toluene, xylene, etc.) that are volatile, toxic and carcinogenic (*Tomić, M. D., Savin, L. Đ., Micić, R. D. et al., 2013*). With this, the advantage of biodiesel is that it does not contain sulfur or aromatic compounds, and the possibility of engine wear is reduced because it is characterized by good lubrication properties compared to fossil diesel and diesel fuels with a low sulfur content (*Lapuerta, M., Armas, O., Rodriguez–Fernandez, J., 2008*).

Oil fuel emissions have a harmful effect on nature. For example, an uncontrolled increase in CO_2 causes an excess of greenhouse gases which consequently results in an increase in temperature (global warming) and a decrease in temperature (global cooling) in nature. Other main harmful emissions are CO, NO_x and UHC. In addition, our energy reserves are decreasing in proportion to the growing demand for energy. (*Demirbas, A., 2007*).

Natural gas, hydrogen, vegetable oil, alcohol and biogas are some of the most important alternative fuels. The use of biofuels and alcohol (ethanol, methanol) in diesel fuels as a mixture has been intensively researched in the last few decades. The performance and exhaust emissions of diesel engines using different biodiesels have been studied by many researchers (*Canakcı, M., Van Gerpen, J., 2001; Altıparmak, D., Keskin, A., Koca, A., et al., 2007*).

The use of biodiesel does not require any engine modifications or fuel injection system modifications, with the exception of older engine designs that require replacement of gaskets and fuel injection hoses (*Fang, T., Lin, Y. C., Foong, T. M., et al., 2009*).

According to Qi, D. H., Geng, L. M., Chen, H., et al. (2009) engine performance (power, torque and fuel consumption) using biodiesel is similar to engine performance produced by fossil diesel combustion.

In addition to the mentioned advantages, the use of biodiesel also has disadvantages. According to previous research, the use of biodiesel increases the content of NO_x in combustion products (*Hazar, H., 2009; Taymaz, I., Sengil, M., 2010*). The higher content of NO_x in combustion products can be explained by the high content of oxygen in biodiesel (*Mustapić, Z., Krička, T., Stanić, Z., 2006*). Due to the unfavorable low –temperature properties of biodiesel, there are problems with starting the engine and using the diesel engine in cold weather, and due to its high hygroscopicity, it absorbs water during storage (*Tomić, M. D., Savin, L. Đ., Micić, R. D. et al., 2013*).

Emissions of HC, CO and particulate matter (PM) are reduced by using biodiesel (*Tomić, M. D., Savin, L. Đ., Micić, R. D. et al., 2013*). CO emission is reduced by 30–50%, depending on the proportion of biodiesel in the mixture, mainly due to higher oxygen content and lower hydrogen and carbon content (*Ozsezen, A. N., Canakci, M., 2010*). *Ramesh, D., Sampthrajan, A. 2008*) found that the emission of CO_2 occurs in the process of burning biodiesel in the limits of 20% to 25% of the total combustion of fossil diesel, while Song, J. T., Zhang, C. H. (2008) give results according to which there is no significant difference in the emission of CO_2.

According to Gökalp, B., Soyhan, H. S., Sarac, H. I. et al. (2009) the addition of biodiesel fuel to standard diesel fuel improves the emission characteristics of diesel engines.

Although biodiesel has many advantages when it comes to fuel properties, it still has several properties that need to be improved, such as its lower calorific value, lower power output and its relatively higher emission of nitrogen oxides (*Gokalp, B., Buyukkaya, E., Soyhan, H. S., 2011*).

Diesel fuel can also be replaced with biodiesel produced from vegetable oils. Today, biodiesel is mainly produced from soybean and rapeseed oil. Soybean oil is of primary interest as a source of biodiesel in the United States of America, while many European countries deal with rapeseed oil, and countries with a tropical climate prefer to use coconut oil or palm oil (*Demirbas, A., 2007*).

After the soybean harvest, the grain is often processed to obtain high–value products, oil and soybean meal. Considering the significant use of soybean meal in animal feed and minor oil refining in Croatia, unused degummed oil can also be used as tractor fuel by mixing it with diesel. Soybean oil degumming is an economically inexpensive method that enables better use of soybean oil in terms of achieving better results of testing vegetable oils, with a simple processing technology (*Haldar S. K, Ghosh B. B., Nag A., 2009*).

It is known that vegetable oil has a positive influence on diesel fuel in terms of the effect of increasing the proportion of oxygen (oxide) in the fuel, which leads to better combustion and higher chemical energy of the fuel, as mentioned in the work of Altin R., Cetinkaya S., Yucesu H. S. et al. (2001) where better results were obtained using the addition of soybean oil to diesel fuel when testing power and torque. Schlick M. L., Hanna M. A., Schinstock J. L. (1988) states that the addition of soybean oil leads to better operation of the injection system precisely because of the increase in fuel viscosity, i.e. the injection pressure increases.

A mixture of soybean oil in concentrations above 60% causes significant changes in the operation of the engine and the formation of coke, but lower concentrations allow the use of soybean oil without modifications to the engine (*Engelman H. W., Guenther D. A., Silvis T. W., 1978; McCutchen, R., 1981*). McCutchen, R. (1981) state that the use of a mixture with indirect injection does not cause significant changes in the operation of the engine, while with the use of direct injection there are changes that are primarily visible in the failure of injectors and sticking of piston rings.

Wagner E. P., Lambert P. D., Moyle T. M. et al. (2013) state that the mixture of soybean oil and diesel causes a drop in power and torque and recommends the possibility of using gasoline in a mixture of diesel and soybean oil to reduce the increased viscosity caused by the addition of soybean oil. The results showed a solution to the viscosity problem, which contributed to solving the problem of power loss and torque both in laboratory research and in long–term operating conditions.

By increasing the concentration of soybean oil, a decrease in hourly and specific fuel consumption was determined compared to diesel fuel (*Pereira R. G., Tulcan O. E. P., Lameira V. J. et al. 2011*). Pereira R. G., Tulcan O. E. P., Lameira V. J. et al. (2011) also investigate the impact of exhaust emissions using soybean oil as a diesel fuel additive. The research results show an increase in the emission of CO, CO_2 and NO_x with the addition of soybean oil compared to the use of diesel fuel. The reason for the increase in emissions is the increase in fuel viscosity, which occurs as a result of the mixing of oil into the fuel, which results in a reduction in fuel dispersion after injection, and thus poorer combustion. In contrast to the aforementioned work, Altin R., Cetinkaya S., Yucesu H. S. et al. (2001) report an increase in CO emissions, but a decrease in CO_2 and NO_x emissions. In addition to the aforementioned influence of viscosity on fuel combustion, it is also necessary to pay attention to the fuel temperature during injection, as stated by Arapatsakos C., Moschou M., Sakalidou F. (2012), because a lower fuel temperature means a higher viscosity and vice versa, which leads to a reduction in combustion, i.e. to an improvement in combustion in case of higher fuel temperature. Also, it is stated that CO emission decreases with increasing fuel temperature, HC emission increases with increasing fuel temperature, and NOx emission shows an increase after the fuel temperature exceeds 30°C.

Based on the aforementioned, the aim of the paper is to determine the impact of mixing raw (degummed) soybean oil into mineral diesel fuel on the operating characteristics of a diesel engine with internal combustion in a tractor, and to determine the impact of using such a fuel mixture on the engine's rated power and exhaust gas emissions.

MATERIALS AND METHODS

The research is divided into two phases, the first is related to testing the technical characteristics of the engine, and the second to gas emissions and changes related to fuel consumption.

The research was carried out in the laboratory for engine characteristics testing at the Department of Agricultural Engineering, University of Zagreb Faculty of Agriculture.

Data on environmental factors (temperature, relative humidity and air pressure) were collected from the meteorological station of the Zagreb–Maksimir, Croatian Meteorological and Hydrological Service, which is located in the immediate vicinity of the laboratory. According to the data, the average temperature during the test was 23.5°C, with a relative humidity of 61% and an air pressure of 1019.2 hPa .

Four types of fuel, diesel fuel, and three mixtures of diesel fuel and soybean degummed oil in a concentration of 5% (S5), 10% (S10) and 20% (S20) were used for the purposes of the test. During the test, values such as braking force (kP), engine and PTO speed (min–1), hourly fuel consumption (l/h) and exhaust gas emissions were monitored.

The technical characteristics that are monitored are engine power and torque in relation to engine revolutions (rpm).

The Torpedo TD 7506 A tractor (Torpedo, Croatia) was used for the test, equipped with a four–cylinder air–cooled F4L 912 engine. According to the manufacturer, the rated power of the engine is 55 kW at 2400 rpm, while the torque is 243 Nm at 1600 rpm. The engine has direct fuel injection at a pressure of 175 bar.

The research of engine characteristics was carried out according to the OECD Code 2 regulations for the official testing of agricultural tractors. Two parts of measurements were carried out in 11 points (Figure 1).

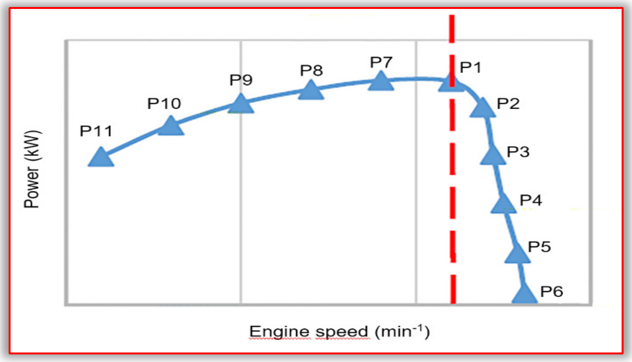

Figure 1 – Engine test points (source: Koronc Z., Filipović D., Fabijanić G., 2018)

The first part of the measurement is carried out in 6 points, where point P1 indicates the nominal power of the motor at the nominal number of motor revolutions. Point P2 represents the power achieved at 85% of the torque obtained at point P1. Point P3 shows the power achieved at 75% of the moment at point P2. Point P4 power at 50% of the moment realized at point P2, then point P5 at 25% of the moment, also at point P2. The last point of the first part of the measurement, point P6 represents the power achieved at the nominal speed without load.

The second part of the measurement was carried out in 5 points, in the range from nominal power to maximum torque, where for each subsequent point the number of revolutions was reduced by 200 engine revolutions per minute (P7 – characteristics at 2150 rpm, P8 – at 1950 rpm, P9 – at 1750 rpm, P10 – at 1550 rpm and P11 – at 1350 rpm).

For the purposes of testing, a hydraulic belt brake Schenck type U1–40 (Schenck RoTech GmbH, Germany) has been used. The hydraulic belt brake is connected to the tractor by means of a cardan shaft, that is, to the tractor's PTO shaft. The brake simulates different loads, i.e. braking forces, which can be used to monitor various parameters, such as tractor power, torque, fuel consumption and the concentration of exhaust gases depending on the applied braking force.

The number of revolutions of the PTO shaft was measured with the help of a digital measuring device Lutron DT 2236 (Lutron Electronics Co., Inc, US) with an accuracy of +/– 0.05 %.

The second part of the research refers to the examination of exhaust gases according to the ISO 8178–4:2017 standard for conducting a test on engine exhaust gases, more precisely to the concentration of CO, CO_2, HC and NO_x that are formed during combustion, and have the greatest impact on air pollution.

Testing is carried out through 8 points using the Maha MET 6.3 exhaust gas analysis device. (MAHA Maschinenbau Haldenwang GmbH & Co. KG, Germany) and probes for measuring exhaust gases, where point 1 represents the measurement of the concentration of gases at maximum engine power at the rated number of revolutions. Point 2 at 75% of the realized moment when measuring at point 1, point 3 at 50% of the realized moment at point 1, point 4 at 10% of the moment realized at point 1. Point 5 indicates the gas concentration at maximum moment, while point 6 indicates values of 75% of the achieved maximum torque, point 7 at 50% of the maximum torque. The last point, point 8, shows the values of the unloaded engine at the minimum number of revolutions.

The obtained values represent the average of the values through 3 measurements carried out in one hour, where statistical analysis using the SAS program was used.

Specific fuel consumption is also determined, which represents the amount of fuel consumed per unit of effective power. It can be expressed in kg/kWh or g/kWh.

Hourly fuel consumption values at different loads were recorded using the Aquametro device Contoil DFM–BC (Aquametro Oil & Marine AG, Germany) which reads the achieved fuel flow on the DFM 8D flow meter.

Statistics analysis of data was brought with computer program SAS (SAS Institute 2002) using analysis of variance (ANOVA). The significance of differences between the observed parameters were indicated by F–test at the level of probability p = 0.05.

RESULTS

The research was carried out on engine characteristics: power, torque, hourly and specific fuel consumption at individual measurement points depending on the number of engine revolutions and load, and are shown in the following tables and graphs. Table 1 and Figure 2 show the achieved power of the diesel engine at individual measurement points when using different types of fuel and the achieved torque when using four types of fuel at individual measurement points.

Table 1. Maximum engine power and torque measured with different fuel types

	Diesel	S5	S10	S20
Max. Power (kW)	45.42 ±0.26 ^{ab*}	44.90 ±0.15 ^{c}	45.79 ±0.19 ^{a}	45.11 ±0.33 ^{bc}
Max. Torque (Nm)	202.92 ±0.29 ^{c}	211.29 ±0.84 ^{a}	211.26 ±0.66 ^{a}	207.73 ±0.57 ^{b}

*Means within the same row with different letters differ significantly ($p < 0.05$)

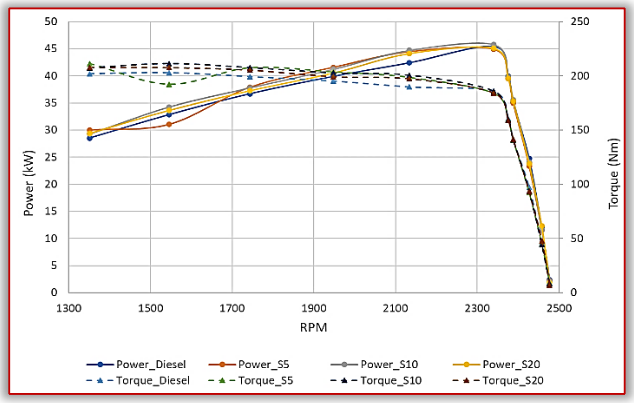

Figure 2 – Engine power and torque characteristics obtained with different fuel types

From point P1 to P6, there are no significant differences in power, somewhat larger differences can only be seen in the area of the curve from the point of the motor's nominal power to the maximum torque, that is, from point P7 to P11. The biggest difference in engine power was observed using S5 fuel at point P10 at 1600 rpm compared to the other three fuels. 9.42% less engine power was achieved when using S5 fuel compared to S10, or 7.81% compared to S20 and 5.56% compared to Diesel fuel. The average power of S10 fuel is higher by 0.99% that is 1.48% and 1.81% in relation to the average power of S20, S5 and diesel fuel.

The highest measured torque was achieved at points P10 and P11, but the biggest difference is visible at point P10 at 1600 rpm, where S5 fuel has the lowest torque compared to the other three fuels. That is, by using S5 fuel, torque was reduced by 5.3%, 7.51% and 9.07% compared to diesel, S20 and S10 fuel. Also, on graph 1, a decrease in torque is clearly visible, which can also be seen on the average value of the measurement. The highest average torque was achieved using S10 fuel, i.e. there is an increase of 0.65%, 1.15% and 2.04% compared to S20, S5 and diesel fuel.

Table 2. Hourly and specific fuel consumption measured with different fuel types

	Diesel	S5	S10	S20
Hourly consumption at max. power (L/h)	12.98 ±0.08 ^{a*}	11.99 ±0.04 ^{b}	13.00 ±0.06 ^{a}	13.01 ±0.09 ^{a}
Specific consumption at max. torque (g/kWh)	212.86 ±0.28 ^{b}	210.84 ±0.34 ^{c}	210.10 ±0.41 ^{c}	214.28 ±0.87 ^{a}

* Means within the same row with different letters diff significantly ($p < 0.05$)

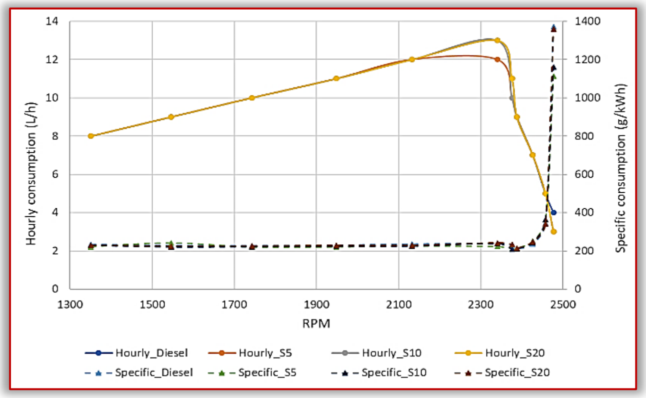

Figure 3 – Hourly and specific fuel consumption of the engine powered with different fuel types

Table 2 and figure 3 show the achieved hourly fuel consumption at individual measurement points when using different types of fuel and the specific fuel consumption when using different types of fuel.

As expected, the highest fuel consumption was achieved at the rated power of the engine, while at the point of rated power, a slightly lower consumption of S5 fuel was achieved, which also has the lowest achieved average fuel consumption. The reduction in consumption using S5 fuel was achieved by 1.02%, or 1.91% compared to S10 and S20 fuel, and the reduction compared to diesel fuel is 3%.

From the table 2 and figure 3, it is observed that there are almost no significant differences between the used fuels. On average, the lowest specific fuel consumption was achieved using S5 fuel, which is 7.46% lower than the highest average specific fuel consumption, i.e. diesel. On average, the highest specific fuel consumption is higher by 0.3%, or 6.74%, compared to S20 and S10 fuel. The lowest specific fuel consumption was achieved at point P2 at 85% of the torque achieved at point P1 using S5 fuel (nominal power point).

The results of the research of exhaust gas emissions are presented in tables, where the test was carried out through eight measurement points using different engine loads according to the standard for exhaust gas analysis ISO 8178–4:2007. The obtained results represent the average value obtained during three measurements carried out in one hour.

Table 3 shows the emission of carbon monoxide (CO) during the use of four different types of fuel at different measurement points.

Table 3. Emission of carbon monoxide at different measurement points

	Load (%)	CO (%) diesel	CO (%) S5	CO (%) S10	CO (%) S20
Rated engine speed	10	0.04	0.04	0.03	0.05
	50	0.03	0.03	0.04	0.04
	75	0.07	0.08	0.08	0.11
	100	0.34	0.44	0.43	0.39
Max. Torque	50	0.07	0.03	0.03	0.03
	75	0.22	0.17	0.16	0.18
	100	0.95	0.80	0.85	0.72

During the test at the nominal speed, an increase in CO emissions is visible with an increase in engine load. By using diesel fuel, the best result was achieved at maximum load at the rated speed compared to other fuels, i.e. by using S5, S10 and S20 fuel there is an increase in CO by 26%, i.e. 29%.

When measuring CO emissions at maximum torque, an increase was found in all three measurement points when using diesel fuel compared to other types of fuel. By using S20 fuel, the best result was achieved at maximum torque (100% load), where CO is reduced by 15.2% compared to S10 fuel. Also, a 24% reduction in emissions was observed when using S20 fuel compared to diesel.

Table 4 and show the measurement results for the emission of carbon dioxide (CO2) at different measurement points.

Table 4. Emission of carbon dioxide at different measurement points

	Load (%)	CO_2 (%) diesel	CO_2 (%) S5	CO_2 (%) S10	CO_2 (%) S20
Rated engine speed	10	2.55	2.49	2.55	2.63
	50	5.45	5.08	5.14	5.14
	75	7.31	7.37	7.41	7.46
	100	12.23	10.54	11.43	9.50
Max. Torque	50	5,76	5.47	5.56	5.37
	75	8.79	8.65	8.65	8.61
	100	11.10	10.60	10.76	10.47

Again, no significant changes occur at the nominal speed up to 75% of the load. The changes are visible during the maximum load, where the best result is achieved by S20 fuel, i.e. a 22% reduction in CO2 emissions was achieved compared to diesel fuel. The other two fuels also show a reduction in emissions during maximum load at rated rpm.

Carbon dioxide emission at maximum torque shows the worst results using diesel fuel in all three measurement points compared to the other three fuels. That is, the use of soybean oil results in a reduction of CO2 emissions at all measurement points. The biggest difference is visible in the maximum torque, where there is a reduction of 5.7% using S20 fuel compared to diesel fuel.

Table 5 shows the emission of NO x when using four different types of fuel and at different measurement points.

When measuring at a rated speed and a load of 50%, there is a 15% reduction in NOx emissions when using S5 and S10 fuel compared to diesel fuel, but with a further increase in load, there is a reduction in emissions in favor of diesel fuel, i.e. when using S20 fuel there is up to a 16% increase in emissions at maximum load at rated rpm compared to diesel fuel.

Table 5. Emission of nitrogen oxides at different measurement points

	Load (%)	NO_x (ppm) diesel	NO_x (ppm) S5	NO_x (ppm) S10	NO_x (ppm) S20
Rated engine speed	10	341.67	329.00	312.00	323.00
	50	997,00	873.33	846.67	957.67
	75	1436.33	1443.67	1402.67	1531.33
	100	1399.67	1473.33	1631.33	1623.33
Max. Torque	50	1092.67	979.67	1015.33	982.67
	75	1588.67	1428.67	1421.67	1562.67
	100	1601.00	1747.00	1838.00	2000.33

When measuring the maximum torque, there is an increase in NOx emissions at 100% load using soybean oil. By increasing the concentration and load there is an increase in NOx, the only decrease is visible at a load of 50% of the maximum torque where the values decreased by almost 10.34% if we look at the ratio of S5 and diesel fuel. An increase in emissions of 24.94% was achieved at maximum torque using S20 fuel compared to diesel fuel.

Table 6 shows the values measured during testing of four different fuels at different measurement points.

By measuring at the nominal speed, clear differences are visible in all measurement points. Increasing the load shows an increase in HC emissions for all types of fuel, and then at maximum load there is a sharp reduction in emissions, with the best result achieved using S20 fuel. The highest values of hydrocarbon emissions were measured using S5 fuel at 75% load at rated rpm.

Table 6. Emission of hydrocarbons at different measurement points

	Load (%)	HC (ppm) diesel	HC (ppm) S5	HC (ppm) S10	HC (ppm) S20
Rated engine speed	10	28.67	29.00	19.67	17.67
	50	29.33	39.00	20.67	28.33
	75	41.00	44.33	38.67	37.00
	100	12.23	15.67	23.00	9.67
Max. Torque	50	15.79	16.00	20.67	19.67
	75	22.30	29.67	29.67	23.67
	100	11.81	9.67	9.67	12.00

When measuring the maximum torque, there is an increase in hydrocarbon emissions at two measurement points using soybean oil as a fuel additive compared to diesel fuel. The biggest differences are visible during 50% and 75% of the maximum torque, with an increase of 30% (50% torque) and 22.1% at 75% torque when we look at diesel and S10 fuel. There are no significant differences in maximum torque, moreover the best result was achieved using S10 fuel.

CONCLUSION

The obtained results show the possibility of using soybean oil as an additive to diesel fuel, since the results of the engine's technical characteristics showed that there is no significant difference between diesel fuel and fuel with 5, 10 and 20% soybean oil. The influence of using soybean oil on engine power showed an increase in engine power. On average, the best result was achieved using S10 fuel. Using 10% soybean oil also achieved the best average result when measuring the maximum torque compared to the worst result achieved using diesel fuel. Energy consumption, i.e. hourly and specific fuel consumption also favors the addition of soybean oil. However, when measuring the emission of harmful gases, there are significant differences between diesel fuel and fuel with the addition of soybean oil, which could be solved with the addition of certain additives that are already used today to reduce the emission of harmful exhaust gases.

References

[1] Altin, R., Cetinkaya, S., & Yucesu, H. S. (2001). The potential of using vegetables oil fuels as fuel for diesel engines. Karabuk Technical Education Faculty, Karaelmas University, Turkey, 533–537
[2] Altıparmak, D., Keskin, A., Koca, A., & Gürü, M. (2007). Alternative fuel properties of tall oil fatty acid methyl ester – diesel fuel blends. Bioresource technology, 98 (2), 241–246
[3] Arapatsakos, C., Moschou, M., & Sakalidou, F. (2012). The Soy Oil Behavior on Diesel Engine. Department of Production and Management Engineering, Democritus University of Thrace, Greece, 175–181.
[4] Barnwal, B. K., & Sharma, M. P. (2005). Prospects of biodiesel production from vegetables oils in India. Renewable and sustainable energy reviews, 9 (4), 363–378
[5] Canakci, M., & Van Gerpen, J. (1998). The performance and emissions of a diesel engine fueled with biodiesel from yellow grease and soybean oil. In 2001 ASAE Annual Meeting (p. 1). American Society of Agricultural and Biological Engineers.
[6] Demirbas, A. (2007). Importance of biodiesel as transportation fuel. Energy policy, 35 (9), 4661–4670
[7] Engelman, H. W., Guenther, D. A., & Silvis, T. W. (1978). Vegetables oil as a diesel fuel. Diesel & Gas Engine Power Division of ASME Paper Number 78–DGP–19., New York
[8] Fang, T., Lin, Y. C., Foong, T. M., & Lee, C. F. (2009). Biodiesel combustion in an optical HSDI diesel engine under low load premixed combustion conditions. Fuel, 88 (11), 2154–2162
[9] Gokalp, B., Buyukkaya, E., & Soyhan, H. S. (2011). Performance and emissions of a diesel tractor engine fueled with marine diesel and soybean methyl ester. Biomass and bioenergy, 35(8), 3575–3583
[10] Gökalp, B., Soyhan, H. S., Sarac, H. I., Bostan, D., & Şengün, Y. (2009). Biodiesel addition to standard diesel fuels and marine fuels used in a diesel engine: effects on emissions characteristics and first–and second–law efficiencies. Energy & Fuels, 23 (4), 1849–1857
[11] Haldar, S. K., Ghosh, B. B., & Nag, A. (2009). Studies of the comparison of performance and emission characteristics of diesel engine using three degummed non–edible vegetables oils. Department of Chemistry, Department of Mechanical Engineering, Kharagpur India, 1013–1018.
[12] Hazar, H. (2009). Effects of biodiesel on a low heat loss diesel engine. Renewable Energy, 34 (6), 1533–1537
[13] Koronc, Z., Filipović, D., & Fabijanić, G. (2018). Karakteristike traktorskog dizel motora s direktnim ubrizgavanjem pri korištenju različitih vrsta dizelskog goriva. 46 Symposium „Actual Tasks on Agricultural Engineering" Opatija, 117–126.
[14] Lapuerta, M., Armas, O., & Rodriguez–Fernandez, J. (2008). Effect of biodiesel fuels on diesel engine emissions. Progress in energy and combustion science, 34 (2), 198–223
[15] McCutchen, R. (1981). Vegetables oil as a diesel fuel–soybean oil. Beyond the Energy Crisis — Oppotunity and Challenge Volume III. Third International Conference on Energy Use Management, Berlin.
[16] Mustapić, Z., Krička, T., & Stanić, Z. (2006). Biodiesel as alternative engine fuel. Journal of Energy: Energy, 55 (6), 634–657. https://hrcak.srce.hr/7868
[17] Ozsezen, A. N., & Canakci, M. (2010). The emission analysis of an IDI diesel engine fueled with methyl ester of waste frying palm tree oil and its blends. Biomass and bioenergy, 34 (12), 1870–1878
[18] Pereira, R. G, Tulcan OEP, Lameira VJ, Filho DMES, & Andrade ET (2011). Use of Soybean Oil in Energy Generation. Fkuimenense Federal University, Bogota, 303–318.
[19] Qi, D. H., Geng, L. M., Chen, H., Bian, Y. Z., Liu, J., & Ren, X. C. (2009). Combustion and performance evaluation of a diesel engine fueled with biodiesel produced from soybean crude oil. Renewable energy, 34 (12), 2706–2713
[20] Ramesh, D., & Sampathrajan, A. (2008). Investigations on performance and emission characteristics of diesel engine with jatropha biodiesel and its blends. Agricultural Engineering International: CIGR Journal.
[21] Sahoo, P. K., Das, L. M., Babu, M. K. G., Arora, P., Singh, V. P., Kumar, N. R., & Varyani, T. S. (2009). Comparative evaluation of performance and emission characteristics of jatropha, karanja and polanga based biodiesel as fuel in a tractor engine. Fuel, 88(9), 1698–1707
[22] SAS Institute (2002). SAS/STAT User's guide. Ver. 9.1, SAS Inst., Cary, NC, USA.
[23] Schlick, M. L., Hanna, M. A., & Schinstock, J. L. (1988). Soybean and Sunflower Oil Performance in Diesel Engine. American Society of Agricultural Engineers, 1346–1348
[24] Song, J. T., & Zhang, C. H. (2008). An experimental study on the performance and exhaust emissions of a diesel engine fueled with soybean oil methyl ester. Proceedings of the Institution of Mechanical Engineers, Part D: Journal of Automobile Engineering, 222 (12), 2487–2496.
[25] Taymaz, I., & Sengil, M. (2010). Performance and emission characteristics of a diesel engine using esters of palm tree olein / soybean oil blends. International Journal of Vehicle Design, 54 (2), 177–189
[26] Tomić, M. D., Savin, L. Đ., Micić, R. D., Simikić, M. Đ., & Furman, T. F. (2013). Effects of fossil diesel and biodiesel blends on the performances and emissions of agricultural tractor engines. Thermal Science, 17(1), 263–278
[27] Wagner, E. P., Lambert, P. D., Moyle, T. M., Koehle, M. A. (2013). Diesel vehicle performance on unaltered waste soybean oil blended with petroleum fuels. University of Pittsburgh, Department of Chemistry, Pittsburgh, 760–764.

Note: This paper was presented at ISB–INMA TEH' 2022 – International Symposium on Technologies and Technical Systems in Agriculture, Food Industry and Environment, organized by University "POLITEHNICA" of Bucuresti, Faculty of Biotechnical Systems Engineering, National Institute for Research–Development of Machines and Installations designed for Agriculture and Food Industry (INMA Bucuresti), National Research & Development Institute for Food Bioresources (IBA Bucuresti), University of Agronomic Sciences and Veterinary Medicine of Bucuresti (UASVMB), Research–Development Institute for Plant Protection – (ICDPP Bucuresti), Research and Development Institute for Processing and Marketing of the Horticultural Products (HORTING), Hydraulics and Pneumatics Research Institute (INOE 2000 IHP) and Romanian Agricultural Mechanical Engineers Society (SIMAR), in Bucuresti, ROMANIA, in 6–7 October, 2022.

ISSN: 2067–3809

[1.]Olunusi Samuel OLUGBENGA, [2.]Promise Goodness ADELEYE, [3.]Sunday Blessing OLADIPUPO

UTILIZATION OF AGRO–WASTES DERIVED BIOCHAR/MODIFIED BIOCHAR AS EFFICIENT ADSORBENTS IN WASTEWATER TREATMENTS – A REVIEW

[1.]Industrial and Production Engineering, University of Ibadan, Oyo State, NIGERIA
[2.]Department of Agriculture, University of Ilorin P.M.B 1515. Ilorin, Kwara State, NIGERIA
[3.]Water resources and environmental Engineering, University of Ilorin P.M.B 1515. Kwara State, NIGERIA

Abstract: Wastewater has been seen as one of the global environmental issues recently. Untreated wastewater left environment polluted and tends to cause health issues. The rate at which environmental contaminants are discharged into our environment are alarming and there is need to seek for solutions to address these issues towards achieving eco–sustainability of the environment in promoting SDG–3 (Ensure healthy lives and promote well–being for all at all ages) through efficient implementation of SDG–6 (Ensure availability and sustainable management of water and sanitation for all). As a result of this, there is need to seek for sustainable adsorbents through utilization of Green Chemistry Principle #7 (Use of Renewable Feedstocks) to address global issues of water scarcity. Utilization of agro–wastes is in frontline towards achieving environmental wastes and as well to produce value–added products such as Activated carbons, Biochar, renewable and eco–friendly chemicals from agro–wastes. Therefore, this mini–review present recent overviews of agro–waste derived adsorbents (biochar) as catalytic materials for the environmental remediation of wastewater
Keywords: Agro–wastes, Biochar, Wastewater, Sustainable Development Goals (SDGs), Circular Economy

INTRODUCTION

Biochar as a renewable and eco–sustainable material obtained from renewable sources with green credentials are gaining attention recently (Afolalu et al., 2022; Li et al., 2022). Biochar is a material suitable for various environmental and energy applications (Li et al., 2022). Biochar is being employed and studied as material with multipurpose in various fields (see Figure 1). Biochar is obtainable from biomass. As we already know that the entire world is facing various issues of which consumption of non–renewable resources is fundamental to it, utilization of non–renewable materials such as petroleum derived materials (Afolalu et al., 2022). Reckless utilization of petroleum derived materials has led to various issues ranging from climate changes to pollution of various types (Aderemi Timothy Adeleye et al., 2021) Petroleum derived materials are not equally distributed equally in all global geographical regions, therefore, there is crisis in continuous using without back–up or sourcing source of renewable materials to complement it (Timothy et al., 2020). Biomass as a material renewable in nature, equally distributed almost across the world and eco–sustainable compliance without environmental degradation are suitable for the synthesis of various materials that are equally obtainable from petroleum such biofuels (e.g ethanol, biodiesel), recently Ning Li et al synthesized biojet fuels from lignocellulose biomass (Timothy et al., 2020). Biomass has also been used for the synthesis of activated carbon (Aderemi Timothy Adeleye et al., 2021), it has been employed as catalytic materials for the synthesis of various materials such value–added chemicals (Chi et al., 2021), for sensor application and as adsorbents for various applications (Li et al., 2022). It is an important renewable feedstock owing to its environmental–friendliness and renewability credentials (Afolalu et al., 2022). Therefore, this is the reason they are being explored for various uses. Agro–wastes are from biomass and are suitable for the applications enumerated above (Aderemi T. Adeleye et al., 2020). This review work is specifically based on the utilization of agro–wastes for the synthesis of biochar as adsorbents for the treatment of wastewater. An environmental and sustainable approach to optimize the use of vast agro–wastes is to use them for the production of value–added materials (Timothy et al., 2020). This will really help in the reduction of accumulated wastes around the globe and further serve as source of income which can as well create job opportunities while agro–economics receive positive boosts (Aderemi T. Adeleye et al., 2020). Apart from plant–derived biomass, biochar can also be synthesized from animal wastes such as bone. For instance, Adeniyi and his colleagues' metal oxide–based biochar from bone via pyrolysis. The biochar synthesized was reported to be suitable as low–cost adsorbent for the treatment of wastewater and catalytic materials to produce biofuel as alternative fuel at lower cost (Chi et al., 2021). The entire production was said to be low–cost and eco–friendly (Li et al., 2022).

The published reports by the United Nations (UN) in 2017 revealed that not less than 2.2 billion people have no access to safe drinking water because of the presence of contaminants in the source of water (Kingsley I. John, Omorogie, Bayode, Adeleye, & Helmreich, 2022).

According to recent report by the year 2030 more 700 million people could be displaced because of inability to have access to potable drinking water.

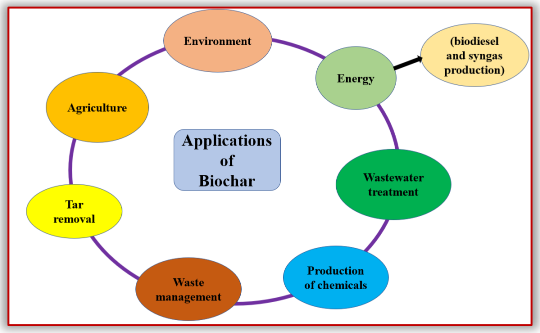

Figure 1. Applications of biochar in various field

According to the United Nations (UN) report, as of 2017, approximately 2.2 billion people were short of safely managed drinking water due to contamination by pollutants (Igenepo John et al., 2021). In order to address this issue in accordance with the SDG–6 (Ensure availability and sustainable management of water and sanitation for all) and SDG–3 (Ensure healthy lives and promote well–being for all at all ages) various techniques have been employed for the treatment of wastewater (Kingsley Igenepo John et al., 2021). Figure 2 shows the current and existing applicable wastewater treatment techniques (Kingsley Igenepo John et al., 2021; Kingsley Igenepo John, Malachy Obu, et al., 2022).

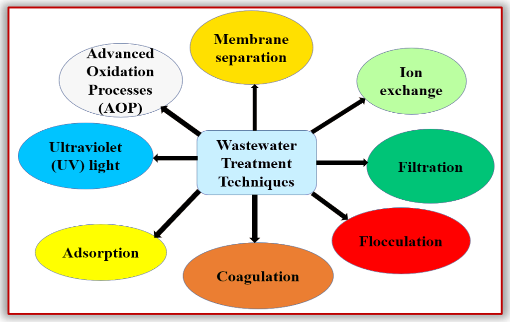

Figure 2. Applicable wastewater treatment techniques

Improper and continuous discard of a large number of organic and inorganic contaminants such as dyes, heavy metals, surfactants, pharmaceuticals, pesticides, and personal care products from households, industries and municipalities into the sources of water have contributed to the scarcity of water for various uses across the globe(Kingsley Igenepo John, Daniel Agbor, et al., 2022). The fact about these contaminants is that they are significantly persistent and recalcitrant in nature thereby causing continuous degradation of our environment in various form. This is a concern and solutions are urgently needed to avert subsequent consequences specially to keep the environment habitable for the future generation while we take care of the present with the available technologies for the wastewater treatment toward achieving sustainable development (Igenepo John et al., 2021). Apart from the wastewater techniques shown in Figure 2, other conventional technologies are applied worldwide for the removal of wastewater contaminants in a single manner or in combination to achieve the purpose efficient treatment. Such as coagulation–flocculation, reverse osmosis, chemical precipitation, ion–electrochemical treatment, solvent extraction, and flotation for the removal of inorganic pollutants (Sarayu & Sandhya, 2012). Though these treatment techniques have pros and cons. Some are inefficient in nature or not cost–effective due to the cost of the required equipment and maintenance, sometimes high consumption of energy made them unaffordable(Rout, Zhang, Bhunia, & Surampalli, 2021). Therefore, efficiency and viability of the method adopted for the treatment must be considered if they are economical affordable, environmental compliance and potential to scale up to industrial adoption. With these credentials treatment approaches could decrease the unaffordable treatment cost and increase the efficiency features of process of the water treatment (Adeyemi, Ajiboye, & Onwudiwe, 2021). The synthesis of biochar is not performed via pyrolysis or thermal decomposition of the employed precursors (i.e carbonaceous biomass) under a limited amount, or absence of oxygen (Fischer et al., 2019). Generally, almost all carbonaceous precursors are suitable to produce biochar precursor such as lignocellulosic biomass, agricultural biomass (i.e., plant or animal derived biomass or even manure), industrial residue, and activated sludge (Fischer et al., 2019). Recently biochar has attracted the attention of the researchers owing to their cost–effectiveness and other characteristic features such presence of oxygen–containing functional groups, interesting high surface areas, high cation exchange capacity and alkalinity (Jung, Lee, Choi, & Lee, 2019), these characteristic features have made them suitable candidates as efficient and sustainable adsorbents in wastewater applications (Fischer et al., 2019). It has been employed as an adsorbent for the remediation of emerging contaminants such as microplastics (Mujtaba Munir et al., 2021), pharmaceuticals (Ihsanullah, Khan, Zubair, Bilal, & Sajid, 2022), dyes, trace metals, pesticides and heavy–metals (Amusat, Kebede, Dube, & Nindi, 2021). Sajjadi B. et al, 2019 (Sajjadi et al., 2019)and Mandal S. et al, 2020 attributes the interesting high sorption feature of biochar to existing disordered valence sheets that engineer incompletely saturated valences and unpaired electrons, that facilitate an improved high number of active sites for adsorption (Mandal et al., 2021; Sajjadi et al., 2019). The presence of a large amount of delocalized π electrons result to a negative charge of the biochar surface; therefore, causes it to act like a Lewis base which subsequently attract Lewis acid via processes of physi– and chemisorption (Mandal et al., 2021). Furthermore, availability of oxygen–containing and nitrogen–containing functional groups on the biochar surface enhances adsorption through acid/base interactions and hydrogen–bond formation (Sajjadi et al., 2019). In addition to that, as biochar possesses carbon matrix, structural defect sites, and various surface functional groups, it is suitable for efficient use in photocatalytic reactions. Biochar has remarkable electrical conductivity, leading to its decreased electron/hole recombination rate during the photocatalytic process, thus enhancing the oxidation rate of the target compound (Mandal et al., 2021; Sajjadi et al., 2019). All of these features make biochar an interesting alternative to activated carbon in the fields of adsorption and photocatalysis (Matos, 2016). Katiyar and his colleagues emphasized on limitations of biochar. Pristine biochar reveals an excellent adsorption capacity for organic substances, it exhibits a very limited adsorption capacity for anionic pollutants (Katiyar et al., 2022). Moreover, raw biochar requires a long equilibrium time, due to its limited surface functional groups and porous structure (Amusat et al., 2021). Additionally, the biomass source, reaction media, and processing conditions determine the biochar properties (Afolalu et al., 2022; Ihsanullah et al., 2022) which means that biochars will differ in the range of molecular structure and topology. Therefore, numerous studies have been conducted to improve biochar properties, including chemical and physical approaches (Amusat et al., 2021; Ihsanullah et al., 2022). To improve its properties for environmental applications, chemical processes such as acid and base modification, metal salt or oxidizing agent modification, and carbonaceous material modification are most often selected (Amusat et al., 2021).

APPLICATION OF BIOCHAR–BASED CATALYST TO WASTEWATER TREATMENT

— Industrial wastewater remediation

Biochar–based catalysts have been used in the treatment of industrial effluent, which composes majorly heavy metals and organic contaminants. Biochar–based catalyst has the potential to be used efficiently as an adsorbent for the adsorption of heavy metals in industrial wastewater(Jung et al., 2019). For instance, Rajapaksha A.U et al emphasized that a successful adsorption of heavy metals (Cu, Pb, As, Cd and other heavy metals) from industrial wastewater using chitosan/ biochar is dependent on the combination ratio of chitosan/ biochar materials (Rajapaksha et al., 2015). Biochar made from bagasse was as well employed to absorb lead from the effluent of the battery production sector to the tune of 13 mg/g, and the adsorptive activity depended on the moderate pH value, contact time, and concentration (Qian, Kumar, Zhang, Bellmer, & Huhnke, 2015). Pan et al. prepared biochar (from peanut, soybean, canola, and rice husk) and showed that adsorption capacity increases as functional groups on biochar increase, suggesting complexation with functional groups as the controlling remediation mechanism for trivalent chromium (Pan, Jiang, & Xu, 2013). Further studies from Chen et al. observed there was a correlation between the absorbed Cr (III) and the released Ca2+ and Mg2+ cations into solution during adsorption. At lower pH (<2.5), surface biochar becomes negatively charged, and trivalent chromium species remains positively charged leading to electrostatic interaction and the removal of the chromium. Majorly, the application of biochar–based catalyst in adsorbing contaminants from industrial wastewater have been carried out in a laboratory environment; however, additional study and deployment in the actual situation are required (Chen, Zhou, Xu, Wang, & Lu, 2015).

— Wastewater treatment in the agricultural sector

Agricultural pollution is unbecoming due to rapid development of new technologies in the agriculture sector. This has led to the release of agro–chemicals containing toxic heavy metals into the environments in large quantities (Amusat et al., 2021). Pesticides such as atrazine and pentachlorophenol are two of the most often used in agriculture. Corn straw and soybean biochars both exhibit strong atrazine reduction potentials, with the adsorption efficiency owing mostly to the pH value and pore volume of the biochars (Fischer et al., 2019). Steam–activated biochar is efficient at eliminating sulfamethazine, and the rate at which it absorbs the substance is dependent on the pH value (Afolalu et al., 2022; Li et al., 2022).

— Data Evaluation of Adsorbents

≡ Calculation of Equilibrium Adsorption Amount of Contaminants

The equilibrium adsorption amount can be calculated using Equation (1):

$$q_e = \frac{(C_0 - C_e)}{m} \quad (1)$$

where qe (mg/g) is the adsorption capacity of the Cm on contaminants, V (mL) refers to the volume of contaminants added, Co (mg/L) represents the initial addition concentration of contaminants solution, Ce (mg/L) denotes the concentration of contaminants solution after adsorption, and m (g) is the weight of the sample (Liu et al., 2022).

≡ Fitting of Contaminants Adsorption Isotherms

Three isothermal adsorption models can be selected on the basis of the adsorption isotherm trend, and the isothermal equation (Equations (2)– (4)) such as follows:

$$q_e = \frac{q_m K_L C_e}{1 + K_L C_e} \quad (2)$$

$$q_e = K_F {C_e}^{\frac{1}{n}} \quad (3)$$

$$q_e = K_H C_e \tag{4}$$

where qm indicates the maximum adsorption amount of contaminants, mmol/kg; and KL, KF, and KH are the Langmuir (eqn. 2), Freundlich (eqn. 3), and Henry adsorption (eqn.4) equilibrium constants of the contaminants adsorption, which can be used to measure the affinity of adsorption (Liu et al., 2022). In the study conducted by Liu et.al., and his colleagues where acid–base modified biochar was employed for adsorption removal of pharmaceutical compound (Chlortetracycline, CTC) by purple soil, the variation of the CTC adsorption capacity of different soil samples with temperature is represented in Figure 3, the sorption capacity of each amended soil for CTC increased with increasing temperatures, showing that the sorption was an endothermic form in nature.

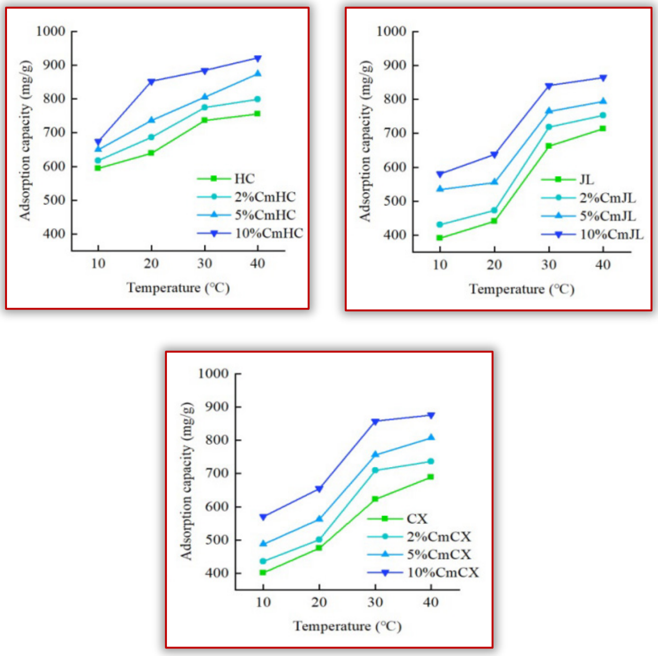

Figure 3: Adsorption capacity of CTC on different soil samples at various temperatures (Liu et al., 2022)

According to the author with the increase in temperature, the adsorption process was more spontaneous because of the thermal movement of molecules, and the collision between the biochar used as adsorbent and CTC was more violent at a high temperature (Liu et al., 2022). A previous study also showed that the adsorption capacity of tetracycline (TC) for different amended soil samples increased with temperature, thereby showing the positive effect of increasing temperature (He et al., 2019)

CHALLENGES AND PROSPECTS OF BIOCHAR CATALYST TO WASTEWATER TREATMENT

Biochar–based catalysts has proven beneficiary in useful applications to catalytic processes and various specific/functional organic reactions. However, all these are currently in their infancy and must be scaled up. Biochar production systems must be set up on an industrial scale to enable the scaling up of these processes. Stephen O. et al. identified to major inhibitors to scaling up biochar production, which are multiple competing end–users, as well as the collection and transportation of raw materials to the facilities that manufacture biochar (Stephen Okiemute, Ifeanyi Michael Smarte, Jeremiah, & Sammy Lewis, 2022). Homagain studied the sensitivity of transportation distance and distinct carbon offset values and found that the system is financially viable at 200 km with good biomass availability (Homagain, Shahi, Luckai, & Sharma, 2016). In addition, the seasonal biomass production cycle makes it difficult to maintain a steady supply of sustainable and reliable fuel. Again, moisture content and particle size are other critical parameters in the synthesis of biochar, because biochar production method requires a lot of energy to drain the moisture and reduce the size. The investigation of high surface area, active sites, and optimal pores is critical to managing the combined impacts of important production process variables (e.g., reagent gas, duration, heating rate, and temperature) and activation process variables (e.g., chemical, and physical) (Amusat et al., 2021; Ihsanullah et al., 2022)

CONCLUSION

This review systematically presented an overview of the emergence of biochar and its significance, different biochar production techniques, characteristics and inherent properties that permit its adsorption capacity, preparation of biochar–based catalysts and its modification mechanisms to enhance its adsorption and absorption properties toward organic and inorganic emerging contaminants, prospective applications to wastewater treatment, present challenges, prospects and recommendations. Therefore, biochar–based catalysts have strong potential for replacing costly and non–renewable conventional catalysts. The versatility characteristics of biochar–based catalysts has been demonstrated effective in remediation of contaminated wastewater, including the adsorption of toxic heavy metals, organic and inorganic elements from effluent, as a support for catalysts, as an immobilization support media for microorganisms and adsorbent of inhibitive compounds during anaerobic digestion.

References

[1] Adeleye, A. T., Akande, A. A., Odoh, C. K., Philip, M., Fidelis, T. T., Amos, P. I., Banjoko, O. O. (2021). Efficient synthesis of bio–based activated carbon (AC) for catalytic systems: A green and sustainable approach. Journal of industrial and engineering chemistry (Seoul, Korea), 96, 59–75

[2] Adeleye, A.T., Odoh, C. K., Enudi, O. C., Banjoko, O. O., Osiboye, O. O., Toluwalope Odediran, E., & Louis, H. (2020). Sustainable synthesis and applications of polyhydroxyalkanoates (PHAs) from biomass. Process biochemistry (1991), 96, 174–193

[3] Adeyemi, J. O., Ajiboye, T., Onwudiwe, D. C. (2021). Mineralization of Antibiotics in Wastewater Via Photocatalysis. Water, air, and soil pollution, 232(5)

[4] Afolalu, S. A., Ikumapayi, O. M., Ogundipe, A. T., Okwilagwe, O. O., Oloyede, O. R., Adeoye, A. O. M. (2022). Development of composite filters from biochars for

wastewater treatment. Advances in materials and processing technologies (Abingdon, England), ahead–of–print(ahead–of–print), 1–18

[5] Amusat, S. O., Kebede, T. G., Dube, S., Nindi, M. M. (2021). Ball–milling synthesis of biochar and biochar–based nanocomposites and prospects for removal of emerging contaminants: A review. Journal of Water Process Engineering, 41, 101993

[6] Chen, T., Zhou, Z., Xu, S., Wang, H., Lu, W. (2015). Adsorption behavior comparison of trivalent and hexavalent chromium on biochar derived from municipal sludge. Bioresource technology, 190, 388–394

[7] Chi, N. T. L., Anto, S., Ahamed, T. S., Kumar, S. S., Shanmugam, S., Samuel, M. S., Pugazhendhi, A. (2021). A review on biochar production techniques and biochar based catalyst for biofuel production from algae. Fuel (Guildford), 287, 119411

[8] Fischer, B. M. C., Manzoni, S., Morillas, L., Garcia, M., Johnson, M. S., Lyon, S. W. (2019). Improving agricultural water use efficiency with biochar – A synthesis of biochar effects on water storage and fluxes across scales. The Science of the total environment, 657, 853–862

[9] He, Y., Liu, C., Tang, X.–Y., Xian, Q.–S., Zhang, J.–Q., Guan, Z. (2019). Biochar impacts on sorption–desorption of oxytetracycline and florfenicol in an alkaline farmland soil as affected by field ageing. Science of The Total Environment, 671, 928–936

[10] Homagain, K., Shahi, C., Luckai, N., Sharma, M. (2016). Life cycle cost and economic assessment of biochar–based bioenergy production and biochar land application in Northwestern Ontario, Canada. Forest ecosystems, 3(1), 1

[11] Igenepo John, K., Abdul Adenle, A., Timothy Adeleye, A., Pearl Onyia, I., Amune–Matthews, C., Omorogie, M. O. (2021). Unravelling the effect of crystal dislocation density and microstrain of titanium dioxide nanoparticles on tetracycline removal performance. Chemical physics letters, 776, 138725

[12] Ihsanullah, I., Khan, M. T., Zubair, M., Bilal, M., Sajid, M. (2022). Removal of pharmaceuticals from water using sewage sludge–derived biochar: A review. Chemosphere (Oxford), 289, 133196–133196

[13] John, K. I., Adeleye, A. T., Adeyanju, C. A., Ogunniyi, S., Ighalo, J. O., Adeniyi, A. G. (2021). Effect of light on concomitant sequestration of Cu(II) and photodegradation of tetracycline by H–MOR/H–β/H–ZSM5 zeolites. Environmental science and pollution research international, 29(8), 11756–11764

[14] John, K. I., Agbor, D., Sani, L. A., Adeleye, A. T., Adenle, A. A., Idris, A. M., Elawad, M. (2022). Adsorption Performance of Zinc Semiconductor Nanoparticles in Tetracycline Removal. Journal of Cluster Science

[15] John, K. I., Obu, M., Adeleye, A. T., Ebiekpe, V., Adenle, A. A., Chi, H., Omorogie, M. O. (2022). Oxygen deficiency induction and boundary layer modulation for improved adsorption performance of titania nanoparticles. Chemical Papers, 76(6), 3829–3840

[16] John, K. I., Omorogie, M. O., Bayode, A. A., Adeleye, A. T., Helmreich, B. (2022). Environmental microplastics and their additives––a critical review on advanced oxidative techniques for their removal. Chemical Papers

[17] Jung, K.–W., Lee, S. Y., Choi, J.–W., Lee, Y. J. (2019). A facile one–pot hydrothermal synthesis of hydroxyapatite/biochar nanocomposites: Adsorption behavior and mechanisms for the removal of copper(II) from aqueous media. Chemical engineering journal (Lausanne, Switzerland : 1996), 369, 529–541

[18] Katiyar, R., Chen, C. W., Singhania, R. R., Tsai, M. L., Saratale, G. D., Pandey, A., Patel, A. K. (2022). Efficient remediation of antibiotic pollutants from the environment by innovative biochar: current updates and prospects. Bioengineered, 13(6), 14730–14748

[19] Li, N., He, M., Lu, X., Yan, B., Duan, X., Chen, G., Hou, L. a. (2022). Municipal solid waste derived biochars for wastewater treatment: Production, properties and applications. Resources, conservation and recycling, 177, 106003

[20] Liu, Z., Fang, X., Chen, L., Tang, B., Song, F., Li, W. (2022). Effect of Acid–Base Modified Biochar on Chlortetracycline Adsorption by Purple Soil. Sustainability, 14(10), 5892.

[21] Mandal, S., Pu, S., Adhikari, S., Ma, H., Kim, D.–H., Bai, Y., Hou, D. (2021). Progress and future prospects in biochar composites: Application and reflection in the soil environment. Critical reviews in environmental science and technology, 51(3), 219–271

[22] Matos, J. (2016). Eco–Friendly Heterogeneous Photocatalysis on Biochar–Based Materials Under Solar Irradiation. Topics in catalysis, 59(2–4), 394–402

[23] Mujtaba Munir, M. A., Yousaf, B., Ali, M. U., Dan, C., Abbas, Q., Arif, M., Yang, X. (2021). In situ synthesis of micro–plastics embedded sewage–sludge co–pyrolyzed biochar: Implications for the remediation of Cr and Pb availability and enzymatic activities from the contaminated soil. Journal of Cleaner Production, 302, 127005.

[24] Pan, J., Jiang, J., Xu, R. (2013). Adsorption of Cr(III) from acidic solutions by crop straw derived biochars. Journal of environmental sciences (China), 25(10), 1957–1965.

[25] Qian, K., Kumar, A., Zhang, H., Bellmer, D., & Huhnke, R. (2015). Recent advances in utilization of biochar. Renewable & sustainable energy reviews, 42, 1055–1064.

[26] Rajapaksha, A. U., Vithanage, M., Ahmad, M., Seo, D.–C., Cho, J.–S., Lee, S.–E., Ok, Y. S. (2015). Enhanced sulfamethazine removal by steam–activated invasive plant–derived biochar. Journal of hazardous materials, 290, 43–50

[27] Rout, P. R., Zhang, T. C., Bhunia, P., Surampalli, R. Y. (2021). Treatment technologies for emerging contaminants in wastewater treatment plants: A review. The Science of the total environment, 753, 141990–141990

[28] Sajjadi, B., Broome, J. W., Chen, W. Y., Mattern, D. L., Egiebor, N. O., Hammer, N., Smith, C. L. (2019). Urea functionalization of ultrasound–treated biochar: A feasible strategy for enhancing heavy metal adsorption capacity. Ultrasonics sonochemistry, 51, 20–30

[29] Sarayu, K., Sandhya, S. (2012). Current Technologies for Biological Treatment of Textile Wastewater–A Review. Applied biochemistry and biotechnology, 167(3), 645–661.

[30] Stephen Okiemute, A., Ifeanyi Michael Smarte, A., Jeremiah, A., & Sammy Lewis, K. (2022). Biochar Development as a Catalyst and Its Application. In B. Dr. Mattia, G. Dr. Mauro, T. Prof. Alberto (Eds.), Biochar – Productive Technologies, Properties and Application (pp. Ch. 25). Rijeka: IntechOpen.

[31] Timothy, A. A., Han, F., Li, G., Xu, J., Wang, A., Cong, Y., Li, N. (2020). Synthesis of jet fuel range high–density dicycloalkanes with methyl benzaldehyde and acetone. Sustainable Energy & Fuels, 4(11), 556–5567

ACTA TECHNICA CORVINIENSIS
Bulletin of Engineering

ISSN: 2067-3809

Fascicule 2
[April – June]
tome [2023] XVI

ACTA Technica CORVINIENSIS
BULLETIN OF ENGINEERING

ISSN: 2067-3809

[1.]Iuliana GĂGEANU, [2.]Adriana BĂDULESCU, [3.]Valentina ISAC, [1.]Ana–Maria TĂBĂRASU, [1.]Cătălin PERSU, [1.]Dan CUJBESCU, [1.]Gabriel GHEORGHE

ENERGY RECOVERY OF BIOMASS IN THE CONTEXT OF EUROPEAN TARGETS

[1.] National Institute of Research – Development for Machines and Installations Designed for Agriculture and Food Industry – INMA, ROMANIA
[2.] National Research–Development Institute for Biotechnologies in Horticulture Ştefăneşti–Argeş, ROMANIA
[3.] Research Institute for Fruit Growing Pitesti–Maracineni, ROMANIA

Abstract: The challenges caused by climate change are becoming inevitable. The main cause is represented by human activities, which are associated with the overexploitation of ecosystem services and natural resources, to meet the ever–growing demand for human needs. This leads to extensive environmental degradation and the release of greenhouse gases into the atmosphere, leading to a dangerous increase in the global average temperature. The benefits of biofuels compared to traditional fuels aim at greater energy security, lower environmental impact, financial savings and socioeconomic aspects related to the rural sector. The concept of sustainable development embodies the idea of inter–connectivity and balance between economic, social and environmental concerns. Romania relies heavily on biomass for the contribution of energy from renewable sources in this sector, biomass being generally used more in rural areas.
Keywords: renewable energy, biomass, conventional energy use reduction

INTRODUCTION

The European Union is moving towards a sustainable energy system, which promotes a much higher consumption of energy produced from renewable sources and energy efficiency in all the sectors. Political instruments have a key role in achieving the assumed objectives (energy efficiency, increasing energy production from renewable sources, biomass utilization, etc.) and implementing this energy system (*ADR Centru, 2018*).

In order to be able to achieve the SDG 7 aim of ensuring an affordable, clean and secure energy system, the EU is seeking to increase the share of renewable energy in gross final energy consumption to at least 32 % by 2030 (*Eurostat, 2022*). The of renewable energy has grown continuously in the EU, with its share doubling since 2005 when renewables covered only 10.2 % of gross final energy consumption. By 2020, this figure had reached 22.1 %, surpassing the target of 20% set for 2020.

The policy framework 2020–2030 envisages improving biomass policies: maximizing resource efficiency techniques, using biomass in multiple sectors, sustainable land use, sustainable forest management (in line with the objectives of the forestry strategy) and ensuring efficient production of biofuel.

In all European countries, different lignocellulosic biomasses have started to be used for the production of renewable energy. Among these, we can mention: agricultural residues (straw, straw containing manure) or fractions of solid municipal waste available in large quantities, but little of this potential is used at the moment. Not all wastes have a suitable content for their treatment with the help of available techniques for transforming lignocellulosic biomass into renewable energy such as anaerobic digestion, ethanol production or thermal recovery (*European Commission – EUR 21350, 2005*).

Biomass has many forms and sources, being the most abundant source of renewable energy in the world that can easily be used by the majority of the population and can be divided in the following major categories:

- wood and wood waste;
- stems of some non–woody plants (annual or perennial); this includes cellulosic agricultural waste (CAW) such as: cereal straw and stalks from different crops as well as those from the processing of some technical plants (textile plants, tobacco stalks), stalks of spontaneously growing plants;
- fractions from municipal waste such as paper waste,
- lignocellulosic agricultural waste (LAW) represents a resource with high global availability and low price, resulting from the harvesting of cereals and some technical plants (the quantities that can be collected depending on the type of crop: wheat straw: 1.4–2.5 t /ha; corn stalks: 4–6.5 t/ha; sunflower stalks 1.9–5.0 t/ha; rape stalks 1.7–3.5 t/ha) (*Marcu, 2008*).

The estimates of biomass supply potential have been the focus of many studies. Different studies quantify the potential of biomass at global, regional and country level for the short– to long term. Studies take into account such factors as differing land use, water and resource availability estimates, as well as varying levels of population and economic growth to arrive at the biomass supply potential.

Romania has sufficient biomass resources to obtain solid of liquid biofuels at small scale or at an industrial level, the raw material being generally agricultural and forestry residues that are available in all regions and to any category of population.

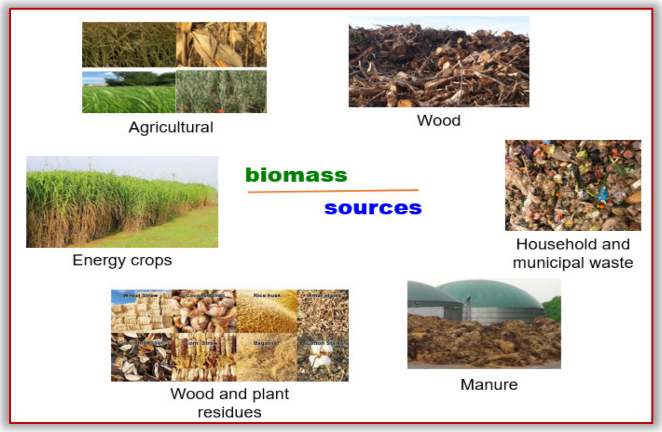

Figure 1 – Main biomass sources available for use to obtain energy

The paper presents the sources and manners of valorizing biomass for obtaining energy, in the context of national and European Union regulations and targets for decreasing the use of conventional energy sources in the following years.

MATERIALS AND METHODS

The most important categories of biomass usable for obtaining and their main uses for obtaining energy are presented below.

— Wood biomass is the most important renewable source of immediately accessible energy in Romania and is used as energy in several ways:

- for the production of heat (including residential buildings) and steam for industrial use;
- for generating electricity;
- as biofuel for transport.

Wood biomass is one of the most used types of biomasses and is divided into four major categories:

- woody residues;
- forest waste;
- urban wood waste;
- biomass resulting from clearing trees.

Forest waste includes waste that can no longer be used, dead trees, trees that do not meet commercial standards, and other trees that cannot be traded and must be cut to clear the forest. Some energy plant species are also part of the woody biomass category, for example fast–growing trees. The harvesting period of such plants varies between 3 and 10 years depending on the tree species, and the period between two plantings can be even more than 20 years (*INMA Bucharest, 2008*).

Forest biomass is the most important renewable energy source immediately accessible in Europe and is used as energy in several ways (Figure 2):

- for the production of heat (including residential buildings) and steam for industrial use;
- for generating electricity;
- as biofuel for transport.

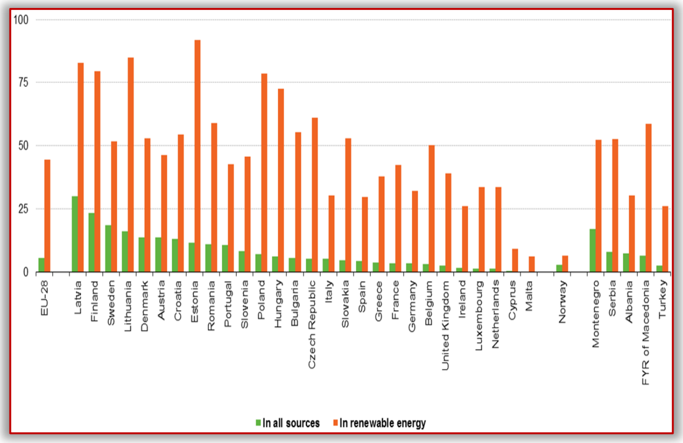

Figure 2 – Wood as a source of energy, 2014 (% share of wood and wood products in gross inland energy consumption, in toe) (*Eurostat, 2016*)

— Agricultural biomass is quantitatively appreciably more than woody biomass. Within it, the types currently most used for energy purposes are: straw; corn stalks and cobs; vine ropes; flax and hemp bushes; agricultural plants; sunflower and soy; biomass from fruits and seeds. Unlike woody biomass, agricultural biomass has an ash content of about 5% (*Vladut et al., 2012*).

Biomass from fruits and seeds. This category includes a number of residual products from agriculture. For example, rice husks are a residue from rice processing (approximately 20% of rice is the husk). This category can also include some solid waste from the food industry, such as the peels or remains of fruits and vegetables, kernels from the production of olive oil, peaches, apricots, etc. In the same way, the residues from the oil production industry, beet and rape constitute biomass that can be used energetically.

— Biomass specially grown for energy purposes includes biomass produced by cultivating plants, used as fuel for electricity generation; such plants are also called "energy plants". In this sense, several species of plants have been developed especially for the production of fuel. Some species of energy plants belong to the category of plant biomass (wheat straw, corn cobs, sunflower, sweet sorghum) and are selected to grow quickly, to be resistant to drought and pests and after harvest to be competitive to be used as fuels (*Vladut et al., 2012*). Energy plants can be grown on agricultural land that is not used for agriculture (usually land that is taken out of the loop for various reasons or land considered unsuitable for growing food plants). Compared to traditional agricultural plants, energy plants require less care and less mineral fertilizers or pesticides.

Energy plants can be divided into:

- annual herbaceous crops (barley, oat, rye, fodder crops, etc.);
- perennial herbaceous crops (reed, Elephant grass, Miscanthus, Cynara etc.);
- oleaginous seed crops (sun flower, soybean, rapeseed, camelina, etc.);
- oleaginous trees (palm tree, coconut tree, manacadamia tree, etc.);
- lignocellulosic annual crops (corn, sorgum, etc.);
- lignocellulosic trees (poplar, willow, eucalyptus, etc.).

— Biomass residues can be divided in primary residues, secondary residues and tertiary residues. Primary residues are produced from plants or forest products. This type of biomass is available "in the field" and must be collected for further use. Secondary residues are produced during the processing of biomass for the production of food products and for the production of finished wood products. They are available in the food industry, paper mills, etc. Tertiary residues result from the use of biomass. Here are included various wastes, (which differ from the point of view of the organic fraction contained) such as: household waste (the resulting amount under Romanian conditions is 0.8–1.5 kg/person/day, and the share of organic matter in urban waste is 40–50%), wood waste, sewage sludge, manure, etc.

RESULTS

Biomass is a renewable energy resource for which, at the national level, there is potential, but the applied technologies are not sufficiently efficient. Biomass is suitable for capitalization both in small–scale applications (individual heating systems) but also in medium/high power applications for the production of energy in cogeneration (electricity and thermal energy), in high energy efficiency systems (*ADR Centru, 2018*).

The energy content of biomass can be used by burning it directly or by chemically converting it into fuels, followed by burning them. Biomass has a very important role in fixing carbon dioxide from the atmosphere, the ambient air with an average concentration of 350 ppm (parts per million) carbon dioxide also representing an important reserve (*Romania's energy strategy 2019–2030, with the perspective of 2050*).

Figure 3 presents an assessment of bioenergy framework worldwide, showing that biomass energy comes from two different sources. The first is represented by primary bioenergy, using farmland or forests to produce biomass and the second is biomass residues that are generated as a by–product of food or wood products throughout their supply–consumption chain.

Even nowadays, approximately 90% of households in rural areas and 15% of those in urban areas are mainly heated with firewood, in inefficient stoves with incomplete combustion, without particle filters. Home heating is usually partial and thermal comfort low. In total, it is about 3.5 million homes, to which are added several tens of thousands of homes in mining areas, heated directly with coal.

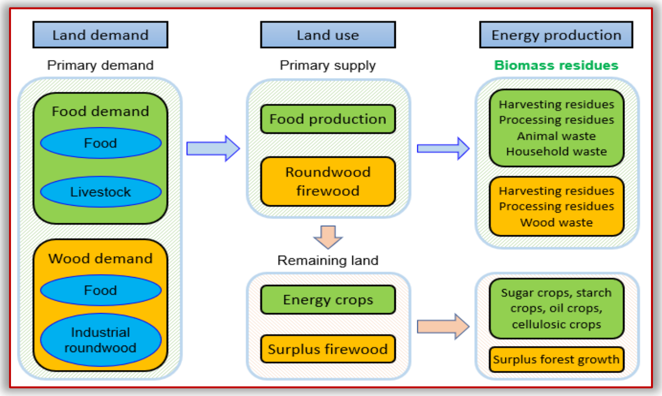

Figure 3 – Supply and demand framework of bioenergy (*INERA, 2014*)

The exploitation of energy sources from domestic resources is on a downward trend, and the dependence on imports is increasing, and despite a continuous reduction of the population, the final energy consumption is increasing. In Romania, approximately one third of energy consumption is related to the residential sector, followed by industry, transport, agriculture and other services (*European Commission, 2020*)

The demand for firewood will enter a downward slope also as an effect of the thermal insulation of rural homes. An increasing number of households, especially new homes, will adopt efficient biomass–based heating installations with complete combustion and no polluting emissions. This transition to more efficient and greener forms of heating with biomass will be increasingly felt in the coming years and will continue beyond 2030 (*European Commission, 2019*).

It is expected that in 2030 there will be in operation power plants that will be powered exclusively by biomass, bioliquids, or waste with a total capacity of 139 MW. The total production of electricity obtained through the utilization of biomass is estimated in 2030 at around 2 TWh (*Senocak and Goren, 2022*).

Final energy consumption from biomass and waste can register a notable increase, from 45 TWh in 2030 to 53 TWh in 2050. The total energy production based on biomass and waste shows, in all scenarios, a consistent increase in the analyzed period, 2030–2050. The tendency to accelerate biomass–based production after 2030, through the development of modern and efficient technologies on a large scale, especially in rural areas, is notable (*European Court of Auditors, 2017*).

By 2030, the consumption of biofuels will increase to the value of 4.1 TWh/year, a value sufficient to reach the national target for 2020, of a 10% SRE share in the transport sector. Biogas will register rapid growth, up to a production of 3,500 GWh in 2030, against the background of the development of the agricultural sector and, to a lesser extent, the modernization of wastewater treatment plants.

For Romania, an increase in the use of renewable sources requires investments of at least EUR 22 billion by 2030 (*Ministry of Economy, Energy and Environment, 2020*) but, to have a just transition, a necessary budget of around EUR 0.7 billion is expected (*Energy policy group, 2020*). To reach a carbon neutral energy system by 2050, additional investments will be needed.

CONCLUSIONS

In the context of climate changes and the need to switch from conventional to renewable energy, biomass has a favourable future. By 2030, biomass could account for 60% of total final renewable energy use and biomass has potential in all sectors. Following the analysis of the potential of solid agricultural and forestry biomass, it was possible to draw the conclusion that Romania has enough biomass to obtain solid biofuels at an industrial level, the raw material being generally agricultural and forestry residues. The biomass potential in Romania is estimated at over 15 million tons of dry biomass, equivalent to 6 million tons of oil, of which agricultural waste is in first place (approx. 63%). Their exploitation and rational use in energy production provides the necessary prerequisites to cover a significant part of the energy needs for domestic and industrial needs, especially in rural areas.

Acknowledgement

This work was supported by a grant of the Romanian Ministry of Agriculture and Rural Development, through ADER Program, project "Technologies for the superior valorization of lignocellulosic waste from horticulture" contract no. ADER 25.4.2/27.09.2019, A.A. 2 / 20.04.2021 and by the Ministry of Research, Innovation and Digitalization through Program 1 – Development of the national research–development system, Subprogram 1.2 – Institutional performance – Projects for financing excellence in RDI, Contract no. 1PFE/30.12.2021.

References

[1] ADR Centru. (2018). Analysis of the evolution of regional, national and european policies regarding bioenergy and energy production through the use of biomass, BIO4ECO Interreg Europe project;
[2] Energy Policy Group. (2020). Accelerated lignite exit in Bulgaria, Romania and Greece;
[3] European Commission. (2005). EUR 21350 – Biomass – Green energy for Europe, Luxemburg Office for Official Publications of the European comunities;
[4] European Commission. (2019). 4th report on the status of the energetic union, Correction of graph entitled "2030 Framework for Climate and Energy";
[5] European Commision. (2020). Energy statistical country datasheet;
[6] European Court of Auditors. (2017). EU actions in the field of energy and climate change;
[7] Eurostat. (2022). Sustainable development in the European Union. Monitoring report on progress towards the SDGs in an EU context, 2022 edition, ISBN 978–92–76–46573–7;
[8] Eurostat. (2016). Archive: Wood as a source of energy;
[9] I.N.M.A. Bucharest. (2008). Determination of thermo–physico–chemical characteristics of solid biomass types. Designing equipment for processing agricultural and forestry biomass in order to obtain pellets and agri–pellets – Bucharest;
[10] IRENA. (2014). Global Bioenergy. Supply and demand projections for the year 2030. A working paper for Remap 2030
[11] Marcu A. (2008). Waste and hazardous waste management – Practical guide for the correct application of environmental legislation;
[12] Ministry of Energy. (2019). Romania's energy strategy 2019–2030, with the perspective of 2050;
[13] Ministry of Economy. (2020). Energy and Business Environment. The National Integrated Plan in the field of Energy and Climate Change;
[14] Senocak A.–A., Goren H.–G. (2022). Forecasting the biomass–based energy potential using artificial intelligence and geographic information systems: A case study, Engineering Science and Technology, an International Journal 26, 100992;
[15] Vlăduţ V., Danciu A., Nicolescu M., Postelnicu E. (2012). Technologies for obtaining and using biomass, Terra Nostra Publishing House, Iaşi.

Note: This paper was presented at ISB–INMA TEH' 2022 – International Symposium on Technologies and Technical Systems in Agriculture, Food Industry and Environment, organized by University "POLITEHNICA" of Bucuresti, Faculty of Biotechnical Systems Engineering, National Institute for Research–Development of Machines and Installations designed for Agriculture and Food Industry (INMA Bucuresti), National Research & Development Institute for Food Bioresources (IBA Bucuresti), University of Agronomic Sciences and Veterinary Medicine of Bucuresti (UASVMB), Research–Development Institute for Plant Protection – (ICDPP Bucuresti), Research and Development Institute for Processing and Marketing of the Horticultural Products (HORTING), Hydraulics and Pneumatics Research Institute (INOE 2000 IHP) and Romanian Agricultural Mechanical Engineers Society (SIMAR), in Bucuresti, ROMANIA, in 6–7 October, 2022

ISSN: 2067–3809

[1.]Thomas Adedayo AYORINDE, [2.]Oseni Kehinde OWOLARAFE

DEVELOPMENT OF TRACTOR MOUNTED KENAF HARVESTER

[1.]Bioresources Development Centre, National Biotechnology Development Agency, Ogbomoso, NIGERIA
[2.]Department of Agricultural and Environmental Engineering, Obafemi Awolowo University, Ile–Ife, NIGERIA

Abstract: The design, fabrication and evaluation of a tractor mounted kenaf harvester was carried out in this study. The machine comprises of a rotary drive mechanism, which was adapted from a forage harvester. A review of kenaf stem properties was done to ensure accuracy of the design calculation for the machine components. The design of the machine was carried out using standard design procedures. A kenaf experimental field was set up at the Obafemi Awolowo University Teaching and Research Farm for the evaluation of the machine. The machine was evaluated using, crop maturity, crop variety and forward speed of the machine as factors. Effective field capacity and field efficiency of the machine were used as performance output parameters. The data obtained was analysed using 3–level factorial response surface methodology (RSM) of design expert software. The effective field capacity was observed to decrease with increase in plant maturity and increase with increase in forward speed of the machine. The highest effective field capacity recorded was 2.13 ha/day with Ifeken 100 at crop maturity of 10 weeks after planting, and forward speed was 5 km/hr. The field efficiency of the machine was found to decrease with increasing crop maturity and forward speed of the machine. The highest field efficiency of 97% was recorded for Ifeken 100 when the crop maturity was 10 weeks after planting and at 2 km/hr forward speed of machine.
Keywords: kenaf varieties, crop maturity, kenaf harvester, forward speed, field efficiency

INTRODUCTION

Kenaf is a dicotyledonous herbaceous annual plant with a high fibre yield. It has three different morphological fragments, which include the bark (with the bast fibre and the pectin), and the core (which contains the hollow centre that has the pith). The bast represents about 30% of the stalk weight and is the outer part of the plant which can produce high quality pulp, while the inner whiter part of the fibre (the core) is about 70% of the dry weight of the stalk, and produces low quality pulp (Makanjuola *et al.*, 2019; Ayorinde, 2022).

The industrial and economic importance of the entire parts of kenaf plant, i.e. leaves, fibre and seeds is enormous as they provide adequate, readily available and quality raw material that would secure the industrial and economic growth of a producing nation (Alexopoulou and Monti, 2013). Kenaf produces high quality pulp, in the stem. Kenaf fibers can be blended with synthetic fibers for making carpet. The fiber can also be used in making coarse bags, ropes, nets etc. Kenaf industrial applications include automobile, agriculture, construction, chemical process and packaging. Apparel fabrics and plastic/fiber composites from the fiber are its major end–use products. Other end use products include fiber board and particle board, oil and chemical absorbents, animal bedding, horticulture potting mix from the core, and livestock feed from the leaf (Makanjuola *et al.*, 2019).

Kenaf's ability to assimilate carbon dioxide, purify water and grow fast, has stimulated nations to consider kenaf as an alternative source of natural fibre. This discovery coincides with the global drive to mitigate environmental degradation due to the effect of oil spill, deforestation and chemical effluent, which made manufacturer to seek the use of agricultural products, wastes, and derivatives, like kenaf and some other fibrous crop, as raw materials, because of their renewability (Makanjuola *et al.*, 2019; Ayorinde, 2022).

Kenaf grows to maturity and is suitable for practical application in less than 3 months after planting. Manual methods are still used in kenaf harvesting and storage. In addition transportation and post–harvest processes are labour– intensive and time–consuming. Therefore, the development of kenaf harvesting technology continues to be an important aspect to explore (Ghahraei *et al.*, 2011; Dauda *et al.*, 2013). The objective of this study was to develop a tractor–mounted kenaf harvester to enhance the productivity of farmers and processors of kenaf in Nigeria.

MATERIALS AND METHODS

— Design consideration of the kenaf harvester

The following design considerations were followed during the development of the machine:

- The machine is not expected to be operated on a ridged field.
- The machine was designed to harvest the kenaf stem at 0.15 m to the ground level.
- The machine was designed to impact the required cutting power for shearing during operation as estimated with equation (1).
- The tractor was designed to travel outside the crop rows, while the harvester travel in the standing crop rows.

- The design concept is simple, easy to operate and repair by village artisans and farmers with minimum technical knowledge.
- It will be able to do large scale harvesting, save labour engagement and time of harvest.

— Description of the Machine

The machine operates with a mechanism of rotary disc harvester, which was mounted on the 3–point linkage of a tractor, driven by the power take–off (PTO) of the tractor and a bailing system, which bails the severed kenaf stem during harvesting. Circular saw blade was fixed on the rotary discs of the rotary disc harvesting mechanism, and was driven at high speed to achieve the cutting of the stem. The drive from the PTO was transmitted to the chain drive, which drives the bevel gear at the design speed. The bevel gear transmitted the drive at constant velocity ratio to the second chain drive, which drove the first cutting blade at constant velocity. The second cutting blade was designed to rotate concentrically with the first cutting blade, by the spur gear design arrangement on the machine. The machine was designed to accommodate a rack, which will enhance the packing of the stem in bundles. The isomeric and exploded views of the machine are as shown in Figures 1 and 2. Figure 3 shows the harvester mounted on a tractor.

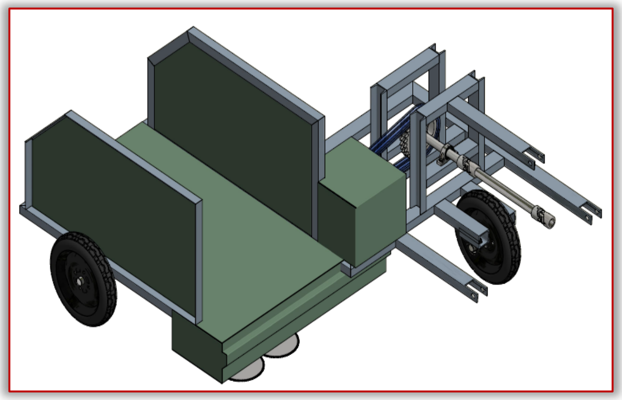

Figure 1: Isometric view of the kenaf harvester

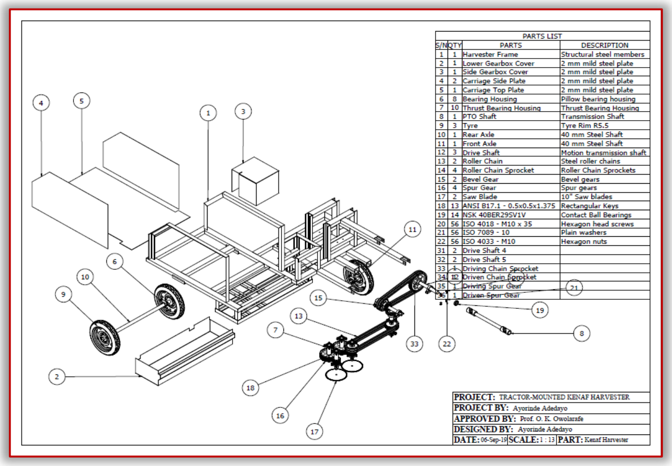

Figure 2: Exploded view of the kenaf harvester

Figure 3: The developed kenaf harvester mounted on a tractor

— Determination of cutting power requirement

The power required to cut kenaf stem was estimated to be 4.88 kW using equation (1), given that the ratio of average to peak cutting force C_f for a typical force–displacement curve is approximately equal to 0.64 (Srivastava *et al.*, 2006). The force required to cut the stem, $F_x$max, was 0.609 kN (Raji and Aremu, 2017), while the depth of material in contact with the blade X_{bu} was 22.98 mm. The cutting frequency, F_{cut} was estimated from the product of speed (647 rpm) by the number of cutting edge per revolution (50). The specifications of the tractor mounted kenaf harvester is shown in Table 1.

$$P = \frac{C_f F_{x\,max} X_{bu} F_{cut}}{60000} \qquad (1)$$

where, P = power for cutting, (kW)

Fx_{max} = maximum cutting force, (kN)

Xbu= depth of material at initial contact with knife, mm

fcut = cutting frequency, cuts/min

Cf = ratio of average to peak cutting force (Srivastava *et al.*, 2006)

$$\text{Cutting power required} = \frac{0.64 \times 0.61 \times 22.98 \times (50 \times 647)}{60000} = 4.84\text{kW}$$

Table 1: Specifications of tractor mounted kenaf harvester

Parameter	Specification
Dimension (L × W × H)	2240 x 2192 x 800 mm
Ground clearance	150 (mm)
Total weight	850 (kg)
Power Source	Tractor PTO
Tractor power required	55–70 (hp)
PTO speed	540 rpm
Transmission	PTO, gears, chain drive, shafts, bevel and spur gears
Height adjustment	Hydraulic
Cutting system	Carbonized Circular saw blade
Cutting width	900 mm
Number of tyres	4

— Performance evaluation of the machine

≡ Experimental design for evaluation

Three varieties of kenaf (Cuba 108, Ifeken di 400 and Ifeken 100) were planted at the Teaching and Research Farm Obafemi Awolowo Univeristy, Ile– Ife, Nigeria and monitored till 10th week. The experimetal design for the evaluation is shown in Table 2, with factors arranged in a 3 x 4 x 5 experiment making 60 experimental runs, with 3 replicates, giving 180 runs.

Table 2: Experimental design for the evaluation

S/N	Independent parameters	Indices
1.	Varieties	Cuba 108, Ife ken 100 and Ife ken Di 400
2.	Age of plant (Stem Diameter, mm)	Week 10,12,14 and 16
3.	Forward speed (km/h)	2, 3.5, 5.0, 6.5 and 7.7

≡ Performance evaluation procedure

The machine was mounted on a tractor and evaluated on the field based on the following parameters;

$$\text{Theoretic field capacity, ha/hr} = \frac{W \times S}{10} \quad (2)$$

where, W = Effective harvest width (m)
S = Forward speed (km/h)

$$\text{Effective field capacity, ha/h} = \frac{\text{Acuatal area covered (Ha)}}{\text{Time required to cover the area (h)}} \quad (3)$$

$$\text{Field efficiency (\%)} = = \frac{\text{Effective field capacity}}{\text{Theoretic field capacity}} \quad (4)$$

(Dauda *et al.*, 2013)

The result of the machine field efficiency was subjected to Box–Behnken randomized methodology of the response surface standard design to get the experimental runs presented in Table 3. Data obtain for field efficiency was statistically analyzed.

Table 3: Kenaf harvester machine performance

Std	Run	WAP (weeks)	Variety	Forward Speed (km/hr)
5	1	10	I4	2
10	2	13	I1	2
7	3	10	I4	7.7
15	4	13	I4	5
12	5	13	I1	7.7
4	6	16	I1	5
8	7	16	I4	7.7
1	8	10	C1	5
2	9	16	C1	5
9	10	13	C1	2
3	11	10	I1	5
13	12	13	I4	5
6	13	16	I4	2
11	14	13	C1	7.7
14	15	13	I4	5

Note: C1 = Cuba 108; I4 = Ifeken di 400; I1 = Ifeken 100

RESULT AND DISCUSSION

— Effect of plant maturity on field efficiency of the machine

The field efficiency of the machine decreased with increasing plant maturity, when other factors remain constant. The maximum field efficiency recorded was 97% at week 10 while the minimum was 22% at week 16. The 3D surface graph in Figures 4 to 9 showed similar trend of drop in the machine efficiency at forward speed and crop variety to as low as 22%. Similar result was reported by Falana *et al.* (2020). The analysis of variance using design expert software showed that all machine operational factors had significant effect on the field efficiency (Table 4)

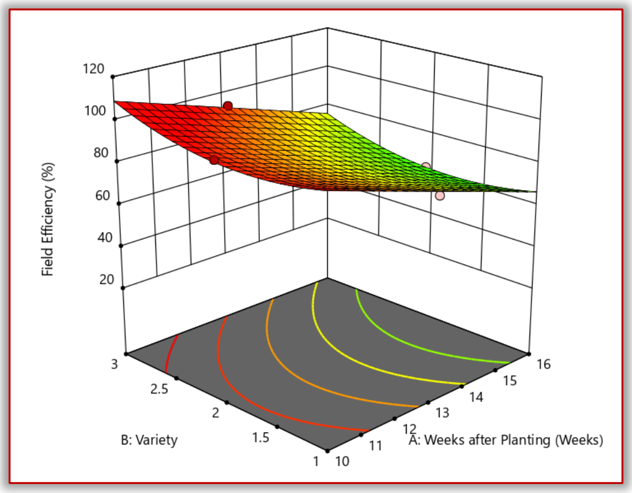

Figure 4: Plot of Effect of variety and weeks after planting on field efficiency when forward speed was 2 km/hr

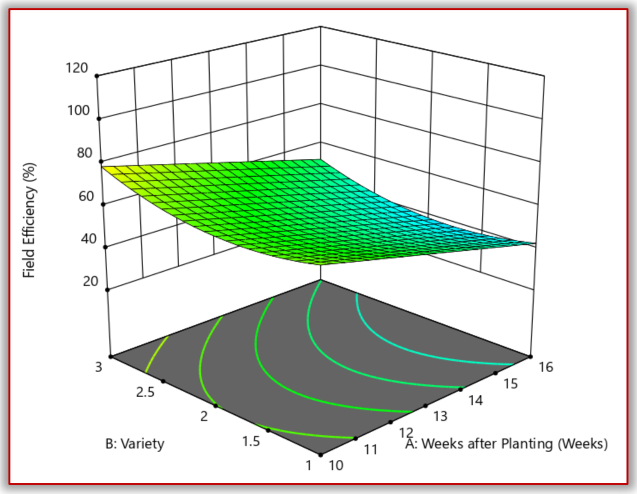

Figure 5: Plot of Effect of variety and weeks after planting on field efficiency when forward speed of tractor was 3.5 km/hr

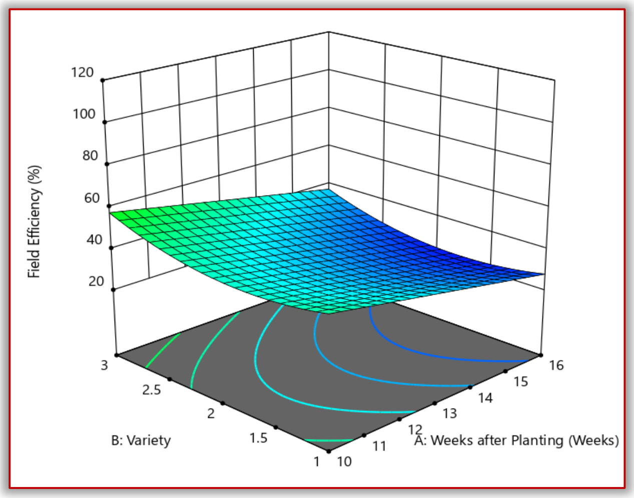

Figure 6: Plot of Effect of variety and weeks after planting on field efficiency when forward speed of tractor was 5 km/hr

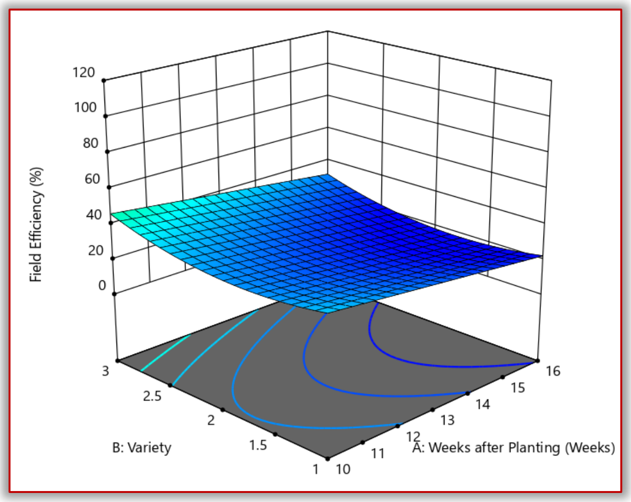

Figure 7: Plot of Effect of variety and weeks after planting on field efficiency when forward speed of tractor was 6.5 km/hr

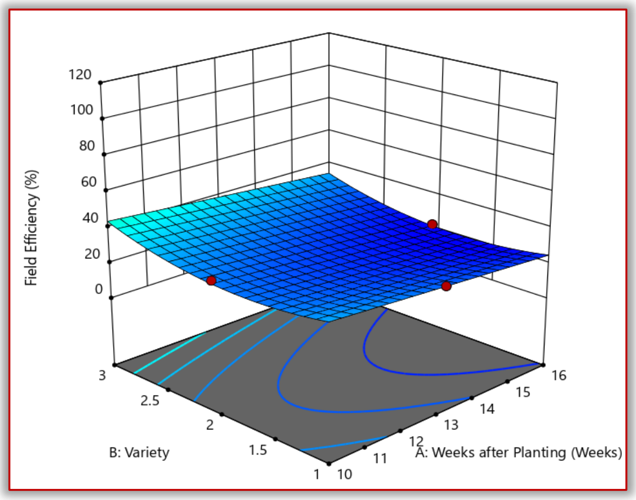

Figure 8: Plot of Effect of variety and weeks after planting on field efficiency when forward speed of tractor was 7.7 km/hr

Table 4: ANOVA of the effect of operation parameters on field efficiency

Source	Sum of squares	DF	Mean Square	F–value	p–value	Remark
Model	8185.65	6	1364.27	357.45	< 0.0001	significant
WAP	913.07	1	913.07	239.23	< 0.0001	significant
V	173.87	1	173.87	45.56	0.0001	significant
FS	5718.38	1	5718.38	1498.27	< 0.0001	significant
WAP*FS	132.41	1	132.41	34.69	0.0004	significant
V^2	261.24	1	261.24	68.45	< 0.0001	significant
FS^2	1055.32	1	1055.32	276.50	< 0.0001	significant
Residual	30.53	8	3.82			
Lack of Fit	30.53	6	5.09			
Pure Error	0.0000	2	0.0000			
Cor Total	8216.18	14				

— Effect of plant variety on field efficiency of the machine

It could be observed from Table 3 that the field efficiency dropped slightly as the variety was changed from Cuba 108 to Ifeken di 400 and increased to the maximum when Ifeken 100 was harvested. The response surface graph in Figures 5 to 9 also confirmed that plant variety had effect on the field efficiency. The highest field efficiency (97%) and the lowest field efficiency (22%) were recorded when Ifeken di 400 was harvested (other machine operation parameters were constant). Similar result was reported by Dauda *et al.* (2013) and Abd–El Mawla and Hameida (2005) in their respective research findings.

— Effect of forward speed of tractor on the field efficiency of the machine

The field efficiency of the machine increased as the forward speed of operation decreased as shown in the response surface graph (Figures 9). The highest and the lowest field efficiencies recorded were 97% and 22%, respectively. The highest field efficiency was recorded when the forward speed of machine was 2.0 km/hr while the lowest field efficiency was at 7.7 km/hr (Table 3). The efficiency of this kenaf harvester is higher than that of the tractor mounted kenaf harvester developed by Dauda *et al.* (2013) which was 76%. The effect of forward speed on the field efficiency was observed to be significant as shown in Table 4.

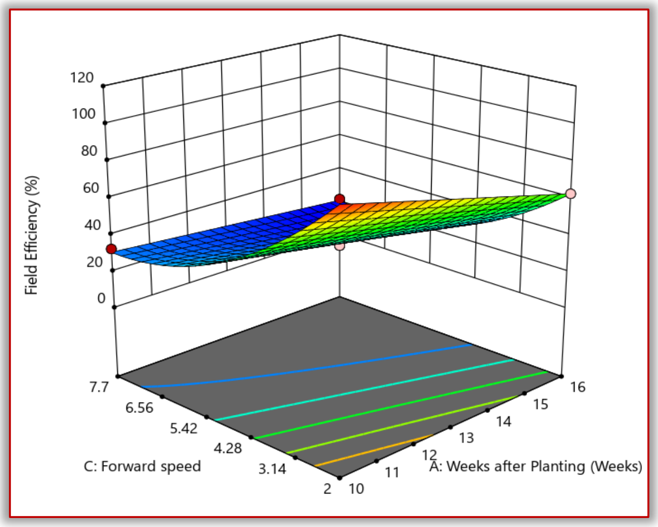

Figure 9: Plot of the effect of forward speed on field efficiency of the machine

CONCLUSIONS

A tractor mounted kenaf havester was developed in this study. The machine harvests the plant stem with a circular blade and it also have a bailing sytem, which make the packing of kenaf stem easy. The result showed that crop maturity, varieties and forward speed during operation have influence on the performance of the harvester. The field efficiency of the machine was found to increase with decreasing crop maturity, and forward speed of the machine. The highest field efficiency was 97% with *Ifeken* 100 harvested, when the crop maturity was 10 weeks after planting, and forward speed of machine was 2 km/hr. The result of the performance evaluation indicates that the harvester has the potential for commercialisation for the use of kenaf farmers.

References

[1] Abd–El Mawla, H.A. and Hameida, B. E. (2015). Sugarcane Mechanical Harvesting Evaluation of local Application. Journal on Soil Science and Agricultural Engineering. Mansoura University. 6(1):129–141

[2] Alexopoulou, E., and Monti, A. (2013). Kenaf: A Multi–Purpose Crop for Several Industrial Applications, 203. London: New Insights from the Biokenaf Project Springer–Verlag.
[3] Ayorinde, T. A. (2022). Development of an improved tractor mounted kenaf harvester. A Ph.D. thesis submitted to the department of Agricultural and Environmental Engineering, Obafemi Awolowo University, Ile Ife.
[4] Dauda, S. M., Ahmad, D., Khalina, A. and Jamarei, O. (2013): Performance Evaluation of a Tractor Mounted Kenaf Harvesting Machine. Academic Research International: 4(2), Pp. 70 – 81.
[5] Falana, O.B., Aluko, O. B., Adetan, D. A. and Osunbitan, J. A. (2020). Determining the efficiency of a modified brush cutter for kenaf (Hibiscus cannabin us) harvesting. Agricultural Engineering Int: CIGR Journal Open access at http://www.cigrjournal.org Vol. 22(2): 59–67.
[6] Ghahraei, O., Ahmad, D., Khalina, A., Suryanto, H. and Othman, J. (2011). Cutting tests of kenaf stems. Transactions of the ASABE, 54(1), 51–56.
[7] Makanjuola, G. A., Ayorinde, T. A., Aluko, O. B., Owolarafe, O. K. and Sanni, L. A. (2019). Performance evaluation of a kenaf decorticator. Agricultural Engineering International: CIGR Journal, 21(1): 192–202.
[8] Raji, A. O. and Aremu D. O. (2017). Mechnaical properties of varieties of kenaf (Hibiscus Cannabius) stem. Global Journal of Science Frontier Researched Agriculture and Veterinary, Volume 17, Issue 6, Version 10.
[9] Srivastava, A. K., Rohrbach R. P. and Goering, C. E. (2006). Engineering Principles of Agricultural Machines, 2nd Edition. ASAE, 2950 Niles Road, St. Joseph, MI 49085–9659 USA. Pp 331 – 341.

ISSN: 2067–3809

Fascicule 2
[April – June]
tome XVI [2023]

ACTA Technica CORVINIENSIS
BULLETIN OF ENGINEERING

ACTA TECHNICA CORVINIENSIS
Bulletin of Engineering

ISSN: 2067-3809

MANUSCRIPT PREPARATION – GENERAL GUIDELINES

Manuscripts submitted for consideration to ACTA TECHNICA CORVINIENSIS – Bulletin of Engineering must conform to the following requirements that will facilitate preparation of the article for publication. These instructions are written in a form that satisfies all of the formatting requirements for the author manuscript. Please use them as a template in preparing your manuscript. Authors must take special care to follow these instructions concerning margins.

INVITATION

We are looking forward to a fruitful collaboration and we welcome you to publish in our ACTA TECHNICA CORVINIENSIS – Bulletin of Engineering. You are invited to contribute review or research papers as well as opinion in the fields of science and technology including engineering. We accept contributions (full papers) in the fields of applied sciences and technology including all branches of engineering and management.

ACTA TECHNICA CORVINIENSIS – Bulletin of Engineering publishes invited review papers covering the full spectrum of engineering and management. The reviews, both experimental and theoretical, provide general background information as well as a critical assessment on topics in a state of flux. We are primarily interested in those contributions which bring new insights, and papers will be selected on the basis of the importance of the new knowledge they provide.

Submission of a paper implies that the work described has not been published previously (except in the form of an abstract or as part of a published lecture or academic thesis) that it is not under consideration for publication elsewhere. It is not accepted to submit materials which in any way violate copyrights of third persons or law rights. An author is fully responsible ethically and legally for breaking given conditions or misleading the Editor or the Publisher.

ACTA TECHNICA CORVINIENSIS – Bulletin of Engineering is an international and interdisciplinary journal which reports on scientific and technical contributions. Every year, in four online issues (fascicules 1–4), ACTA TECHNICA CORVINIENSIS – Bulletin of Engineering [e-ISSN: 2067-3809] publishes a series of reviews covering the most exciting and developing areas of engineering. Each issue contains papers reviewed by international researchers who are experts in their fields. The result is a journal that gives the scientists and engineers the opportunity to keep informed of all the current developments in their own, and related, areas of research, ensuring the new ideas across an increasingly the interdisciplinary field. Topical reviews in materials science and engineering, each including:

- surveys of work accomplished to date
- current trends in research and applications
- future prospects.

As an open-access journal ACTA TECHNICA CORVINIENSIS – Bulletin of Engineering will serve the whole engineering research community, offering a stimulating combination of the following:

- Research Papers – concise, high impact original research articles,
- Scientific Papers – concise, high impact original theoretical articles,
- Perspectives – commissioned commentaries highlighting the impact and wider implications of research appearing in the journal.

ACTA TECHNICA CORVINIENSIS – Bulletin of Engineering encourages the submission of comments on papers published particularly in our journal. The journal publishes articles focused on topics of current interest within the scope of the journal and coordinated by invited guest editors. Interested authors are invited to contact one of the Editors for further details.

BASIC MANUSCRIPT REQUIREMENTS

The basic instructions and manuscript requirements are simple:

- Manuscript shall be formatted for an A4 size page.
- The all margins of page (top, bottom, left, and right) shall be 20 mm.
- The text shall have both the left and right margins justified.
- Single-spaced text, tables, and references, written with 11 or 12-point Georgia or Times New Roman typeface.
- No Line numbering on any pages and no page numbers.
- Manuscript length must not exceed 15 pages (including text and references).
- Number of the figures and tables combined must not exceed 20.
- Manuscripts that exceed these guidelines will be subject to reductions in length.

The original of the technical paper will be sent through e-mail as attached document (*.doc, Windows 95 or higher). Manuscripts should be submitted to e-mail: redactie@fih.upt.ro, with mention "for ACTA TECHNICA CORVINIENSIS".

STRUCTURE

The manuscript should be organized in the following order: Title of the paper, Authors' names and affiliation, Abstract, Key Words, Introduction, Body of the paper (in sequential headings), Discussion & Results, Conclusion or Concluding Remarks, Acknowledgements (where applicable), References, and Appendices (where applicable).

THE TITLE

The title is centered on the page and is CAPITALIZED AND SET IN BOLDFACE (font size 14 pt). It should adequately describe the content of the paper. An abbreviated title of less than 60 characters (including spaces) should also be suggested. Maximum length of title: 20 words.

AUTHOR'S NAME AND AFFILIATION

The author's name(s) follows the title and is also centered on the page (font size 11 pt). A blank line is required between the title and the author's name(s). Last names should be spelled out in full and succeeded by author's initials. The author's affiliation (in font size 11 pt) is provided below. Phone and fax numbers do not appear.

ABSTRACT

State the paper's purpose, methods or procedures presentation, new results, and conclusions are presented. A nonmathematical abstract, not exceeding 200 words, is required for all papers. It should be an abbreviated, accurate presentation of the contents of the paper. It should contain sufficient information to enable readers to decide whether they should obtain and read the entire paper. Do not cite references in the abstract.

KEY WORDS

The author should provide a list of three to five key words that clearly describe the subject matter of the paper.

TEXT LAYOUT

The manuscript must be typed single spacing. Use extra line spacing between equations, illustrations, figures and tables. The body of the text should be prepared using Georgia or Times New Roman. The font size used for preparation of the manuscript must be 11 or 12 points. The first paragraph following a heading should not be indented. The following paragraphs must be indented 10 mm. Note that there is no line spacing between paragraphs unless a subheading is used. Symbols for physical quantities in the text should be written in italics. Conclude the text with a summary or conclusion section. Spell out all initials, acronyms, or abbreviations (not units of measure) at first use. Put the initials or abbreviation in parentheses after the spelled-out version. The manuscript must be writing in the third person ("the author concludes... ").

FIGURES AND TABLES

Figures (diagrams and photographs) should be numbered consecutively using Arabic numbers. They should be placed in the text soon after the point where they are referenced. Figures should be centered in a column and should have a figure caption placed underneath. Captions should be centered in the column, in the format "Figure 1" and are in upper and lower case letters.

When referring to a figure in the body of the text, the abbreviation "Figure" is used illustrations must be submitted in digital format, with a good resolution. Table captions appear centered above the table in upper and lower case letters.

When referring to a table in the text, "Table" with the proper number is used. Captions should be centered in the column, in the format "Table 1" and are in upper and lower case letters. Tables are numbered consecutively and independently of any figures. All figures and tables must be incorporated into the text.

EQUATIONS & MATHEMATICAL EXPRESSIONS

Place equations on separate lines, centered, and numbered in parentheses at the right margin. Equation numbers should appear in parentheses and be numbered consecutively. All equation numbers must appear on the right-hand side of the equation and should be referred to within the text.

CONCLUSIONS

A conclusion section must be included and should indicate clearly the advantages, limitations and possible applications of the paper. Discuss about future work.

Acknowledgements

An acknowledgement section may be presented after the conclusion, if desired. Individuals or units other than authors who were of direct help in the work could be acknowledged by a brief statement following the text. The acknowledgment should give essential credits, but its length should be kept to a minimum; word count should be <100 words.

References

References should be listed together at the end of the paper in alphabetical order by author's surname. List of references indent 10 mm from the second line of each references. Personal communications and unpublished data are not acceptable references.

- *Journal Papers:* Surname 1, Initials; Surname 2, Initials and Surname 3, Initials: Title, Journal Name, volume (number), pages, year.
- *Books:* Surname 1, Initials and Surname 2, Initials: Title, Edition (if existent), Place of publication, Publisher, year.
- *Proceedings Papers:* Surname 1, Initials; Surname 2, Initials and Surname 3, Initials: Paper title, Proceedings title, pages, year.

ISSN: 2067-3809

INDEXES & DATABASES

We are very pleased to inform that our international scientific journal ACTA TECHNICA CORVINIENSIS – Bulletin of Engineering completed its 15 years of publication successfully [2008–2022, Tome I–XV].
In a very short period the ACTA TECHNICA CORVINIENSIS – Bulletin of Engineering has acquired global presence and scholars from all over the world have taken it with great enthusiasm.
We are extremely grateful and heartily acknowledge the kind of support and encouragement from all contributors and all collaborators!

ACTA TECHNICA CORVINIENSIS – Bulletin of Engineering is accredited and ranked in the "B+" CATEGORY Journal by CNCSIS – The National University Research Council's Classification of Romanian Journals, position no. 940 (http://cncsis.gov.ro/).
ACTA TECHNICA CORVINIENSIS – Bulletin of Engineering is a part of the ROAD, the Directory of Open Access scholarly Resources (http://road.issn.org/).

ACTA TECHNICA CORVINIENSIS – Bulletin of Engineering is also indexed in the digital libraries of the following world's universities and research centers:

WorldCat – the world's largest library catalog
https://www.worldcat.org/
National Lybrary of Australia
http://trove.nla.gov.au/
University Library of Regensburg – GIGA German Institute of Global and Area Studies
http://opac.giga-hamburg.de/ezb/
Simon Fraser University – Electronic Journals Library
http://cufts2.lib.sfu.ca/
University of Wisconsin – Madison Libraries
http://library.wisc.edu/
University of Toronto Libraries
http://search.library.utoronto.ca/
The University of Queensland
https://www.library.uq.edu.au/
The New York Public Library
http://nypl.bibliocommons.com/
State Library of New South Wales
http://library.sl.nsw.gov.au/
University of Alberta Libraries – University of Alberta
http://www.library.ualberta.ca/
The University of Hong Kong Libraries
http://sunzi.lib.hku.hk/
The University Library – The University of California
http://harvest.lib.ucdavis.edu/

ACTA TECHNICA CORVINIENSIS – Bulletin of Engineering is indexed, abstracted and covered in the world–known bibliographical databases and directories including:

INDEX COPERNICUS – JOURNAL MASTER LIST
http://journals.indexcopernicus.com/
GENAMICSJOURNALSEEK Database
http://journalseek.net/
DOAJ – Directory of Open Access Journals
http://www.doaj.org/
EVISA Database
http://www.speciation.net/
CHEMICAL ABSTRACTS SERVICE (CAS)
http://www.cas.org/
EBSCO Publishing
http://www.ebscohost.com/
GOOGLE SCHOLAR
http://scholar.google.com
SCIRUS – Elsevier
http://www.scirus.com/
ULRICHSweb – Global serials directory
http://ulrichsweb.serialssolutions.com
getCITED
http://www.getcited.org
BASE – Bielefeld Academic Search Engine
http://www.base-search.net
Electronic Journals Library
http://rzblx1.uni-regensburg.de
Open J–Gate
http://www.openj-gate.com
ProQUEST Research Library
http://www.proquest.com
Directory of Research Journals Indexing
http://www.drji.org/
Directory Indexing of International Research Journals
http://www.citefactor.org/

ACTA TECHNICA CORVINIENSIS
Bulletin of Engineering
ISSN: 2067-3809

Faculty of Engineering Hunedoara,
5, Revolutiei, 331128, Hunedoara, ROMANIA
http://acta.fih.upt.ro